Complexity in the entangled bank : On the structure and dynamics of empirical mutualistic networks

Claudia Payrato Borras

Thèse de doctorat pour l'obtention du titre de

Docteur en Sciences Physiques

délivré par

CY Cergy Paris Université

Complexity in the entangled bank:

On the structure and dynamics of empirical mutualistic networks

---

présentée et soutenue publiquement par

Clàudia Payrató Borràs

le 17 Décembre 2020

Directeurs de thèse:

Laura Hernández
Yamir Moreno Vega

Jury:

M. Fernando Peruani LPTM CY Cergy Paris Président du jury
Mme. Susanna Manrubia National Centre for Biotechnology (CSIC) Rapporteur
M. Diego Garlaschelli IMT School for Advanced Studies Rapporteur
M. Raúl Toral IFISC (CSIC) Examinateur
M. Luis Mario Floría University of Zaragoza Examinateur

¡Qué encanto este de las imaginaciones de la niñez, Platero, que yo no sé si tú tienes o has tenido! Todo va y viene, en trueques deleitosos; se mira todo y no se ve, más que como estampa momentánea de la fantasía... Y anda uno semiciego, mirando tanto adentro como afuera, volcando, a veces, en la sombra del alma la carga de imágenes de la vida, o abriendo al sol, como una flor cierta, y poniéndola en una orilla verdadera, la poesía, que luego nunca más se encuentra, del alma iluminada.

Platero y yo, J. R. Jiménez

La ciencia siempre ha tenido para mí el regusto de los juegos infantiles, ese maravillarse que acompaña el descubrimiento de lo que ocurre más allá de nosotros mismos y que solo más tarde podemos ordenar, con el tesón y probablemente la sencillez, del que completa un puzzle, clasifica sus figuritas o colorea escrupulosamente un dibujo. Está, asimismo, en la fascinación obstinada del que se inventa un nuevo juego o el que busca, en el antiquísimo *escondite*, a sus hermanos, con esa certeza tan arraigada de que les encontrará.

El recuerdo de esos momentos me ha visitado a menudo durante la escritura de esta tesis, y me gustaría pensar que he conseguido condensar algún resto de su brillo –aunque a veces casi se apagara– en estas páginas. El documento que sigue no deja de ser, porque así se pide y tal vez así deba ser, el resultado visible y atemperado de las ilusiones y las desilusiones, las alegrías y las frustraciones, al fin y al cabo, lo aprendido y –muy a mi pesar– lo ignorado durante los cuatro años que ha durado mi tesis doctoral. También es, sin duda, un reflejo de las personas que me han acompañado.

Ahora, como les habrá ocurrido a tantos otros antes que a mí, dar por terminado este ejercicio de desprendimiento despierta una melancolía prematura. Hay quienes detestan la melancolía por sentimental o improductiva. Muy al contrario, yo creo que del mismo modo que una fruta una vez azucarada acaba fermentando en un sabor agridulce, sin melancolía no tendríamos la certeza de haber vivido, aunque sea un instante, algo bueno.

Acknowledgments

There are many people with whom I am in debt because of this thesis, sometimes for obvious reasons, sometimes in indirect or mysterious ways. To start with, I want to thank my two supervisors, Laura and Yamir, for their support and mentoring during these years. Moreover, I am grateful to the people from LPTM for their warm welcome and help. I am also very happy of having had the opportunity to work in the BIFI: I have had countless interesting conversations and funny moments there, and I was lucky enough to find some good friends inside the walls of the office. This thesis is better thanks to many of you. I wish I could name all the people with whom I have shared a scientific discussion or a nice moment in the office along these four years, but you know who you are.

De otro lado, le tengo mucho que agradecer a mi familia, sobretodo a mis padres, por todo lo que han hecho y hacen por mí. También a los amigos que me han acompañado, especialmente a mi amigo de siempre, Yeray. Y finalmente a Enrico, por todo lo que se pueda imaginar (y también por lo que no).

Abstract

Mutualistic relationships, that in the past had been long overlooked as fascinating but marginally relevant, are today known to play a crucial role in shaping ecosystems. In this thesis we look into the complexity of how these ecological relationships are intertwined in natural systems, or what Darwin famously called the 'entangled bank', from the viewpoint of the network formalism.

In the first part of the thesis, we investigate the origin of the architecture of mutualistic networks. In detail, by applying concepts from information theory and statistical physics, we address the question of the emergence of a widespread pattern known as nestedness. By analyzing a large dataset of empirical networks, we show that the interplay of a few minimum assumptions on the number of mutualistic interactions per species and the effect of chance are sufficient to reproduce the observed structure, precluding the introduction of selective pressures or mechanistic processes. In this sense, our results show that the global structure of mutualistic communities can be explained, in statistical terms, by the lower-order features of the system. With these results at hand, we then explore how the different metrics proposed in the literature quantify nested patterns, evaluating their overall performance on real and synthetic networks. Our results indicate that the ranking and comparison of nested patterns among different ecosystems is hampered by the presence of undesired dependencies on other network parameters.

In the second part of this thesis, we continue examining the organization of mutualistic communities but tackling another challenge, namely that of moving beyond the still-prevailing aggregated paradigm. To start with, we characterize a set of empirical networks and assess how incorporating information about the temporal variability modifies the static network description. Next, we propose a group of models to generate, under diverse assumptions, synthetic configurations of phenology for a given network. We find that, while the adequacy of mechanistic models to produce realistic configurations is highly system-dependent, a statistical model based on the maximum entropy principle performs generally well independently of the network details. Elaborating further upon this line of thought, we then briefly explore the dynamical consequences for species persistence of taking into account the phenology. We find that species with a short period of activity face a larger uncertainty in their robustness against perturbations. This preliminary approach, though, calls for further research, especially in the context of a changing climate.

On the whole, along this thesis we analyze how the network language can be used to disentangle the complexity of natural mutualistic systems, by assessing on the one hand the minimum information required to understand the 'entangled bank', and on the other hand, identifying the limitations of the static representation that still predominates in the field. The works we will present and discuss here relate to the following publications:

- Payrató-Borràs, C., L. Hernández, and Y. Moreno (2019). Breaking the spell of nestedness: The entropic origin of nestedness in mutualistic systems. *Physical Review X 9* (3), 031024.

- Payrató-Borràs, C., L. Hernández, and Y. Moreno (2020). Measuring nestedness: A comparative study of the performance of different metrics. *Ecology and evolution*, 10(21), 11906-11921.

- Payrató-Borràs, C., C. Gracia-Lázaro, L. Hernández, and Y. Moreno (2020). Beyond the aggregated paradigm: characterizing phenology in mutualistic networks. *In preparation.*

Resumé

Les interactions mutualistes, qui dans le passé avaient longtemps été considérées comme fascinantes mais marginales, sont aujourd'hui reconnues par le rôle crucial qu'elles ont dans la formation des écosystèmes. Dans cette thèse, nous examinons comment la complexité de ces interactions écologiques intervient dans les systèmes naturels, ce que Darwin a appelé le 'rivage luxuriant', en appliquant le formalisme des réseaux.

Dans la première partie de la thèse, nous considérons l'origine de l'architecture des réseaux mutualistes. Dans le détail, en appliquant des concepts du théorie de l'information et de la physique statistique, nous abordons la question de l'émergence d'une propriété très générale, connue sous le nom d'imbrication. En analysant un vaste ensemble de données de réseaux empiriques, nous montrons que la considération de quelques hypothèses minimales sur le nombre d'interactions mutualistes par espèce et l'effet du hasard sont suffisantes pour reproduire la structure observée, excluant l'introduction de pressions sélectives ou de processus mécanistes. En ce sens, nos résultats montrent que la structure globale des communautés mutualistes peut être expliquée, en termes statistiques, par les propriétés locales du système. Ensuite, nous explorons comment les différentes métriques proposées dans la littérature permettent de quantifier le degré d'imbrication, évaluant leur performance globale sur des réseaux réels et synthétiques. Nos résultats indiquent que la comparaison et le classement des niveaux d'imbrication entre différents écosystèmes sont entravés par la présence de dépendances par rapport à d'autres paramètres des réseaux.

Dans la deuxième partie de cette thèse, nous continuons à étudier l'organisation des communautés mutualistes, mais en se concentrant sur un autre défi: celui de dépasser le paradigme de l'agrégation temporelle encore dominant. Pour commencer, nous caractérisons un ensemble de réseaux empiriques et évaluons comment l'incorporation d'informations sur la variabilité temporelle modifie la description statique du réseau. Ensuite, nous proposons un groupe de modèles qui génère, sous diverses hypothèses, des configurations synthétiques de phénologie pour un réseau donné. Nous constatons que, bien que l'adéquation des modèles mécanistes pour produire des configurations réalistes dépend fortement du système, un modèle statistique basé sur le principe d'entropie maximale fonctionne généralement bien, indépendamment des détails du réseau. En développant cette ligne de pensée, nous explorons ensuite brièvement les conséquences dynamiques de la prise en compte de la phénologie sur la persistance des espèces. Nous constatons que les espèces qui ont une courte période d'activité sont confrontées à une plus grande incertitude quant à leur robustesse face aux perturbations. Cette approche préliminaire, cependant, appelle a des recherches supplémentaires, en particulier dans le contexte du changement climatique.

Somme tout, nous analysons au long de cette thèse comment le langage des réseaux complexes peut être utilisé pour démêler la complexité des systèmes mutualistes naturels, en évaluant d'une part l'information minimale nécessaire pour comprendre le 'rivage luxuriant', et d'autre part, en identifiant les limites de la représentation statique qui prédomine encore dans le domaine.

Resumen

El mutualismo, que durante largo tiempo había sido considerado un tipo de interacción fascinante pero marginalmente relevante, es reconocido hoy en día por desempeñar un papel crucial en la formación de los ecosistemas. En esta tesis analizamos la complejidad del rico entrelazado que forman estas relaciones ecológicas en los sistemas naturales, o lo que Darwin célebremente llamó el 'ribazo enmarañado', desde el punto de vista del formalismo de redes.

En la primera parte de la tesis nos centramos en estudiar el origen de la arquitectura de las redes mutualistas. En detalle, a partir de la aplicación de conceptos de la teoría de la información y la física estadística, abordamos la cuestión de la emergencia de un ubicuo patrón estructural conocido como anidamiento. A través del análisis de un vasto conjunto

de redes empíricas, mostramos que unas pocas asunciones mínimas sobre el número de interacciones mutualistas por especie junto con el efecto del azar son condiciones suficientes para reproducir la estructura observada –sin necesidad de suponer la intervención de fuerzas selectivas o procesos mecanicistas. En este sentido, nuestros resultados muestran que la estructura global de las comunidades mutualistas puede explicarse, en términos estadísticos, a partir de las propiedades locales del sistema. En segundo lugar, exploramos también cómo las diferentes métricas propuestas en la literatura cuantifican el anidamiento, evaluando su eficacia tanto en redes reales como sintéticas. Nuestros resultados indican que la comparación y clasificación de patrones anidados correspondientes a distintos ecosistemas es entorpecida, sustancialmente, por la existencia de dependencias respecto a otros parámetros de la red.

En la segunda parte de esta tesis, continuamos profundizando en el estudio de la organización de comunidades mutualistas pero abordando un desafío distinto, concretamente el de superar el paradigma de agregación temporal de las redes ecológicas. Para empezar, caracterizamos un conjunto de redes empíricas y evaluamos cómo la incorporación de información detallada sobre la variabilidad temporal modifica la descripción estática del sistema. A continuación, proponemos un grupo de modelos que permite generar, bajo diversos supuestos, configuraciones sintéticas de fenología compatibles con una red determinada. Encontramos que, si bien la idoneidad de los modelos mecanicistas para producir configuraciones realistas depende en gran medida del sistema estudiado, un modelo estadístico basado en el principio de máxima entropía se comporta generalmente bien independientemente de los detalles de la red. Basándonos en estos resultados, exploramos brevemente las consecuencias dinámicas, específicamente para la persistencia de las especies, de tener en cuenta la dimensión temporal de la red de interacciones. En particular, observamos que las especies con un período de actividad corto se enfrentan a una mayor incertidumbre frente a perturbaciones externas. Este enfoque preliminar, sin embargo, requiere investigaciones más detalladas, especialmente en el contexto del cambio climático.

En conjunto, a lo largo de esta tesis analizamos cómo se puede utilizar el lenguaje de redes para estudiar la complejidad de los sistemas mutualistas naturales, evaluando por un lado la información mínima requerida para comprender el 'ribazo enmarañado', y por otro lado, identificando las limitaciones de la aún predominante representación estática de los ecosistemas.

Contents

CHAPTER 1

Introduction

1.1 Some definitions of Complex Systems

According to the 'Concise etymological dictionary of the English language' (Skeat Walter, 1980), the word *complex* comes from the ancient Latin word *complexus*, composed by the prefix *com* –which means 'together', 'jointly'– and the past participle form of the root *plectere* -which means 'to plait', 'to weave'-. This origin stands in contrast with the etymology of the word *simple* from the Latin *simplex*: the root remains the same but the prefix changes to *sim*, that translates into 'one' or 'as one'. Interestingly, this notion of complexity as a large aggregate of elements intricately tangled, and moreover as multiplicity as opposed to singleness, is surprisingly close to the modern scientific concept of a Complex System. Indeed, Simon (1991) wrote:

> *Roughly, by a complex system I mean one made up of a large number of parts that interact in a nonsimple way. In such systems, the whole is more than the sum of the parts [...] in the important pragmatic sense that, given the properties of the parts and the laws of their interaction, it is not a trivial matter to infer the properties of the whole.*

This tentative definition already points out several features that are commonly attributed to Complex Systems, namely: multiplicity of components, non-trivial interactions among them and *emergent* behavior. The latter consists in the fact that as the scale of a system changes (i.e. the number of elements involved increases) novel properties and phenomena appear. Hence, quantitative differences transform into qualitative ones, or as Anderson (1972) put it, *more is different*. Thus, we should not expect to be able to explain the collective behavior of complex systems by solely adding up scientific concepts and laws that have been derived through a reductive approach, that is, by reducing such systems to a microscopic description of their parts.

Truth be told, however, there is no agreed-on formal definition of Complex Systems or Complexity Science (Mitchell, 2009; Kwapień and Drożdż, 2012), neither there exists scientific consensus about what is the optimal way to quantitatively measure complexity (Lloyd, 2001). Since it is not our aim to enter in this sort of comparative discussions though, we will instead elaborate a bit further on the fundamental properties and phenomena that are generally identified in Complex Systems. In order to do so, we introduce the definition proposed by Mitchell (2009), which reads:

> *[...] I can propose a definition of the term complex system: a system in which large networks of components with no central control and simple rules of operation give rise to complex collective behavior, sophisticated information processing, and adaptation via learning or evolution.*

This interpretation reiterates several of the aforementioned properties, but it also introduces some novel ones. First, the capability of these systems to exchange information with its environment. Indeed, Siegenfeld and Bar-Yam argue that, in order to be efficient, a system should be at least as complex as its environment (Siegenfeld and Bar-Yam, 2019). Otherwise, it would not be able to process and respond accordingly to the wide range of varied

external stimuli it receives. In a sense, the second feature outlined by Mitchell is related to this variability: complex systems show generally an adaptive and evolving character. It must be said, nonetheless, that evolution is not always considered relevant, either because it does not play a major role in the dynamics, either because its effects are negligible at the time-scale at which we study the system (Mitchell, 2009).

Admittedly, the set of features that we have discussed so far are some of the more commonly referred, but there are many more that we are not considering which may be of special relevance in a particular domain. In fact, the interesting thing about all these general properties is that they are shared by a vast variety of systems of disparate natures: from insect colonies to the World Wide Web, from the human brain to the natural language (Mitchell, 2009; Kwapień and Drożdż, 2012). All these examples of Complex Systems exhibit, despite the differences in their microscopic description, similar complex behaviors at a macroscopic scale.

The question that naturally arises is, then, whether it is possible to describe such phenomena using a common language. The definition of Complex Systems suggested by Mitchell also provides a hint in this sense: she calls the web of interactions among constituents a *network*. Reviewing the network representation of Complex Systems and how it can contribute to our understanding of them is, actually, the subject of the next section.

1.2 Through the network glass, and what we found there

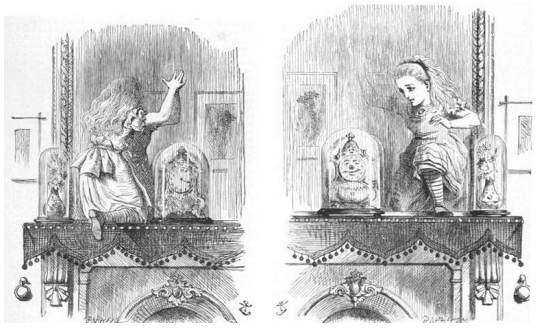

Alice through the looking glass, original illustration by John Tenniel (Carroll, 1872).

As discussed before, Anderson criticized the notion of a naive scientific constructivism according to which macroscopic behaviors may be explained by aggregatively applying microscopic laws. But what if, in order to explain macroscopic patterns, not only novel laws and concepts need to be introduced, but also some microscopic details can be safely neglected? This is, in very general terms, the idea in which the network language is grounded.

In short, a network is a set of components where some of them are pairwise connected. The components are typically referred to as the *nodes* or *vertexs*, while the connections are called the *links* or *edges*. This simple object can be used as an abstract representation of a strikingly vast range of systems. Indeed, the few examples of Complex Systems we mentioned before –the brain, human language or financial markets– can all be effectively represented by networks. In what follows, we will briefly discuss the history and consequences of viewing complex systems 'through the networks glass'.

From graphs to networks

The development of network science begins with the birth of graph theory, which is generally attributed to the mathematician Leonhard Euler (1707-1783) for his solution to the problem known as the *Seven Bridges of Königsberg* (Biggs et al., 1986). Königsberg (today Kaliningrad, Russia) was an old East Prussian city across which flew the river Pregel, spanned by a total of seven bridges (see Fig. 1.1). The mathematical riddle that occupied Euler may be formulated as succinctly as follows: is it possible to devise a walk through the city that

crosses each bridge once, and only once? Despite the simplicity of the question, answering it is not a trivial task. A brute force attempt would entail, in fact, trying every different possible path across the map, resulting in an overwhelming combinatorial effort.

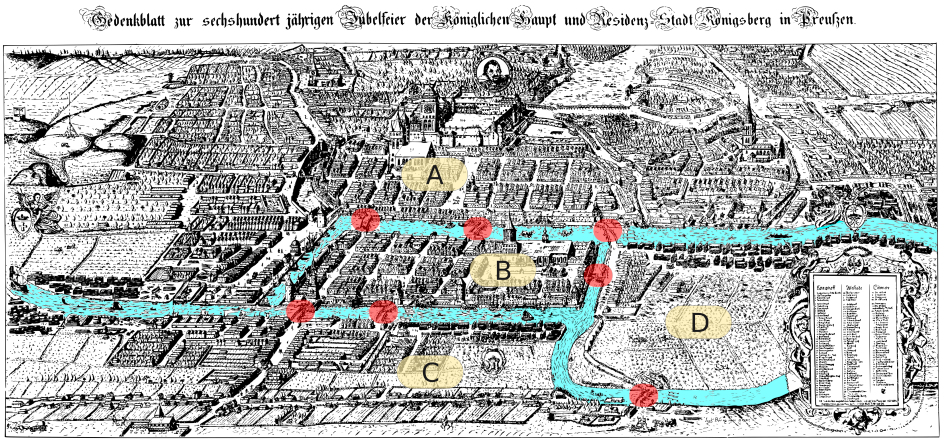

Figure 1.1: Map of Königsberg, adapted from Joachim Bering 1613's original engraving. The seven bridges are highlighted in red, the Pregel river is colored in blue and the island and the different mainland portions are named by capital letters.

Nonetheless, Euler showed that there is an alternative, less painful, approach. In an article published in 1736 (Euler, 1741), he proposed to look at this puzzle from an abstract perspective, overlooking the individual details of the bridges and portions of lands in order to work, instead, with an stylized portrayal. In such graph representation (see Fig. 1.2), land portions are depicted by nodes while the bridges are represented by links. Interestingly, the puzzle may be solved using one of the key properties of a node: its number of connections, or in the graph language, the *degree*. In order of the non-redundant walk to exist, it must be possible to arrive to a node through one link and leave it from a different one. In other words, all nodes must have an *even* degree. This necessary condition is, in fact, not verified in the Königsberg map. As can be seen in Fig. 1.2, all four nodes have an *odd* number of connections, thus implying that a walk that visits each link exactly once, actually called an *Eulerian path*, does not exist.

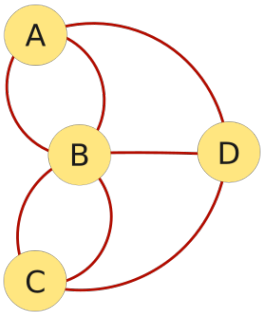

Figure 1.2: Graph representation of the Königsberg' bridges problem. Each node represents a portion of land, as named above, while the bridges are depicted by links.

After the death of Euler, the field of Graph Theory continued growing thanks to the contributions of several mathematicians, like Kirkman, Hamilton or Cayley (Harary, 1969). Although the bulk of production in the field was undoubtedly primary theoretical, it is still possible to find some instances of empirical inspiration, as illustrate the Kirchhoff's studies on electric networks, the work of Cayley on molecular graphs to represent chemical isomers or the developments of Sylvester and Brunel on graph chemistry (Harary, 1969). All these

examples may be regarded as predecessors of the explosion of network science that started at the beginning of the twentieth century within the field of Sociology, and then extended in the most recent decades to an astonishing range of areas as disparate as economics, neuroscience, epidemiology, genetics or ecology, to mention just a few of a much longer list. Indeed, the concept behind the term *network* differs from that of *graph* in that, in a strict sense, the graph refers to the pure mathematical object while the network is a representation (or model) of a real system (Barabási et al., 2016). As we will now see, this common network language has permitted unveiling some universal properties and behaviors of, otherwise, fairly distinct systems.

Looking at real systems

According to Bar-Yam (2000), macroscopic systems may be characterized by a 'complexity profile' that indicates how the amount of information needed to describe it changes at various levels of detail, that is, at different scales. He argues that, broadly speaking, three distinct types of systems may be distinguished: random, coherent and correlated. The random type requires the largest amount information at the smallest scale, but this quantity rapidly declines as the scale grows. On the other hand, describing coherent structures demands a constant and relatively small level of information across all scales, since the behavior of each of the parts is exactly known. Finally, correlated systems lie somewhere in between: they are neither entirely random, neither completely regular, but instead they exhibit significant emergent complexity at all scales.

Interestingly enough, this stylized classification recalls the seminal paper by Watts and Strogatz (1998) about the small world phenomenon, where they show how a complex network architecture arises in the middle-way among a random graph and a regular graph. In short, the small world structure implies high clustering together with a small characteristic path length. This combination leads to the peculiarity that any pair of nodes are typically separated by just a few steps, a situation that recalls the 'seven degrees of separation' hypothesis, according to which any pair of persons in the world are separated, in average, by only seven links. Such particular structure has singular effects on the dynamics, as accelerating the spread of dynamical processes like epidemics or rumors. Watts and Strogatz not only proposed a simple network model that reproduces this effect, but they also revealed that it naturally arises in a vast myriad of systems, from the power grid to the neuronal network of C. Elegans (Amaral et al., 2000).

The historical relevance of the Watts and Strogatz's article stems from the fact that it is one of the first evidences of how simple models of networks may fail to describe the complex architecture of real networks. Another example of a rather universal feature that has been extensively explored across disciplines is the family of scale-free networks, whose degree distribution follows a power law (Barabási and Albert, 1999). The consequent degree heterogeneity translates into a considerable diversity in the roles of the network's components: many nodes have few links, while a small portion of nodes hold many connections, acting as hubs. This special topology results into a 'robust yet fragile' effect on the dynamics, such that the network's connectivity is resilient against random failure but extremely vulnerable to targeted attacks (Albert et al., 2000). Once again, this particular structural property is exhibited by a wide variety of systems, although recently some debate took place questioning whether the power law degree distribution is indeed as ubiquitous as some claim, or instead empirical degree distributions are merely heavy-tailed (Broido and Clauset, 2019). In any case, high inhomogeneity in the degrees is, undoubtedly, a key and widely observed feature of real systems.

In the recent years, the study of real networks has certainly evolved well beyond these paradigmatic examples. However, reviewing it is fairly beyond the scope of this thesis. Instead, by shortly introducing the small world and scale free architectures, our aim is to provide a quick glimpse of how the network language can capture some complex features of real systems. It is as well an attempt of conveying the idea that, although the present work is mainly concerned with ecological communities, our conclusions will be sometimes translatable to other systems and disciplines, since the structural patterns and dynamical features we will study here are more than once shared by a broad range of different systems.

Basic quantities, types of networks and notation

Before continuing, we will introduce, for the sake of clarity, some of the basic concepts in network theory. We will also summarize, as concisely as possible, the main types of networks that can be distinguished, generally speaking, in terms of the link's properties on the one hand and the overall network structure on the other hand.

For a given network, the information of the connectivity among nodes is typically enclosed in an object called *adjacency matrix*. From now on, we will depict this quantity by the letter **A**. In the simplest case, it is defined as a square matrix that fulfills that:

$$A_{ij} = 1 \text{ if node } i \text{ and node } j \text{ share a link,} \tag{1.1}$$

$$A_{ij} = 0 \text{ otherwise.} \tag{1.2}$$

The second most basic quantity that we may define in a network is the number of interactions per node, so-called the *degree* of a node, commonly represented by the letter k. Using the adjacency matrix, the degree of a node i is straightforwardly calculated as:

$$k_i = \sum_j A_{ij}, \tag{1.3}$$

while the set composed by all network's degrees, $\{k_1, ..., k_i, ...\}$, is what we call the *degree sequence*. A closely related measure is the *degree distribution*, namely the probability distribution obtained by calculating the fraction of nodes p_k whose degree is equal to k. Despite their elementariness, the degree and the degree distribution can be highly informative quantities both at an individual and at a global level, and indeed along this thesis we will pay great attention to them and their relation with other structural patterns.

The picture we have drawn up to now corresponds to the most basic scenario, in which links only inform about *which* node is connected to which but not about *how* they are connected. At least two fundamental modifications exist that permit incorporating more complex properties to the link: *(i)* direction and *(ii)* weight. When introducing (i), the links are provided with a direction, which turns the symmetric interaction into an asymmetric one such that one node acts as the 'sender' and the other as the 'receiver'. By adding *(ii)*, the connections are pondered by their relative importance or strength in a gradual scale, in opposition to the binary case where interactions are merely existing (a one in the adjacency matrix) or not (a zero).

Introducing these two properties of links already brings up four possible types of networks: directed/undirected and binary/weighted. By moving into a more general perspective on the structural configuration of the whole network, we may distinguish the following classes of networks:

- **Bipartite networks**. A network is said to be bipartite if it can be partitioned into two separate sets (normally called *guilds)*, such that links exist only among the nodes of distinct guilds, but not among the members of the same guild (see Fig. 1.3). Moreover, the separation of nodes into two groups usually represents as well the existence of two kinds of nodes, distinguished by either their identity, function or role. A typical example of a bipartite network is that of films and actors: a link is placed between a movie and an actor if he or she appeared on it (Newman, 2010). Given that no intra-guilds connections exist, the adjacency matrix of bipartite networks –in the case of undirected and binary interactions– has the following particular form:

$$\mathbf{A} = \begin{pmatrix} 0 & \mathbf{B} \\ \mathbf{B}^\intercal & 0 \end{pmatrix}, \tag{1.4}$$

  where **B** is what we call the *bi-adjacency matrix*. In the most general case, **B** is a rectangular matrix of size $n \times m$, where n and m represent the number of nodes belonging to each guild. As before, $B_{kl} = 1$ when node k and node l share a link

and $B_{kl} = 0$ when they don't, with the peculiarity that the nodes k and l belong to different guilds. Networks which can not be partitioned into two guilds are called *monopartite*.

- **Multilayer networks.** The idea behind multilayer networks is to divide the network into various *layers*, in order to incorporate into a sole network different kinds of nodes and links. Each single layer, in isolation, may be regarded as a network where nodes are connected between them via intra-layer links, while the nodes in diverse layers are connected through inter-layer links (see Fig. 1.3 for an example). Such increase of complexity in the representation permits typifying different kinds of interactions and nodes through the obvious distinction among layers and inter/intra-layer links, as well as modeling how the perturbations and dynamics in one layer transfer to the others. A classic example of this class of networks is the network of urban transport, where each layer represents a different system of public transportation (i.e. bus, train, subway, etc) and the links represent the connections among lines (Gallotti and Barthelemy, 2015; Aleta et al., 2017). A particular case of multilayer networks are the so-called multiplex networks, characterized by the fact that the same set of nodes is represented in all the layers, yet the type of interactions represented in each layer differs.

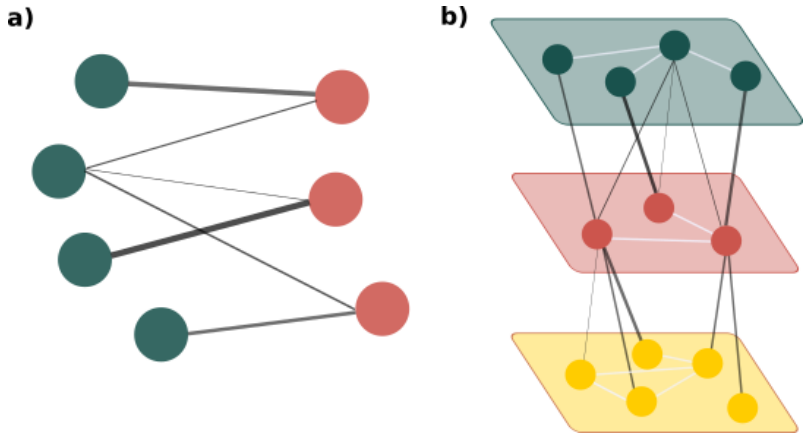

Figure 1.3: Illustration of different network types. In **a)**, bipartite network, where one guild is represented in teal and the other in red. In **b)**, multilayer network composed by three layers. The inter-layer links are drawn in grey, while the intra-layer links are depicted in white.

This classification provides a very basic sketch of how the network representation can be modified and adapted to address different problems. Having introduced already the basic notions of complex systems and how the language of networks may offer a suitable framework to study them, we will now turn our eyes into ecological systems, in order to understand how the concepts discussed up to now apply to natural ecosystems.

1.3 Complexity in the entangled bank

The notion of complexity we have discussed so far may be certainly recognized in a bundle of examples, including natural ecosystems. Indeed, Levin (1998) argues that ecosystems in particular and the biosphere in general conform paradigmatic cases of complex adaptive systems, primary characterized by its significant biodiversity and by being subject to evolutionary change. As such complex systems, they exhibit patterns of aggregation and hierarchical organization. One crucial question, as Levin remarks, is whether such complex structures are driven by self-organization processes, contingent environmental factors, or a path-dependent evolutionary history.

In any case, the idea that complexity pervades nature appeared considerably earlier, and we may trace it back to Darwin's famous picture of the *entangled bank*. Indeed, in the last paragraph of his seminal work *On the origin of the species*, Darwin wrote:

> *It is interesting to contemplate an entangled bank, clothed with many plants of many kinds, with birds singing on the bushes, with various insects flitting about, and with worms crawling through the damp earth, and to reflect that these elaborately constructed forms, so different from each other, and dependent on each other in so complex a manner, have all been produced by laws acting around us.*

Despite its poetic simplicity, this description points out several key aspects of ecosystems: the presence of an intrinsic heterogeneity of species and functions, interconnected among them as well as with the environment. Moreover, such organized variety is not the product of a global design by a chief controller, but the emergent result of what Darwin called the 'laws'. Although here Darwin surely refers to evolution, we may extend his view to include, in general, any set of rules which leads to complex behavior.

This intrinsically complex character of natural systems has led ecologist like Odum (1977) to advocate for a holistic approach to study them, which would complement the reductionist researching agenda on the components of ecosystems. With this perspective in mind, the aim of this subsection is to offer a short introduction to the development of ecology as a science and, especially, to review the recent incursion of complex networks as a language for modeling, explaining and predicting the complex structure and functioning of ecosystems.

A young science

The early historical development of ecology as a science is in fact a disputed subject, and, like in the best of royal intrigues, there is no agreed consensus on who is the 'father' of the discipline (McIntosh, 1986). Although Darwin (1809-1882) is often credited for unwillingly setting the basis of ecological theory, some historians of science consider its predecessor Humboldt (1769-1859) as the real founder, due to his pioneering works on biogeography. Others track the origin still earlier in time to White (1720-1793) and his observations of the natural life in Selborne, a fresh view that has often been categorized as 'Arcadian'.

Curiously enough, the term 'ecology' was not coined by any of these authors but by the zoologist and naturalist Haeckel (1834-1919), who introduced it to German from the ancient Greek root 'oikos' which means 'house', 'habitat'. In this sense, the term was introduced to name the study of the relation of animals –including humans– with the environment. Indeed, as anachronistic and incomplete as it might be, the definition given by Haeckel of the term ecology is still cited in may textbooks and offers a nice picture of what relations try to capture, in particular, ecological networks:

> *By ecology, we mean the whole science of the relations of the organism to the environment including, in the broad sense, all the "conditions of existence." These are partly organic, partly inorganic in nature; both, as we have shown, are of the greatest significance for the form of organisms, for they force them to become adapted. (...)*
>
> *As organic conditions of existence we consider the entire relations of the organism to all other organisms with which it comes into contact, and of which most contribute either to its advantage or its harm. Each organism has among the other organisms its friends and its enemies, those which favor its existence and those which harm it. (...)*

On the whole, as the historian of ecology McIntosh (1986) argues, this difficulty on re-constructing the origin of ecological theory is aggravated by the intrinsic problematics in defining the scope and limits of the very own discipline. To this, it should be added a long-standing human interest on the composition and functioning of natural systems, manifested through history in various manners since, at least, the Ancient Greece. The birth

of ecology at the interface between natural history, evolutionary theory, biogeography and population dynamics somewhat reflects this lasting plurality, and as McIntosh nicely puts it: "*[...] what I call 'retrospective' ecology encounters problems in identifying roots simply because ecology is, to continue the botanical metaphor, more a bush with multiple stems and a diffuse rootstock than a tree with a single, well-defied trunk and roots*".

In any case, as May et al. (2007) point out, during these blurry beginnings and the latter first developments, the contributions to the field of ecology remained mostly observational and descriptive, with punctual exceptions of mathematical incursion like the Lotka and Volterra work on population dynamics. It was not until the second half of the twentieth century that this qualitative perspective on theoretical ecology was re-framed into more analytical terms, mainly thanks to the works of Hutchinson (1903-1991) and MacArthur (1930-1972). On the methodological side, this shift was followed by major advances in the fields of non-linear dynamics and chaotic systems, which were often applied to –if not intertwined with– the study of population dynamics and pattern formation-. Finally, regarding field ecology, there was as well a transformation from an observational approach to nature into a more experimental attitude.

All this led to what McIntosh calls theoretical mathematical ecology or, as named in the sixties, the 'new ecology'. In addition to the incorporation of statistical, analytical and computational tools typically employed by physicists and mathematicians, Scoones (1999) argues that it also entailed a change in the conception of ecosystems. The prior image of ecosystems as well-balanced, static systems at equilibrium was challenged by the novel recognition that, in fact, they are stochastic by nature and often placed out of equilibrium (Scoones, 1999). Such recognition resulted in both an empirical and theoretical effort to understand the variability of ecosystems across scales, time and space; as well as a struggle to model and predict their stability. The translation of ecosystems into complex networks (Heleno et al., 2014), which will be the topic of the rest of this section, partly contributed to addressing these challenges.

To finish with this short glance at the historical development of ecology, it is worth noting that in the very recent years, especially with the appearance of the Internet and Big Data, the field has experienced an unprecedented rise of data gathering and sharing. Carmel et al. (2013) showed that the main research subjects have not, from a general perspective, notoriously changed during the last 30 years, except for a significant increase in the number of data-based studies. The complex networks approach, and in particular the research presented in this thesis, has probably much to do with this latter trend.

A question of scale

One of the key challenges of ecology is tackling the relevant scales to observe and describe ecosystems. Darwin himself noted, in his afore-mentioned description of the entangled bank, that species are 'elaborately constructed forms' in their own, which in turn compose a complex web of interactions. What level of description, then, is more appropriate to understand biodiversity: single-species, the community level, even the planetary scale? Levin (1992) argues that there is in fact not a single, naturally relevant scale, but rather a multiplicity of scales along which processes take place and across which information is transferred. At lower-order scales, the description of the systems gains in richness of details, due to a natural increase of the heterogeneity and variability. At higher-order scales, some of these details are blurred in favor of a simplified view, which unveils sometimes hidden patterns. The scientific question is, thus, how to balance this trade-off between accuracy and explanatory power in order to obtain some insights into the mechanisms that determine the ecosystem's features and functioning.

The complex networks framework addresses this very same challenge by modeling systems, as we have discussed before, as a stylized web of nodes and links. Applied to ecosystem, networks can depict a variety of components' and interactions' types, and the choice of one scale or another will determine this representation as well as the sort of scientific questions that may be asked. As Levin remarks, the multiplicity of scales does not only refer to space and time, but also to the organizational level (Levin, 1992). In this sense, when tackling for instance the problem of biodiversity, organisms may be grouped following different criteria,

i.e.: by species, by function, by importance in the ecosystem, by body mass, by diet, etc. This choice of scale can have a decisive role in the observation and measurement of ecosystem's patterns. For example, in their review of ecological networks, Ings et al. (2009) discuss how the aggregation of individuals in food webs into different classes affected the quantification of the predator-prey body mass ratio. In particular, grouping individuals into species (by their average traits) or trophic species (by their shared predators and preys) masked the allometric relations, that is, the feeding hierarchy of bigger-eats-smaller, which instead became evident when analyzing the interactions on an individual-individual basis.

All this serves as a no-free-lunch remainder that ecology is not exempt from the burden of choosing a non-biased observer, neither the construction of a network is always an obvious election. Along this text, we will mainly study ecological networks where nodes represent species and links depict the ecological interactions among them, and accordingly we will adhere to the simple definition of biodiversity as the total number of species. However, it is worthy to keep in mind that this representation is not unique or self-evident. Indeed, understanding on the one hand which patterns remain unchanged across scales -i.e., they exhibit scaling behavior-, and which instead appear or disappear at different levels of description is one of the key questions of theoretical ecology.

Ecological networks in a nutshell

Types and more types

Any attempt of reviewing the state of the art of ecological networks should probably begin with an explanation of the distinctions among its different types. Truth be told, however, there is not a unique way of classifying ecological networks, and the criterion eventually chosen will typically depend on which aspect of the network representation is emphasized. Therefore, we will start by summing up some of the most common classifications of ecological networks, while keeping in mind that these criteria are neither exhaustive nor mutually exclusive –since any network representation will certainly fit in different classes at the same time. In any case, ecological networks might be grouped, at least, by the following four criteria:

- **By perspective.** Ings et al. (2009) distinguish among two historical trends in the way of addressing the study of natural ecosystems: those who stress the importance of the biotic community, like Elton (1927), by prioritizing the study of the relation between the organisms; and those who place the emphasis on the whole ecosystem, like Odum (1977), by taking a holistic perspective that tackles the relations between organisms and the environment in a language of flows and transfers of biomass, nutrients, energy, etc. Since the focus of this thesis is on mutualistic interactions, in what follows we will pay special attention to the first approach. Nonetheless, it is important to remind that interactions within a community also imply transfers of energy and biomass, even if they are not always explicitly modeled (Ings et al., 2009).

- **By interaction type.** In this case, the network is primary distinguished by the ecological interaction(s) captured. Traditionally, three broad types are distinguished: *(i)* food-webs, characterized by depicting predator-prey relationships, *(ii)* mutualistic networks, where species are engaged in mutually beneficial interactions, and *(iii)* host-parasite networks, where one individual is parasitic to another. The first and third types tackle antagonistic relationships, characterized by being detrimental to at least one of the agents (i. e. the prey, the host), while in the second case the relationship retrieves a benefit to both of the participating species, often providing as well an ecosystem service (e.g. pollination). All in all, it is worthy to remark that the distinction per interaction type can be sometimes blurry, given that the beneficial or detrimental nature of an ecological interaction is not always self-evident and may gradually vary in time or across individuals. By way of example, not only food webs but also mutualistic and host-parasite networks involve, in fact, trophic exchanges: both the parasite and one of the mutualistic partners may get feed through their interaction (Ings et al., 2009).

In addition to the difficulty of classifying interaction types, a major problem is that communities are composed by an entwine of diverse ecological relationships, being the predominance of solely one interaction type an exception rather than the rule. We will come to this again later, since addressing this limitation poses both a theoretical and an experimental challenge.

- **By dimensionality.** As afore-mentioned, ecosystems exhibit significant heterogeneity in many aspects, including the temporal an spatial variability. Spatial networks attempt to incorporate spatial effects by embedding the web of interactions into a topological representation of space, or by weighting the interactions as a function of the distance among the partners. On the other hand, the representation of ecological systems as temporal networks aims at describing seasonal or daily turnover of species, as well as appearance or disappearance of links and changes in interaction strengths. Spatial networks have been often used to explore landscape biotic composition and robustness, particularly the patchiness of species' distribution (Bascompte and Jordano, 2013). Ecological temporal networks, instead, have been scarcely used up to date, despite a long-lasting ecological concern regarding the seasonal changes in species abundances and composition. All in all, during the recent years the field has witnessed an increase of interest in understanding and modeling the temporal dimension of ecological communities using networks. To finish, in opposition to spatially extended or temporal networks stand the so-called *aggregated* networks, where the temporal and spatial dimensions are simply dismissed by gathering together the observations made across a region or along a certain timespan. Despite their obvious limitations, aggregated networks have been extensively used as they already provide us with remarkable insight into the organization and functioning of natural ecosystems.

- **By network type.** To finish, a probably quite obvious way of classifying ecological networks is according to their overall structure, as defined previously in section 1.2. Again, this classification may be done generally speaking in: directed/undirected, weighted/binary, bipartite/monopartite and multilayer/monolayer networks. To start with, bipartite networks have been extensively used in ecology to represent interactions among two different groups, distinguished by species' type (e.g. plants and animals in mutualistic networks) or by role (e.g. hosts and parasites in antagonistic networks). Concerning multilayer networks, Pilosof et al. (2017) recently proposed them as a pertinent framework to refine the description of ecosystems, in particular by increasing the complexity of their representation. The authors explored a myriad of possible applications of the multilayer setting, including, for instance, the modeling of spatial and temporal networks, the codification in a single network of different kinds of ecological interactions, or, still, the representation of the relations among different levels of organization. Some of these applications have been already explored, as illustrated the work by Kéfi et al. (2016) in which they use a multiplex network to analyze the organization of a highly-resolved empirical network, for which both trophic and non-trophic interactions had been observed, or the work by Gracia-Lázaro et al. (2018) in which they convert a bipartite mutualistic network into a bilayer network by incorporating competitive interactions among members of the same guild.

This generic classification already illustrates the pluralism of approaches in the application of complex networks to ecology, yet it also brings up some of the current challenges in the field. Such challenges are mainly related with the limitations of the aggregated, single-interaction-type network representation, which has lead ecologists to call for an increase in the complexity of the description by considering, for example, the co-existence of various interactions types in a community or the presence of temporal and spatial heterogeneity (Ings et al., 2009; Heleno et al., 2014).

A brief historical account

From the historical point of view, the early development of ecological networks remained intimately linked to the study of food webs. According to Bersier (2007), the first documented

food web dates back to 1880 and is attributed to Lorenzo Camerano, who depicted in a diagram the trophic relation among several functional groups of animals and insects, with the ultimate aim of pondering the detrimental or beneficial effects of these various species to human crops. However, the influence of this work was seemingly scarce (Egerton, 2007), and it was not until the 1910's that the diagrammatic portrayal of food webs –precursory of the network representation– was used almost simultaneously by Pierce et al. (1912) (see Fig. 1.4) and Shelford (1913). From then on, the study of food webs in the form of diagrams gradually became a commonplace in community and ecosystem ecology, mainly thanks to Elton in the afore-called community approach, and by the hand of Lindeman and Odum in the ecosystem perspective (Bersier, 2007).

a) Food-web diagram

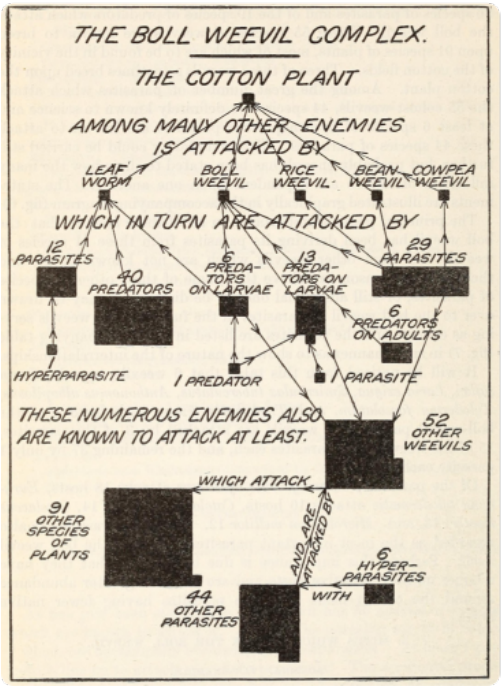

b) Host-parasite interactions

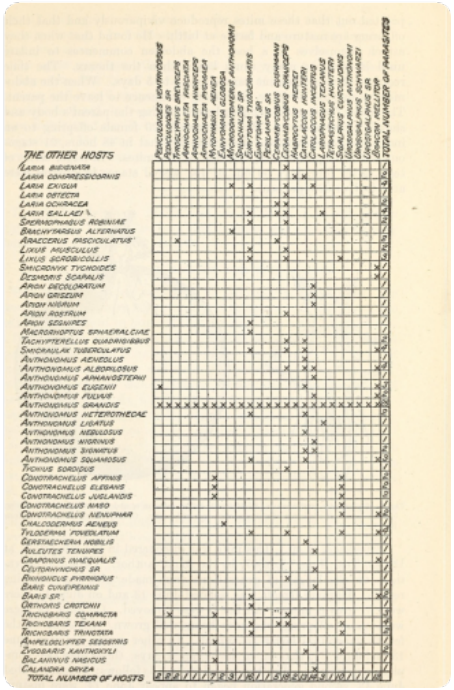

Figure 1.4: Original food web by Pierce et al. (1912) that focus on cotton pests, primary boll weevil, and their secondary and tertiary trophic relationships. In **a)**, the original diagram depicting the various predator-prey relationships. In detail, Pierce et al. reported the pests that affected the cotton plant, secondly its predators and parasites, and in a third place the predators and alternative hosts of the cotton plant's parasites. The result is a complex food-web which includes various trophic levels. Once again, the construction of this food web was driven by a practical interest on controlling pests that affected crops, by getting some insight on the natural predators of the pests that could be encouraged in order to eventually diminish the pest population. In **b)**, a graphic representation of the relationships between the parasites of boll weevil and their others hosts. This table can be seen as the bi-adjacency matrix of the host-parasite network -probably the first one to be documented, in historical terms-. Both images are extracted from the original book, which is now public domain.

These pioneering studies focused on empirical food webs, constructed by reporting the observed interactions among species or functional groups. The first model of ecological networks did not appear until 1972, and was proposed by May. The model consisted in a randomly assembled community where the interaction strengths were randomly assigned (May, 1972). This seminal work advanced the application of mathematical tools to analytically study the stability of ecosystems, and at the same time promoted the use of synthetic networks as models of real ecosystems.

The interest in food webs not only has been sustained in time since then, but has exhibited an astonishing outbreak from the 90's until now, probably in part related to the simultaneous

explosion of network science (Heleno et al., 2014). The history of mutualistic networks, last but not least, exhibits an important temporal delay with respect to that of food webs. Despite an intermittent interest on mutualistic interactions, especially pollination, since the middle of the 18th century (Bascompte and Jordano, 2013), the network language was not used to represent mutualistic communities until the very end of the last century with the seminal paper by Jordano (1987). Since the discovery of universal patterns no more than two decades ago (Bascompte et al., 2003), the field has witnessed a spectacular growth, and so has the study of host-parasite networks. Yet, this remarkable increase of popularity has not sufficed to emulate that of food webs (Ings et al., 2009).

May and beyond

The seminal work by May (1972) presented as well an interesting result: the stability analysis of the random adjacency matrix depicting the ecological network showed that, as the number of species or connectance in the system increases, stability is hindered. In particular, when exceeding a particular critical point the system moves from a dynamically stable state to an unstable one. Such prediction was thought-provoking all the more it contradicted prior ecological intuitions: real ecosystems are indeed large and complex, and previous field studies at the time pointed out that simple communities –like cultivated land– are more prone to respond with large fluctuations to perturbations than more complex ones (McCann, 2000).

This paradox initiated what is sometimes called the 'diversity-stability debate', that has led both theoreticians and field ecologists to design models and perform experiments that would confirm –or dismiss– the inverse relationship among diversity and stability (McCann, 2000; Montoya et al., 2006). Several attempts have been made up to nowadays to resolve this problem, from assuming that ecosystems may naturally work at an out-of-equilibrium regime (McCann, 2000), to considering that real systems' dynamics can be described by a selected set of parameters other than random (Montoya et al., 2006). The approach that interest us the most, however, is that which challenges May's assumption that ecosystems can be explained by a random network of interactions. Empirical observations, in fact, have revealed that the natural webs of interactions are anything but trivially organized. In this sense, the study of the structural properties of real ecological networks has often revealed the existence of common, regular features like the degree heterogeneity or the compartmentalization of links into modules. Such recognition has resulted in a research effort for understanding the effect of these complex architectures on ecosystem's functioning and robustness (Bascompte et al., 2003; Thébault and Fontaine, 2010). Indeed, this is yet another form of the classic question in network theory regarding the relation between structure and dynamics.

As we have reviewed here, the study of ecological networks is a rich and expanding field. Yet, in this thesis we are particularly interested in the modeling of mutualistic networks, hence in the next section we will focus on the story, organization and challenges behind mutually beneficial relationships in nature.

1.4 A network perspective on *friends will be friends*

Mutualistic relationships pervade nature, to the point that it has been claimed that every living organism is engaged in a mutualistic interaction at least once in a lifetime (Bronstein, 2001). This kind of ecological interactions, characterized by reporting an advantage to both agents, can occur among individuals of the same species -the so-called conspecific mutualism-, or among individuals of unrelated species –allospecific mutualism– which will be the one occupying us here. In both cases, the outcome of the interaction normally translates into an increase of the organisms' fitness, either because a resource is consumed or because the reproduction success of one or both of the agents is enhanced. In addition to positively affecting the fitness of individuals and, by extension, modulating the dynamics of the whole community, mutualistic interactions provide essential ecosystem functions worldwide, from pollination services to nitrogen fixation.

All in all, mutualism often does also involve a cost: the net outcome between the provided advantage and the damage is what eventually determines the sign and strength of the

interaction, resulting in a continuous, gradual range of possibilities from pure mutualism to antagonism (Bronstein, 2001). Therefore, variation in interaction strengths due to these differences in outcome are expected among individuals of the same or different species, as well as across time and space.

In any case, mutualistic interactions of different types and grades are ubiquitous in nature, including both marine and terrestrial habitats. In the case of terrestrial ecosystems, Bascompte et al. (2003) classify multispecies mutualism into five main groups, that we summarize below:

- **Pollination**. In this case, the pollination of flowering plants by animals, mainly insects, provides the pollinators with nutrients extracted from pollen and nectar, while pollinated plants enhance its reproductive success.
- **Seed-dispersal**. This kind of mutualism involves the dispersal of plants' seeds by animals, typically birds, that in turn get feed by consuming the plants' fruits.
- **Protective plant-ant interactions**. This represents a particular relationship between plants and ants, where plants provide ants with shelter, food and other resources in exchange of ants' defense from herbivorous animals or competitive plants.
- **Harvest mutualisms**. This group includes those mutualistic interactions in which individuals reciprocally obtain and provide nutrients and energy to each other. Widespread examples are: the gut flora and fauna in vertebrate species, rhizobia bacteria that fix nitrogen in some plants' roots, or lichens, which are birthed from the mutualistic association of a fungi species and an algae or a cyanobacteria.
- **Human crops and domestication**. Agriculture and animal husbandry can be also considered as two instances of human-plant and human-animal mutualistic interactions.

All these mutualistic interactions can be encoded in a network representation. In this section, the second-to-last of this introduction, we will briefly review the origin of mutualistic networks and its main structural characteristics, unveiled thanks to the observation of empirical communities.

From orchids to webs

As we discussed above, the interest on mutualistic networks arose not more than fifty years ago. Truth to be told, though, it was not the network translation of mutualistic communities alone which took long to appear, but the overall attention payed to mutualistic interactions had been rather scant until recently. Indeed, Bascompte and Jordano (2013) argue that for a long time mutualistic interactions remained perceived more as a fascinating curiosity than as a relevant component of ecological communities. Instead, the emphasis was placed on antagonistic relations, which until the 70's were believed to predominantly shape and drive the ecosystem's dynamics.

This early notion of mutualism under the form of peculiar, singular interactions was basically influenced by early observational studies, which mostly focused on highly specialized mutualistic interactions. A renowned example is that of the astounding morphological matching between the Darwin's orchid and its pollinator, which was unknown until Darwin (1877) predicted its existence and it was eventually discovered in Madagascar forty years later (see Fig. 1.5 for a more detailed explanation). This sort of tightly coevolved mutualistic relationships offered beautiful examples of extreme adaptive specialization, but also lead to overemphasizing the importance of specialist-to-specialist interactions that, at the level of the community, are in fact rare (Waser et al., 1996).

It was in the decade of the seventies that the focus on pairwise interactions was shifted towards a community-wide perspective (Bascompte and Jordano, 2013). This viewpoint change was spurred by the recognition that generalism is an ubiquitous feature of mutualistic communities, which moreover plays an equally important role to that of specialized interactions (Waser et al., 1996), in both ecological and evolutionary terms. Here

a) Darwin's orchid and moth **b)** Hawk moth

Figure 1.5: **a)** On the left, illustration of *Angraecum sesquipedale*, also known as Darwin's orchid, and its hypothetical moth pollinator. The orchid has an extremely long nectar spur, which lead Darwin to hypothesize the existence of an unknown moth, endowed with an equally long proboscis (the "tongue" of the moths) which would allow it to pollinate the flower (Darwin, 1877). The moth was discovered in 1903, 21 years after Darwin's death, and named Hawk Moth or *Xanthopan morganii praedicta* which in latin means 'predicted moth' (Arditti et al., 2012). The drawing is extracted by the essay *Creation by Law* by Wallace (1867), who supported Darwin's idea and imagined the form of the hypothetical pollinator. **b)** On the right, actual photography of the *Xanthopan morgani praedicta* kept at the Natural History Museum of London.

again, we find an example of how a reductive approach, consisting in disentangling the web of interactions into its basic components -the pairwise interactions-, is insufficient to account for the complexity of the whole ecosystem. The introduction of mutualistic networks as models of mutualistic webs in the 90's aimed at tackling the challenge of considering the entire community, by exploiting this novel framework and its powerful set of analytical and numerical tools.

The structure of mutualistic networks

As aforementioned, mutualistic networks are commonly represented in a bipartite embedding where each guild depicts a different mutualistic partner or group of species, like in the example in Fig. 1.6 of a plant-pollinator community. Despite the particular characteristics that each mutualistic system may have, some general features have been identified in terms of structure. Heterogeneity, modularity, nestedness or asymmetric interactions are some of these topological regularities, to which we will now pay some attention.

Although we will describe each of these structural features separately, it is worth noting that most of them co-occur simultaneously in the network, and what is more, they are sometimes not independent of one another. Indeed, a great bulk of work has been devoted to explore the interrelations between structural properties, and in this thesis we will as well address this question for the particular case of nested patterns.

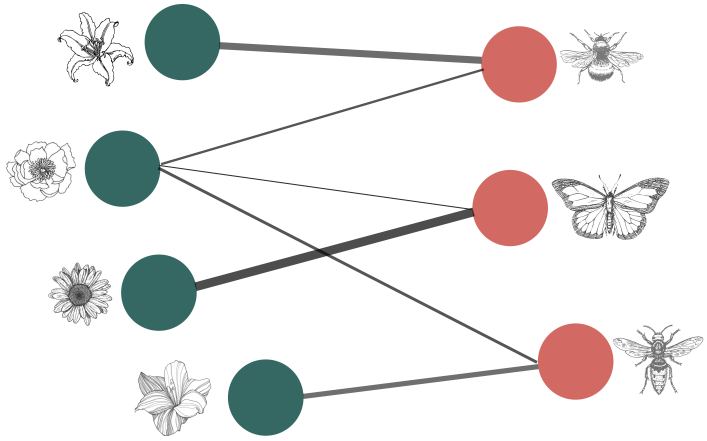

Figure 1.6: Example of a mutualistic networks composed by plants and their pollinators, represented in a bipartite setting. The links among the two guilds can be weighted, which we represent here by varying the thickness of the line.

Degree heterogeneity

Along with the recognition that mutualism can be highly generalized (Waser et al., 1996) came the acknowledgement that mutualistic networks are significantly heterogeneous, in the sense that in the same community coexist species that hold many contacts –the generalists, which consequently have a large degree– with others that interact with just a small subset of the possible mutualistic partners -the so-called specialists, that have a small degree-. Accordingly, special efforts have been dedicated to characterize the functional form of the degree distributions of both guilds. Indeed, it has been claimed that for an important majority of real systems, their degree distribution can be fitted by a truncated power-law (Jordano et al., 2003). Nevertheless, the significance of such fit is greatly hindered by the fact that, since mutualistic networks are in general relatively small, their empirical degree distributions spans just a few orders of magnitude.

Independently of what the best fitting function might be, what seems clear is that the pattern of connectivity is significantly heterogeneous, similarly to what happens in many real systems (see Section 1.2). Nonetheless, here the tail of the degree distributions departs from that of a scale-free network. This implies that several species have a few interactions, while just a few species hold many interactions but not as many as could be, a priori, possible. This limitation in the degree of the most connected species has been linked to the existence of forbidden links due to ecological barriers determined, for instance, by morphological, phenological or phenotypical traits (Bascompte and Jordano, 2013).

Besides degree distributions, if the network is weighted one can study the distribution of strengths. In the context of mutualistic networks, the weight is typically associated to the frequency or intensity of the ecological interaction, although this quantity may be difficult to measure and sometimes it is instead estimated from the relative species' abundances. In any case, the strength is the weighted analogue to the degree, which provides information about the connectivity at the species level. The strength's distributions of mutualistic networks have been claimed to be even more heterogeneous than the degree distribution (Bascompte and Jordano, 2013), suggesting that the heterogeneity in the connectivity emerges not only in a qualitative representation of who interacts with whom, but also when we include quantitative information on how much they interact.

Asymmetric interactions

The study of quantitative mutualistic networks revealed that the distribution of interaction weights is significantly right-skewed, reflecting a majority of weak mutualistic connections against just a few strong interactions (Bascompte et al., 2006). Moreover, the intensity of

a mutualistic interaction is not necessarily symmetric. This means that, for instance, in a plant-pollinator community the dependency of a flower on a plant is not, forcibly, the same as that of the plant on the flower.

Indeed, the study of empirical systems has shown that this strength heterogeneity is patterned in a particular way: the few intense interactions present in the network are, typically, highly asymmetrical. In a plant-pollinator system, this translates into the fact that if a plant relies significantly on the pollination services of a given animal, this pollinator depends weakly on the resources of the plant (Bascompte et al., 2006). Such asymmetry may play an important role in sustaining biodiversity by preventing positive feedback loops, that can act as amplifiers of possible disturbances in the population.

Small world

Moving from a species-level description of the connectivity to a community-wide perspective, mutualistic networks exhibit several regularities. One of them is a widespread phenomenon across real systems, the afore-mentioned 'small world' property (see section 1.2 for a more detailed discussion of its ubiquity in empirical complex networks).

Olesen et al. (2006) studied its prevalence in mutualistic communities by converting the bipartite network of mutualistic interactions into two one-mode networks of shared neighbors, one per guild, such that species of the same guild are connected whenever they share a common mutualistic partner. The analysis of these projected networks revealed that the majority of species are placed just a few links away from each other, with an average path length typically smaller than two together with a relatively large clustering coefficient. Such combination implies that perturbations may spread quickly along the community, or as Montoya et al. (2006) put it: "*Every species is closely linked to every other, so –metaphorically– when a tree falls in a rainforest, every species in that species-rich, complex system would seem to 'hear' that event quickly*". This has contributed to the paradoxical notion that natural mutualistic communities may be fragile, leading to the proposal of the presence of alternative structural properties or mechanisms that would enhance the system's resilience, like the afore-mentioned interaction asymmetry.

Modularity

Another way of inspecting the closeness between species is looking at the presence of modules, that is, groups or clusters of species characterized by being tightly connected, in the sense that connections among the members of the same module are significantly more frequent than links among different modules. The existence of such modules has been related to the action of environmental, ecological and evolutionary forces, in particular since modules tend to group together species with convergent morphological traits (Olesen et al., 2007; Dupont and Olesen, 2009). Accordingly, modules have been advocated to be the building blocks of mutualistic networks, revealing habitat compartmentalization at the big scale and coevolutionary pressures at a closer look.

Nestedness

Besides the general features mentioned so far, the most notorious and widespread property of mutualistic networks is probably nestedness. This community-wide pattern entails that the interactions of a given species result to be a subset of the interactions of more generalized –higher degree– species. This special organization of the interactions, which has been found to be ubiquitous across natural ecosystems regardless of their differences in habitat, climate or species composition (Bascompte et al., 2003), has fueled in the recent years an important number of works focusing on its causes and consequences. In particular, special efforts have been made to explain its implications for the assembly and stability of ecosystems.

Anyway, given that the study of nested patterns is the topic of the first part of this thesis, we will not elaborate further on it now. Instead, we will devote the entire first chapter of this thesis to discuss, in greater detail, its definition, origin, dynamical implications and several ways of measuring it.

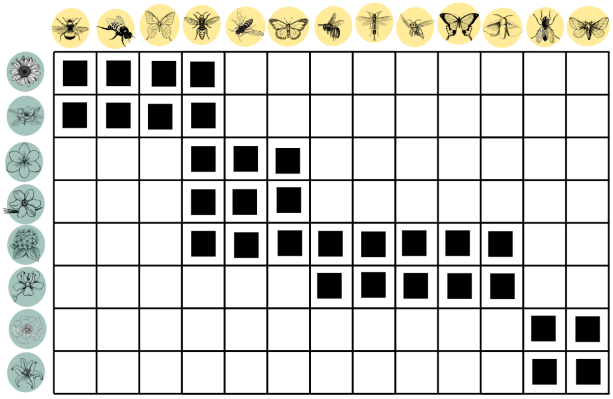

Figure 1.7: Example of a perfectly modular network of plants and pollinators, divided into four modules.

Mutualism outside ecology

Although the study of mutualism has mainly concerned ecologists, it has also played a role in the study of human organizations ever since the publication of the book 'Mutual aid' by Kropotkin et al. (1902), which explored the prevalence of mutualistic relations in society as well as the natural world. By challenging the idea that competition dominates nature, Kropotkin revalued the importance of cooperation and mutualistic interactions as crucial factors for the survival of human and animal communities. Curiously enough, it has been argued that its association with anarchist communism may have contributed to the general dismissal of mutualistic forces, considered almost as incidental until the 70's (Bascompte and Jordano, 2013).

Outside ecology, mutualism takes the form of win-win relationships among two entities or agents, whose identities span diverse contexts and levels of organization, from individuals to entire countries. In the economic context, some examples of mutualistic webs are manufacturer-contractor networks (Saavedra et al., 2009) or seller-buyers networks (Hernández et al., 2018). In sociology, communication networks made of individual users and memes (e.g. hashtags in Twitter) have been as well studied through the lens of mutualism (Borge-Holthoefer et al., 2017).

In the recent years, there has been an increasing interest in exploring whether the structural features and dynamical properties of ecological mutualistic communities hold for mutualistic networks outside ecology (Burgos et al., 2008; Hernández et al., 2018; Straka et al., 2018; Mariani et al., 2019). In the light of this, while the focus on this thesis will be mainly on ecological systems, the conclusions we may attain are expected to often have an implication, as well, for mutualistic networks of economical, sociological or technological systems.

1.5 Where we are now, and where we aim to go

In spite of its youth, the field of ecological networks –and in particular that of mutualistic networks– has witnessed an impressive growth during the last decades (Heleno et al., 2014), in parallel with the expansion of network science and, certainly, spurred by an accompanying increase of data gathering and sharing (as illustrates for instance, the Web of Life project [1]). Nevertheless, several questions remain still unresolved (Ings et al., 2009; Heleno et al., 2014; Pilosof et al., 2017) calling for a combination of conceptual, methodological and experimental endeavors. Such challenges can be framed along the lines of the aforementioned trade-off between explanatory power and simplification, a tension which appears intrinsically attached to the construction of a network.

[1] Database of ecological networks, especially mutualistic, available at: http://www.web-of-life.es/

On the one hand, ecologists have been advocating for ameliorating the realism of mutualistic networks by adding further information about their temporal and spatial variation, as well as considering pairwise interactions' specificities or the existence of differential traits at the level of the species or even the individuals (Ings et al., 2009; Heleno et al., 2014). This could lead to a more detailed representation of the natural complexity, at the cost of increasing the heterogeneity of both nodes and links. All in all, exploring the implications of changing the level of organization is a necessary step in order to dismiss the presence of an observer's bias, which could result in artifacts like those regarding the measure of the allometric relation in foodwebs (Ings et al., 2009). The aforementioned transformation of binary, qualitative networks into weighted, spatially extended, or temporal networks, are all different ways of refining the realism of the network, by paying the price, however, of potentially complicating the models.

On the other hand, the observation and study of patterns even in the most simplified networks has posed several questions, some of which are still open. As Levin (1992) recalled, the detection of patterns is interesting to the extent to which it reflects hidden mechanisms, and indeed the implications of structural properties of mutualistic networks, like nestedness, are controversial up to date. Furthermore, a crucial aspect of the interplay between pattern and scale is exploring whether a given feature or phenomena is invariant across scales. Otherwise, the natural question that arises is how information is transferred and transformed from one level of description to another, in order to lead to the emergence –or disappearance– of the pattern. In this sense, defining the structural determinants of mutualistic networks is a long-standing problem in ecology, that concerns community-wide properties –e.g. nested patterns– as much as species-centered features –like the degree.

The challenges we have mentioned so far call for both theoretical and experimental advances. Theoretical, since appropriate conceptual and methodological frameworks are to be developed in order to refine the network representation of ecosystems, as well as to characterize patterns across scales and investigate the dependency between structural features at different levels. Experimental, on the other side, because to be able to model details one needs rich and reliable data, that should moreover take into account spatial and temporal variability. This requires an increase of sampling effort in quality and quantity terms alike, together with the elaboration of protocols to measure –and possibly enhance– the degree of completeness of empirical networks (Ings et al., 2009). All this implies that future advances in ecological networks are not only an interdisciplinary endeavor, concerning together pure ecologists, mathematicians or physicists, but also a multi-approach task, since theoretical advances are intimately conditioned by field work –and vice versa.

In this thesis, we will study mutualistic networks from a theoretical viewpoint, considering in detail two main topics: *(i)* the characterization and emergence of nestedness and *(ii)* the introduction of temporal information on plant-pollinator networks. This partitioned research reflects the perennial tension between simplification and realism in models that we have just discussed here. Indeed, while in the first part we will focus on explaining nested patterns that appear in the most basic representation of mutualistic networks –binary, aggregated and monolayer–, in the second part we will work towards a more realistic characterization of communities, by modeling their temporal dimension through empirical data on the periods of activity of plants and pollinators, the so-called *phenology*. Before definitely beginning with the main body of this thesis, let us discuss a bit further how these two subjects will be addressed.

Nested patterns and the three witches

Why is it relevant to look for patterns in ecology? Beyond the search of natural order, regularities can reflect dynamical process of different kind, concerning either the past, the present or the future of ecosystems. In a symbolic way, this recalls the figure of the three witches. In the first part of Shakespeare's famous play *Macbeth*, three witches encounter the main character Macbeth and, when greeting him, each hails him differently: one of them by his past rank ('thane of Glamis'), the second by his present position ('thane of Cawdor') and the third witch by his future title ('the future king'). This has lead to the interpretation that, while the three witches held Macbeth's fate in their hands, each of them

represents a different temporal moment, respectively the present, the future and the past. In a metaphorical sense, an analogue triad can be defined in the study of the implications of ecological patterns and what information they convey: about the ecosystem's past, in particular its assembly and eco-evolutionary history; about the present state, for instance how species coexist and function together, leading to the observed biodiversity; and of course about the possible future, in the sense of how the ecosystem would react against external perturbations. All three aspects of the triad are equally important to the understanding of the fate of mutualism.

Figure 1.8: The three witches of the Shakespeare's play *Macbeth*, also called the three weird sisters. Engraving by Lorsay, that appeared in 'Magasin Pittoresque' in 1863, after a 1782 drawing by Fuseli.

Nevertheless, not every observed pattern is equally informative, as neither every observed regularity is forcibly significant. In the first part of this thesis, we will address the question of the significance of nested patterns in mutualistic networks, or in other words, how lower-order structural properties of the network can determine the global nestedness. In particular, we will start with an introductory chapter reviewing the definition and implications of nestedness, as well as the main metrics that have been developed to quantify it. In the subsequent chapter we will use null models to try to resolve the aforementioned question of the origin and significance of nestedness. Finally, in the third chapter of this first part, we will use the developed methods to investigate the performance of a varied set of nestedness metrics.

The *phenos* of mutualism

Phenology is the science that studies the timing of biological cycles along the life of organisms, from seasonal patterns to circadian rhythms. Returning, as we started this introductory chapter, to etymology, the world *phenology* is composed by the prefix *phenos*, that comes from the Ancient Greek 'phaino' which means 'to appear', and the conventional suffix *ology*, from the Greek 'logia' that means 'the study of'. Phenology, therefore, would translate as 'the study of appearance'.

Given that an important part of ecological mutualisms takes the form of plant-animal interactions, they can be greatly conditioned by the seasonal cycles of the partners. In particular, plants tend to exhibit marked seasonal life events, like leaf-producing, fruiting or flowering. Although such effects may change considerably among habitats and climates, in general they are not negligible. In the latter years, the interest in modeling the phenology

of mutualism has been spurred by the fact that climate change may severely affect species' phenology, leading to a potential disrupt of plant-pollinator or plant-disperser systems.

In this thesis, we will approach this topic in the second part of the manuscript. The first chapter will be devoted to the characterization of two empirical datasets and the proposal of some models to generate synthetic configurations of phenology under different constraints. Subsequently, we will address the question of the dynamical consequences of introducing phenology by examining a model that incorporates both mutualism and competition for resources.

PART I

Revisiting Nested Patterns

CHAPTER 2

The three W's and one H of nested patterns

Almost two decades ago, a seminal work by Bascompte et al. (2003) revealed that nested patterns are widespread in mutualistic communities. Indeed, mutualistic networks gathered across the globe appear to be regularly nested, despite differences in ecosystem's geographical location, climate, or species composition. The discovery of such ubiquity awoke considerable interest within and beyond the ecological community and, as a result, many works have been devoted since then to understanding the extension, impact and origin of nested patterns.

In this chapter, we summarize the main conclusions of these efforts. We start providing a exact definition of nestedness (the 'what'), and continue with the real systems where it has been detected (the 'where'). Next, we briefly review some of the hypothesis that have been handled as possible explanations of its origin, as well as its dynamical consequences (the 'why'). Finally, we introduce the main metrics that have been proposed to measure and quantify nested patterns (the 'how').

2.1 The what

Nestedness is a global property of networks that addresses the overlap between interactions, in particular to what extent the mutualistic partners of a given species are shared by its more generalized counterparts. Strictly speaking, a *perfectly nested* structure is defined by the fact that the interactions of a given node are invariably a subset of the interactions of all nodes with larger degree (see Fig. 2.1). That is, if $\mathbf{B}$ is the biadjacency matrix of a $N_R \times N_C$ bipartite network, the system will be perfectly nested only if the following conditions are both true:

$$\mathbf{B}_{i,j} = 1 \text{ and } \mathbf{B}_{i,k} = 1 \iff \text{given a pair } j \text{ and } k \text{ such that } \sum_{i}^{N_R} \mathbf{B}_{i,j} \leq \sum_{i}^{N_R} \mathbf{B}_{i,k}\,, \quad \forall i\,; \tag{2.1}$$

$$\mathbf{B}_{i,j} = 1 \text{ and } \mathbf{B}_{l,j} = 1 \iff \text{given a pair } i \text{ and } l \text{ such that } \sum_{j}^{N_C} \mathbf{B}_{i,j} \leq \sum_{j}^{N_C} \mathbf{B}_{l,j}\,, \quad \forall j\,; \tag{2.2}$$

where N_R and N_C are, respectively, the number of rows and columns of the biadjacency matrix $\mathbf{B}$.

The conditions above translate into the fact that specialist species, that is, species with few interactions and thus a small degree, are seldom interacting with other specialists. Instead, they tend to exhibit degree disassortativity, appearing attached to generalist species. Generalists, in turn, have a large degree and hence are connected to a variety of neighbors, including other generalists. This confers to nested biadjacency matrices its distinctive triangular shape, composed by a robust core of connections among generalists to which specialist cling (see Fig. 2.1).

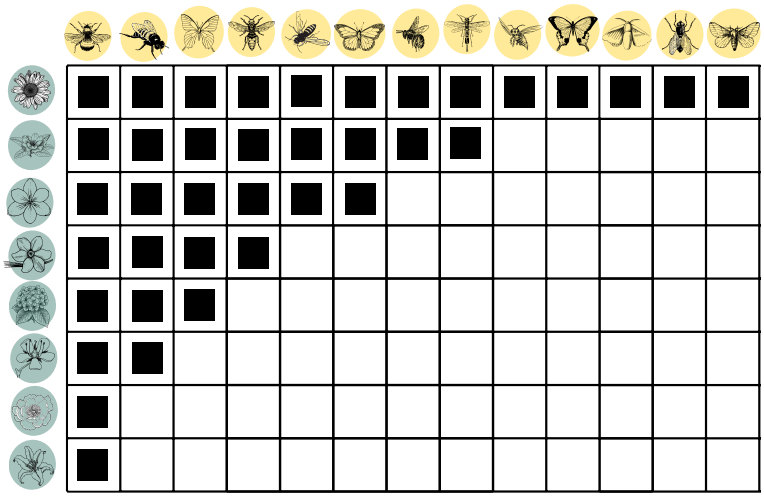

Figure 2.1: Example of a perfectly nested biadjacency matrix, for a bipartite plant-pollinator network. Each node represents a different species and black boxes represent a mutualistic interaction between a plant and a pollinator. It can be observed that the interactions of any species form part of a subset of the interactions of all species with larger degree.

As we will discuss below in the 'where' section, real networks are rarely perfectly nested. However, the study of hypothetical, maximally nested scenarios is necessary in order to define the pattern, as well as to set a benchmark against which to compare imperfect systems. Interestingly enough, if we take a perfectly nested network and order the nodes of one guild by decreasing (or increasing) degree, the nodes of the other guild appear automatically ordered in the same way. Additionally, the corresponding bi-adjacency matrix would have all of its non-zero elements below an ideal curve called 'isocline of perfect nestedness' (IPN). This curve was first proposed by Atmar and Patterson (1993), and later on refined by Rodríguez-Gironés and Santamaría (2006). Moreover, Medan et al. (2007) examined still a third definition of the IPN, and proved that this curve, defined in a continuous approximation of the biadjacency matrix, is closely related to the cumulative degree distribution of both guilds. As we will review in the 'how' section, the interest in properly characterizing the IPN is not merely theoretical but has a pragmatic justification, since several metrics aimed at quantifying nestedness rely in its calculation.

A related notion to the IPN is the *maximally packed configuration*. Given a particular network, this corresponds to the arrangement of the matrix which better reveals and maximizes its nestedness. However, there is not a unique choice of what particular quantity should be optimized, and accordingly various methods to pack the matrix can be found in the literature (Rodríguez-Gironés and Santamaría, 2006; Domínguez-García and Muñoz, 2015; Lin et al., 2018). Indeed, while the strict definition of nestedness explained above calls for an ordering by degree, it has been shown that this does not necessarily produce the best 'packing' of the matrix -in the sense of clearly separating the regions with and without interactions of the biadjacency matrix- neither it does maximize the nestedness as measured by certain metrics (Domínguez-García and Muñoz, 2015). Given the role that this choice of packing may have when ranking the relative importance of nodes for the global nestedness, we will turn later on to this topic both when reviewing the nestedness metrics and in the next chapter.

2.2 The where

Although here we will pay special attention to nested patterns in the context of mutualistic networks, as a matter of fact the concept of nestedness was first introduced among ecologists in the field of biogeography. According to Ulrich et al. (2009), since the decade of the

thirties several works independently proposed this property in order to describe the spatial distribution of species in fragmented habitats, like islands and compartmentalized landscapes. Nonetheless, the concept did not become genuinely popular until the publication of the seminal paper by Patterson and Atmar (1986), which examined the geographical composition of mammal fauna in different locations, unveiling a regular nested structure.

In these early biogeographical studies, the distribution of species is encoded by a bipartite network where one guild represents the species and the other the geographical sites (i.e. islands or habitat compartments). Therefore, if a species is observed in a given site, the corresponding element of the biadjacency matrix is non-zero, particularly a one -in the binary representation- or the value of its relative abundance -in the weighted case-. In this context, a nested pattern implies that species present in smaller communities or patches are also part of larger sites. Various ecological hypothesis have been handled to explain such structure, concerning the processes of dispersion and extinction of species across the sites.

What interests us the more here is, however, the extension of this concept to the study of mutualistic networks. As aforementioned, Bascompte et al. (2003) first showed that this pattern systematically appears in plant-animal mutualistic communities, including both systems of plant-pollinators and plant-dispersers, and their findings have been ratified later for other mutualistic systems (Guimaraes Jr et al., 2006; Olesen et al., 2007). Beyond mutualism, whether ecological networks in general are nested is a debated subject. On the one hand, host-parasite networks are an example of antagonistic systems that have been shown to be naturally nested (Vázquez et al., 2005; Poulin, 2010). On the other hand, Bascompte et al. (2003) and Thébault and Fontaine (2010) claimed that real food webs are significantly less nested than mutualistic networks, although Kondoh et al. (2010) rebutted the results of the former by arguing they were biased due to the small size of the systems considered. Instead, by analyzing an alternative dataset of real food webs, Kondoh et al. (2010) found that their degree of nestedness was not significantly different to that of empirical mutualistic communities.

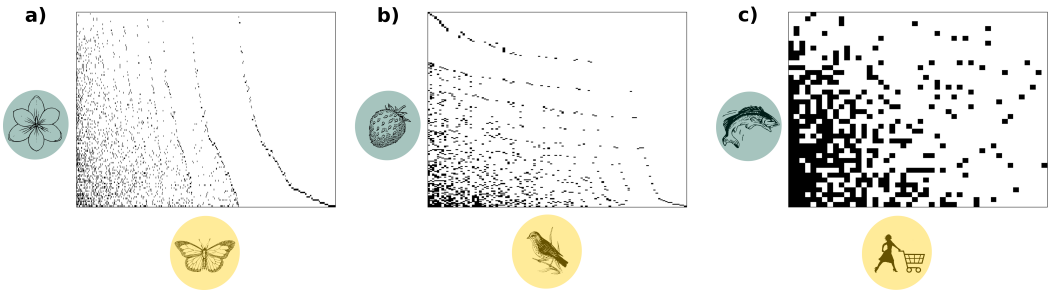

Figure 2.2: Examples of three different kinds of real nested networks, all of them depicting mutualistic communities. Species are ordered by degree. In **a)**, plant-pollinator network of a phrygana ecosystem, which is a characteristic Mediterranean scrubland, gathered in Daphní -near Athens, Greece- by Petanidou (1991). In **b)**, seed-disperser network by Silva (2002), observed in the natural park of Intervales, near Sao Paulo, Brazil. In **c)**, seller-buyer network of the Boulogne-sur-Mer fish market, in France, studied by Hernández et al. (2018).

In fact, the detection of nestedness in mutualistic and non-mutualistic systems is jumbled by its coexistence with other structural patterns, particularly modularity (Fortuna et al., 2010). Modularity (see its definition in section 1.4 of the first chapter) is theoretically expected to be more common in antagonistic networks -driven by competition- than in mutualistic ones -dominated by cooperation- (Thébault and Fontaine, 2010). Such theoretical divergence, together with the fact that the characterization of real food webs seems to confirm these dynamical predictions (Prado and Lewinsohn, 2004; Thébault and Fontaine, 2010), have traditionally promoted the analysis of each pattern separately. All in all, the evidence that nestedness and modularity do actually coexist in many real systems (Lewinsohn et al., 2006; Olesen et al., 2007; Fortuna et al., 2010), has recently motivated the refinement of appropriate methodology to asses them conjointly (Solé-Ribalta et al., 2018).

Finally, in the latter years the study of nested patterns has permeated other areas of complex systems, as varied as economy, sociology or anthropology. Indeed, nestedness has been detected as well in trading networks between countries (De Benedictis and Tajoli, 2011; König et al., 2014) and individuals (Hernández et al., 2018), in manufacturer-contractor relationships (Saavedra et al., 2009), communication systems (Borge-Holthoefer et al., 2017), cultural assemblages (Kamilar and Atkinson, 2014) and even scientific production (Cimini et al., 2014). Although along this text we will focus on the case of ecological mutualistic systems, we will surely return to some of these non-ecological examples which illustrate the ubiquity and generality of nested patterns.

2.3 The why

As we discussed in the introduction, the increase of attention in nestedness is better explained by the interest in its causes and consequences rather than in the pattern itself. Accordingly, different hypothesis describing the origin of nested patterns have been proposed over the recent years (Vázquez et al., 2009; Ulrich et al., 2009). In general terms, we can classify these explanations into two main groups: first, those that emphasize the role of ecological factors, like species' abundances, the matching of traits or the spatio-temporal distribution of species; second, those that explore the evolutionary processes that have led to the observed patterns, like its natural selection, its emergence as a byproduct of assembly processes or its relation to the phylogeny of species. Given the existence of an important interplay between the results we will be presenting in the next chapter and the different justifications of the origin of nestedness, we now briefly discuss the most relevant of such explanations. Of course, although the separation between ecological and evolutionary factors may be an illustrative simplification, both causes are often not independent from one another.

Regarding the role of ecological factors, one of the first hypothesis that was explored as a possible justification for the origin of nested patterns is related to species' abundance. In particular, several studies have examined the role of the relative abundance of species as a predictor of the probability that two species interact. This assumption, sometimes called the *passive sampling* hypothesis (Ulrich et al., 2009) or *neutrality* (Krishna et al., 2008; Vázquez et al., 2009), postulates that more abundant species are prone to have more contacts, in a rich-get-richer fashion determined by the number of individuals of each kind. In other words, as a result of the fact that some species are more frequent in the system, they are 'easier to find' by mere statistical sampling and gather a larger number of interactions. However, this process alone has been shown to be insufficient to account for the macroscopic structure of real mutualistic networks (Vázquez et al., 2007; Krishna et al., 2008). Instead, including additional information regarding the phenology of species or their spatial overlap allows predicting the macroscopic structural properties, but not the frequency of occurrence of pairwise interactions (Vázquez et al., 2009; Olito and Fox, 2015). Altogether, these works suggest that abundance might be an important factor driving the structure of mutualistic networks, but certainly not the only one.

The neutrality hypothesis is often confronted with the existence of the so-called *forbidden links* (Jordano et al., 2003). This concept refers to the existence of biological constraints that hinder certain mutualistic interactions to occur, mainly due to mismatching traits or the lack of spatio-temporal overlap among the species. Such restrictions contradict the aforementioned neutral assumption that any two species can virtually interact, and several studies have examined how they may shape the structure of a network. For instance, Santamaría and Rodríguez-Gironés (2007) studied two different kinds of mechanistic constraints related to traits: *(i)* the presence of complementary traits, such that only those species that share them interact, like the Darwin's orchid and its pollinating Hawk moth; and *(ii)* barrier traits, that explicitly forbid certain species to profit from particular resources, like a pollinator that is unable to access the nectar of a certain flower. They concluded that the first mechanism alone produces highly unrealistic patterns, and that the best predicting model was a mixed compound of both effects. In a similar fashion, Eklöf et al. (2013) studied the number of traits needed to reproduce the real structure of ecological networks, and concluded that such number is rather small (<10) but increases with the size of the network. Moreover,

such minimal set of traits greatly depends on the type of ecosystem considered. To finish, it is worth mentioning that some works have incorporated both the effect of matching traits and the abundance (for instance, morphological traits related to body size), showing that it enhances the predictions made by considering the passive sampling mechanism alone (Stang et al., 2007). Therefore, although traits seem to play an important role in determining ecological interactions, and by extension nestedness, there is still no general indications on which minimal group of traits is needed to reproduce the observed nested patterns.

While ecological effects may play an important role in explaining the emergence of nestedness, another important set of determinants that has been largely explored is evolutionary history. To start with, some early attempts had been made to relate nestedness with the phylogeny of species. Phylogenetics study how heritable traits are transmitted and transformed over the evolutionary history of organisms, resulting in that species whose historical evolutions are close, are told to be phylogenetically related. In this sense, Bascompte and Jordano (2013) discuss two possible consequences of phylogenetical proximity: related species may exhibit strong similarities in their pattern of interactions, and, on the other hand, a given species may only interact with species that are phylogenetically close among them. Rezende et al. (2007) explored the possibility that such relatedness accounts for the structure of mutualistic networks, including nestedness. Although they reported a significant phylogenetic signal in some empirical networks (a quarter part of the set analyzed), it correlated poorly with the observed interactions. Indeed, Perazzo et al. (2014) showed later that the empirical structure of real networks differs greatly to the one obtained by producing synthetic networks which minimize phylogenetic distances, in particular among species that share a common mutualistic partner.

A second justification of the emergence of nestedness that takes into account its evolutionary history, posits that it may arise as the outcome of natural selection. A good example of this line of thought is the work by Suweis et al. (2013), who showed that nested patterns naturally appear when applying an optimization principle which seeks to maximize the individual abundance of species as well as the total abundance of the community, and moreover that the degree of nestedness of networks correlates positively with the total number of individuals. Therefore, nestedness could also be understood as resulting from evolutionary pressures that select those properties that carry out advantageous functions. Or, as Suweis et al. (2013) put it: 'nested architectures in mutualistic communities could emerge from different initial conditions as a result of a rewiring of the interactions according to a variational principle aimed at maximizing either the fitness of the individual insect/plant (...) or the fitness of the whole community (...)'. It is important to note that this assumption approaches the problem from a different perspective in comparison with the aforementioned explanations. Here, the origin of the pattern is not related to the identity of the species, understood in a broad sense -i.e., involving its ecological, phenotypical or phenological characteristics-, but is sought instead on the dynamical role of the pattern. The nature of such role remains in fact a debated subject, since the study of the consequences of nested patterns for biodiversity persistence and stability has led to mixed conclusions. Indeed, on the one hand and similarly to the results we have presented up to now, several works have supported the idea that nestedness promotes species coexistence (Memmott et al., 2004; Bastolla et al., 2009; Thébault and Fontaine, 2010). On the other hand, more recent works have challenged such results by arguing that nestedness does not correlate with community persistence (James et al., 2012; Feng and Takemoto, 2014; Grilli et al., 2017) or, even more, that it may be negatively influenced by it (Allesina and Tang, 2012; Staniczenko et al., 2013). Admittedly, during the recent years the latter hypothesis has gained increasing evidence, triggering, as we will discuss in the next chapter, a reconsideration of the relevance of nestedness in favor of other network parameters.

Such aim of revisiting the importance of nested patterns is related to the last -but not least- of the interpretations that has been given to the origin of nestedness in evolutionary terms. In particular, it has been proposed that this pattern may actually emerge as a byproduct of an assembly process that, in opposition to the mechanism described above, does not explicitly seek to generate nestedness. Two recent works have shown that, indeed, some structural properties like nestedness may be *network spandrels*, which result from simple mechanisms of assembly alone, precluding any evolutionary selective force (Valverde

et al., 2018; Maynard et al., 2018). The notion of 'spandrel', that we will in fact discuss in more detail in Chapter 3, attempts to enclose the fact that such patterns are often -and misleadingly- presupposed to be selected due to their complex appearance.

2.4 The how

To conclude this chapter on the basic notions of nested patterns, we will address the question of *how* it is measured, that is, which methods exist to quantify the degree of nestedness of a given network. Since the proposal of this patterns in biogeography studies, the arousal of interest in nestedness has been reflected as well in an increase in the number of nestedness *metrics* -with their corresponding *indexes*- coexisting in the literature. A review of the early nestedness metrics is due to Ulrich et al. (2009), while a more recent review by Mariani et al. (2019) provides a very detailed and updated summary of the most common nestedness metrics. In what follows, we will explain the functioning of several nestedness metrics, involving both the most popular indexes together with recent or less known proposals. All in all, it is worth noting that, even if this review attempts to be fairly exhaustive, including all the nestedness metrics present in the literature would be a massive task, and hence some of them have been left out of this description.

At least two basic distinctions can be made when it comes to classify nestedness metrics. The first and most basic one is according to its means of calculation: *(a)* analytically, that is, with an expression that depends on the biadjacency matrix, and *(b)* algorithmically, i.e. through a numerical procedure that often involves reorganizing the interactions of the network. Although this differentiation may seem rather naive, we will see in Chapter 3 that it actually plays a role. Secondly, nestedness metrics may be grouped by their conceptual basis, particularly which network property they emphasize in order to characterize the pattern. Both Ulrich et al. (2009) and Mariani et al. (2019) distinguish between the following types of metrics: *(i)* gap-counting metrics, which quantify the number of missing or unexpected interactions in the real configuration as compared to its perfectly nested equivalent matrix; *(ii)* overlap metrics, which quantify the amount of redundancy in the interactions between neighbors; *(iii)* distance-based metrics, that weight the relevance of the deviations from a perfectly nested network by pondering their distance to the isocline of perfect nestedness; and *(iv)* spectral metrics, which rely on the spectral properties of the biadjacency matrix. We would add to this classification a fifth category: *(v)* robustness metrics, which are based on the study of the effects of node-removal.

This final section will provide helpful information for the following chapters. Indeed, in chapter 3 we will use two of the described metrics to address the question of the emergence of nestedness. Furthermore, in chapter 4, we will examine the performance of all the reviewed metrics, by quantifying their dependencies and flaws. Therefore, a pragmatic reader may chose to read only the descriptions of the NODF and spectral radius before going through chapter 3, and the rest of metrics when reading chapter 4.

The Atmar and Patterson temperature

This nestedness metrics is based on the idea of quantifying the deviations of a real matrix from a perfectly nested matrix by measuring the distance of the misplaced interactions from the IPN curve (see Fig. 2.3).

In particular, the mathematical basis of this metrics relies on the mapping of the maximally packed version of a $m \times n$ bipartite adjacency matrix into a continuous rectangle (Medan et al., 2007), leading to the analytic expression of the IPN in terms of two continuous variables $a \in [0, n]$ and $p \in [0, m]$, which constitute the continuous approximation to the discrete labels of the columns and rows of the biadjacency matrix, respectively. This approximation is expected to be correct in the limit of very large systems. Then, the non zero elements of the biadjacency matrix correspond, in the rectangular surface of size $m \times n$, to an area proportional to the density of contacts $\phi = E/(m \times n)$, where E is the total number of edges. This area may be assumed to be coloured and so the empty area represents the amount of zero elements of the adjacency matrix. The IPN can be analytically expressed as a function of m, n and ϕ (Medan et al., 2007).

Because real systems are not perfectly nested, the temperature (T_{AP} from now) measures the distance, along the diagonal of the unit square, of the misplaced points (presence or absence of a contact above or below the IPN) (Atmar and Patterson, 1993). Various implementations of this metrics can be found in the literature (Rodríguez-Gironés and Santamaría, 2006; Atmar and Patterson, 1995; Guimarães and Guimaraes, 2006), however the most popular nowadays is probably BINMATNEST, developed by Rodríguez-Gironés and Santamaría (2006). Indeed, in this work the authors proposed to quantify the *unexpectedness* of a given interaction of the matrix, mapped into the unit square, by the following function:

$$u_{ij} = \left(\frac{d_{ij}}{D_{ij}}\right)^2 , \tag{2.3}$$

where d_{ij} and D_{ij} correspond, respectively, to the distance between the unexpected interaction and the IPN in the first case and to the total length of the diagonal in the second (see Fig. 2.3). The final temperature is then calculated as follows:

$$T_{AP} = \frac{100}{U_{max} \cdot n \cdot m} \sum u_{ij} , \tag{2.4}$$

where the sum runs over all the unexpected interactions and U_{max} is a constant given by Atmar and Patterson (1993). Accordingly, the T_{AP} will be large if there are several $'1s'$ and $'0s'$ on the wrong side of the IPN. It will be even larger if those misplaced points are located far from the IPN. Then, the lower the measure of the T_{AP} of a given system, the more nested it is.

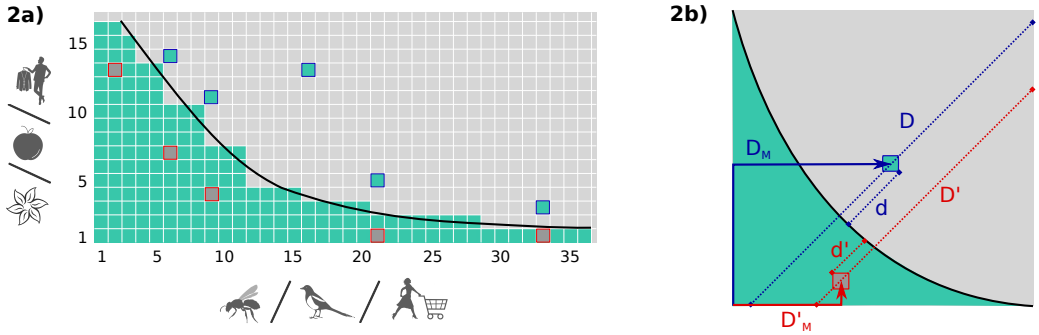

Figure 2.3: Distances and continuous approximations for measuring nestedness. Panel **a)** shows the scheme of a non-perfectly nested network. Green squares depict the interactions and the black curve represents the *Isocline of perfect nestedness* (IPN) which separates, in an ideally perfect nested matrix, the region where all the nodes are connected from the region with no interactions. The unexpected interactions above the IPN are highlighted in blue, while absent interactions below the IPN are highlighted in red. Panel **b)** represents the mapping of a matrix into the unit square. The black curve corresponds to the IPN, and unexpectedly present (absent) interactions are highlighted in blue (red). The figure shows two different kind of distances that may be used for measuring nestedness: D, D', d and d' (traced in dashed lines) are used in the calculation of the temperature, while D_M and D'_M (represented by solid arrows) are used by the nestedness index based on the Manhattan distance (NMD).

The nestedness index based on the Manhattan distance (NMD)

This metrics by Corso et al. (2008) follows the same idea as the T_{AP} metrics, in the sense that it counts the number of unexpected presences or absences with respect to a nested matrix of the same characteristics (size and fill) as the studied matrix, when both are brought to their maximally packed form. Again, it introduces a mapping of the matrix into the unit square. On this rescaled continuous approximation, it measures the distance to the corner of

the matrix where the nested core is expected (see Fig. 2.3 for an example). Distances are measured in terms of the Manhattan distance, which means that the distance between a rescaled element $b_{i,j}$ of the matrix and the origin is $d_{i,j} = x_i + y_i$. This nestedness index is given by:

$$\tau = \frac{d - d_{nest}}{d_{rand} - d_{nest}}\,, \tag{2.5}$$

where d is the sum over all the elements' distances $d = \sum d_{i,j}$ of the real matrix (maximally packed) and d_{nest} represents an analogous sum but over the corresponding perfectly nested matrix with the same size and fill as the empirical one. Their difference is then normalized by the maximum difference in average distances between a null model and the perfectly nested matrix. There are various options for the null model used to calculate d_{rand}, but a common choice is to keep constant size and fill. In this way $0 \leq \tau \leq 1$, and the smaller τ the more nested the system is.

The nestedness metrics based on overlap and decreasing fill

This index (hereafter NODF), introduced by Almeida-Neto et al. (2008), involves two contributing factors to nestedness: *decreasing fill*, that quantifies to what extent, after ordering the rows and columns of the matrix, the degree sequences strictly decrease; and *paired overlap*, that accounts for the number of shared partners between all pairs of columns (rows), normalized by the smaller degree. By gathering together the operational definition indicated by Almeida-Neto et al., we proposed the following compact expression to calculate NODF (Payrató-Borràs et al., 2019):

$$\begin{aligned}\mathrm{NODF}(\mathbf{B}) = &\frac{1}{K}\sum_{i<j}^{N_P}\left\{[1-\theta(v_j - v_i)]\cdot\frac{\sum_{a=1}^{N_A} b_{ia}b_{ja}}{v_j}\right\} + \\ &\frac{1}{K}\sum_{k<l}^{N_A}\left\{[1-\theta(h_l - h_k)]\cdot\frac{\sum_{p=1}^{N_P} b_{pk}b_{pl}}{h_l}\right\},\end{aligned} \tag{2.6}$$

$$\text{where } K = \frac{N_P(N_P-1) + N_A(N_A-1)}{200}. \tag{2.7}$$

Here we have used the following notation: v_p is the degree of plant p and h_a the degree of animal a. The double sums run over two indexes and we consider that the bipartite adjacency matrix is labeled such that row i is placed above row j and column k at the left of column l. The K factor contains the normalization over the number of all possible pairs, and the fact that NODF is defined to take values between 0 and 100. Finally, the θ stands for the Heaviside step function, which is zero when its argument is negative, and one if its argument is positive or zero. As a result, the $1-\theta(v_j - v_i)$ term encapsulates the decreasing fill condition.

As can be seen, the NODF metrics separately informs on the contribution of rows and of columns to the observed nestedness. It is important to emphasize that the overlaps between all the possible pairs of rows (columns) are only taken into account if the considered pair is ordered in decreasing degree, otherwise it assigns a null value to the overlap. Moreover, the higher the index, the more nested the system is.

The NODF metrics correctly assigns a very low nestedness value to modular networks because, in general, elements within the same block have similar degree. However, as remarked by Staniczenko et al. (2013), it may give a false negative in the case of a nested network with multiple rows or columns with the same degree. This is due to the decreasing fill factor, which heavily penalizes degree degeneracy. Unfortunately, this situation is quite

common for mutualistic ecosystems that are in general very sparse and often eccentric –with typically much more animal species than plant species–, which altogether leads to a non negligible degree degeneracy. For this reason, a variant of this metrics called **stable-NODF** has recently been proposed by Mariani et al. (2019). The definition of this index (also named s-NODF) is analogous to the classic metric NODF except for the decreasing fill term. In particular, keeping the same notation, it reads:

$$\text{s-NODF}(\mathbf{B}) = \frac{1}{K}\sum_{i<j}^{N_P}\frac{\sum_{a=1}^{N_A} b_{ia}b_{ja}}{v_j} + \frac{1}{K}\sum_{k<l}^{N_A}\frac{\sum_{p=1}^{N_P} b_{pk}b_{pl}}{h_l}, \tag{2.8}$$

$$\text{where } K = \frac{N_P(N_P-1)+N_A(N_A-1)}{200}. \tag{2.9}$$

Note that the definition above requires the network B to be ordered by decreasing degree in both guilds. This variant does not incorporate the decreasing fill term and hence does not penalize the degree repetition, therefore solely measuring the number of shared partners among pairs of rows and columns. This results in this metric being more robust against slight variations in the degree sequence and, importantly, in solving the drawbacks outlined by Staniczenko et al. (2013).

The Brualdi and Sanderson discrepancy

This metrics is, after the temperature, one of the firstly proposed indexes. Starting from the real matrix in its maximally packed state, this metrics counts the number of misplaced absences or presences of contacts, called *discrepancies*, that should be 'corrected' in order to produce a perfectly nested matrix with equal size and fill (Brualdi and Sanderson, 1999). Instead of focusing on the distances, though, it is based on the gap-counting approach mentioned above.

Since such measure is based on the comparison of the real matrix with a perfectly nested one of the same parameters (number of rows, number of columns and number of links), it is independent of any particular null model. However, given that there may be some ambiguity on the maximally packed configuration, the result depends on the chosen one. Therefore, an optimal calculation would involve averaging over the different initial maximally packed configurations, which can be however a quite demanding process in computational terms.

Furthermore, given that the number of possible discrepant links is directly proportional to the total number of links, the result greatly depends on the network's fill. To prevent such dependency, it has been proposed to normalize the discrepancy by the total number of links (Greve and L. Chown, 2006). As it was the case of the temperature T_{AP}, the definition of this metrics implies that the lower the value of the index, the more ordered the system is.

The nesting index based on network's robustness

This metrics (shortened as NIR hereafter) is based on the notion of the robustness of a network, that is, the capacity of the system to remain connected when subject to node removal (Burgos et al., 2007; Memmott et al., 2004). This metrics uses two extreme node removal procedures, or *attack strategies*, whose outcomes reveal the amount of nestedness of the network. On the one hand the nodes of one guild are removed in *decreasing degree order* (DDR strategy), and of the other in *increasing degree order* (IDR strategy). The fraction of species of the other guild that still keeps contacts as the counterparts are removed leads to the *Attack tolerance curve* (ATC).

Once the attack strategy is fixed, the ATC depends on the degree of nestedness. Fig 2.4 illustrates three different typical behaviors of the ATC for each strategy, when the procedure is applied on a perfectly nested network, on a real network and on a null model with the same size and fill. The DDR strategy better reveals the differences of structure of the three networks.

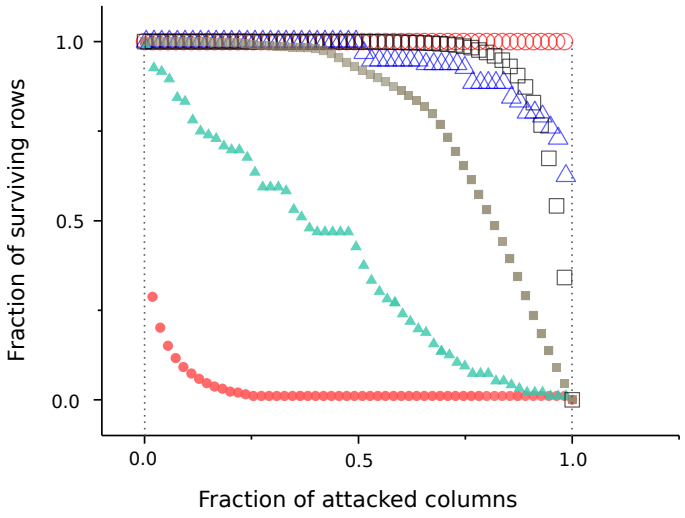

Figure 2.4: Attack Tolerance Curves for three different networks having the same parameters. Triangles correspond to the real mutualistic ecosystem of Clements and Long (1923), squares to a randomization of this system and circles to an artificial perfectly nested network with the same parameters (size and number of links). Open and full symbols correspond to the IDR and DDR attack strategies, respectively.

It can be easily shown that, for the perfectly nested network, the area under the ATC is $R_{IDR} = 1$ for IDR strategy, while it is $R_{DDR} = \phi$ for the DDR (Burgos et al., 2009). Thus, this index is normalized by the area between two extreme curves, which is maximum for a nested network. Moreover, the area is minimum for a random network, while for the real networks the area lies between these two extremes. Altogether, the contribution to the nestedness coefficient of rows or columns is defined as:

$$NIR = \frac{R_{IDR} - R_{DDR}}{1 - \phi}, \tag{2.10}$$

which measures, like NODF, the contribution to nestedness of rows and columns, separately.

On the other hand, NIR looses sensitivity as the density of links increases, which is not a problem for ecosystems that are, in general, very sparse. Finally, this index may in principle slightly depend on the chosen matrix ordering with respect to the degrees of the guild being suppressed. As such order is not unique due to degree degeneracy, averaging over a set of equivalently ordered matrices would preclude any possible biases.

The spectral radius

The spectral radius was recently proposed by Staniczenko et al. (2013) as an alternative metric for nestedness that directly relies on the spectral properties of the adjacency matrix. Let us call $\mathbf{I}$ the identity matrix and $\mathbf{A}$ the adjacency matrix of a bipartite matrix $\mathbf{B}$, such that:

$$\mathbf{A} = \begin{pmatrix} 0 & \mathbf{B} \\ \mathbf{B}^{\intercal} & 0 \end{pmatrix}, \tag{2.11}$$

which is a square, symmetric and non-negative matrix, given that $a_{i,j} \geq 0$. The spectral radius of the matrix $\mathbf{A}$ (also called *dominant eigenvalue* or *largest eigenvalue*) is defined as follows:

$$\rho(\mathbf{A}) = \max\{\, |\lambda_i| \,\}. \tag{2.12}$$

Where λ_i for $i \in \{1, ..., n\}$ are the eigenvalues of $\mathbf{A}$, thus the roots of the equation: $\det(\mathbf{I}\lambda - \mathbf{A}) = 0$. Since $\mathbf{A}$ is a symmetric matrix, $\lambda_i \in \text{Re}$, $\forall i$.

The capability of the spectral radius for quantifying the degree of nestedness of a network is rooted in a theorem by Bell et al. (2008), that states that within the set of networks having the same number of links and nodes, the one yielding the maximum spectral radius will be perfectly nested. In fact, Staniczenko et al. (2013), showed that more nested networks *tend* to have larger spectral radius. However, importantly, this relation is only true in statistical terms. Indeed, their results reveal that, if we take two slightly different networks, the one with a largest spectral radius is *not*, necessarily, the most nested (see, for instance, Fig. 1 from Staniczenko et al. (2013)). Therefore, the sensibility of the spectral radius at a fine scale (i.e. to distinguish between small differences in the degree of nestedness of two networks) is rather limited. This important flaw, however, is scarcely -if at all- reported in the literature, and to our knowledge we were the first one to draw attention to it in Payrató-Borràs et al. (2019).

Another caveat of the spectral radius is, furthermore, that it is not normalized. This implies that nestedness measures are affected by network properties like the density of links or the size, thus hindering the comparison among networks which do not share those characteristics. We will explore with more caution this characteristic in Chapter 4, and propose -and study- a possible normalization.

CHAPTER 3

Nestedness and chance

Non omne quod nitet aurum est
(All that glitters is not gold)

Ancient Latin Proverb

Hopefully, the previous chapter would have served to illustrate, at least partly, how the discovery of nested patterns stirred an avid interest not only among ecologists, but among network scientists in general. Admittedly, this resulted in a growing number of evidences of their ubiquity, reflected as well in the quantity of hypothesis and observations brought out regarding its causes and consequences. Along the present chapter, perhaps paradoxically, we will attempt to undo this constructed notion of nestedness. Indeed, we will try to show that nested patterns are not independent, significant patterns in their own, but just the macroscopic result of imposing certain constraints on the level of generalization of each species. That is, nestedness emerges from the combination of lower-order properties of the network with chance, a result that calls for revisiting its overall relevance.

From the point of view of a busy reader, it may seem a pointless roundabout to elaborate so much upon the importance of nestedness, in order to subsequently argue that it is not, in fact, a relevant pattern. However, only by doing so it is possible to account for the extent of the implications of such result, since, as the popular saying typically attributed to Mark Twain says: 'It is easier to fool people, than to convince them that they have been fooled'.

In particular, we will show how nested patterns can emerge in real systems as an entropic consequence of the degree sequences alone, i.e., of the number of contacts held by each species. The discussion of this result, which has been published in Payrató-Borràs et al. (2019), will be the central part of this chapter (section 3.3). However, before addressing this core problem, we will introduce in section 3.1 the effect of chance in the structure of ecological networks, which will require a general -yet short- account of the main principles of evolutionary theory. Secondly, in section 3.2, we will summarize the different types of null models that have been proposed to deal with -and possibly rule out- the effect of chance in determining the structure of a network. Finally, this chapter will be closed exploring the ecological interpretation, as well as the potential applications, of a meaningful set of parameters of the null model that are empirically determined -the so-called Lagrange Multipliers-.

3.1 Nature does play dice

In 1926, Einstein wrote a letter to Max Born where he famously said: '*The theory yields much, but it hardly brings us closer to the Old One's secrets. I, in any case, am convinced that He does not play dice*'. The 'theory' mentioned by Einstein is Quantum Mechanics, about which, despite having contributed to it himself, he held serious doubts. In his celebrated quote, Einstein criticizes the inherent probabilistic nature of the quantum theory, arguing that its embracing of chance and the resulting challenge of traditional determinism was merely epistemological -but not ontological. In other words, he argued that the probabilistic basis of the quantum description of reality was due to the incompleteness of the theory, and

not a property of the physical world [1]. Despite the undeniable commotion that Quantum Mechanics supposed to the scientific conception of reality, truth to be hold the importance of the role of *chance* in shaping nature had been made evident some years before, with the introduction of the theory of *evolution*. Darwin, who casts a long shadow across this thesis -or to inverse the negative meaning of the phrase, a long-lasting glow-, is at the heart of the scientific revolution which transformed the conception of the origin of life, including that of humans. Indeed, his theory has been sometimes considered as a complementary stage of the Copernican Revolution, which set the basis of the modern scientific view of the world (Ayala, 2007).

While the theory was originally conceived to explain, primary, the evolution of living organisms, it has been later applied as well to the selection of relationships among species, particularly cooperation (Nowak, 2006), and even more, to the study of non-biological systems like culture, technology or language (Arthur et al., 1993; Solé and Valverde, 2020) –all of which have been often defined as complex adaptive systems, as discussed in the introductory chapter. Of course, the latter forms of evolution can not be exactly translated from the original theory, but may still involve, at least in part, analogous principles or rules. In what follows we will briefly summarize the general notion of evolutionary theory in order to better frame the importance of chance in ecology, and particularly the emergence of the so-called *spandrels*.

God as a gambler

The part played by chance in biological evolution may seem trifling, yet Darwin had to face an established preconception of his time: that there could not be 'design without designer' (Ayala, 2007). The existence of organs that performed complex tasks, moreover seemingly appropriate to their environment, lead the predecessors of Darwin, like William Paley (1743-1805), to think that, in words of Ayala: '*The purposeful function reveal, in each case, an intelligent designer, and the diversity, richness, and pervasiveness of the designs show that only the omnipotent Creator could be this Intelligent Designer*'. Darwin challenged this view by arguing, not only that species evolve over time -which was already a sound idea at his time-, but also that the eventual complexity of organs and organisms is the result of an unsurveilled and unplanned process called natural selection, or what Dawkins famously called 'the blind watchmaker'. In this process, chance is present in the appearance of random mutations which may increase, or decrease, the fitness of a species. In fact, if Paley's God was to be seen as the bettor in this mutation game, he would be a rather a spendthrift, since it is estimated that more than 99% of the species that have ever lived have become extinct (Ayala, 2007).

In principle, this selection-of-the-fittest mechanism may shape as well the observed networks of interactions, particularly in mutualistic communities. As discussed in the previous chapter, natural selection can manifest itself at a system-wide level by filtering out less resilient configuration (Suweis et al., 2013). Besides, it may also act upon individual traits that regulate inter-species interactions -for instance, those that determine exploitation barriers or those that determine the eventual benefit and cost of a mutualistic relationship-, reinforce certain pairwise interactions through the effect of coevolution or even sculpt the structure of the entire network (Nuismer et al., 2013).

Selection on the eye of the beholder

Natural selection offered a scientific answer to the problem of design. Nevertheless, just as the observation of a particular complex element does not entail the existence of a creator, such complexity does not necessarily imply, likewise, the presence of selective pressures. In a seminal paper, Gould and Lewontin (1979) criticized what they called 'panselectionism', that is, the belief in 'the near omnipotence of natural selection in forging organic design and fashioning the best among possible worlds'. Gould and Lewontin prevented against the fallacy

[1] This lead Einstein to propose, together with Podolsky and Rosen, his famous EPR paradox, which hypothesized the existence of some local hidden variables.

of assuming that, since natural selection is able to produce evolved complex structures, every evolutionary process or complex structure is forcibly the product of natural selection. In short, the whole criticism can be summed up by the popular saying that goes: 'if all you have is a hammer, everything looks like a nail'

In particular, Gould and Lewontin proposed the existence of the aforementioned *spandrels*, defined as structures that could seem to be evolutionary selected –but are not. The term spandrel originally refers, in fact, to an architectonic element, namely the void space between an arch and a transversal frame or between two (or more) adjacent arches (see Fig. 3.1). Such empty space has no primary use and is merely a byproduct of the configuration of the supporting structural elements. Yet, architectonic spandrels are usually filled with ornaments such as paintings or sculpted reliefs, which may trick the observer into thinking that such space is intentionally designed and carries out a key purpose.

Figure 3.1: Example of an architectural spandrel in the doorway of the Saint Georges Church in Great Bromley (Essex, UK). The spandrel is decorated with a Dragon, as part of the representation of Saint Geroge's legend. Picture adapted from an original photography by Michael Garlick (CC BY-SA 2.0)

In the analogy proposed by Gould and Lewontin (1979), the architectonic constraints related to the construction of the building are translated as biological constraints that may drive and restrict the evolution of an organ or an organism through non-selective mechanisms. In what concerns us here, the notion of spandrels was introduced from evolutionary theory into the network language by Solé and Valverde (2006). In their article, the authors proposed that motifs found in cellular networks are in fact network spandrels. Indeed, while certain network motifs are significantly abundant in comparison to random models (Milo et al., 2002), Solé and Valverde reviewed several evidences pointing at the fact that no particular selective pressure seem to work upon such motifs, and moreover simple models of random duplication and mutation can reproduce their observed abundances. More recently, Valverde et al. (2018) in the first place, followed by Maynard et al. (2018), showed that the structure of ecological networks, including mutualistic systems, can emerge as a by-product of the assembly process. Therefore, non-trivial topological properties of such networks, like degree heterogeneity of nestedness, could be network spandrels that are not specifically optimized through natural selection.

In the next sections we will try to show that, from a purely structural point of view, empirical nested patterns of mutualistic systems turn out to be non-significant when taking into account information about the degree sequences. This view is complementary to the one exposed up to now, where the notion of spandrel is justified by exploring the dynamics of assembly and evolution of mutualistic systems. Instead, in what follows we will focus on studying the properties of static, aggregated networks, in order to show that nestedness is an entropic effect, in the sense that it appears as the most probable macroscopic configuration of the interactions given certain constraints on the number of contacts of each species.

3.2 Null models or how to filter chance

The concept of *null model* is closely related to the notion of *null hypothesis*, a term that was coined by Fisher (1935). In his seminal book, Fisher illustrated the idea with a simple, yet well-known experiment: the *lady tasting tea*. In such thought experiment, a woman declares to be able to differentiate whether an English cup of tea has been prepared by pouring first the tea and secondly the milk, or vice-versa. Fisher proposed to challenge her claim by carrying out a blind tasting test, involving several cups of tea differently mixed. Such test is based on a simple null hypothesis, namely that the lady's statement is false and, in fact, she is guessing the order of the mix haphazardly. In order to *reject* this hypothesis -i.e. to show that her ability to distinguish the tea taste is not simply a matter of luck- we would need to know how many cups she *could* correctly identify when playing randomly. Then, if in comparison to that quantity she actually does a sufficiently large number of correct guesses, we can dismiss the option that she is just tossing a coin to decide.

Following this line of thought, the idea of a null model originates in the context of network theory, where we need to test a particular null hypothesis on a graph –typically whether a given property can be produced by the effect of chance alone. In this sense, the null model is used to produce a set -or ensemble- of randomizations, traditionally synthetic networks where a certain number of parameters have been constrained, against which to compare the original network. This permits assessing whether a particular observation, for instance community structure (Barber, 2007) or degree assortativity (Newman, 2002; Park and Newman, 2003; Johnson et al., 2010), is a relevant property generated by non-trivial mechanisms of network formation, or, on the contrary, it can be merely explained by statistical correlations naturally emerging from other restrictions on the graph, e.g. the network's finite size, a particularly high or low density of links, or the presence of degree heterogeneity.

In what follows, we will use a null model in order to determine whether, as aforementioned, nestedness can emerge as an entropic consequence of the degree sequences. In fact, the application of null models to the analysis of ecological networks is not new. Far from it, there is a long history of debate about which null model is more suitable to assess the significance of patterns –including nestedness– dating back to the first studies in biogeography (Connor and Simberloff, 1979; Gotelli and Graves, 1996) followed by a later extension to interaction networks– (Bascompte et al., 2003), which has remained a lively topic until today –see for instance Strona et al. (2018) for a recent contribution and the review of the topic by Mariani et al. (2019).

The majority of the early null models rely on algorithmic procedures that numerically randomize the network by strictly keeping some constraints, what we will call the *hard constraints* approach. On the other hand, it is also possible to relax such conditions, what results in a general family of null models based on *soft constraints*. Within this group, a particular class of null model has been recently proposed (Squartini and Garlaschelli, 2011), that the authors named *canonical* ensemble following statistical mechanics terminology. It consists in constructing a statistical ensemble where constraints are kept only on average, by imposing some key conditions on the entropy and likelihood of the distribution of probability of existence of each graph in the ensemble. Such novel framework offers several technical and conceptual advantages with respect to former methods, which is why we will exploit it to test whether nestedness is a significant pattern. Before doing so, we summarize below the main families of null models with their characteristics and flaws, keeping in mind that we are especially interested on ecological networks and in keeping the degree sequences as constraints.

Hard constraints

As aforementioned, this family of null models is characterized by enforcing a set of constraints strictly. Given that statistical mechanics terminology is often used to describe different types of network ensembles –a practice that was inaugurated, likely, by Park and Newman (2004)– we could also identify this class of null models with the *micronanical* ensembles (Squartini and Garlaschelli, 2011). Indeed, just like some constraints on the network parameters are preserved *exactly*, in physics the micronanical ensemble includes the set of all microstates

that share a precise, completely specified total energy. In theory, the number of conditions that one could impose to the null model is virtually as large as the number of observable quantities, ranging from the most basic properties to elaborated and system-wide patterns. Nonetheless, in most cases we are interested in understanding whether fundamental network properties –that we may also call *lower-order* features– are able to determine global –or higher-order– ones. Accordingly, most null models are constructed by controlling one or various of the following parameters: *(i)* network size, *(ii)* number of links and *(iii)* degree sequences.

In the particular case of bipartite networks, it is important to note that both *(i)* and *(iii)* can be disentangled per guild, that is, not only the total number of nodes is given but also how many of them belong to each kind. Likewise, we do not have *one* but *two* degree sequences. This bipartite character of mutualistic networks multiplies as well the spectra of possible combinations of constrains, because a particular condition may be applied to just one guild, its counterpart, or both. Following Ulrich and Gotelli (2007), the subsequent classification can be made:

- **Equiprobable model.** In this null model only the size of the network and the number of links is preserved. Consequently, the ensemble is constructed by imposing that, within a guild, each node has in theory the same probability of having a link (hence the name *equiprobable*). Since both guilds are randomized fulfilling this condition, this null model is traditionally named in short as EE (*equiprobable-equiprobable*).

- **Fixed models.** In this case, not only the size and density of links are kept, but also the degree sequences are conserved strictly (that is, the degrees are *fixed*). The most restrictive null model, the so-called *fixed-fixed* (FF), constraints the degree sequences of both guilds to meet strictly the original ones. Nonetheless, it is also possible to relax this condition upon one of the guilds, resulting on the *fixed-equiprobable* model (FE) or its complementary *equiprobable-fixed* (EF), depending on which of the two degree sequences (rows or columns) is kept constant.

This classification was originally developed in the context of biogeography (Connor and Simberloff, 1979; Gotelli, 2000), but was rapidly adapted and adopted in the context of mutualistic networks (Bascompte et al., 2003; Ulrich et al., 2009). In the bigger picture, similar null models are used in the analysis of network structure. Indeed, the EE model produces Erdős-Rényi random graphs with a fixed number of edges m and nodes n, a model that in graph theory is often named as $G(n, m)$ (Newman, 2010). A straightforward implementation of this methods is to take the original network and randomly rewire the interactions, picking and reshuffling them following a uniform distribution. Alternatively, it is possible to 'fill' the network, assigning interactions randomly among not-previously linked nodes, until the number of links matches the empirical one (Gotelli, 2000). However, as discussed in the introduction, this sort of null models produce synthetic graphs that are in general very different from real examples, given that they show very low clustering –that tends to zero in the limit of large networks– and virtually no community structure or degree correlations. Therefore, the EE null model is traditionally regarded as a loose benchmark against which to challenge empirical observations.

In what regards the FF null model and its variants, there is a rather prolific literature on what is the optimal –or in other words less statistically biased– implementation. Here again we find that this question is not exclusive to ecology, since network scientist have been for long interested in generating more realistic degree sequences, particularly resembling the heterogeneous, right-skewed degree distributions that are typically found in empirical systems (Newman, 2010). Despite this multiplicity of methods, we can find, fundamentally speaking, two principal ways of attacking the problem of constructing a network matching a specific degree sequence:

- **Swapping algorithms**. In a sense, this approach pursues fairly closely the notion of *randomization* proposed by Fisher, conceived as disordering a given system in order

to compare the resulting, decorrelated structure with the originally observed pattern. Indeed, this implementation starts with the real biadjacency matrix and exchanges pairs of links between nodes of different guilds, as shown in Fig. 3.2 –what is called *rewiring*. This can be visualized as interchanging two pairs of elements in the biadjacency matrix, each pair composed by a zero and a one, in such a way that the total row and column sums are unaltered (Gotelli and Entsminger, 2001). Moreover, interactions are chosen and replaced according to a set of conditions: first, newly connected nodes must not be previously linked, which hinders the introduction of double edges, and second, the rewiring must occur only among nodes of different guilds, which preserves the bipartite character of the network and avoids the appearance of self-loops. It is important to note that such impositions go beyond the mere preservation of the degree sequences, since in fact neither introducing self-links or double edges would violate the condition of keeping the degrees constant. Hence, this sort of requirements reduces the size of the ensemble of compatible randomized networks. Furthermore, in the specific challenge of assessing the significance of nested patterns, Ulrich and Gotelli (2007) remarked on two major limitations when using the FF null model. First, the number of novel configurations available is small for networks that have either a remarkably high or a remarkably low degree of nestednes (Ulrich et al., 2009). Secondly, even for medium values of nestedness, the number of possible reshufflings is very much influenced by finite size effects. This means that the search in the phase space is confined to a reduced set of possible reconfigurations, which turns to be smaller as the networks' size decreases or the density of links increases.

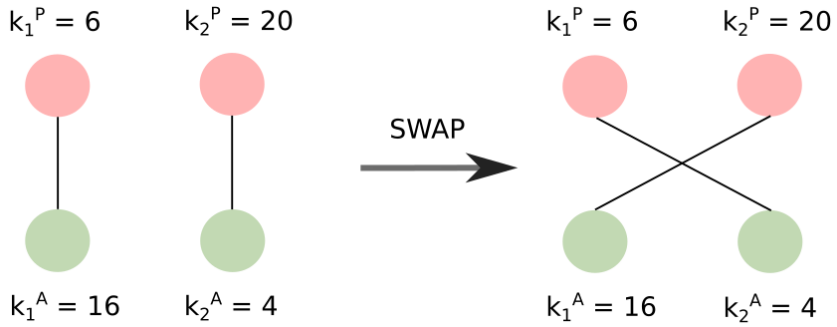

Figure 3.2: Example of the swapping algorithm for a plant-animal bipartite network. The links of two pairs of nodes, represented in pink for plants and in green for animals, are exchanged. Some hypothetical degrees (k_1^P,k_1^A,..., etc) are shown, illustrating that the degree sequences are kept constant.

- **Configuration model**. In this approach, we start with a disconnected network where initially only the 'half-links', also called 'stubs', are assigned in such a manner that the degree sequences are already fixed. The challenge is then to connect, randomly, all pairs of stubs in order to complete the network, as illustrated in Fig. 3.3. Here again, this simple process can break down if one wishes to avoid the appearance of self-loops and multi-edges, which may lead to a non-uniform sampling of the ensemble of null networks (Newman, 2010).

As can be seen, the major difference between the two approaches is the initial configuration: in the swapping algorithm, we take the real network and attempts to randomize it by sequentially rewiring pairs of links, while in the configuration model we start working with a 'voided' network where all links have been cut and thus has to be entirely reconnected. In ecology, the most popular methodology is probably the swapping algorithm, which has been used in numerous papers dating back to its proposal in 1979 (Connor and Simberloff, 1979), to its later application to study mutualistic networks (Bascompte et al., 2003; Ulrich et al., 2009; Joppa et al., 2010; Saavedra and Stouffer, 2013; Staniczenko et al., 2013). All in all,

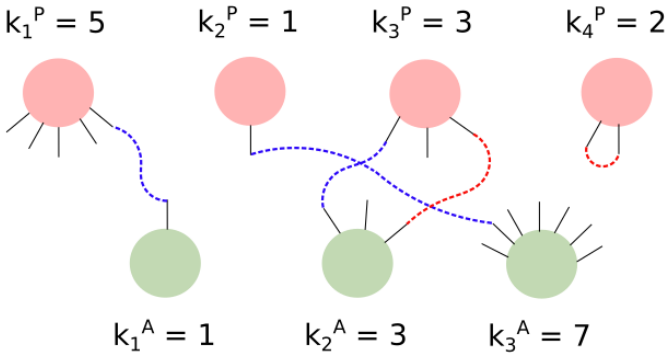

Figure 3.3: Example of the functioning of the configuration model for a plant-animal bipartite network. Each node is assigned a number of stubs, depicted in black, according to the degree sequence that has to be kept. Then stubs are matched randomly, as shown in blue dashed lines. Some particular matchings are forbidden, represented here in red dashed lines, to avoid the presence of self-loops and double-edges.

the limitations we have mentioned above may translate into several drawbacks that introduce undesired correlations and statistical bias into the ensemble. That is why in the following subsection we introduce another family of null models that prevent some of these problems by relaxing the constraints and keeping them only in average, imposing the so-called *soft constraints*.

Soft constraints

By softening the constrains we mean that enforced network parameters are no longer strictly kept but they are allowed to vary across the ensemble, with the condition that the average is still controlled for. Here again, several different network properties could be imposed, but building upon the previous subsection we will focus mainly on two cases: the restriction of the number of nodes and links, in analogy to the EE null model; and the preservation of the degree sequences of both guilds, equivalently to the FF null model.

The softening of the EE null model would lead, in the graph's language, to a modification of the Erdős-Rényi random graph proposed by Gilbert, and typically referred to as $G(n, p)$. At variance with the $G(n, m)$ model, here the probabilities of placing a link between any two nodes have all the same value p and, importantly, they are independent of one another. This entails that the ensemble can be directly constructed by performing a sampling of the probabilistic biadjacency matrix, and randomized networks will differ in their number of connected nodes and links while the average will be kept.

On the other hand, it is also possible to adapt the FF model by enforcing the dependence on the degree through the probability of having a link, what is often called the *proportional-proportional* (PP) null model (Gotelli, 2000; Ulrich and Gotelli, 2012). This approach is characterized by assigning a link between a species i and j –from different guilds– according to the following probability:

$$p_{i,j} = \frac{k_i k_j}{L^2}, \tag{3.1}$$

where k_i is the degree of node i, k_j the degree of node j and L the total number of links. This dependence on the product of the degrees resembles the classical form of the encounter rate between particles in a homogeneous, well-mixed system, which in a first order approximation is a direct function of the product of their concentrations. Moreover, it represents as well the theoretical probability that two nodes have a link in the hard configuration model (Newman, 2010), although here sampling this probability will of course produce randomized networks where the number of links and degrees are not exactly kept. This null model is a fairly common choice not only in ecology (Gotelli, 2000; Ulrich and

Gotelli, 2012; Jonhson et al., 2013; Solé-Ribalta et al., 2018) but also among network scientists in general (Caldarelli et al., 2002; Chung and Lu, 2002; Garlaschelli and Loffredo, 2008). Nevertheless, we will argue later that, regardless of its popularity, this null model has some relevant limitations as well, and it is not exempt of statistical bias even if it already resolves some of the problematics of the FF null model.

A third null model that stands in the midway between the random graph $G(n,p)$ and the PP null model is the one proposed by Bascompte et al. (2003). Unlike in the $G(n,p)$ model, here each link has a different probability of appearance that depends on the degrees of the two species considered. Nevertheless, this probability differs from the one shown in Eq. 3.1, and reads instead:

$$p_{i,j} = \frac{k_i}{2N_R} + \frac{k_j}{2N_C}, \tag{3.2}$$

where N_R is the number of rows and N_C the number of columns of the biadjacency matrix. It is straightforward to see that, despite this null model introduces a certain dependence between the degree and the interaction probability, it does not preserve the degree sequences, and instead tends to homogenize their distribution in a similar fashion to the EE null models (Saavedra and Stouffer, 2013). This is mainly due to the fact that, given that the probability here depends on the sum rather than on the product of the degrees, the term will be dominated by the largest degree. Therefore, in the randomized versions of the matrix, specialist species will tend to become more generalists and generalists will tend to become more specialists. All in all, what exact information is conveyed by this particularly form of the probability remains rather unclear. Indeed, this was made manifest in the debate between James et al. (2012, 2013) and Saavedra and Stouffer (2013). Despite these shortcomings, we can find still several examples of applications of this model in the ecological literature (Bascompte et al., 2003; Saavedra et al., 2009, 2011).

On the whole, in the three classes of soft null models we have discussed so far the only constraints that are imposed concern the link probability among nodes. Nonetheless, it is also possible to enforce additional conditions that warrant that the ensemble has maximum entropy and thus it is statistically non-biased. This is what we will explore now, by introducing the so-called canonical approach.

The canonical approach

The family of canonical null models is constructed by adopting a statistical mechanics perspective, as proposed by Park and Newman (2004). In such framework the null model is completely defined by the probability of appearance of each graph in the ensemble. That is, if we refer to the ensemble's graphs by the general name $\mathbf{G}$, then the probability of existence of each of its elements is given by $P(\mathbf{G})$. The null ensemble is then composed by a large set of graphs, $\{\mathbf{G}\}$, including the real network that, adhering to the notation introduced by Squartini and Garlaschelli (2011), we will name $\mathbf{G}^*$.

Following Park and Newman (2004), the present methodology can be regarded as an analogy, in network language, of the construction of the canonical ensemble in statistical physics. Such ensemble is characterized not only by the soft constraining, but also by the fact that the entropy is maximized. In particular, the Shannon-Gibbs entropy is defined as:

$$S = -\sum_{\mathbf{G}} P(\mathbf{G})\, lnP(\mathbf{G}), \tag{3.3}$$

where the sum runs over all the graphs G in the ensemble. The optimization of this quantity under some given set of constraints $\vec{C}$ leads to the *Exponential Random Graph model*, which reads:

$$P(\mathbf{G}/\vec{\theta}) = \frac{e^{-H(G,\vec{\theta})}}{Z(\vec{\theta})}, \tag{3.4}$$

being H the graph Hamiltonian such that $H(G,\vec{\theta}) = \vec{\theta}\cdot\vec{C(G)}$, and Z the normalizing partition function $Z = \sum e^{-H(G)}$. The set of variables $\vec{\theta}$ are the *Lagrange multipliers*, issued

from the maximization of Eq. 3.3 under the chosen constraints $\vec{C}$. In particular, these constraints represent, in the first place, a normalization condition:

$$\sum_{\mathbf{G}} P(\mathbf{G}) \, = \, 1 \tag{3.5}$$

and, secondly, the preservation of the average of a certain property, that following the standard notation we will call X:

$$\langle X \rangle \, = \, \sum_{\mathbf{G}} X(\mathbf{G}) \, P(\mathbf{G}), \tag{3.6}$$

and which can be extended to include a set of multiple properties $\{X_1, ...X_i, ...\}$. This second requirement represents, in fact, the soft enforcing of the desired constraints, translated now into a maximum entropy framework.

This particular condition on the entropy ensures that the ensemble is maximally disordered, or in terms of information theory, contains maximal *uncertainty*. Moreover, it is equivalent to the Boltzmann distribution with conserved mean energy, that in statistical physics provides the distribution probability of microstates in a system at equilibrium with a thermal bath. The general idea behind this choice is that, in the absence of better insight into the particular microstates –in our case of other network parameters–, the best distribution is that which maximizes the disorder while still keeping, as averages, the observed properties –in our case, some particular network properties. Here, by the *best* we mean that it entails a minimal number of assumptions about the uninformed and hence unconstrained properties of the graphs across the ensemble, which translates into a maximization of the uncertainity (Jaynes, 1957; Newman, 2010).

Exponential random graphs have been extensively used in the latter years, especially in the field of social networks where they also receive the name of p^* models (Robins et al., 2007). Nonetheless, the ensemble as defined in Eq. 3.4 is not fully determined. The Lagrange multipliers, whose introduction is required to constrain the optimization with the conditions of Eqs. 3.5-3.6, are a priori unknown and hence stand as *hidden variables* (Garlaschelli and Loffredo, 2008), that need to be fixed in order to complete the definition of the null model. As a matter of fact, several methods to estimate these parameters can be found in the literature[2], ranging from considering these parameters as fitness values and extracting them from either empirical or theoretical distributions (Caldarelli et al., 2002), to fitting the observed properties using generative models like Markov random graphs (Robins et al., 2007). Here, we will follow the procedure developed by Garlaschelli and Loffredo (2008) and Squartini and Garlaschelli (2011) in order to construct a maximum entropy ensemble that, specifically, is aimed at randomizing the real network, represented by the graph $\mathbf{G}^*$. Given that we are interested in constructing a null model to evaluate the significance of empirical nested patterns, this seems indeed the most sensible choice.

According to Garlaschelli and Loffredo (2008) and Squartini and Garlaschelli (2011), a correct randomization of a real network entails that the model parameters are those for which the real network is found in the ensemble with maximum probability. To illustrate this procedure, let us start defining the log-likelihood of observing the real network:

$$L(\vec{\theta}) = ln(P(\mathbf{G}^* \mid \vec{\theta})), \tag{3.7}$$

which, replacing the exponential graph model in $P(\mathbf{G})$, can be rewritten as:

$$L(\vec{\theta}) = -H(\mathbf{G}^*, \vec{\theta}) - lnZ(\vec{\theta}). \tag{3.8}$$

The proposal of Garlaschelli et al. is to maximize the quantity in Eq. 3.8, which leads to a set of optimal values for the Lagrange Multipliers that we will call $\vec{\theta^*}$. With this values at hand, the maximum entropy ensemble is fully determined, with the peculiarity that the real

[2]Truth to be told, there is a huge literature on how to estimate the model parameters on Exponential Random Graphs, including as well several packages to construct the ensemble. However, reviewing them is beyond the scope of this thesis and we will focus on reviewing the method proposed by Garlaschelli and Loffredo (2008) and Squartini and Garlaschelli (2011).

network –or to be more precise, the observed properties we aim to enforce– will be found with maximum probability. This ensures not only that the constraints are met on average, but also that they are the most expected value, which is a warranty of non-bias, in particular always fulfilled by the exponential random graph model but not generally true for other types of ensembles.

The framework we have described up to now is a general approach that could serve, in principle, to construct a wide variety of null models concerning different network types and constrains. Nonetheless, given that we are particularly concerned with bipartite networks with softly fixed degree sequences, we will now explain the details of how this methodology applies to this special case.

Bipartite networks and local constraints

The adaptation of the maximum-entropy and maximum-likelihood framework to bipartite networks is due to Saracco et al. (2015), who applied it to the study of the international trade network. Although the general scheme remains mostly the same to the monopartite case, some peculiarities arise.

To begin with, we construct the Hamiltonian for a bipartite network, whose biadjacency matrix we call $\mathbf{B}$. Differently to the monopartite case, we confront *two* degree sequences (one for each of the guilds) which need to be taken into account separately. Although the scheme is equally valid for any mutualistic network (seed-dispersers, ant-plants...), for the sake of clarity we restrict our notation to the paradigmatic case of plant-pollinator communities. Thus, we will speak of systems with N_P number of *plants* and N_A pollinating *animals*. Accordingly, the real degree sequences will be represented respectively by $\vec{v}$ and $\vec{h}$, where v_p is the diversity of *visiting* animal species that a plant species p receives, while h_a is the number of different *hosting* plant species with which a pollinator species a interacts.

As aforementioned, the Hamiltonian could virtually enclose any network constrain, yet for the sake of continuity we will explore two basic types of soft constraints: the density of links –in analogy to the EE model–, and the degree sequences –similarly to the FF model–. In the first case, that is, if the number of links is kept on average, it is straightforward to see that one recovers the $G(n, P)$ model, i.e. the soft random graph model (Park and Newman, 2004). Instead, introducing the degree sequences leads to a more complicated case, that we will now derive in detail.

To begin with, in order to enforce both distributions as constraints we introduce two sets of Lagrange multipliers, $\vec{\alpha}$ for plants and $\vec{\beta}$ for animals. Subsequently, the graph Hamiltonian can be written as:

$$H(\mathbf{B}, \vec{\alpha}, \vec{\beta}) = \vec{\alpha} \cdot \vec{v} + \vec{\beta} \cdot \vec{h}. \tag{3.9}$$

This means that the probability of encountering a bipartite graph $\mathbf{B}$ in the exponential random graph ensemble of Eq. 3.4 becomes:

$$P(\mathbf{B} \mid \vec{\alpha}, \vec{\beta}) = \frac{e^{-\vec{\alpha}\cdot\vec{v}-\vec{\beta}\cdot\vec{h}}}{\sum_B e^{-\vec{\alpha}\cdot\vec{v}-\vec{\beta}\cdot\vec{h}}}. \tag{3.10}$$

To simplify the notation we introduce the variable change $x_p = e^{-\alpha_p}$ and $y_a = e^{-\beta_a}$, as suggested by Squartini and Garlaschelli (2011). After this modification, the log-likelihood of encountering the real network reads:

$$L(\vec{x}) = \sum_{p=1}^{N_P} v_p \, ln(x_p) + \sum_{a=1}^{N_A} h_a \, ln(y_a) - \sum_{a=1}^{N_A}\sum_{p=1}^{N_P} ln(1 + x_p y_a), \tag{3.11}$$

which, as discussed above, we need to maximize in order to find the optimal variables $\vec{x^*}$ and $\vec{y^*}$ that ultimately define our ensemble. By doing so we are enforcing that both the degree sequences of plants and animals are found, in the maximum entropy ensemble, with maximum probability. Indeed, by requiring that $\vec{\nabla} L(\vec{x}, \vec{y}) = \vec{0}$, we obtain the following set of equations:

$$v_p = \sum_{a=1}^{N_A} \frac{x_p y_a}{1 + x_p y_a} \quad \text{for } p = 1, ..., N_P, \tag{3.12}$$

$$h_a = \sum_{p=1}^{N_P} \frac{x_p y_a}{1 + x_p y_a} \quad \text{for } a = 1, ..., N_A. \tag{3.13}$$

It can be easily shown that these equations are equivalent to imposing that the average degrees (right hand side) are equal to the degree sequence from the real network (left hand side). Firstly, we need to note that the ensemble probability can be factorized in terms of the *probability of existence of a link between a plant species 'p' and animal species 'a'*, which we call p_{pa}. In effect, by taking:

$$p_{pa} = \frac{x_p y_a}{1 + x_p y_a}, \tag{3.14}$$

replacing it into Eq. 3.10 and doing some little algebra, one finds:

$$P(\mathbf{B} \mid \vec{\alpha}, \vec{\beta}) = \prod_{p,a} {p_{pa}}^{b_{pa}} (1 - p_{pa})^{1 - b_{pa}}, \tag{3.15}$$

where b_{pa} is the (p,a) element of the bipartite matrix of interactions. Then, using expression 3.15, it is almost immediate to see that $\langle b_{pa} \rangle = p_{pa}$, and thus in turn, the average matrix element reads:

$$\langle b_{pa} \rangle = \frac{x_p y_a}{1 + x_p y_a}. \tag{3.16}$$

This demonstrates that, as we had said, the right hand-side of equations 3.12-3.13 is a sum over the column or row of expected values of the randomized bipartite matrix. It is noteworthy to observe that this form of the link probability is radically different to the ones proposed in other soft null models, like the configuration model of Eq. 3.1 or the linear model of Eq. 3.2. Indeed, Garlaschelli and Loffredo (2008) showed that the popular form of the probability in 3.1 is in fact a biased choice, since it produces non-maximum likelihood ensembles, that is, ensembles where the degree sequences are kept in average but, strikingly, they are not the most probable outcome.

Furthermore, the possibility of factorizing $P(\mathbf{B} \mid \vec{\alpha}, \vec{\beta})$ essentially entails that the probabilities p_{pa} of having a link are independent among them. In other words, when the constraints enforced are local –like the degrees, the probability of existence of different links can be disentangled. This was already assumed in previous models that softly constrain the degree, but this maximum-entropy and maximum-likelihood scheme provides a theoretical derivation showing that it is indeed possible to do so.

Therefore, this factorization automatically permits the construction of the exact expected randomized matrix of interactions across the ensemble:

$$\langle \mathbf{B}^* \rangle = \begin{pmatrix} p_{11} & p_{12} & \cdots & p_{1a} & \cdots & p_{1N_A} \\ p_{21} & p_{22} & \cdots & p_{1a} & \cdots & p_{2N_A} \\ \cdots & \cdots & \cdots & \cdots & \cdots & \cdots \\ p_{p1} & p_{p2} & \cdots & p_{pa} & \cdots & p_{pN_A} \\ \cdots & \cdots & \cdots & \cdots & \cdots & \cdots \\ p_{N_P 1} & p_{N_P 2} & \cdots & p_{N_P a} & \cdots & p_{N_P N_A} \end{pmatrix} \tag{3.17}$$

To sum up, we have described a randomizing framework that allows enforcing some soft constraints on the degrees while ensuring that the ensemble is statistically well-behaved, offering some solid basis as compared to other, simpler null models. With these results at hand, we will show now, following Squartini and Garlaschelli (2011), how it is moreover possible to estimate the average and standard deviation of networks properties using either analytical approximations or numerical methods.

General analytical expressions of the first two moments of the distribution of a given property of the network.

The randomizing scheme discussed up to now may be exploited to achieve the final goal of this whole procedure: to measure a given network property across the statistical ensemble. As aforementioned, in general there are two possible ways of performing this calculation. On the one hand, as long as the property that we aim to evaluate can be analytically formulated in terms of the elements of the bipartite adjacency matrix, Squartini and Garlaschelli (2011) showed that it is possible to obtain, at first order, the analytical expression of the first and second moments of the corresponding distribution. These expressions depend only on the link probabilities. In other words, it is not necessary to sample the ensemble, instead the mean and the standard deviation of the nestedness index can be analytically calculated. On the other hand, one can always sample the ensemble in order to study the statistics of the target property on a generated, unbiased sampling (Squartini et al., 2015)

Let us start reviewing the analytical procedure. We will call a network property by X and its average across the statistical ensemble by $\langle X \rangle^*$. The asterisk superscript indicates that the statistical ensemble is built for a given real bipartite matrix $\mathbf{B}^*$. If this property X can be calculated through an analytical expression –that is, as a function of the matrix elements of $\mathbf{B}$–, then Squartini and Garlaschelli (2011) showed that it is possible to perform an approximate but accurate measure of the first and second moment of X, *directly* on $\langle \mathbf{B}^* \rangle$. In particular, for the bipartite case, the expressions for the average and the standard deviation of X read:

$$\langle X \rangle^* \simeq X(\langle \mathbf{B}^* \rangle), \tag{3.18}$$

$$\sigma_X \simeq \sqrt{\sum_{p=1}^{N_P} \sum_{a=1}^{N_A} \left(\frac{\partial X(\mathbf{B})}{\partial b_{pa}} \right)^2 \sigma^2_{b_{pa}}}, \tag{3.19}$$

where $\sigma_{b_{pa}}$ is the standard deviation for the bipartite matrix element b_{pa}. These two expressions can be regarded as the result of linearly approximating the dependence of X on the matrix elements, where second-order terms are neglected. In particular, Squartini and Garlaschelli (2011) showed that this estimation is accurate as long as that the property X is Gaussian-distributed in the random ensemble, which warrants that higher order corrections will be comparatively small.

Secondly, any property –having an analytical expression or not– can always be measured in a sample of the statistical ensemble. The sampling consists in generating networks by placing links among species according to the probabilities provided by the matrix elements of $\langle \mathbf{B}^* \rangle$ (Eq. 3.17). The fact that the probabilities p_{pa} are independent from one another offers a great advantage with respect to other randomizing methods, like the swapping algorithm described above. Moreover, given that these probabilities are obtained imposing the maximum-entropy and maximum-likelihood conditions, the resulting sample will be significantly less biased than other choices (Squartini et al., 2015).

We have described in great detail this randomizing framework since it will be the basis of calculations in the rest of this chapter, as well as part of chapter 4. Indeed, in what follows we will apply these results to the study of nested patterns, in order to elucidate whether nestedness is –or is not– an independent, significant property. Besides, the description of alternative null models will have hopefully provided a glimpse of the bigger picture, and certainly will help us explain how our work relates to prior investigations on the relevance of nested patterns.

3.3 Breaking the spell of nestedness

As it has been discussed in Chapter 2, recently the pertinence of nestedness as a suitable indicator to characterize the dynamics of mutualistic communities has been challenged by various works. In fact, it has been argued that either nestedness has no significant impact on the coexistence of mutualistic communities (James et al., 2012; Grilli et al., 2017),

either it detrimentally affects local stability (Allesina and Tang, 2012; Staniczenko et al., 2013). Moreover, other properties of the observed networks have been claimed to be key drivers of the community dynamics (James et al., 2012; Feng and Takemoto, 2014). In particular, the networks' degree assortativity or the degree heterogeneity have been identified as determinants of biodiversity persistence. This leads to the aforementioned key question of whether nestedness, conceived as a global trait of the emerging architecture, is actually a genuine and independent property, or contrarily, it just derives from lower order features of the interaction network. In what follows we will attempt to answer this question from a structural point of view. In particular, this section starts with a brief discussion on previous works that addressed a similar problem; next, we will describe how we implemented the maximum-entropy and maximum-likelihood framework to construct a null model for ecological networks; and, finally, we will apply this scheme to evaluate the significance of the nestedness of a large dataset composed by 167 empirical networks representing diverse types of plant-animal mutualistic communities across the globe.

Predecessors

Earlier investigations on the structural determinants of nestedness were concurrent on the relevance of the degree sequences. Firstly, Medan et al. (2007) theoretically showed that the isocline of perfect nestedness can be ultimately related, in the continuous limit approximation, to the degree distributions of both guilds. On the other hand, Joppa et al. (2010) identified the degree sequences as a feature that considerably explains empirical nestedness, although they still claimed to find '*a statistically significant excess of networks with unusual nestedness patterns*'. Last but not least, Jonhson et al. (2013) explored the emergence of correlations in a finite size configuration model, and notably argued that degree heterogeneity together with dissasortativity are two crucial determinants of nestedness, or in their words: '*... most of the empirically found nestedness stems from heterogeneity in the degree distribution. Once such an influence has been discounted – as a second factor – we find that nestedness is strongly correlated with disassortativity and hence – as random networks have been recently found to be naturally disassortative – they also tend to be naturally nested just as the result of chance*'. Indeed, the results derived in this section have much in common with their conclusions, although we take a different methodological path in order to demonstrate such dependencies.

Furthermore, in the context of building null models to measure the significance of empirical nested patterns, other works had been confronted to the relationship between nestedness and heterogeneity of degrees, yet without fundamentally addressing it. Instead, the majority of such studies placed the focus on the technical capability of each family of null models to 'detect' nestedness –resulting into the well-known classification between *conservative* and *non-conservative* tests, and the arousal of Type I and Type II errors– and leaving aside any further, conceptual implications of the obtained nestedness significance. Moreover, the actual existence of randomizing issues often monopolized the discussion. A good example of this situation is the debate about the aforementioned *fixed-fixed* model, which has been extensively used to assess nested patterns. A common caveat of this model is that the number of null networks compatible with the constrained degree sequences might be highly limited. For instance, Ulrich and Gotelli (2007) and Ulrich et al. (2009) observed poorly significant nested patterns when using this null model. Howbeit, they explained such result arguing that the FF null model induces a bias in the sampling, due to the fact that the generated null matrices closely resemble the real network, contrarily to the case where a randomization that relaxes the degree sequences –for instance the EE model– is applied. In the words of Ulrich and Gotelli (2007): '*This similarity makes it more difficult for the FF algorithm to detect nestedness*'. Likewise, Staniczenko et al. (2013) pointed out the limitations of the FF model, given that the number of possible null networks decreases as the nestedness or density of links of the real network increases.

In spite of all these different hints pointing at the crucial question of the structural relevance of nestedness, the debate still remains open (Allesina, 2012). On the whole, the difficulty in obtaining a definitive answer to this problem is related to the nature of the methodology followed in previous studies. As it has been explained, such methodology mainly relayed on statistically correlating the observed degree of nestedness in real systems with the

expectation provided by the null model(s) of choice. Given that, as discussed above, previous null models typically randomize algorithmically the observed network under some constraint, they are more often than not flawed by the emergence of undesired bias —enhanced, in turn, by the typical small size of ecological networks. In what follows, we take a different methodological path that allows us to test, in a non-biased randomizing framework, the significance of nested patterns.

Construction of the statistical ensemble

The maximum-entropy and maximum-likelihood ensemble introduced above solves many of the drawbacks of alternative null models that, either softly or hardly, constrain the degree sequences. In the particular case of ecological data, this canonical approach has the advantage that possible missing links or overrated interactions, which might lead to impoverished ecological data (Blüthgen et al., 2008; Olesen et al., 2010), are dealt with in a proper way. In other words, from a theoretical perspective relaxing such constraints reflects the fact that the observed degree sequences may provide imperfect information, i.e., the reported network may be incomplete or contain noisy data like mislead interactions. Indeed, enforcing the randomized degree sequences to be equivalent to the empirical ones only on average limits the possible impact of these shortcomings, while assuring that results are not dependent on specific details. Moreover, from a methodological viewpoint, the fact that this null model provides an analytic expression for the probability of interaction between species, results in the computational generation of null networks being fast, efficient and demanding few numerical resources (Squartini and Garlaschelli, 2011).

In order to apply the framework described above to the study of mutualistic networks, first we need to construct a maximum entropy statistical ensemble for each one of the empirical networks we aim to examine, under the constraint that the degree sequences in the ensemble match on average the empirical ones –this being true for the two guilds of the corresponding bipartite graph. Eventually, this provides a set of coupled equations to solve for the Lagrange multipliers (Eqs. 3.12-3.13 above). Hence, determining the statistical random ensemble for each real mutualistic network entails solving the corresponding optimization problem. In particular, for each network in the empirical dataset we numerically found the Lagrange multipliers that maximize the likelihood using two different, independent algorithms: *(i)* simulated annealing, which is a global, pseudo-random numerical method for optimizing the likelihood, and *(ii)* a deterministic, gradient-based algorithm for solving non-linear systems of equations. Further details on how these methods are implemented are given in the Appendix B. Moreover, the codes to produce this ensemble for any network are published as an open repository named *nullnest* in github (see Appendix G).

As it has already been discussed, a primary advantage of constructing a maximum likelihood and maximum entropy ensemble is that, in the case of local constraints, the probability of existence of a graph in the ensemble can be exactly factorized into the probabilities of existence of a link between any two species (see Eq. 3.15). Therefore, after numerically determining each optimal set of Lagrange multipliers, we built the matrix containing the average probability of interaction corresponding to each empirical network, as illustrated in Fig. 3.4 for the empirical network reported by Inoue et al. (1990). The resulting dataset, comprising 167 probabilistic networks, is as well made public as part of the *nullnest* repository.

Statistical measures of nestedness

We performed the statistical measures on the ensemble applying both the analytical and the numerical approach described in the section 3.2. In what follows, though, we focus on deriving the analytical expressions for the mean and the standard deviation of the distribution of nestedness across this ensemble. In particular, we do so for the two indices of nestedness for which this is possible: the well-known *nestedness metric based on overlap and decreasing fill* (NODF) (Almeida-Neto et al., 2008), and the recently proposed *spectral radius* (Staniczenko et al., 2013). The measures performed by numerically sampling the ensemble are detailed in Appendix E.

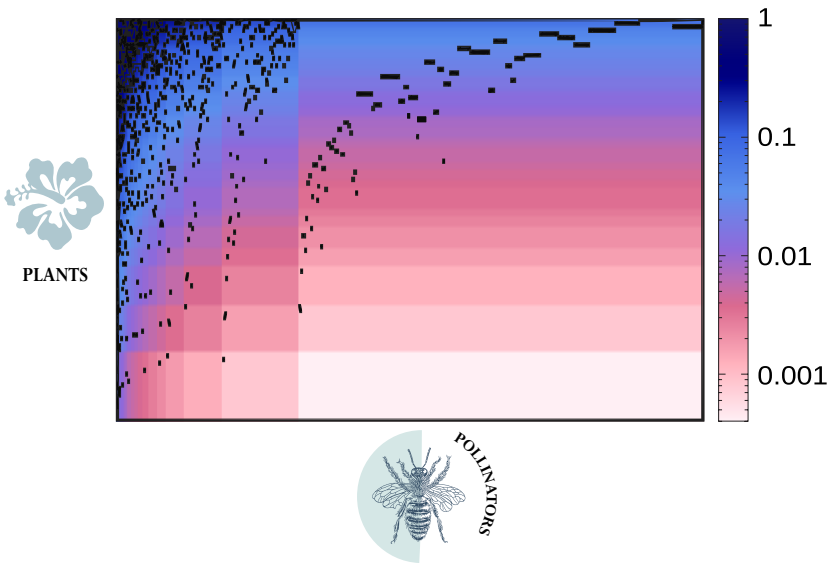

Figure 3.4: Comparison between empirical mutualistic interactions and probability of interacting in the ensemble. The probability of interaction between species in the statistical ensemble given by $\langle \mathbf{B}^* \rangle$ is shown as a color heatmap, for the plant-pollinator network recorded by Inoue et al. (1990). The empirical corresponding bipartite matrix of interactions $\mathbf{B}^*$ is superimposed in black. Both plants and pollinators species have been ordered in decreasing order of their degrees (from top to bottom and from left to right). As it can be seen at a glance, the obtained probabilities are consistent with the observed interactions, with the dark regions delimiting an upper left triangle, as in an ideally nested structure. Note that the color legend is in logarithmic scale.

Derivation of the analytical expressions for NODF

In this subsection, we derive the analytical expressions for the average and the standard deviation of nestedness measured by the index known as *nestedness metric based on overlap and decreasing fill* (NODF). We chose this metric among the vast range of indices in the literature due to a variety of reasons: first, it can be calculated through an analytical and compact expression in terms of the matrix elements; second, and contrarily to other metrics, its definition is based on a clear and explicit quantification of conditions in Eqs. 2.1-2.2, precluding any type of geometric or algorithmic approach; and finally, it is widely used not only in ecology but also in network applications to economics (Saracco et al., 2015; Hernández et al., 2018) or sociology (Borge-Holthoefer et al., 2017).

Definition and distribution of NODF

As we explained in Chapter 2, the NODF index quantifies two aspects of nestedness: on the one hand, the *decreasing fill*, that quantifies the variation in the degree sequence; and on the other hand the *paired overlap*, that weights the overlap of interacting partners among the nodes of a guild. To encapsulate this calculation, we will use the analytical definition proposed in the previous chapter (see Eq. 2.6), which, for the sake of clarity –and at the expense of some redundancy–, we remind:

$$\mathrm{NODF}(\mathbf{B}) = \frac{1}{K}\sum_{i<j}^{N_P}\left\{[1-\theta(v_j-v_i)]\cdot\frac{\sum_{a=1}^{N_A} b_{ia}b_{ja}}{v_j}\right\} + \frac{1}{K}\sum_{k<l}^{N_A}\left\{[1-\theta(h_l-h_k)]\cdot\frac{\sum_{p=1}^{N_P} b_{pk}b_{pl}}{h_l}\right\}, \tag{3.20}$$

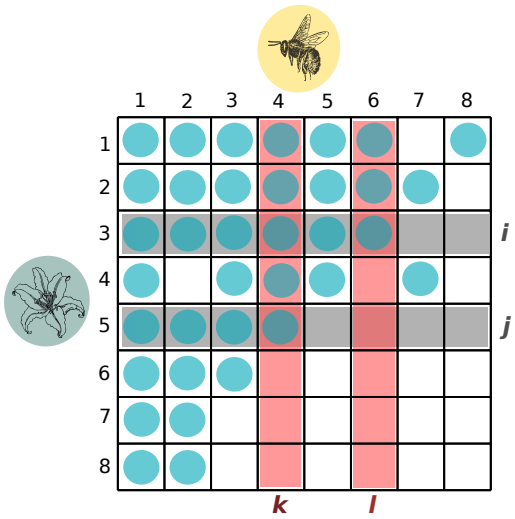

Figure 3.5: Example of an ordered matrix of interactions, not perfectly nested. Species of both guilds have been ordered in decreasing degree, and the numbered labels indicate their rank (the larger the degree, the smaller the rank). The indexes i, j, k and l illustrate our notation for rows and columns.

$$\text{where } K = \frac{N_P(N_P-1)+N_A(N_A-1)}{200}. \tag{3.21}$$

Here we consider that the bipartite adjacency matrix is labeled as shown in Fig. 3.5, such that row i is placed above row j and column k at the left of column l. The K factor introduces the normalization and the θ stands for the Heaviside step function.

In fact, from now on we will use the following abbreviations for the decreasing fill term:

$$\begin{gathered} DF_{ij} = 1-\theta(v_j - v_i) \\ \text{such that, if } v_j \geq v_i \text{ then } DF_{ij} = 0, \\ \text{and if } v_j < v_i \text{ then } DF_{ij} = 1 \end{gathered} \tag{3.22}$$

$$\begin{gathered} DF_{kl} = 1-\theta(h_l - h_k) \\ \text{such that, if } h_l \geq h_k \text{ then } DF_{kl} = 0, \\ \text{and if } h_l < h_k \text{ then } DF_{kl} = 1 \end{gathered} \tag{3.23}$$

Despite being a popular metrics, some authors have raised concerns about the use of NODF to measure nestedness. In particular, as discussed in Chapter 2, Staniczenko et al. (2013) argued that, due to the DF factor, the NODF is unable to detect nested patterns when the proportion of repeated degrees in the network is large. In order to ensure that our results are not affected by this limitation in the sensitivity of NODF, we obtained as well the analytical expressions of the first two moments of the alternative version of the metric called *stable-NODF*, proposed by Mariani et al. (2019). As discussed in Chapter 2, this variant relaxes the decreasing fill condition and hence solves the drawbacks outlined by Staniczenko et al. (2013). The analytical expressions of the first two moments of its distribution in the ensemble can be found in Appendix C. Still, we keep our main focus in NODF given its widespread use for measuring nestedness, together with the fact that the mentioned lack of sensibility is not particularly relevant but for small or highly dense networks (see Appendix C).

We next verify that NODF is Gaussian-distributed in the ensemble, as required if we aim to apply Eqs. 3.18-3.19, by performing a check on a subset of the empirical networks. To this end, for each of the corresponding statistical ensembles we generated a sample of 10^4 networks obeying the probability of link existence given by $\langle \mathbf{B} \rangle^*$. We then computed the nestedness of each sampled network, using NODF, in order to generate the nestedness

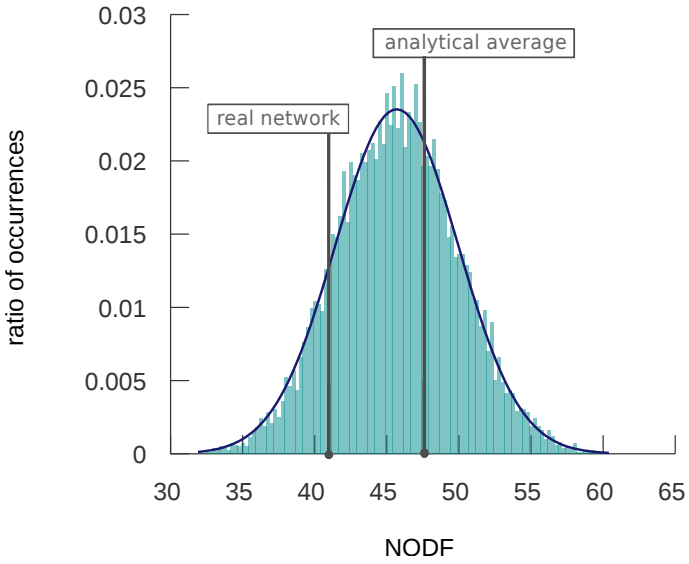

Figure 3.6: Nestedness distribution, measured by NODF, for a sampling of the statistical ensemble corresponding to the empirical networks by Small (1976). In blue, fit of a Gaussian function using the mean and standard deviation extracted from the distribution (mean $\mu = 45.8$ and standard deviation $\sigma = 4.2$). In grey, values of the nestedness of the real network and of the analytical average, which corresponds to the average computed using the analytical expression in Eq. 3.24.

distribution. In all cases we could successfully fit a Gaussian function (see Fig. 3.6 for an example).

Analytical expression for the first moment of NODF

The analytical and packed expression for NODF that appears in Eq. 3.20 can then be plugged into Eq. 3.18. Accordingly, we obtain that the first moment of the randomized NODF for a given real bipartite matrix $\mathbf{B}^*$ reads:

$$\langle \mathrm{NODF}(\mathbf{B}) \rangle^* = \frac{1}{K} \sum_{i<j}^{N_P} \left\{ DF_{ij} \cdot \frac{\sum_{a=1}^{N_A} \langle b_{ia} \rangle \langle b_{ja} \rangle}{\sum_{a=1}^{N_A} \langle b_{ja} \rangle} \right\} + \frac{1}{K} \sum_{k<l}^{N_A} \left\{ DF_{kl} \cdot \frac{\sum_{p=1}^{N_P} \langle b_{pk} \rangle \langle b_{pl} \rangle}{\sum_{p=1}^{N_P} \langle b_{pl} \rangle} \right\}. \tag{3.24}$$

Note that $\sum_{a=1}^{N_A} \langle b_{pa} \rangle = v_p$ and $\sum_{p=1}^{N_P} \langle b_{pa} \rangle = h_a$, given that the randomized matrix necessarily fulfills the enforced constrains. Additionally, this warrants that the ordering of the matrix is equal to the original one, which is important since NODF is ordering-dependent through the decreasing fill terms. It is also of interest to remark that the previous expression can be understood in probabilistic terms. Indeed, given that $\langle b_{pa} \rangle = p_{pa}$, where p_{pa} are independent link probabilities, the overlap term might be seen as a joint probability of two independent events, divided by a normalizing factor which is the union of independent probabilities. For example, for the pair of animal species k and l, the overlap term results in:

$$\frac{\sum_{p=1}^{N_P} \langle b_{pk} \rangle \langle b_{pl} \rangle}{\sum_{p=1}^{N_P} \langle b_{pl} \rangle} = \frac{\sum_{p=1}^{N_P} p_{pk}\, p_{pl}}{\sum_{p=1}^{N_P} p_{pl}}. \tag{3.25}$$

Analytical expression for the second moment of NODF

The standard deviation is given by Eq. 3.19, which for NODF reads:

$$\sigma_{\mathrm{NODF}} = \sqrt{\sum_{p=1}^{N_P}\sum_{a=1}^{N_A}\left(\frac{\partial \mathrm{NODF}(\mathbf{B})}{\partial b_{pa}}\right)\Bigg|^{2}_{\mathbf{B}=<\mathbf{B}>^{*}} \sigma^{2}_{b_{pa}}} \qquad \text{with} \quad \sigma^{2}_{b_{pa}} = p_{pa}\,(1-p_{pa}) \quad , \tag{3.26}$$

where we have used the fact that the existence of a link in the network is a Bernoulli process. Furthermore, the derivative with respect to a general matrix element b_{rc} (the index r stands for rows and c stands for columns) can be split into the contributions of plants and of animals:

$$\frac{\partial\ \mathrm{NODF}(\mathbf{B})}{\partial b_{rc}} = \frac{\partial\ \mathrm{NODF}(\mathbf{B})_{\mathrm{plants}}}{\partial b_{rc}} + \frac{\partial\ \mathrm{NODF}(\mathbf{B})_{\mathrm{animals}}}{\partial b_{rc}}. \tag{3.27}$$

After deriving, we obtained that:

$$K\ \frac{\partial\ \mathrm{NODF}(\mathbf{B})_{\mathrm{plants}}}{\partial b_{rc}} = \sum_{j=r+1}^{N_P} DF_{rj}\ \frac{b_{jc}}{v_j}\ + \sum_{i=1}^{r-1} DF_{ir}\ \frac{b_{ic}}{v_r}\ - \sum_{i=1}^{r-1}\sum_{a=1}^{N_A} DF_{ir}\ \frac{b_{ia}\ b_{ra}}{{v_r}^2} \tag{3.28}$$

$$K\ \frac{\partial\ \mathrm{NODF}(\mathbf{B})_{\mathrm{animals}}}{\partial b_{rc}} = \sum_{l=c+1}^{N_A} DF_{cl}\ \frac{b_{rl}}{h_l}\ + \sum_{k=1}^{c-1} DF_{kc}\ \frac{b_{rk}}{h_c}\ - \sum_{k=1}^{c-1}\sum_{p=1}^{N_P} DF_{kc}\ \frac{b_{pk}\ b_{pc}}{{h_c}^2}, \tag{3.29}$$

which after being plugged into Eq. 3.26 provides an analytical expression for the standard deviation of the distribution of NODF in the ensemble.

Derivation of the theoretical expressions for the *spectral radius*

In this subsection, we derive the theoretical expressions for calculating the average and standard deviation of nestedness using the so-called *spectral radius* (Staniczenko et al., 2013). We performed the statistical measures using this metric due to its increasing popularity among nestedness indices, and, moreover, to its computational advantages: firstly, it is a mathematical property of the graph which does not depend on the ordering of the matrix and, secondly, its numerical calculation is fast. Nonetheless, it is worthy to remind as well that the measures obtained with the spectral radius should be handled with care, since as discussed in Chapter 2 this metric does not reliably quantify nestedness at a fine scale and, moreover, it is not normalized.

Definition and distribution of the spectral radius

The spectral radius was recently proposed by Staniczenko et al. (2013) as an alternative metric for nestedness that directly relies on the spectral properties of the adjacency matrix. Although we already introduced this metrics in Chapter 2, to improve the readability of this thesis we will remind its definition here. Let us call $\mathbf{I}$ the identity matrix and $\mathbf{A}$ the adjacency matrix of a bipartite matrix $\mathbf{B}$, such that:

$$\mathbf{A} = \begin{pmatrix} 0 & \mathbf{B} \\ \mathbf{B}^{\intercal} & 0 \end{pmatrix}, \tag{3.30}$$

which is a square, symmetric and non-negative matrix, given that $a_{i,j} \geq 0$. The spectral radius of the matrix $\mathbf{A}$ (also called *dominant eigenvalue* or *largest eigenvalue*) is defined as follows:

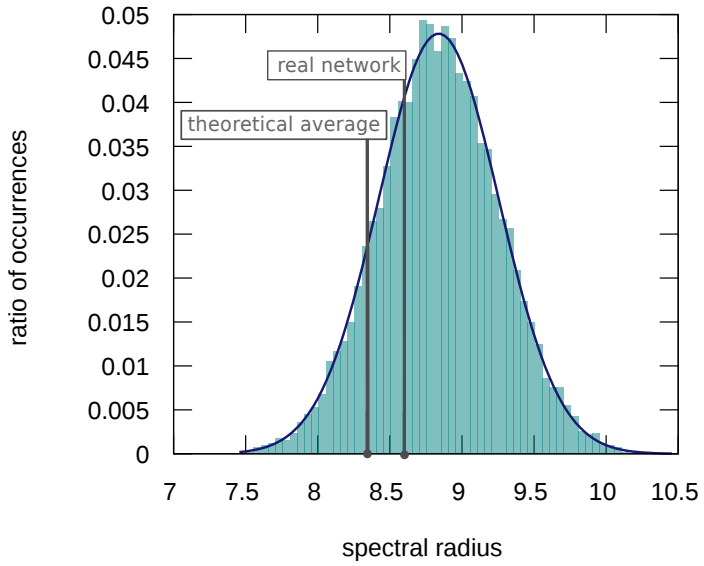

Figure 3.7: Distribution of the spectral radius over the ensemble calculated for the real network collected by Small (1976), for a sampling made of 10^4 networks. In blue, fit of a Gaussian function using the mean and standard deviation extracted from the distribution (mean $\mu = 8.8$ and standard deviation $\sigma = 0.4$). In grey, values of the nestedness of the real network and of the theoretical average, which corresponds to the average computed using the theoretical expression in Eq. 3.33.

$$\rho(\mathbf{A}) = \max\{\,|\lambda_i|\,\}. \tag{3.31}$$

Where λ_i for $i \in \{1, ..., n\}$ are the eigenvalues of $\mathbf{A}$, thus the roots of the equation: $\det(\mathbf{I}\lambda - \mathbf{A}) = 0$. Since $\mathbf{A}$ is a symmetric matrix, $\lambda_i \in \mathrm{Re} \quad \forall i$.

In order to apply the analytical expressions for the first two moments of its distribution, first we checked whether the spectral radius is Gaussian-distributed over the ensemble. In particular, for each network in our dataset, we generated a sample of 10^4 networks obeying the probability of link existence provided by $\langle \mathbf{B} \rangle^*$. Then, we calculated the spectral radius of each sampled network algorithmically using the R package $rARPACK$ (Qiu and Mei, 2016). Finally, we verified that the resulting distribution is indeed normal, as can be seen in Fig. 3.7.

Theoretical expression for the first moment of the spectral radius

Given that $\rho(\mathbf{A})$ is a function of the matrix entries of $\mathbf{A}$, we can apply the linear approximation proposed by Squartini and Garlaschelli in Eq. 3.18, in order to estimate the average over the ensemble computed for a real bipartite matrix $\mathbf{B}^*$:

$$\langle \rho(\mathbf{A}) \rangle^* \approx \rho\left(\langle \mathbf{A} \rangle^*\right), \tag{3.32}$$

where:

$$\langle \mathbf{A} \rangle^* = \begin{pmatrix} 0 & \langle \mathbf{B} \rangle^* \\ \langle \mathbf{B} \rangle^{*\intercal} & 0 \end{pmatrix} \tag{3.33}$$

This means that the average spectral radius can be found as:

$$\rho(\langle \mathbf{A} \rangle^*) = \max\{\,|\langle \lambda_i \rangle|\,\}, \tag{3.34}$$

where $\langle \lambda_i \rangle$ are the roots of the equation:

$$\det(\mathbf{I}\langle \lambda \rangle - \langle \mathbf{A} \rangle^*) = 0\,. \tag{3.35}$$

In practice, Eq. 3.35 has to be solved numerically, which implies that no analytical expression for the average of the spectral radius exists. In particular, we numerically implemented the calculation of the spectral radius of each matrix $\langle \mathbf{A} \rangle^*$ using again the R package *rARPACK* (Qiu and Mei, 2016).

Analytical expression for the second moment of the spectral radius

Using Eq. 3.19, the standard deviation of the spectral radius over the ensemble can be estimated by:

$$\sigma_\rho \simeq \sqrt{\sum_{p=1}^{N_P} \sum_{a=1}^{N_A} \left(\frac{\partial \rho(\mathbf{A})}{\partial A_{pa}} \right) \Bigg|_{\mathbf{A}=<\mathbf{A}>^*}^2 \sigma^2_{A_{pa}}}. \tag{3.36}$$

Here, the calculation of the derivative of the spectral radius, $\frac{\partial \rho(\mathbf{A})}{\partial A_{pa}}|_{\mathbf{A}=<\mathbf{A}>^*}$, is non-trivial, given that there is no general analytical expression for the spectral radius because Eq. 3.35 needs to be solved numerically. Nonetheless, we will now show how is it possible to obtain such derivative by applying the results by Deutsch and Neumann (1984).

Let us start by assuming that $\mathbf{M}$ is a square, non-negative and irreducible matrix. Then, it has been shown that its spectral radius $\rho(\mathbf{M})$ is a simple eigenvalue and it is equal to its Perron root. Since $\rho(\mathbf{M})$ is a simple eigenvalue, it has multiplicity one and it is possible to obtain its first derivatives with respect to $\mathbf{M}_{ij}$. Indeed, if we denote by $\mathbf{D}$ the matrix whose matrix elements are:

$$\mathbf{D}_{ij} = \frac{\partial \rho(\mathbf{M})}{\partial \mathbf{M}_{ij}}, \tag{3.37}$$

then, following Deutsch and Neumann (1984), $\mathbf{D}$ can be computed using the expression:

$$\mathbf{D} = \left(\mathbf{I} - \mathbf{Q}\mathbf{Q}^{\#} \right)^{\mathsf{T}}. \tag{3.38}$$

Here, $\mathbf{Q}$ is a special type of matrix known as *M-matrix* (Kirkland and Neumann, 2012) and defined as:

$$\mathbf{Q} = \rho(\mathbf{M})\,\mathbf{I} - \mathbf{M}, \tag{3.39}$$

while $\mathbf{Q}^{\#}$ is the *group inversion* of $\mathbf{Q}$ (Ben-Israel and Greville, 2003). The group inversion is a more general type of inverse that can be applied as well to singular matrices. For a certain type of matrices, the group inverse is equivalent to another class of inversion known as *Moore-Penrose inverse*. This is true if and only if the matrix of study is *range-Hermitian* (Ben-Israel and Greville, 2003). One of the conditions that warrants that a matrix is range Hermitian is the following:

$$range\,(\mathbf{Q}) = range\,(\mathbf{Q}^H) \tag{3.40}$$

where $\mathbf{Q}^H$ is the conjugate transpose (also called Hermitian conjugate) of $\mathbf{Q}$. If we now assume that $\mathbf{Q}$ is range-Hermitian, expression 3.38 can be rewritten into:

$$\mathbf{D} = \left(\mathbf{I} - \mathbf{Q}\mathbf{Q}^{\dagger} \right)^{\mathsf{T}}, \tag{3.41}$$

where $\mathbf{Q}^{\dagger}$ represents the Moore-Penrose inverse of $\mathbf{Q}$.

Let us show now that Eq. 3.41 can be used to calculate the derivative with respect to our matrix of interest $\mathbf{A}$, in particular in the case where $\mathbf{A} = \langle \mathbf{A} \rangle^*$. Firstly, we will show that $\langle \mathbf{A} \rangle^*$ fulfills the conditions that allow us to apply equation 3.38. Next, we will prove that a matrix $\mathbf{Q}_A$ defined as:

$$\mathbf{Q}_A = \rho\left(\langle \mathbf{A} \rangle^*\right) \mathbf{I} - \langle \mathbf{A} \rangle^*, \tag{3.42}$$

is a range-Hermitian matrix and, consequently, $\mathbf{Q}_A^{\#} = \mathbf{Q}_A^{\dagger}$.

First, we know already that $\langle \mathbf{A} \rangle^*$ is a square and non-negative matrix, yet it remains to be shown whether it is irreducible. A matrix is said to be irreducible if and only if its corresponding graph is strongly connected, that is, if it is possible to find a path that connects any pair of nodes of the network. Because $\langle \mathbf{B} \rangle^*$ is a complete bipartite graph ($\langle b_{ij} \rangle^* > 0 \ \forall i, j$), then it is clear that it is strongly connected and therefore $\langle \mathbf{A} \rangle^*$ is an irreducible matrix.

Second, the condition for the matrix $\mathbf{Q}_A$ to be range-Hermitian is provided by Eq. 3.40. In our case, $\rho(\mathbf{A}) \in \text{Re}$ and $\mathbf{A}_{ij} \in \text{Re} \ \ \forall i, j$, therefore $\mathbf{Q}_{A,ij} \in \text{Re} \ \ \forall i, j$. From this follows that:

$$range\,(\mathbf{Q}_A^H) \ = \ range\,(\mathbf{Q}_A^\intercal) \tag{3.43}$$

Where we have used that the conjugate transpose of a real matrix is simply its transpose. We still need to prove that:

$$range\,(\mathbf{Q}_A^\intercal) = range\,(\mathbf{Q}_A). \tag{3.44}$$

This condition is equivalent to:

$$\text{row space of } \mathbf{Q}_A = \text{column space of } \mathbf{Q}_A. \tag{3.45}$$

Note that this is not true in general. In our case, given that $\mathbf{Q}_A$ is a square and symmetric matrix, its row and column spaces are equal and therefore Eqs. 3.44 and 3.45 are verified. This proves that $\mathbf{Q}_A$ is range-Hermitian and consequently its group inverse is equivalent to its Moore-Penrose inverse. With this we have shown that a matrix $\mathbf{D}_A$ defined by:

$$\mathbf{D}_{A,ij} \ = \ \left. \frac{\partial \rho(\mathbf{A})}{\partial \mathbf{A}_{ij}} \right|_{\mathbf{A}=<\mathbf{A}>^*}, \tag{3.46}$$

can be computed using the following expression:

$$\mathbf{D}_A \ = \left(\mathbf{I} \ - \mathbf{Q}_A \mathbf{Q}_A^\dagger \right)^\intercal, \tag{3.47}$$

which completes Eq. 3.36 and thus provides an analytical expression for the calculation of the standard deviation of the spectral radius. We implemented Eq. 3.47 using the *R* MASS package (Venables and Ripley, 2002), in particular the function *ginv* to calculate the Moore-Penrose inverse.

Significance of empirical nested patterns

With these analytical expressions characterizing the nestedness' distribution at hand, one can now attempt to examine how the nestedness of real networks relates to its null expectation. Indeed, we do so for each of the 167 empirical networks in our dataset. This empirical set includes three different kinds of mutualistic communities (plant-pollinator, seed-disperser and plant-ant), covering a wide variety of geographical locations, climate conditions and species compositions (see Appendix A for further details).

Using expressions 3.24 and 3.26 it is possible to compute the expectation value of nestedness measured by NODF, $\langle \text{NODF}(\mathbf{B}) \rangle^*$, and its standard deviation, for each empirical network in our dataset. A comparison between the expected value of nestedness calculated over the statistical ensemble corresponding to each real network and the actual nestedness of the real network shows a striking agreement, see Fig. 3.8. As reported in Table 3.1, the absolute difference between these two quantities is less than *one* standard deviation for 100 out of 167 networks (59.9%), raising to 158 out of 167 networks (94.6%), if we account for *two* standard deviations. After performing a multiple testing correction (see Appendix D), we find that only 3 out of the 167 empirical networks show significant nestedness (corrected p-value < 0.01). The three of them, which are of a relatively small size (≤ 55 species), were found to be *less* nested than predicted by the statistical ensemble.

Moreover, we verified that these results are not affected by the shortcomings related to the decreasing fill factor, by repeating the above calculations using the index stable-NODF, as detailed in the Appendix C. In fact, the mentioned conclusions not only hold but are also

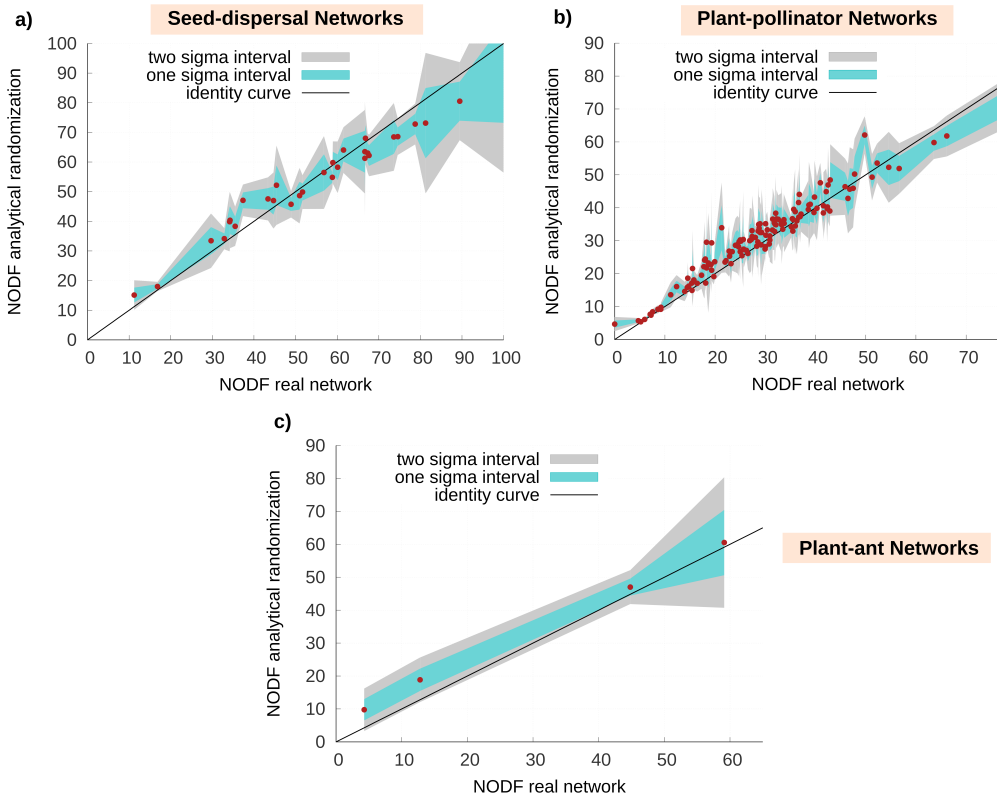

Figure 3.8: Significance of the nestedness of real networks. The figure shows the empirical measure of nestedness against the average value of nestedness in the generated statistical ensemble (red dots) for the 167 real mutualistic networks. The 3 panels correspond to different kinds of mutualistic systems as indicated. The shadowed areas represent one (teal) and two (light gray) standard deviations of the mean. Further details about the number of networks whose nestedness are within these boundaries are provided in Table 3.1. A detailed significant test results in only 3 networks having a statistically significant (in all cases under-represented) nestedness value. Overall, the results indicate that the nestedness of these mutualistic networks is not significant.

Type of community	Fraction of ntws with $\|$z-score$\| \leq 1$		Fraction of ntws with $\|$z-score$\| \leq 2$	
plant-pollinator	82 out of 133	61.7%	126 out of 133	95.5%
seed-disperser	16 out of 30	53.3%	28 out of 30	93.3%
plant-ant	2 out of 4	50.0%	4 out of 4	100.0%

Table 3.1: Results, disentangled into communities, showing the fraction of networks (abbreviated above as 'ntws') whose discrepancy between the real and randomized nestedness is less or equal than one or two sigma. Nestedness is measured with NODF.

strengthen when using this metric, since we find 118 out of 167 networks (70.7%) within a distance of one standard deviation to the mean, and 162 out of 167 networks (97.0%) within two standard deviations.

Additionally, in order to ensure that our findings are not an artifact of using the NODF metrics, we have performed the same analysis for the spectral radius using the analytical expressions in Eqs. 3.34- 3.36. As shown in Fig. 3.9 and Table 3.2, this supplementary

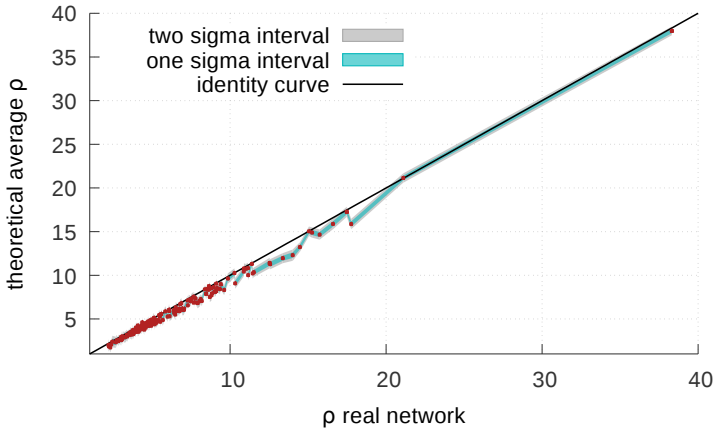

Figure 3.9: Significance of the nestedness of real networks, measured with the spectral radius ρ. The figure shows the theoretical average value of nestedness in the statistical ensemble against the empirical measure of nestedness (red dots) for the 167 real mutualistic networks. The shadowed areas represent one (teal) and two (light gray) standard deviations of the mean.

analysis produces results that are generally in agreement with those reported above for the NODF metric. After performing the multiple testing correction, we found 22 out of 167 networks unexpectedly nested (corrected p-value < 0.01). Although this proportion is larger than the one found by NODF, it can be argued that, given the poor performance of the spectral radius metric at fine scales, it is not necessarily an indication of significant nested patterns but a consequence of the intrinsic limitations of the metric.

Fraction of ntws with $\lvert$z-score$\rvert \leq 1$		Fraction of ntws with $\lvert$z-score$\rvert \leq 2$	
67 out of 167	40.1%	114 out of 167	68.3%

Table 3.2: Fraction of networks whose discrepancy between the real and randomized nestedness is less or equal than one or two sigma, for nestedness measured by the spectral radius.

Finally, as detailed in the Appendix E, we also verified that performing the measures by sampling the ensemble and then computing the distribution of nestedness gives compatible results, both for NODF and the spectral radius. Indeed, this procedure leads to qualitatively analogous conclusions about the non-significance of nestedness. Noteworthy, when performing nestedness measures on a sample of the ensemble it is especially important to consider a proper normalization for NODF. Otherwise, badly normalized calculations can lead to biased observations, a situation which is further discussed in the first section of Appendix E.

Network properties determining nestedness emergence

In the light of the previous results, the next question to be considered is whether we can determine which characteristic of the degree sequences controls how much nested a network is. Taking into account that the degree distributions of mutualistic communities have been reported to commonly follow a (truncated) power-law (Jordano et al., 2003), we propose, as a plausible candidate, the *heterogeneity* in the number of contacts per species. Thus, the hypothesis addressed is that for two networks with identical number of species and connections but diverse degree sequences, the most heterogeneous one –taking into account both guilds– will be as well the most nested.

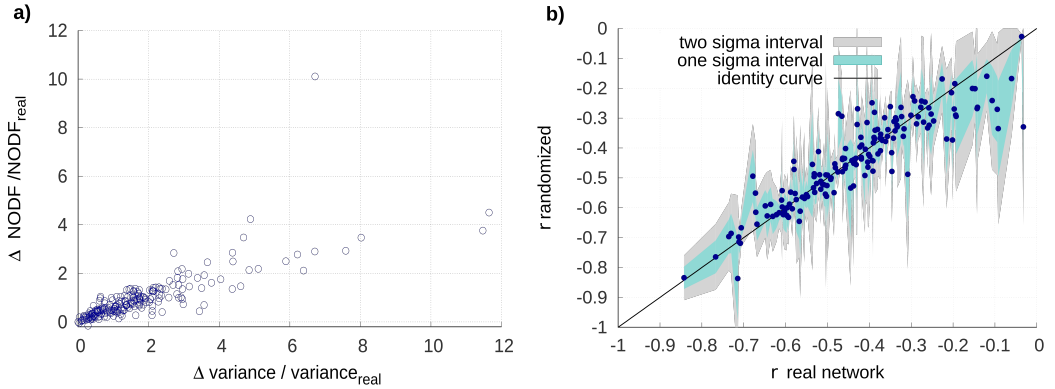

Figure 3.10: Determinants of nestedness. Panel *(a)*: relative change in nestedness and the corresponding change in heterogeneity, measured for the set of 167 empirical networks and the average over the respective rewired ones. We used the rewiring algorithm described in Appendix D. Nestedness is measured using the NODF metric, whereas the heterogeneity is measured through the variance of the degree sequence of the unipartite adjacency matrix. We found a correlation index for a linear fit (excluding the top outlier) of $R = 0.88$. This closely linear relationship discovers a tight bound between nestedness and heterogeneity. Panel *(b)* shows a comparison between the real observation of the degree assortativity r (Pearson's coefficient among degrees) and the average estimation in the statistical ensemble, for the 167 networks of our study. The fact that $r < 0$ for all values indicate that both real networks and the average of the randomized ensemble are naturally disassortative.

To evaluate this conjecture, we made use of a self-organizing network model that is devised with the aim of optimizing the nestedness of a network (Burgos et al., 2007) by rewiring existing links (see Appendix D). After applying this algorithm to our empirical set of networks, we found that the resulting degree sequences are, with respect to the original ones, more heterogeneous and that the final networks are more nested, see Fig. 3.10. This allows to bridge the gap between two structural features that have been classically treated separately, although previous works have already suggested their connection (Perazzo et al., 2014; Jonhson et al., 2013). Interestingly enough, the relationship between network's heterogeneity and nestedness also explains why dynamical implications once attributed to nestedness like the sustainability of communities with a large number of different coexisting species (Bastolla et al., 2009) or the network's structural stability (Thébault and Fontaine, 2010; Rohr et al., 2014), have recently been successfully associated with other properties such as the heterogeneity itself (Feng and Takemoto, 2014) or the species' degree (James et al., 2012; Gracia-Lázaro et al., 2018).

Moreover, accounting for the heterogeneity offers some further insight on the process of emergence of nestedness out of the degree sequences. At first glance, it might not be evident why our null model reproduces so well the empirical nestedness. A priori, we would naively expect that the random ensemble contains both nested and non-nested structures alike, in which specialists appear attached, respectively, to generalists or to other specialists. Although a given number of connections are certainly imposed by the existence of super-generalists as well as by finite size effects, usually there is still room for reshuffling links –like in the "swapping algorithm" (Gotelli and Entsminger, 2001). In terms of mixing, we would say that, concerning specialists, both assortative configurations (nodes have neighbors with degrees similar to their own) and disassortative ones (neighbors have dissimilar degree) are in theory feasible.

Why, then, our algorithm generates disassortative networks as shows Fig. 3.10? Here, the particularity that we used a maximally-entropic ensemble plays a crucial role. Johnson et al. (2010) demonstrated that, in the case of heterogeneous systems, disassortativity is generally more entropic, that is, it is more likely as long as no external pressures are at work. This occurs, to put it simply, because for a species with few interactions there exist many

more chances to engage with another species with numerous connections than matching to a low-connected partner. Therefore, the low significance of empirical nested patterns reported here is directly related to the fact that the number of mutualistic interactions per species is a highly heterogeneous quantity. Jonhson et al. (2013) also observed this fundamental relationship between heterogeneity, disassortativity and nestedness, yet using a finite size configuration model as the one discussed in section 3.2. In our null model, on the other hand, finite size correlations are tempered since the degree sequences are allowed to vary, thus showing that the emergence of nestedness is a genuine entropic consequence of degree heterogeneity.

Discussion

The findings above allow us to finally attempt to answer the question that has motivated this Chapter: is nestedness an irreducible, relevant pattern –or on the contrary, is it just a redundant consequence of lower-order features? The statistical analysis performed clearly demonstrate that, given the degree sequence of real networks, the observed nestedness is not significant –at least for almost all networks considered. Therefore, this suggests that nestedness is not an independent pattern, in sharp contrast to the widely extended belief that it is so. In other words, the observed nested structure of the ecological communities studied is, in fact, a mere entropic effect of the degree sequences of the two guilds.

In the bigger picture, the dependence of nestedness on the number of interactions per species has implications beyond the purely structural construction of the network. As aforementioned, in the recent years several hypothesis regarding the origin of nestedness have been handled, being one of them that it emerges as a byproduct of non-selective processes such as the assembling rules (Valverde et al., 2018; Maynard et al., 2018). In this sense, our observations support the claim that no selective pressures are required for nestedness to emerge, which does not exclude, however, that such pressure could have shaped the degree sequences. That is, our findings demonstrate that nested patterns are not *more* informative of the evolutionary history of real systems than their degree sequences alone. Furthermore, as an additional argument for the non-selection of nestedness, it is important to recall that the networks of our study are, often, both spatially and temporally aggregated. Given the significant variability of species' interactions along time (Chacoff et al., 2018) and space (Trøjelsgaard et al., 2015), the fact that nestedness emerges from a local property like the degrees is a parsimonious explanation. Indeed, degree heterogeneity is a general feature, not only characteristic of the aggregated network but also of its spatial and temporal counterparts. On the other hand, if nestedness were an independent pattern, its emergence would require a specific selection of interactions across time and space, which is a much more intricate process and hence a less simple justification of the origin of nestedness.

All in all, as aforementioned, structural analysis are not sufficient to determine what is the exact mechanism of network formation in ecological mutualistic systems, even if our results clearly support the 'spandrel' hypothesis. In this sense, it is worthwhile making as well some remarks on the limitations of our approach. From the perspective of information theory, the fact that constructing a model where disorder is maximized except for some informed features (what in our case corresponds to the maximization of the entropy given some constraints) eventually succeeds in reproducing the features of a real system, does not entail that the uninformed properties of the system are *truly* random (Gotelli and Graves, 1996). Indeed, it can also happen to be the case that the confluence of a large number of diverse factors sump up into an apparently random aftermath. In the particular context of the factors shaping ecological networks' structure, what we observe is that in order to reproduce empirical observations of nestedness, it is sufficient to provide some information on the degree sequences, leaving everything else unconstrained. Of course, in the absence of further insight on particular formation mechanisms, we will keep calling this the effect of chance –but it is important to keep in mind that our observations are not incompatible with the actual existence of various, or mutually canceling, non-random ecological and evolutionary drivers.

Turning now into the methodological side, these findings have some implications as well. Regarding the long-standing controversies about the use of a proper null model for nested

networks discussed above, our conclusions point out once more the need of incorporating the information contained in the degree sequences. This claim is not new and it can be traced back to the first analysis of nested patterns in biogeography (Connor and Simberloff, 1979), and has been later on reflected in the number of null models that incorporate fewer or more details about the degree sequence. However, null models that involve the degree sequences as a constraint are often intricate and result easily biased. In this sense, the results presented in this section indicate that an appropriate null model for bipartite networks is the set of exponential random graphs for which the probability of finding a graph having the empirical degree sequences is maximized. Indeed, besides the methodological and conceptual unbiased statistical grounds for this maximum entropy framework, this approach exhibits at least two main advantages with respect to alternative methods. On the first place, it overcomes the finite size effects of the FF model, which does not allow for a proper algorithmic randomization (Gotelli and Entsminger, 2001; Ulrich and Gotelli, 2007; Ulrich et al., 2009), hence restraining too narrowly the exploration of the phase space of null matrices. With respect to the PP models, that preserve the degrees on average by constructing a probability of interaction proportional to the species degrees (Ulrich and Gotelli, 2012), it has been shown that the common form of the probability in Eq. 3.1 is subject to bias since it is not a maximum-likelihood choice (Garlaschelli and Loffredo, 2008).

Altogether, while exponential random graph models have been extensively used in other fields like sociology (Robins et al., 2007) or economics (Garlaschelli and Loffredo, 2008; Saracco et al., 2015), their possible application to ecological networks is still largely unexplored. Thus, the methodology implemented here could be a general tool to assess nestedness' significance in a variety of contexts, not necessarily restricted to ecological mutualistic network. Indeed, to facilitate the application of the developed methods to any bipartite network of choice, we provided an open and fully-documented package with the software and several key results of this section (see Appendix G).

In concluding, our results highlight the interest of focusing on the ecological and evolutionary mechanisms that have led to the coexistence of both specialized and generalized mutualisms in the same community (Johnson and Steiner, 2000; Bronstein et al., 2006), giving raise to the observed high heterogeneity of the degree sequences. This is a fundamental challenge, since understanding the way in which structural properties emerge in ecological communities can provide critical clues to depict ecosystems' past assembling, present functioning and future responses –the three witches of the fate mutualism mentioned the introduction. Finally, given that nested patterns have been recurrently detected across systems as diverse as biological, social and technological networks, such findings are expected to have relevant implications beyond the present analysis of ecological mutualistic communities.

3.4 More on the Lagrange Multipliers

The maximum-entropy and maximum-likelihood formalism introduced above not only has allowed us to tackle the question of the origin of nested patterns, but also has provided us with a null model that, interestingly, generates fairly realistic bipartite networks. Indeed, with the only enforcing of the degree sequences in average, the encountered ensembles based on the family of exponential random graphs (ERG herein) reproduce several features of empirical mutualistic networks: first, its density of links, as it would be trivially expected, but also its nestedness and its degree assortativity, which is a surprising finding. A key ingredient of this network model are the Lagrange multipliers, which we may determine by maximizing the probability of encountering the real degree sequences across the ensemble. A natural question that emerges with these results at hand is: what do these Lagrange multipliers represent? Can we assign them an intuitive interpretation, and in particular, do they convey any relevant ecological information?

In this section we briefly explore the possible meaning of the Lagrange multipliers, understanding them as parameters that are closely related to the structural determinants of the ecological community. Indeed, in order to attempt to understand the information carried by Lagrange multipliers (LMs from now on), we can address the problem from different angles. To begin with, we can take once more the perspective of statistical mechanics. In

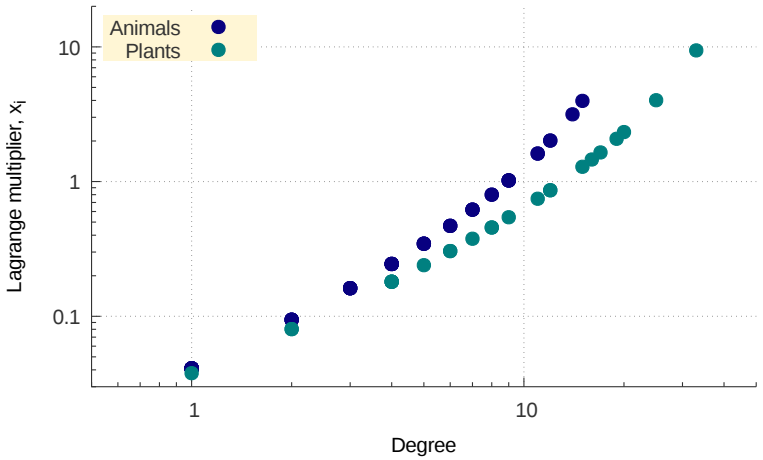

Figure 3.11: Relationship between the Lagrange multipliers and the degrees, for the plant-pollinator network reported by Burkle et al. (2013). The LMs are encountered following the procedure explained in section 3.2 and the Appendix B. In particular, the y-axis shows the x_i and y_j, that correspond to the change of variables used in Eqs. 3.12-3.13, such that $x_i = e^{-\alpha_p}$ and $y_j = e^{-\beta_p}$. The points in light blue correspond to the animals –pollinators–, and those in dark blue to the plants. Both axis are in logarithmic scale.

this case, it is possible to draw an analogy between the canonical ensemble in the network world and the ensemble of states of a physical system in thermodynamic equilibrium with its environment, where the measurable features are thermodynamic properties and one can constrain, for instance, the energy and/or the number of particles (Jaynes, 1957). In this line of thought, the LMs we determined would represent the network analogy to the inverse of the temperature –in the canonical ensemble– and the chemical potential –in the grand-canonical ensemble–. However, despite the theoretical interest of tracing relations between the two applications of the maximum entropy formalism, these analogies do not tell us much more about the specific role of the Lagrange multipliers in the ecological context.

Adopting the viewpoint of network theory instead, we introduced the LMs as the parameters that permit enforcing the chosen constraints. In the particular case of a bipartite network with known degree sequences, we showed above that the relation between the degree of a plant v_p and the LMs is:

$$v_P = \sum_{a=1}^{N_A} \frac{e^{-\alpha_p} e^{-\beta_a}}{1 + e^{-\alpha_p} e^{-\beta_a}}, \tag{3.48}$$

where, keeping the same notation as in section 3.2, α_p represents the Lagrange multiplier of plant p and β_a that of animal a. As aforementioned (see Eqs. 3.12- 3.13), we can write an analogous expression for the degrees of the other guild. Up to now, we have treated these variables simply as undetermined parameters that have to be fixed in order to fulfill the conditions above. Indeed, when determined using the maximum-likelihood approach, we encounter a non-linear relationship between the values of the LMs and the real degrees (see Fig. 3.11 for an example). Howbeit, one can also ask whether it is possible to identify these variables with non-topological quantities, i.e., measurable properties of the nodes related to the intrinsic nature of the empirical system.

As a matter of fact, this has been done both from a theoretical and a empiricist standpoint using the so-called *fitness* models. From a theoretical perspective, this approach consists in assigning a quenched value to each node, such that, as discussed in section 3.2, this quantity eventually determines the vertex's probability of interaction with other neighbors, hence the name 'fitness'. This type of generative models have been proved useful in reproducing non-trivial network structures such as scale-free networks (Caldarelli et al., 2002). The empiricist turn consists, in place of extracting fitness values from a more or less ad-hoc

theoretical distribution, assigning them according to the distribution of a real feature. A successful example that carries out this idea is the work by Garlaschelli and Loffredo (2004), where the authors find that the gross domestic product (GDP) of countries can be identified as the fitness variables determining the topology of the network of commercial interactions among them, i.e. the World Trade Web (WTW). An even more interesting study, that moreover finally relates to the central question of this section, is a continuation work in which Garlaschelli and Loffredo (2008) showed that such fitness values, and thus in turn the GDP, coincide with the Lagrange multipliers obtained when constructing a canonical null model for the WTW –that is, by maximizing the probability of occurrence of the real degree sequence of the WTW in a maximum-entropy ensemble with constrained degree sequences.

Altogether, this suggests that in the present application of the ERG formalism to ecological mutualistic networks, the LMs are not only a theoretical tool but could convey some relevant information about the structural construction of the web of interactions. Therefore, following the spirit of the relationship found by Garlaschelli and Loffredo (2004, 2008), we examined whether the species' abundances could be playing the role of the fitness variables. As aforementioned, the distribution of abundance has been recurrently identified as one of the significant factors shaping the structure of ecological communities (Vázquez et al., 2009), particularly modulating the degree of mutualistic generalization (see section 2.3, especially the discussion on the passive sampling hypothesis).

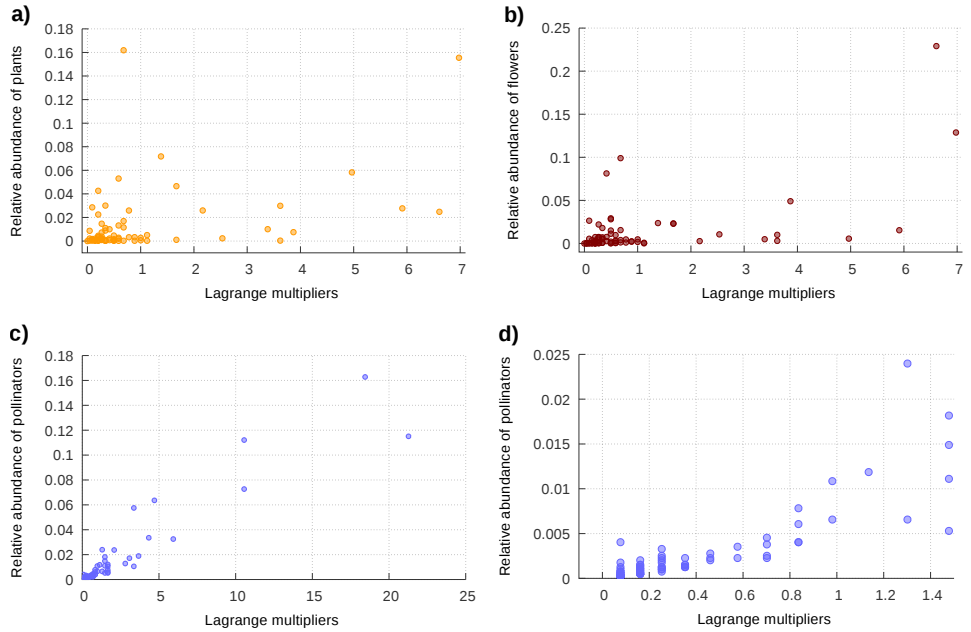

Figure 3.12: Relation among the relative abundance and the lagrange multipliers for: **a)** plants, **b)** flowers and **c)** pollinators. The **d)** panel shows the detail of plot c). The Lagrange multipliers are rescaled to the mean. The data correspond to a plant-pollinator network, collected in the restored site by Kaiser-Bunbury et al. (2009).

In order to address this question, at least preliminary, we analyze two plant-pollinator networks reported by Kaiser-Bunbury et al. (2009, 2010). Both networks were observed in Mauritian ecosystems, but one of them corresponds to a recently restored habitat, while the second one was recorded in a unrestored site. Kaiser et al. also provide the abundances of species, but while the measures of relative abundance of plants were directly estimated through a sampling method based on counting individuals – and the flowering density was estimated similarly–, for pollinators the authors provide an inferred measure, taking as the total abundance per species its total number of observed visits.

Our results (Figs. 3.12-3.13) clearly indicate a positive correlation between LMs and relative abundance for pollinators, but instead we find no correlation for plants species in any of the possible measures of abundance –i.e. flowers abundance or whole plants abundance.

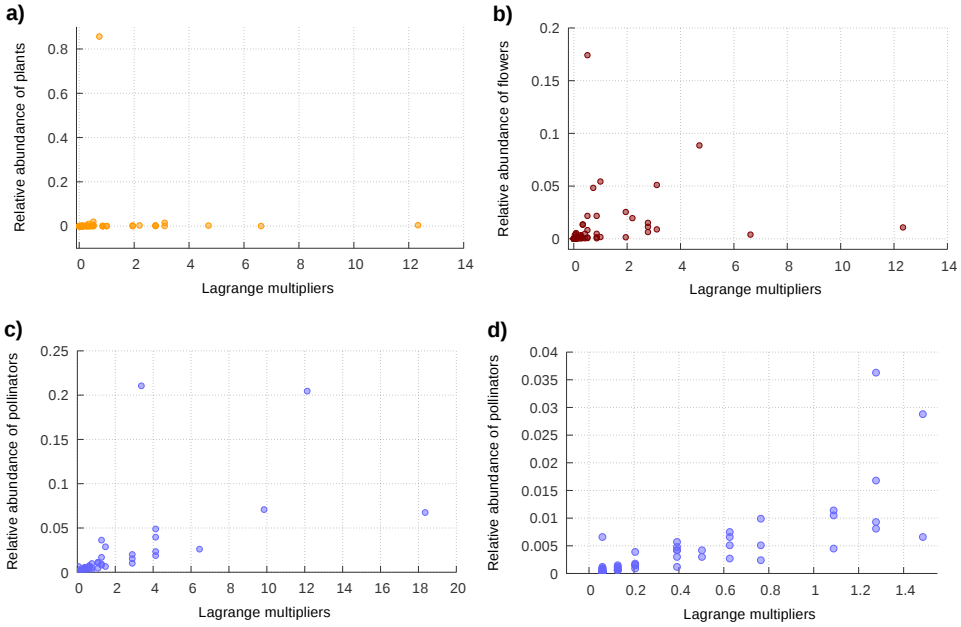

Figure 3.13: Relation among the relative abundance and the lagrange multipliers for: **a)** plants,**b)** flowers and **c)** pollinators. The **d)** panel shows the detail of plot c). The Lagrange multipliers are rescaled to the mean. The data correspond to a plant-pollinator network, collected in the unrestored site –also named control site– by Kaiser-Bunbury et al. (2009). As can be seen, in comparison to the restored site, here the plant population is dominated by a superabundant species.

As a matter of fact, the latter result is in accordance with other studies which claim that, while abundant species tend to be generalists, not all generalists are abundant (Fort et al., 2016). Moreover, considering the observed correlation for pollinators, we can not dismiss the possibility of it being an artifact of the measuring techniques. [3]

On the whole, this suggests that we may be facing a more complex relationship than the one encountered by Garlaschelli and Loffredo (2008) in the context of international trading and calls for further research. Prospectively, other factors such as phenology or traits could be taken as well into account in order to be evaluated as candidates for fitness variables that, hopefully, explain the ecological meaning of the LMs.

3.5 Conclusions and perspectives

Along this chapter we have examined the tight relation between nestedness and chance, by looking first at how evolution might –or in fact might not– account for the complex architecture of interactions within ecological communities, and secondly focusing on the emergence of structural patterns in mutualistic networks.

In particular, by exploiting a powerful randomizing framework based on a maximum entropy and maximum likelihood ensemble, we have demonstrated that the degree sequences ultimately determine the observed nestedness and degree disassortativity of real mutualistic systems. The emergence of these non-trivial features is justified by their highly entropic character, that is, by the fact that they are the most probable configuration of links given the condition of softly constraining the degree sequences, in the absence of other forces. As it has been extensively discussed, such finding has broad implications for the understanding of the origin and the role of nested patterns in ecological communities. Indeed, it alludes that,

[3]Indeed, Kaiser-Bunbury et al. sampling method was based on an equal repartition of observational time among plants, in order to minimize the possible undersampling of rare species. However, this methodology could easily lead to a biased quantification of pollinators' abundance, given that generalist animal species could have a larger probability of being observed.

despite nested patterns entail a certainly non-trivial organization of mutualistic interactions, their complexity is not the product of natural selection –as the so-called panselectionists would assume– but rather the macroscopic consequence of other pertinent structural features, particularly the degree sequences.

Moreover, the adequacy of this null model to accurately reproduce the observed structure of real networks suggests the possibility of developing further applications beyond the present analysis of the significance of nested patterns. For instance, the encountered Lagrange multipliers can be regarded as fitness variables that not only stand as a methodological tool to determine the null ensemble, but also may carry some relevant content about the empirical drivers of the network's architecture. As aforementioned, though, our results concerning this topic are still inconclusive and require future investigations. Another, more direct application of the methods developed along this chapter is the evaluation of other nested metrics, in order to assess their performance and unveil their dependencies on other network parameters. This topic is, indeed, the endeavor of the next Chapter.

CHAPTER 4

Many rulers for one length: how to quantify nested patterns

Admittedly, as a result of the effort to quantify nestedness, a variety of *metrics* with their corresponding *nestedness indices* coexist in the ecological literature. However, since they are based on diverse but not necessarily independent properties of the nested networks, how to compare the degree of nestedness of different ecosystems remains unclear. The situation recalls the well-known history of the definition of temperature in Thermodynamics. Initially defined operationally, i.e., by listing the protocol to measure it, the obtained temperature values suffered from the flaw that they depended on the thermometer used. This problem was solved by the theoretical definition of the temperature based on the Second Principle of Clausius, and finally the notion of temperature was completely understood by the microscopic approach of Statistical Physics introduced by Boltzmann and Gibbs. Interestingly, the first metrics of nestedness defined by Atmar and Patterson (1993) was called *temperature*. This initial proposal was followed by a long struggle to find the best index to measure nestedness, with the development of various approaches ranging from algorithmic procedures to analytical methods. In this chapter we address the question of how to quantify nested patterns by focusing on the comparison between the most relevant of such metrics and their philosophy, performance and details.

As a matter of fact, the metrics defined to quantify nestedness suffer from a critical drawback: as they are strongly dependent on different network parameters like size, fill, etc, the comparison among ecosystems is difficult, even in the case where the same metrics (the same thermometer) is used to measure all the systems. These problems have been reported by several authors, notably on the occasion of the introduction of each new index and/or package devoted to correct some of the shortcomings of previously existing ones (Rodríguez-Gironés and Santamaría, 2006; Almeida-Neto et al., 2008; Dormann et al., 2009; Burgos et al., 2009; Galeano et al., 2009). Still, these works mainly focus on the dependence on the size and the density of links of the network of a few metrics, leaving aside other important nestedness indices as well as the interdependencies among network parameters.

In order to overcome the aforementioned difficulties when measuring and comparing the nestedness of different networks, the standard procedure is to contrast the nestedness value of a given real network with that of a null model (see section 3.2), both calculated using the same metrics. However, while the majority of nestedness metrics have been tested for algorithmically-based null models (Ulrich and Gotelli, 2007; Almeida-Neto et al., 2008), their behavior in maximum-entropy ensembles is still largely unexplored.

In this chapter, we focus on the problem of measuring nestedness by presenting a comparative study of the behavior of the six nestedness metrics reviewed in section 2.4, most of which are commonly included in popular packages and cited in the literature. Our purpose is two-fold: first, we aim to test the performance of these metrics under the maximum-entropy null model explained in Chapter 3 and recently used in Payrató-Borràs et al. (2019), and secondly, we intend to critically assess the functioning of each metrics by analyzing its dependencies with network parameters. By doing this we mean to, first, fill a gap in the literature concerning null models, and second, to provide a practical guide of the advantages and disadvantages of each nestedness metrics.

This chapter is structured as follows. The first section is devoted to introducing a normalized version of the spectral radius. Secondly, we measure the nestedness in the ensemble built for each of the real networks according to each of the metrics and we compare the results with the corresponding nestedness value of the observed network. In the subsequent section, we perform various statistical analyses to determine the relation of each metrics with network properties, like size, fill, degree degeneracy, etc. Next, we discuss the implications of these findings for the performance of each metrics; and we finish the chapter with some general remarks and conclusions on how to choose a nestedness metrics.

4.1 Normalizing the spectral radius

As discussed in section 2.4, the spectral radius is a recently proposed nestedness metrics that exploits the spectral properties of nested graphs (Staniczenko et al., 2013), characterized by being independent of the ordering of the graph and fast to calculate. Nonetheless, an important drawback of the spectral radius is that it is not normalized. Remarkably, the theorem on which it is based (Bell et al., 2008) requires the size of the matrix and the number of links to be fixed, a condition that should be considered in order to set a benchmark against which to rescale the final measure. Although the FF null model respects the required hypothesis, we already discussed that it leads to a poor statistics due to the relatively few number of networks matching these constraints in finite and small systems. For these reasons, we propose to normalize the spectral radius obtained for each system with that of the perfectly nestedness matrix having the same size and fill, as was already suggested by Staniczenko et al. (2013). That is, if ρ represents the spectral radius of a real network and ρ_{max} the spectral radius of a perfectly nested graph with the same size and fill, the normalized index ρ_{norm} is given by the expression:

$$\rho_{norm} = 100\,\frac{\rho}{\rho_{max}} \tag{4.1}$$

In order to calculate the normalized version of this metrics, we need an estimation of the largest spectral radius of a perfectly nested network of the same size and fill. To estimate each of these values, for each real network in our dataset we produced 100 new networks, characterized by being perfectly nested. These networks were generated using the SNM algorithm introduced by Burgos et al. (2007), which preserves the number of connected nodes and links, but modifies the pattern of connections and the degree sequences. This algorithm is divided into two procedures. First, the real network is randomized preserving only the fill and the size –that this, ensuring that every node has at least one connection. Second, the SNM algorithm is performed, which consists of iterating over the following rules:

- *i* We attempt to modify a link by proposing a new partner, randomly selected but different to the original node. The rewiring is susceptible of being accepted only if the new partner has a larger degree than the previous one. This step performs a static version of preferential-attachment.
- *ii* If the proposed reconnection leaves one of the nodes with zero degree, the move is discarded. This ensures that the number of connected nodes does not change, thus preserving the network size.

By iterating over these steps *i* and *ii*, one generates a new matrix which is more nested as well as more heterogeneous in its degree sequences than the original one (see Fig. 3.10). The iteration stops when no more moves are allowed. However, given condition *ii*, this process is not unique and might end up in multiple perfectly nested configurations. To handle this, we generated several optimal configurations per each real network. Specifically, we generated 100 new networks for each empirical network, and exceptionally, for computational reasons, 50 networks for the very large Robertson network. This means that the normalized spectral radius is actually calculated as:

$$\rho_{\mathrm{norm}} \;=\; 100\;\frac{\rho}{\sum_i^{N_{\mathrm{perf}}}\frac{\rho_{\mathrm{perfect},i}}{N_{\mathrm{perf}}}}, \tag{4.2}$$

where ρ is the spectral radius of the real network and $\rho_{\text{perfect},i}$ represents an optimal configuration with the same size and fill of the real network, produced by the SNM algorithm. N_{perf} corresponds to the number of perfectly nested generated, that in general we set to 100.

When sampling the ensemble, we generated 10 perfectly nested networks per each null network ($N_{\text{perf}} = 10$), and in order to keep the calculations computationally feasible we reduced the sampling size to 500 null networks ($N_{\text{samp}} = 500$).

Accordingly, the average normalized spectral radius is calculated as:

$$\langle \rho_{\text{norm}} \rangle = 100 \sum_{j}^{N_{\text{samp}}} \frac{\rho_{\text{null},j}}{N_{\text{samp}} \sum_{i}^{N_{\text{perf}}} \frac{\rho_{\text{perfect},i,j}}{N_{\text{perf}}}} , \tag{4.3}$$

where $\rho_{\text{null},j}$ represents a null network sampled from the statistical ensemble and $\rho_{\text{perfect},i,j}$ represents a perfect configuration produced with the SNM algorithm, having the same size and fill as the corresponding null network.

In the next sections, we study both versions of this metrics: the unnormalized original one along with the normalized modification given by Eq. 4.1.

4.2 Metrics' behavior in the canonical ensemble

To start with, we have measured the nestedness of 191 empirical ecological networks extracted from the *Web of Life* as well as 8 economic networks which represent the trading interactions between the buyers and the sellers of two different fish markets studied by Hernández et al. (2018) (see Appendix A for a detailed account of the dataset). In order to compare the average nestedness over the ensemble with that corresponding to empirical networks, we have used the six metrics described in the section 2.4 plus two variations, namely: the Temperature, the nestedness metrics based on the Manhattan distance (NMD), the NODF and its recent variant the stable NODF, the discrepancy, the nestedness index based on robustness (NIR), and finally the spectral radius and the above introduced normalized modification.

As it has been shown analytically and numerically in the previous chapter, the nested structure of mutualistic networks is a consequence of the double heterogeneity in the degree sequences which results from entropic effects. In order to investigate if the other nestedness indices are able to reveal this dependence, we built a null model for each real network –as explained in section 3.2 and Appendix B– and we compared the nestedness of real networks with their corresponding average over the ensemble. In particular, for each real network in our dataset, we sampled 10^4 null networks with the obtained probability interaction matrix of Eq. 3.17. Across the same sample, each of these null matrices may vary in its size (number of connected nodes), density of links, degree sequence, redundancy of degrees or bipartite matrix eccentricity. Nevertheless, the degree sequences are maintained, on average, equal to the empirical ones.

Next, for each of the studied metrics, the average value of nestedness over the randomized ensemble has been obtained by numerically calculating each metrics over the sampled networks and then constructing the total estimated distribution. The details of the implementation of these measures are given in the Appendix F. For the sake of clarity and to homogenize the reading of the diverse figures, we have transformed the definition of the temperature, the NMD and the discrepancy indices so that the larger the index the more nested the system is. We have also rescaled these indices so that they vary between 0 and 100. These modifications read as follows:

$$T = 100 - T_{AP} , \tag{4.4}$$

$$NMD = 100\ (1 - \tau) , \tag{4.5}$$

$$\Delta' = 100 \left(1 - \frac{\Delta}{E}\right) . \tag{4.6}$$

$$\tag{4.7}$$

where T is the temperature, NMD the nestedness metrics based on the Manhattan distance, Δ is the discrepancy index, and E the total number of edges in the network.

The Fig. 4.1 shows the nestedness measured over the ensemble versus the nestedness of the corresponding real network. Consistently with the results obtained in the previous chapter using NODF and the spectral radius, NIR and NMD also show that the nestedness values of the empirical networks are statistically equivalent to the average of the corresponding randomized ensemble. This leads to the conclusion that the observed nestedness measured by these indices is not significant. On the contrary, the discrepancy and temperature indices show a clear bias, with an important fraction of the real networks being *less* nested than the random average.

4.3 Influence of network features

The results presented in Fig. 4.1 reveal that the metrics studied behave in different ways under the same null model, showing distinct levels of fluctuations and sometimes a systematic bias, as it is the case for the discrepancy and temperature indices. This finding suggests that the different algorithms implemented by each metrics may eventually translate into non-equivalent nestedness measures. We explore further this situation in Fig. 4.2, where we compare the values of nestedness obtained for a group of mutualistic networks when measured using each of the metrics. As it can be observed, for the same dataset not only the value of nestedness itself but also the ranking of the networks according to their degree of nestedness is strongly metrics' dependent.

Ideally, as it has been recalled by several authors (Staniczenko et al., 2013; Ulrich et al., 2009; Almeida-Neto et al., 2008), a well-behaved nestedness metrics ought to be independent of the particular network parameters and, furthermore, rank the degree of nestedness of a given set of networks *universally*. The results discussed above put in evidence that the second condition is not always true. Regarding the first requirement, we next explore more carefully how the nestedness values given by each metrics depend on the network parameters. In particular, since the networks of the dataset cover a wide range of parameter values (see Fig. 4.2 for an example), we analyze the effects of three characteristic network properties: size, density of links and eccentricity. These quantities are defined as follows:

$$\text{size} \equiv s = n + m\,, \tag{4.8}$$

$$\text{density of links} \equiv \phi = \frac{E}{n+m}\,, \tag{4.9}$$

$$\text{eccentricity} \equiv \epsilon = \left|\frac{n-m}{n+m}\right|\,, \tag{4.10}$$

$$\tag{4.11}$$

where, as before, n and m are, respectively, the number of rows and columns of the bi-adjacency matrix, while E is the total number of links. The eccentricity quantifies the difference between the number of nodes of the two guilds, or in other words, the deviation from a square-shaped bi-adjacency matrix. Indeed, $\epsilon = 0$ for a square matrix and $\epsilon \to 1$ when one of the guilds is much larger than the other. Interestingly, most of the large ecological networks observed show more columns (animal species) than rows (plant species), with a frequent ratio of 1 to 3. This observation, though, cannot be generalized to all mutualistic networks, specially to small networks (which can be much more eccentric) or to non ecological systems.

Additionally, we study the dependence of nestedness on a fourth parameter, the degree degeneracy. In particular, a perfect nested matrix with an arbitrary ϕ might have several species of each guild with the same degree. We measure this quantity as:

$$\text{degeneracy in degrees} \equiv g = \frac{\text{number of species with the same degree}}{n+m}\,. \tag{4.12}$$

The study of this parameter remains a special case, since the known connection between the nested patterns and the degree sequences entails that a certain dependency with the

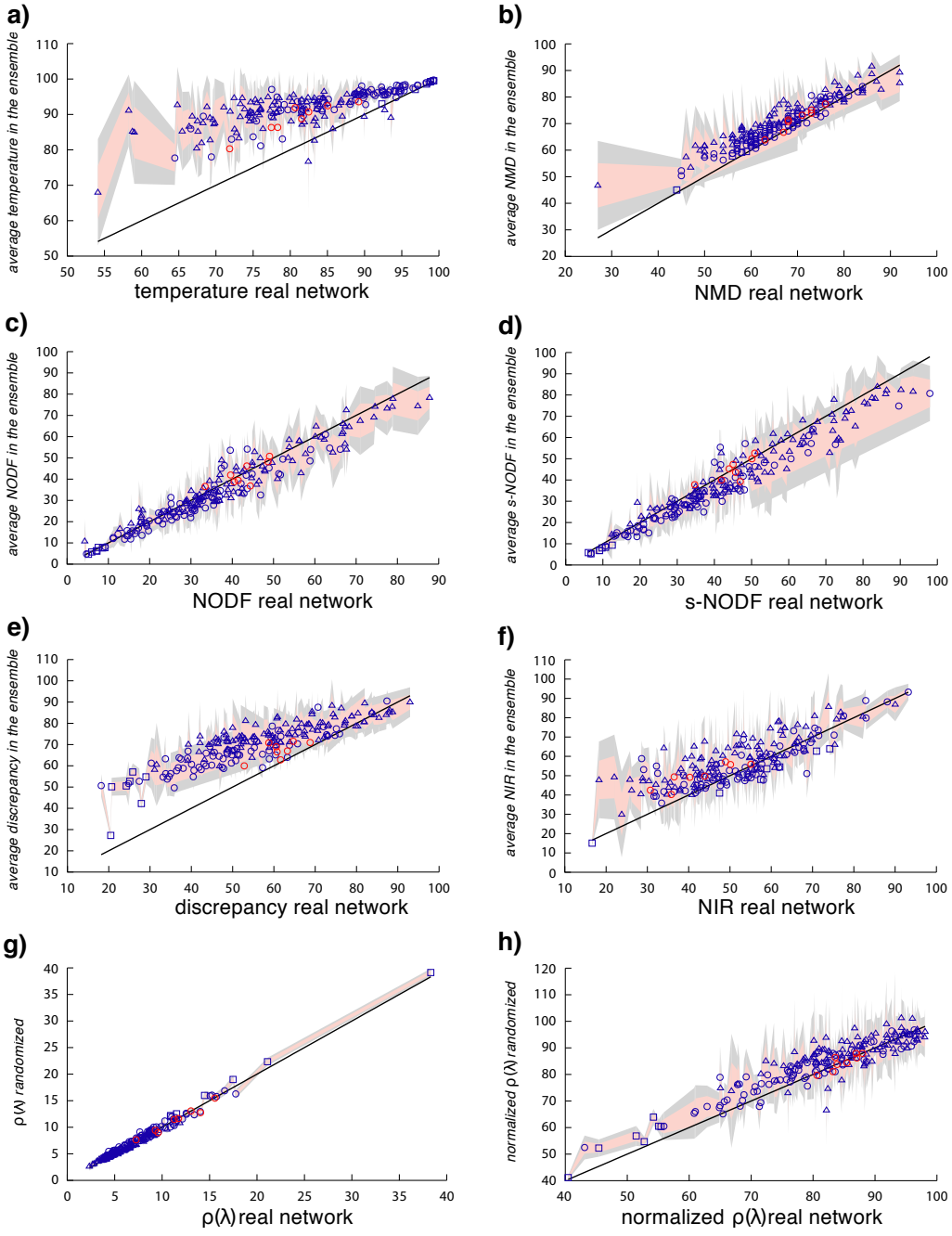

Figure 4.1: Significance of the nestedness of real networks. The figure shows the empirical measure of nestedness against the average value of nestedness in the generated statistical ensemble for the 199 empirical networks in our dataset. The different panels correspond to different metrics: (a) temperature, (b) NMD, (c) NODF, (d) stable-NODF, (e) discrepancy, (f) NIR, (g) spectral radius and (h) normalized spectral radius. The shadowed areas represent one (salmon color) and two (light gray) standard deviations of the mean. The black line depicts the identity curve. Triangle symbols stand for small networks (less than 50 nodes), circles for medium size networks (more than 50 nodes and less than 410) and squares for large networks (more than 410 nodes). Ecological networks are colored in blue, economic networks in red.

degree degeneracy is in fact expected. All in all, we analyze its influence given that each

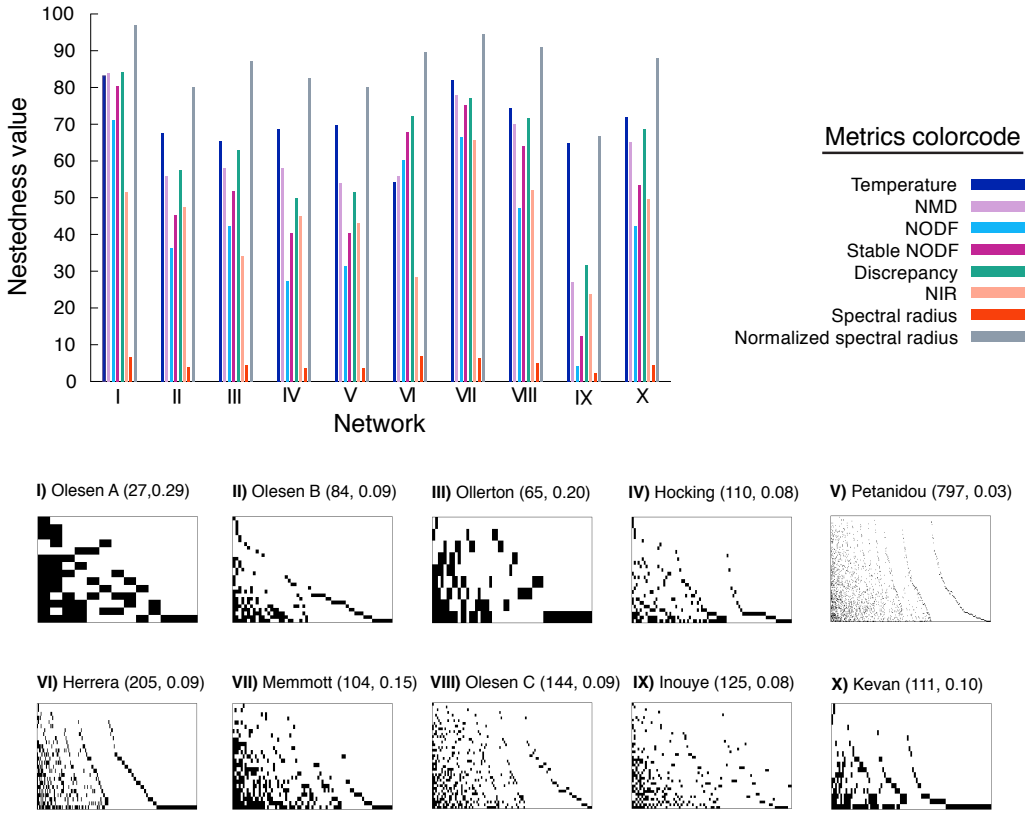

Figure 4.2: Comparison among nestedness indices. The histogram on the top of the figure shows how eight different metrics measure the nestedness of several real networks. Each network, indexed I to X, is represented in the bottom of the figure by its bi-adjacency matrix ordered by decreasing degree, with the interactions among species represented by black pixels. All networks represent plant-pollinator mutualistic communities extracted from the Web of life dataset (Bascompte Lab). Each network is labeled with the name of the first author of the corresponding reference, followed within brackets by, first, its total number of species (number of plants plus number of animals), and second, its density of links.

metrics deals with degree degeneracy in a different way.

In order to quantify the dependencies discussed above we have performed a two-fold analysis. First, we have calculated the Spearman's rank correlation between the nestedness index given by each metrics and the different network parameters. This coefficient allows to assess the relation between both variables without assuming a linear behavior. Fig. 4.3a summarizes the result of the analysis, showing the Spearman coefficient along with its statistical significance for all pairs of nestedness values and network parameters (see the Appendix F for the details on the numerical calculation). Secondly, we have performed a multi-linear regression. In particular, we have taken the nestedness values obtained by each metrics as the dependent variable while the network parameters behave as the explanatory variables. Importantly, in this second analysis we do not consider the effect of the degree degeneracy, since we are mainly interested on the dependence on parameters that should *not*, in principle, determine nestedness. The linear function we have fitted has the following standard form:

$$\nu_j = \beta_{0,j} + \beta_{1,j} s + \beta_{2,j} \phi + \beta_{3,j} \epsilon + \varepsilon \,, \tag{4.13}$$

where ν_j, $j = 1, ..., 8$ represents the nestedness metrics indexed by j, $\beta_{0,j}$ is the intercept and $\beta_{i,j}$, $i = 1, .., 3$ are the partial regression coefficients. The ε represents an error term. This sort of regression informs on the effect of a single network parameter when the rest of parameters are kept fixed. Such consideration is specially important given that, in natural

systems, networks' properties are often correlated (for instance, larger networks tend to be less dense) and therefore bi-variate regressions may misleadingly quantify the influence of a certain property due to the uncontrolled coupled influence of another one. On the other hand, our model assumes a linear relation among the variables which might not always be accurate. Fig. 4.3b shows the results of the regression for each nestedness metrics, in particular, the significance of the partial coefficients corresponding to the different network parameters as well as the value of the adjusted coefficient of multiple determination (see the Appendix F for more details).

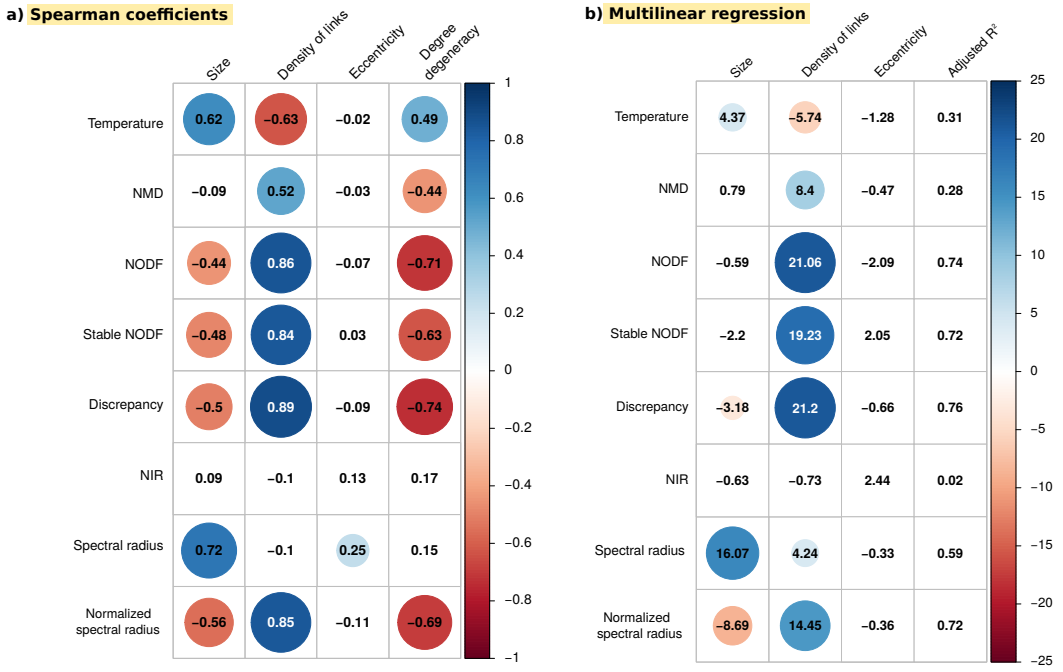

Figure 4.3: Dependency of nestedness metrics on network parameters. The left panel, **a)**, shows the Spearman correlation factor between the networks parameters (columns) and the eight nestedness metrics under study (rows). The numbers represent the value of the Spearman rank coefficient for each corresponding pair of nestedness value and network parameter. Only those coefficients that are statistically significant (p-value < 0.01) are highlighted by a colored circle, being the size and the color of the circle proportional to the coefficient. The right panel, **b)**, summarizes the results of the multi-linear fit detailed in Eq. 4.13. Each row corresponds to a different nestedness metrics. The first column from the right shows the adjusted coefficient of multiple determination (*adjusted* R^2). The other three columns show the *t-ratio* of the regression coefficient corresponding to each explanatory variable (as labelled by the column name). Only those coefficients that are statistically significant (p-value < 0.01) are highlighted by a colored circle, being the size and the color of the circle proportional to its t-ratio.

Once we have quantified the dependencies of the various nestedness metrics on different network parameters, we next explore whether we can explain the deviations with respect to the null model observed in Fig. 4.1. In particular, we perform a multi-linear fit of the type detailed in Eq. 4.13, where we replace the nestedness values by the *z-scores* obtained for each metrics when applying the null model discussed in sections 3.2 and 4.2. Such z-scores are calculated as follows:

$$\text{z-score}_j = \frac{\nu_j - \langle \nu_j \rangle}{\sigma_j} \,, \tag{4.14}$$

where ν_j represents, as before, the real values obtained with a nestedness metrics indexed by j, $\langle \nu_j \rangle$ represents the average nestedness value calculated with metrics j over the null ensemble and σ_j represents the standard deviation of the distribution of nestedness in the

ensemble for the same metrics. By fitting a linear function analogous to Eq. 4.13 we obtained, thus, the partial coefficients which account for the contribution of each network parameter to the corresponding z-scores. A summary of these results can be found in Fig. 4.4.

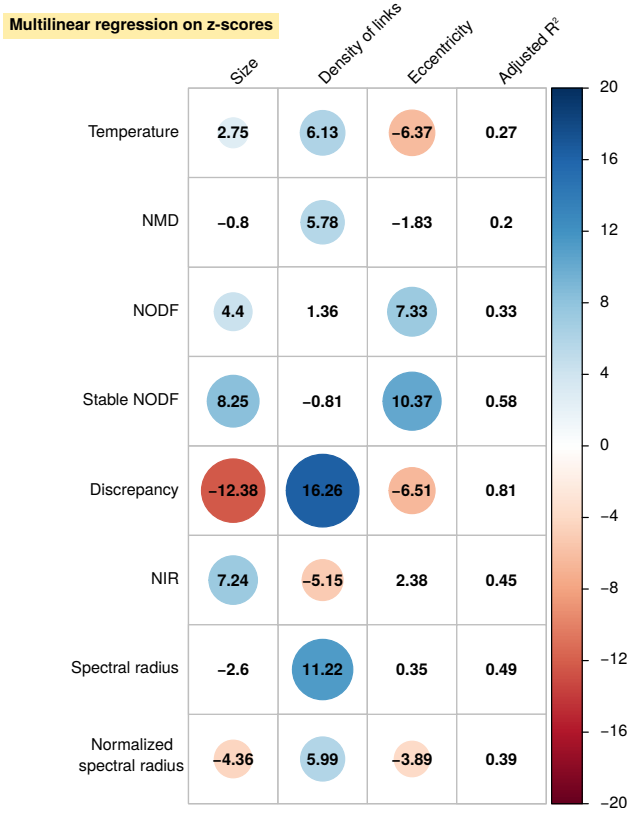

Figure 4.4: Dependency of z-scores on network parameters. The figure summarizes the results of a multi-linear regression between the z-scores values corresponding to each nestednes metrics and network properties. Each row corresponds to the z-scores obtained by applying to each metrics the null model discussed in section 3.2. The first column from the right shows the adjusted coefficient of multiple determination (*adjusted* R^2). The other three columns show the *t-ratio* of the regression coefficient corresponding to each explanatory variable (as labelled by the column name). Only those coefficients that are statistically significant (p-value < 0.01) are highlighted by a colored circle, being the size and the color of the circle proportional to the t-ratio.

4.4 Critical analysis of each metrics

In the previous section, we have quantified the influence of several network properties on various nestedness metrics, taking into account how each metrics measures the nestedness of empirical networks as well as how they compare to the null model of section 3.2. With this information at hand, we now proceed to critically evaluate the performance of each metrics by discussing and framing the observed dependencies in a general context.

Temperature

Despite its popularity, this metrics was already known to have several flaws (Almeida-Neto et al., 2008) and various authors have outlined the presence of ambiguous steps in its calculation (Rodríguez-Gironés and Santamaría, 2006; Mariani et al., 2019). Indeed, Almeida-Neto et al. (2008) called up on its dependency on the density of contacts, ϕ, and on the size of the matrix. We confirmed these dependencies since our statistical analysis shows that real values correlate positively with size and negatively with the density of links (see Fig. 4.3).

Interestingly enough, the temperature is as well the only metrics to show a significant positive correlation with the degree degeneracy, while the rest of metrics penalize the repetition of degrees.

Moreover, when tested against the null model, the temperature exhibits a clear bias (see Fig. 4.1). In fact, the average nestedness in the ensemble is systematically larger than the real observations. The multilinear regression performed using the z-scores shows that they correlate significantly with the size, the density of links and the matrix eccentricity. As shown in Fig. 4.1, the bias of this metrics shows a negative z-score value, therefore its modulus (which gives the relative distance to the identity curve) increases when the size of the network is smaller, less dense and more eccentric. Given that mutualistic ecological networks usually present low density and a pronounced eccentricity, these conclusions point out that the temperature metrics should be applied, if at all used, with care in the ecological context.

NMD

Our analysis of the nestedness metrics based on the Manhattan distance shows that it correlates positively with size and negatively with the degree degeneracy. Interestingly, the deviations with respect to the null model are sensibly smaller than in the temperature metrics, though a slight but systematic positive deviation still appears leading again to a negative z-score. The multilinear regression indicates that the z-scores are mainly explained by the density of links, which have a positive influence meaning that denser networks fall closer to their null expectation.

Overall, the NMD metrics exhibits notably less dependencies than its close metrics temperature, which with the NMD shares a common spirit given that both metrics measure somehow the distance of unexpected interactions. This dissimilarity is probably due to the different normalization of the NMD given in Eq. 2.5. On the other hand, such normalization is dependent on the null model used (Corso et al., 2008), and hence the metrics is inevitably subject to the same limitations (see the Appendix F for more details on the implementation of NMD, in our case using the FF null model).

NODF and stable NODF

In the work in which the NODF metrics was firstly proposed, Almeida-Neto et al. (2008) found a positive dependency with the matrix fill. In our analysis, we recover this result and observe as well a negative correlation with the network size (see Fig. 4.3a) which is nonetheless a veiled consequence of the variation in the density of links, as can be understood after performing the multilinear regression (see Fig. 4.3b). Furthermore, this nestedness index exhibits a good agreement with the null prediction, as was already found in the previous chapter. The differences with the null model, quantified by the z-score, are explained mainly by the size and the eccentricity. As expected from a statistical point of view, the small and eccentric networks show the largest difference with the null expectation.

Although the NODF metrics is nowadays extensively used, some authors have raised a few concerns about its adequacy. In particular, Staniczenko et al. (2013) criticized the decreasing fill factor in its definition, which penalizes degree degeneracy. Indeed, we do observe a strong negative correlation with degree degeneracy for NODF in Fig. 4.3a. As a solution, Mariani et al. (2019) proposed an alternative version of the metrics called stable-NODF, which does not incorporate this decreasing fill. Our analysis determines that dependencies of both versions of the metrics are very similar: on the one hand, the stable-NODF does moderate the correlations exhibited by NODF both on degree degeneracy and density of links, but on the other hand, the correlations of the z-scores with the size and eccentricity are strengthened.

Discrepancy

The discrepancy index shows a significant dependency on the size and the density of links, being the latter parameter the dominant one as it can be seen from the multilinear regression (see Fig. 4.3). These dependencies had been noted already (Almeida-Neto et al., 2008).

Interestingly, these findings are very similar to the correlations observed for NODF and stable-NODF, despite the fact that the metrics are based on distinct strategies for measuring nestedness.

On the other hand, the test against the null model reveals that for an important fraction of networks the real value of nestedness is smaller than the average in the ensemble, resulting in a systematic deviation with negative z-scores. This shift is very well explained by the regression of the z-scores summarized in Fig. 4.4, where it can be observed that the three network parameters studied correlate significantly with the z-scores. Indeed, the larger, less dense and more eccentric the network, the more distance there is between the null expectation of nestedness and the empirical value.

NIR

The nestedness index based on network robustness exhibits no dependencies on the network parameters. Indeed, our statistical analysis reveals no significant correlation with any of the studied properties (see Fig. 4.3). This suggests that, despite not being particularly popular, the NIR metrics is a reliable option for measuring nestedness. At the same time, the analysis done using the null model indicates that the nestedness value of smaller and denser networks tends to fall further apart from their null expectation. Indeed, this is a consequence of its definition, which relies on the difference between the areas of the ATCs obtained by the DDR and IDR node removal strategies. As the curvature of the former reproduces the shape of the IPN, it becomes less convex as the density increases, leading to a loss of sensitivity of this index. Therefore, this metrics is well adapted for ecological networks that usually show low densities, but less suited for other bipartite networks, like the aggregated market networks.

Spectral radius

Among the metrics described, the spectral radius shows a significant dependency on both the size and the density of links, specially the former one. Indeed, larger and denser networks tend to have a larger spectral radius. This is a consequence of the lack of normalization, as mentioned above. However, the spectral radius shows a remarkable agreement between the average over the ensemble and the value of the corresponding real network, along with a very low dispersion. Nonetheless, the z-scores correlate significantly well with the density of links, being the most denser networks the ones that exhibit a larger discrepancy with the null model.

In order to hinder the strong dependency on the network size, we evaluate as well a normalized version of the spectral radius. In particular, we weight the nestedness of each network with respect to the maximally ordered matrix with the same parameters as explained in the Methods section. Taking into account this normalization, it is now possible to compare the degree of nestedness of networks of different sizes, and to study how different network parameters affect the nestedness index. We find that this normalized version of the spectral radius correlates positively with the density of links, and negatively with the size and the eccentricity of the matrix. Notably, these dependencies are analogous to the ones shown by the NODF, stable NODF and discrepancy indexes. At the same time, the analysis against the null model reveals a slight deviation towards a larger value of the average in the random ensemble with respect to the empirical value. This deviation is stronger for larger, less dense and more eccentric networks.

Besides the mentioned dependencies, when using the spectral radius, it is essential to consider its underlying basis for measuring nestedness. As we pointed out in the introduction, the relation between the spectral radius and the degree of nestedness is not strictly monotonic, but only holds on statistical terms. This hampers its usefulness to rank networks according to their nestedness.

4.5 Conclusions: how to choose a metric?

In this chapter we have addressed the question of how to quantify nested patterns, taking into account the large variety of metrics available in the literature. Indeed, although it has

recently been shown that nestedness is not an emergent irreducible property of the network, it still remains an interesting quantity to measure, as it constitutes a global property that informs on the heterogeneity of the degree distributions of the guilds. This is particularly relevant for ecological networks because of their typical, rather small sizes preclude a correct fit to a fat tail distribution, like a power law, on the available data. Because of the interest in ecology for this property, different definitions of nestedness coexist in the literature. These metrics usually quantify some property of the network following a precise protocol, leading to *operational definitions*. Moreover, several of these metrics are integrated into packages widely used by network ecologists to assess the nestedness values of different networks. This lack of a unique definition generates confusion when it comes to the comparison between the nestedness values of different networks.

In this chapter, we have performed a systematic comparative study of the performances of six different metrics and the variants of two of them, addressing their dependency on various network parameters. Based on a large database of real systems, our results clearly put in evidence that the different metrics show diverse dependencies on size, density of contacts, eccentricity and degree degeneracy. Therefore, if the same group of networks is ranked according to their nestedness, the outcome will depend on the metrics used. Understanding these dependencies for each metrics has helped us to explain, as well, the systematic shifts between the real values of nestedness and the average over a null model based on a maximum-entropy, maximum-likelihood ensemble.

Altogether, our results point out that the NIR index is, by far, the most independent metrics with respect to the considered network parameters, although it suffers from a lack of sensitivity when the density of contacts is high. Moreover, the NODF, the stable NODF, the discrepancy and the normalized spectral radius all show very similar dependencies, that is: a positive correlation with the density of links and, for the latter two, a negative correlation with the size. While a dependency with the size is undesired and ought not to appear when using a proper normalization, some authors have claimed that a positive correlation between nestedness and fill is in fact expected (Almeida-Neto et al., 2008).

From a methodological perspective, this analysis could provide a useful guide addressed at practitioners since it compiles the different characteristics, advantages and drawbacks of the most popular nestedness metrics. Moreover, it complements the theoretical results discussed in the previous chapter by extending the use of maximum-entropy-based null models to a large set of metrics. Finally, this study is accompanied by a repository called *Nullnest* that allows to calculate all the nestedness indicators studied, generate the null ensemble for any network, as well as a database with the already calculated probabilities allowing to generate the null models for the 199 networks studied here (see Appendix G).

PART II

Mutualism in motion

CHAPTER 5

Beyond the aggregated paradigm

This chapter inaugurates the second part of the thesis, along which we will continue looking at mutualistic networks yet from a fairly different perspective. Indeed, while in the previous part we were occupied disentangling the existence of redundant patterns in empirical systems, here we will try to bring our attention to a very diverse, almost opposite -in terms of the general spirit- task. In particular, we will attempt to understand how by neglecting the temporal dimension of real mutualistic communities, that is, by working with the aggregated version of the interaction networks, we can loose relevant insight into the organization and functioning of natural ecosystems. In this sense, we will try to incorporate into the network formalism the information about empirical phenology, namely the biological activity cycles of species that, to a certain extent, constrain and articulate how ecological relationships occur among individuals.

This endeavor is certainly not entirely new (Olesen et al., 2008; Encinas-Viso et al., 2012; Sajjad et al., 2017; Ramos-Jiliberto et al., 2018; Chacoff et al., 2018) and, in fact, during the recent years the need of moving towards a more realistic depiction of ecological communities has been stressed more than once (Ings et al., 2009; Heleno et al., 2014). All in all, aggregated networks are still paradigmatically used in the characterization of the structure and dynamics of mutualistic systems. Along the following sections we will address this issue by examining the effects on the perceived network architecture of taking into account -at least partly- the temporal dimension of mutualism, while the next chapter will be devoted instead to exploring its implications for species persistence by using dynamical population models.

Accordingly, the present chapter is organized as follows: we will start introducing some basic notions on phenology; next, we will characterize two real datasets and how their networks of interactions vary along the season; and, in the third place, we will propose a set of synthetic models for phenology that permit assessing and contrasting the effect of temporal variability beyond the scarce number of open datasets.

5.1 A short tale on phenology

From cherry blossom to digital cameras

The bloom of flowers in spring, the arrival of the first migratory birds or the shedding of leaves at fall are all simple yet beautiful examples of phenological events that undeniably shape, since ancient ages, our perception and narration of time, especially the passage of the seasons. Our language and culture is full of references to this sort of phenomenon and their timing, from words like 'late bloomer' to Aristotle's famous phrase '*one swallow does not make a summer*'. Naturally, hence, we can find as well remarkably old instances of documented phenological patterns, not only related to agricultural needs –as was the case for the first empirical ecological networks described in Chapter 1– but also in cases in which their timing marked the date of religious or traditional festivities. A fascinating illustration is the viewing of cherry blossom in Japan, known as *hanami*, a celebration that started in the eight century as an elitist ceremony and gradually became a general festivity. Nowadays, it is so popular that the cherry blossom is nightly forecast in Japan and the advance of the front of blossom across the country -the so-called *sakura zensen*- is keenly followed (see Fig. 5.1). As

a result, it is possible to find extensive datasets on the phenology of various species of cherry tree along the years –mainly the *Prunus serrulata*-, comprising more than seven centuries of blossoming information (Aono and Kazui, 2008). In fact, this kind of sequential data have been used to reconstruct springtime temperatures of undocumented old periods. Similarly, analogous studies have been carried using alternative species' phenology around the globe, such as the grape plant to produce wine in France (Chuine et al., 2004).

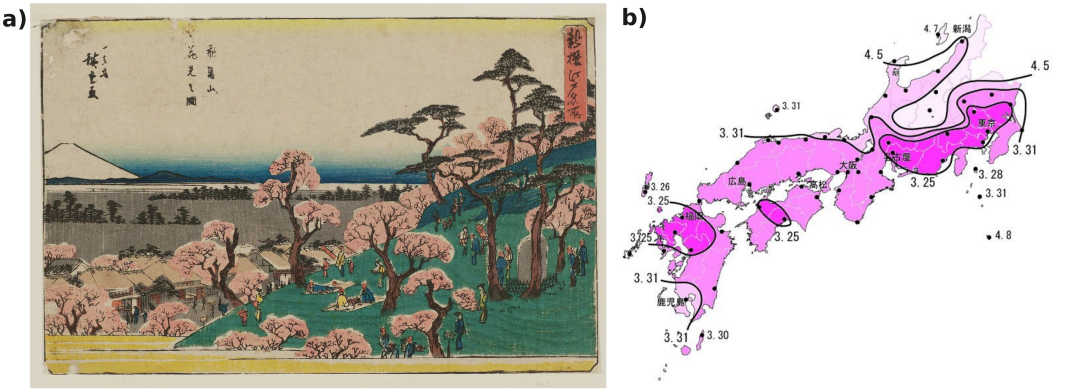

Figure 5.1: In **a)**, picture called *Asukayama hanami no zu* (Cherry-blossom viewing at Asuka hill) by Utagawa Hiroshige, dated about 1831. In **b)**, forecasting of the dates of blossoming across Japan in 2007. The numbers represent the month and day of the blossoming, being the darker areas the ones where blossoming is expected earlier. Source: Wikimedia commons.

While these datasets were constructed by relying, basically, on visual and small-scale observations, during the last decades technological advances have permitted a multiplication and diversification of the means to measure phenology of both plants and animals. Such methodology ranges from citizen science projects where participants format and share individual observations of phenology in their local area (Havens and Henderson, 2013), to the use of sophisticated remote sensing tools based on satellite data (Zhang et al., 2003). A particularly ingenious case among these novel approaches is the work by Graham et al. (2010), in which they process the images recorded by public cameras connected to the Internet -primary related to traffic surveillance or national parks- to gather information on vegetation phenology across North-America, exploiting a free source of glances of trees and plants unintendedly caught by the cameras. Nurtured by these methodological advances as well as spurred by the investigations on how climate change influences phenology (Memmott et al., 2007; Hegland et al., 2009) –a topic that we will discuss in some more in detail in the next chapter–, nowadays we face an undeniable increase in the quantity and the quality of documented phenology.

Paradoxically, though, this copious amount of phenological data comes at little help, at least directly, when trying to better understand mutualism along time. This is due to the fact that public empirical data on both the network of interactions *and* the timing of their mutualistic activity is, to put it mildly, scarce. Consequently, previous studies examining the effect of phenology on mutualistic communities either focus on a very reduced number of highly-resolved networks (Olesen et al., 2008; CaraDonna et al., 2017; Ramos-Jiliberto et al., 2018), either they succeed in keeping the big numbers of phenological data at the expense of roughly approximating the patterns of mutualistic relationships –that is, by neglecting the real complex networks of interactions (Duchenne et al., 2020). A third approach, yet, to address the lack of data, is to explore instead synthetic models either for phenology or for the network of interactions (Kallimanis et al., 2009; Encinas-Viso et al., 2012). In what follows, these limitations will condition us as well. But before jumping into that, let us summarize the main characteristics of the phenology of plant-pollinator communities.

Ecological and evolutionary determinants of phenology

Although phenology certainly plays a part in different types of ecological mutualism, in this thesis we will focus on its implications for plant-pollinators communities, both because it is a paradigmatic example in which seasonality is strongly marked and also because, despite the aforementioned data limitations, the phenology of plants and pollinators is in general better documented than that of other mutualistic species (Rafferty et al., 2015).

The study of the phenology involves all temporal aspects of species' life cycle, regarding on the one hand the timing of their various stages of development, i.e. egg/seed, larvae, adult, etc; and on the other hand the onset and duration of different biological processes such as flowering, germination, pollination, leaf falling, etc. Such timing is determined by a myriad of factors, similarly to what occurs with mutualistic interactions as described in section 2.3. Indeed, both biotic and abiotic forces shape the phenology of species, which, in addition, is thought to be subject to evolutionary change (Rathcke and Lacey, 1985; Forrest and Miller-Rushing, 2010). To complicate things further, several sources of intra-species phenological variability occur simultaneously: inter-annual (Olesen et al., 2008; Cirtwill et al., 2018) –that is, among different seasons–, geographical (Post et al., 2018) –for the same species but on diverse sites– and last but no least, individual, i.e. among different individuals of the same population, even those coexisting on the same site and at the same season (Forrest and Miller-Rushing, 2010).

All in all, from a statistical viewpoint a few general patterns have been identified that, hopefully, will permit us gain further insight into the general rules governing phenology. In particular, we will focus on two fundamental phenological quantities of plant-pollinator systems: first, we will look at the *starting dates*, that is, the time at which the flowering –in the case of plants– or the pollination –for animals– begins, and secondly we will consider the so-called *periods*, that is, the length or duration of this active state, during which mutualistic interactions are, on paper at least, possible. Of course, this selection of phenological indicators is far from being exhaustive, and other works have modeled the different stages of plants and pollinators in more realistic detail (Ramos-Jiliberto et al., 2018). Instead, in our approach we will approximate this complex landscape of temporal variability by focusing only on the adult phase of the species, and moreover, reducing the whole possible set of biological processes and stages to a couple of states: *active*, namely when the species could potentially hold a mutualistic relationship –i.e. pollinate or be pollinated–, or *inactive*. In Fig. 5.2 we depict this schematic representation for an hypothetical plant and its pollinator. Indeed, this sort of simplification is not novel and other works have adopted analogous approaches (Memmott et al., 2007; Encinas-Viso et al., 2012; Burkle et al., 2013).

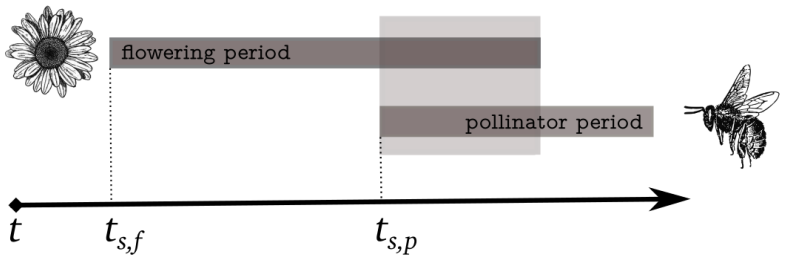

Figure 5.2: Schema of the phenology of a plant and a pollinator, represented by their *active* states. Each species is defined by its period and its starting date, called here $t_{s,f}$ for the flowering plant and $t_{s,p}$ for the pollinator. The section of time during which the two species overlap and can actually interact is highlighted in grey.

Regarding the periods of activity, in general both plants' and pollinators' periods tend to follow right skewed distributions, with a small number of species exhibiting a long phenophase while a large number of species are active only during a short time (Bawa et al., 2003; Kallimanis et al., 2009). Particularly, Kallimanis et al. (2009) examined the statistical

distribution of period's lengths in a Mediterranean scrub community observed along four years by Petanidou et al. (1995), and concluded that the distribution of pollinator's periods could be fitted by a decreasing exponential, while plants' followed a lognormal distribution. On the other hand, in a plant-pollinator system in the Arctic, Olesen et al. (2008) identified a lognormal shape for both plants and pollinators' periods, and a normal distribution for plants in one of the years of their observation.

In what concerns the onset of flowering and pollinating activity, a complementary measure that is often used is the *middle date*. In this sense, evidence suggests that they tend to be relatively synchronized (Rathcke and Lacey, 1985; Tébar et al., 2004). For example, both Olesen et al. (2008) and Bawa et al. (2003) observed that most active periods temporally coexist at a peak, probably due to a similar reaction to a common set of physicochemical stimuli such as temperature, photo-period, humidity, etc (Rathcke and Lacey, 1985). In statistical terms, this would correspond to a scenario where the middle dates are relatively clustered, as modeled for instance by Kallimanis et al. (2009) using a normal distribution. At the same time, genetic factors seem to play as well an important role in determining the timing of flowering or pollinating activity, which hence contributes to explain the heterogeneity of starting dates. On the other hand, it has also been hypothesized that species may spread along the season in order to minimize competition. Although the evidence supporting this hypothesis is controversial (Rathcke and Lacey, 1985), some authors have proposed that such minimization could still occur within a temporal range determined by genetic and environmental constraints (Kochmer and Handel, 1986).

In conclusion, this short summary illustrates the complexity of the temporal dimension of plant-pollinators communities. Indeed, temporal variability not only appears at different scales, from days to decades and from individuals to species, but it is furthermore regulated by a multiplicity of factors. In the next section, we analyze two empirical datasets of phenology in order to examine whether the statistical characteristics aforementioned hold, and then we use them to evaluate how our understanding of mutualistic networks can change when moving beyond the aggregated paradigm.

5.2 Phenology in a network: characterization of two datasets

In this section we will focus on studying two empirical examples of plant-pollinator systems, that contain, at the same time, detailed information about their phenology and their web of mutualistic interactions. In particular, we will analyze the plant-pollinator community recorded by Burkle et al. (2013) together with the community measured by Kantsa et al. (2018), which includes two consecutive years of observations and hence two networks. The specificities regarding each dataset and how we processed them before the analysis can be found in Appendix A. In what follows, for the sake of convenience we will refer to them simply as the *Burkle dataset* and the *Kantsa dataset*.

With the aim of understanding how the network description changes when we introduce temporal variability, this section is divided into two parts: first, we will examine the main characteristics of the empirical phenology under study; secondly, we will monitor how the structure of the network varies on a daily basis beyond the static description we are already familiarized with. In detail, we will characterize how it affects both mutualistic and competitive interactions within the community.

Statistical properties of phenology

We begin by exploring the statistical characteristics of the two phenological datasets. We will first look into the distribution of periods lengths and compare them with the literature discussed above. Secondly, we will address the effect of coupling this phenological information with the network of interactions, which results in a distribution of mutualistic and competitive overlaps. These analysis will pave the way for, eventually, introducing some synthetic models to recreate the effects of phenology on the network's structure at the end of this chapter.

Distribution of periods

We start by examining the distribution of the duration of the activity of plants and pollinators. In particular, we fitted a variety of functional forms on the cumulative distributions using a maximum likelihood estimation. Then, we tested the quality of the fit by performing a Kolmogorov-Smirnov test by bootstrapping, as explained in detail in Appendix H.1.

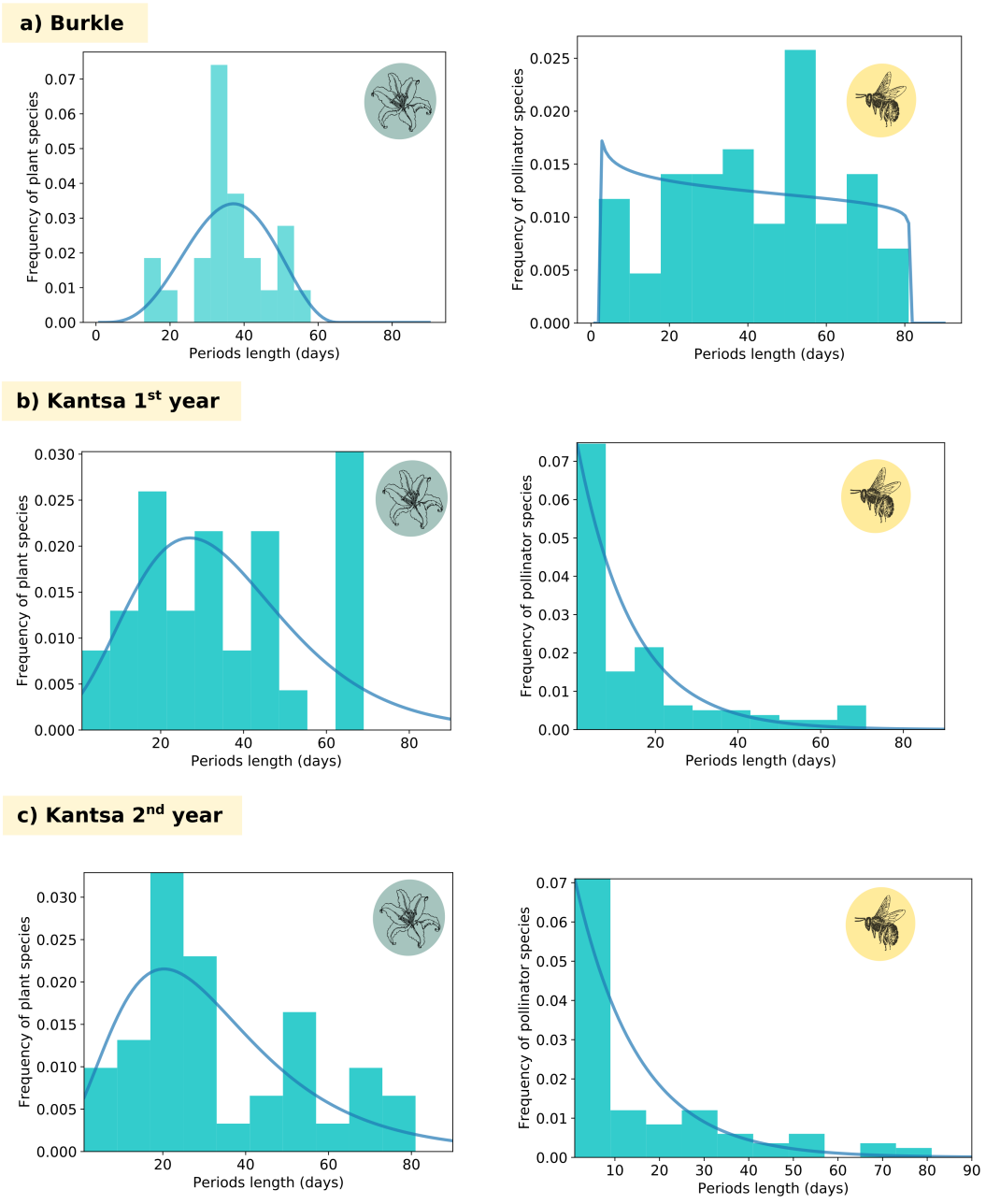

Figure 5.3: Empirical distribution of the periods length for plants (right pannel) and pollinators (left pannel), corresponding to three different real datasets. We show the fitted beta distribution for the Burkle's dataset, for both plants and animals. For the Kantsa dataset, we could fit a lognormal for plants and we fitted an exponential for pollinators. In Table 5.1 we summarize the significance of each fit. Although we show here the binned histograms, the parameters of each fitting function were estimated using the unnbined, discrete empirical distributions.

In more detail, we tested three different functional forms: lognormal, exponential and the beta function. As aforementioned, the first two distribution types have been claimed to correctly describe some empirical observations, while we introduce the latter as a generic fitting. The results of the p-value for the KS-test are reported in Table 5.1, where we highlighted in bold the good-quality fits. As can be seen in Fig. 5.3, the two datasets exhibit very different shapes: the Burkle dataset is better fitted by the beta function, while in the Kantsa dataset we could fit a lognormal to the distribution of plants' periods but we found no unique fit for the pollinators. In general terms, the distribution of periods of the Burkle dataset is less heterogeneous, while the Kantsa distributions are clearly righter-skewed. This is especially notorious for the periods of the pollinators, among which we find a large proportion of species with very short period -one or two days- as can be seen in Fig. 5.3. This particularity is what makes this case especially difficult to fit, although its plot suggests an exponential shape.

Dataset	Lognormal fit		Exponential fit		Beta function fit	
	Plants	Pollinators	Plants	Pollinators	Plants	Pollinators
Burkle	0.021	0.018	0.001	0.001	**0.63**	**0.18**
Kantsa 1st year	**0.67**	0.014	0.029	0.001	**0.41**	0.001
Kantsa 2nd year	**0.50**	0.001	0.018	0.001	0.02	0.001

Table 5.1: Results of fitting different functional forms, disentangled into plants and pollinators. We show the p-value of the fit, and highlight in bold the good quality fits, that is, those which do not significantly differ from the estimated distribution (p-value > 0.05). The p-values are obtained by performing a Kolmogorov-Smirnov test between the fitted distribution and the empirical sample, then comparing it to the corresponding K-S distribution sampled by bootstrap as explained in Appendix H.1.

Distribution of overlaps

As a matter of fact, the relevance of phenology goes beyond the individual characterization of species' traits. Indeed, it regulates as well the ecological interactions within the community, affecting both their occurrence and intensity. Such relationships involve of course the different kinds of mutualism we have been considering so far, but also indirect interactions like competition for shared mutualistic resources (Jones et al., 2012), which naturally emerges among species of the same kind. The negative effects of these antagonistic interactions are known to coexist with mutualism, leading to a trade-off between costs and benefits as explained in Chapter 1 (Bronstein, 2001). This means that addressing how phenology impacts antagonistic interactions might be just as important as understanding its effect on mutualism.

In order to be able to calculate the consequence of temporal variability not only among mutualistic partners but also among competitors, we need to compute the network of competitive interactions based on shared resources. We do so following the proposal by Gracia-Lázaro et al. (2018), namely, projecting the empirical biadjacency matrix of mutualistic interactions $B_{i,k}$ into the subspace of intra-guild interactions such that:

$$\text{if} \quad B_{i,k}B_{j,k} = 1 \quad \text{then plants } i \text{ and } j \text{ compete for the pollinating services of animal } k, \tag{5.1}$$

$$\text{if } B_{i,k}B_{j,k} = 0 \text{ then } i \text{ and } j \text{ do not compete for the resources of pollinator } k, \tag{5.2}$$

which leads to a competitive network between all pairs of plant species i and j. Analogously, we can define the competitive interactions among two pollinator species k and l as follows:

if $B_{i,k}B_{i,l} = 1$ then pollinator species k and l compete for the flower resources of plant species i, (5.3)

if $B_{i,k}B_{i,l} = 0$ then k and l do not compete for the resources of plant species i. (5.4)

This completes the description of the ecological community in the sense that the observed network of pollinating contacts not only mediates the explicit mutualistic interactions, but also the implicit, competitive relationships among species of the same guild.

Returning to our main problem, the most straightforward consequence of introducing phenology into an ecological network is the modification of the amount of temporal coexistence –the so-called *overlap*– among species. Indeed, we find a continuum of possible scenarios ranging from full concurrence to absence of overlap, as shown in Fig. 5.4. These overlaps concern either two species in the mutualistic case, or three species –two species of the same kind and the shared resource– when considering competition.

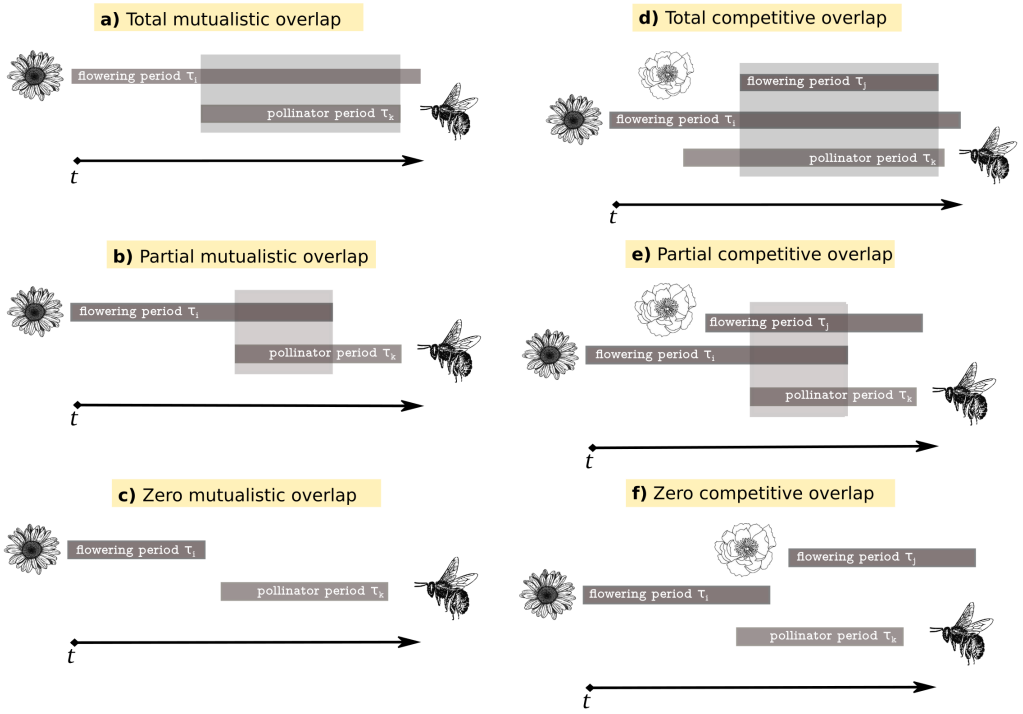

Figure 5.4: Diversity of phenological configurations giving rise to different types of mutualistic and competitive overlap. The pannels on the left represent the mutualistic overlap between the pollinator species k and the plant species i, from the viewpoint of the pollinator species k. In **a)** there is full mutualistic overlap, in **b)** there is only partial overlap and in **c)** there is no overlap at all. Pannel **d)** depicts the competitive overlap between three species, particularly two plants i and j competing for a shared pollinator species k. In this case the overlap is referred to the first pollinator species, j. In **d)** the competitive overlap is full, in **e)** there is only partial overlap and in **f)** there is no overlap at all between the competitors.

Within this framework, we can introduce a set of phenological coefficients $\{\Phi\}$ and $\{\Omega\}$ to quantify the effect of the phenological overlap on, respectively, the mutualistic and the competitive interactions. In the particular case of a plant species i interacting mutualistically with a pollinator k and competitively with another plant j, we define these coefficients as follows:

$$\Phi^P_{ik} = \frac{\tau_{ik}}{\tau_i}, \tag{5.5}$$

$$\Omega^{P}_{ijk} = \frac{\tau_{ijk}}{\tau_i}, \tag{5.6}$$

where τ_i stands for the period of flowering of the plant species i, τ_{ik} represents the temporal overlap between the plant species i and its pollinator k (see Fig. 5.4 a-c for a graphical representation), and finally τ_{ijk} stands for the overlap between plants species i and j and their pollinator k (see Fig. 5.4 d-g for an example). An analogous set of coefficients can be drawn for the pollinators.

Note that, as can be seen in Eqs. 5.5-5.6, the overlaps are pondered by the period of activity of the species –in the example above, the plant i–, which means that each coefficient is always referred to a certain plant or animal species. This particular normalization implies, moreover, that the effect of the temporal overlap is non-symmetric among the interacting partners. Although this might not seem very relevant now, we will see its consequences in the next Chapter when we address the study of the community dynamics.

In order to obtain some insights into the impact of phenology at a network level, we calculated the distribution of phenological overlaps $\{\Phi\}$ and $\{\Omega\}$ for each dataset. The results presented in Fig. 5.5 show that the two empirical cases we have at hand exhibit clearly different shapes. In what follows, we will explore how these quantities can contribute to changing our perception of the structure of the community along time.

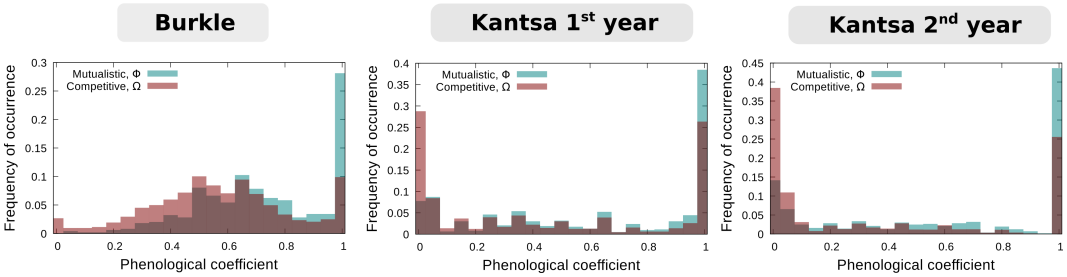

Figure 5.5: Histogram of the phenological coefficients $\{\Phi\}$ and $\{\Omega\}$ defined in Eqs. 5.5-5.6 to account for the mutualistic (in blue) and the competitive (in red) overlap. Each pannel corresponds to a different dataset, as indicated on the top of the figure.

Disentangling the structure

With this summary about the general characteristics of each dataset at hand, we can now turn our attention into the aforementioned question: how does the perceived structure of the network change if we take this empirical information into account? In order to attempt to answer this problem and depict the temporal variation of the network's structure, we construct a discrete temporal sequence of networks, where each element corresponds to a different *snapshot* of the system, taken at a different moment of the season. In particular, given that the level of detail of both empirical phenologies is narrowed to *days*, we construct a set of daily networks, representing the mutualistic interactions observed among plants and pollinators on a given date. To do so, we use the empirical information on the starting and ending dates of activity of plants and pollinators, and remove from the daily network certain mutualistic links among species whenever they do not coincide in time – i. e., when their phenological overlap, as defined in Eq. 5.5, is zero. Additionally, we also remove inactive species as well as active species with zero degree. On the whole, this provides a coarse-grained description of the community as shown in Fig. 5.6, that, even if it is not a pure temporal network, it does account to a great extent for the intra-annual temporal variation, moving beyond the static network formalism.

Using this information, we measure a set of fundamental structural features for the different networks of the sequence, in particular: the number of active nodes, the number of active links, and the maximum degree. Fig. 5.7 provides a summary of the evolution of these properties along time, for each of the empirical networks in our dataset. To begin

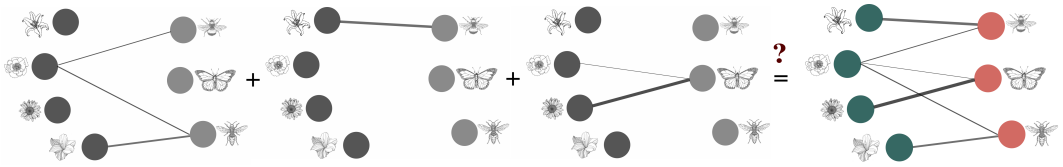

Figure 5.6: Schematic representation of the coarse-grained description of temporal variation. Each network in grey-scale corresponds to a different day of the season, where certain species and interactions might be absent. Summing up these interactions produces the aggregated network, depicted in color, where the information on the turnover of species and interactions is lost. Despite this aggregation process is indeed quite simple, a pertinent question is whether the structure and dynamics of the temporal snapshots is comparable to that of the aggregated network.

with, in both cases the temporal measures are significantly smaller than their aggregated counterparts, although this was already expected. What is more interesting is that the evolution of the two datasets exhibits a clearly different behavior over the season: while in the Burkle dataset the three quantities show a marked peak approximately at the middle of the season, in the Kantsa dataset they stay relatively stable around a certain value, showing an almost flat shape. Moreover, in the Burkle dataset the maximum of the peak represents around the 75-80% of the aggregated counterpart, whereas in both instances of the Kantsa dataset this quantity descends to less than 30-40%.

In the bigger picture, there are very few studies which permit assessing the generality –or rarity– of these observations, although a recent work by Sajjad et al. (2017) examined the structure of a plant-pollinator system in analogous terms and obtained similar results to those described for the Burkle dataset. Overall, the remarkable differences among empirical examples suggest that introducing the phenology into the network formalisms does not yield a unique pattern, but instead the resulting patterns are highly system-dependent. Truth be told, this finding raises more questions than answers, ranging from the reasons beneath the divergences among the communities to the implications for the stability and robustness of ecosystems. The inherent difficulty in addressing these issues is aggravated by the lack of publicly available datasets beyond the few examples we study here. As a result, we devote the next section to explore a set of synthetic models, constructed using a minimal number of assumptions, and seeking those that better reproduce the observed characteristics of empirical systems.

5.3 Going synthetic

The idea of constructing synthetic models that account for unobserved features of the community, either mutualistic interactions or phenology, has been partly addressed before as we recalled in section 5.1. Nevertheless, the majority of these previous works incorporate empirical phenology as a fixed input while focusing, hence, on modeling the ecological network. An illustrating pair of examples of this approach are the works by Kallimanis et al. (2009) and Vázquez et al. (2009), in which the authors propose a diverse set of null models to explore the role of phenology as a possible determinant of the interaction probability among species.

In this section we adopt an almost inverse perspective and consider, instead, the problem of modeling the undocumented phenology of a system whose network of mutualistic interactions is known. That is, we place the emphasis on modeling the temporal variability of the system. As aforementioned, this is a persistent problem given that, despite the existence of large repositories of real ecological networks, such datasets ordinarily lack the details about the species' phenology. Shifting the focus onto modeling the phenology of a given network permits, therefore, addressing questions that traditionally revolved around the network's structure, like the emergence of patterns or their implications for the community dynamics.

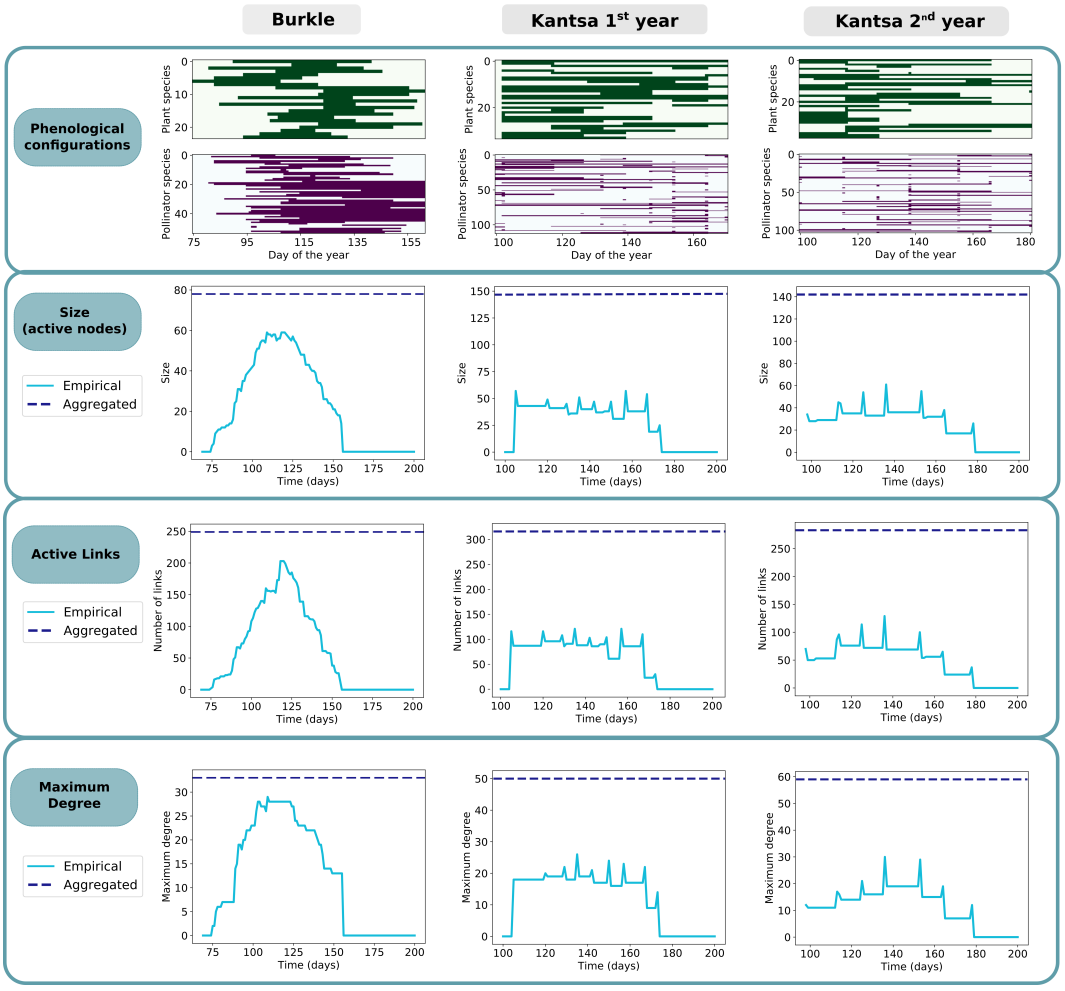

Figure 5.7: Phenological configurations and temporal evolution of three fundamental structural features. On the top, schema of the temporal arrangement of the periods of activity of plant species (green) and pollinators (purple) along the season. Below, the temporal variation of three basic structural parameters, measured on a daily basis: number of active nodes, active links and maximum degree. Each column corresponds to a different dataset as indicated on the top of the figure.

Accordingly, here we will propose and explore a group of models designed to generate synthetic phenological configurations building into different assumptions. The remaining of the section is organized as follows: first, we describe and discuss the conceptual basis behind each null model; and secondly, we compare the generated phenology with the real datasets characterized above, in order to determine which null model better reproduces empirical examples.

Description of the synthetic models

As explained in section 5.1, we will work with a stylized representation of the temporal variability, where the phenology of each species is defined by two elements: the starting date and the period of activity. These two quantities are thus the parameters to be set by the synthetic model, under the condition that mutualistic partners share a non-zero mutualistic overlap. This requirement ensures that the binary mutualistic network is preserved equal to the observed one, constituting a formalism that focus explicitly on modeling the phenology.

Determining these two groups of phenological parameters is non-trivial given that, as we reviewed at the beginning of this chapter, the seasonal patterns of species' activity are driven

by a multiplicity of factors. However, in what regards the periods, a straightforward solution could be to extract them from either one of the realistic distributions tested in Table 5.1 (see for instance the work by Encinas-Viso et al. (2012) for a similar approach), either following a general, not necessarily realistic function that can serve for hypothesis testing. On the other hand, the specification of the starting dates under the mentioned constraints is slightly more challenging, which is why here we will pay special attention to it. Subsequently, we will assume that the periods are already given, and focus on how the starting dates might be fixed in order to warrant that mutualistic partners share a certain phenological overlap.

Before entering into further details about the different synthetic models, let us briefly discuss the particularities and consequences of preserving the network of interactions. As aforementioned, we will construct a model under the requirement that the phenological overlap among mutualistic partners is comprised in the range $(0, 1]$, excluding the zero in order to ensure that the two species still interact. This means that, strictly speaking, we will only keep the *binary* mutualistic network. In other words, the general idea consists in constructing a synthetic phenology that is *compatible* with the given network treated in binary terms.

In this line of thought, the constraint that mutualistic partners share non-zero phenological overlap may be written as an inequality for each species' starting date. For instance, let us take a plant i with period p_i^P and unknown starting date $t_{0,i}^P$, who is interacting with an animal j with period p_j^A and an unknown starting date $t_{0,j}^A$. In order to ensure that their periods overlap, it must be fulfilled that:

$$t_{0,j}^A - p_i^P + 1 \leq t_{0,i}^P \leq t_{0,j}^A + p_j^A - 1\,, \tag{5.7}$$

where we have assumed a daily coarse-graining, such that the minimal overlapping unit is one day. In order to ensure that all interacting species share phenological overlap, we may write an inequality analog to Eq. 5.7 per each link in the bipartite network. Then, if we take the starting dates as unknown variables, we can view the problem of constraining the starting dates as a multivariate system of linear inequalities composed by N unknown variables and L inequalities (where N and L are respectively the number of nodes and the number of links of the network). Note that both $\{t_0^P\}$ and $\{t_0^A\}$ are unknown variables, which means that the system of inequalities is coupled.

Furthermore, in order to ensure that the resulting distribution is realistic, we can introduce an additional set of constraints. In particular, we impose a lower and upper bound for the starting dates of activity, which ensures that the community exhibits some seasonality, a characteristic that has been empirically observed (Rathcke and Lacey, 1985; Kallimanis et al., 2009). If we represent by l the lower bound and by u the upper bound delimiting the season, then the condition on the starting date of a general species i can be written as:

$$l \leq t_{0,i} \leq u - p_i + 1. \tag{5.8}$$

Overall, Eqs. 5.7-5.8 represent a coupled system of linear inequalities, where the parameters to be determined are the starting dates. Although a problem of this kind might not generally have a feasible solution, in our particular case the existence of some trivial solutions –e.g. the same starting dates for all species– warrants that the system is consistent.

Within this framework, we present a group of approaches that, under different assumptions, permit determining the set of synthetic starting dates while fulfilling the conditions in Eqs. 5.7-5.8. In particular, we explore four possible scenarios, corresponding to different fundamental hypothesis about the main factor governing the species' phenology, namely: *(i)* species' periods tend to be synchronized, *(ii)* species seek to organize their activity as to minimize their intra-guild competition for mutualistic resources, *(iii)* species periods get maximally dispersed along the season, *(iv)* in the absence of further information, the starting dates can be determined using a minimal model of maximum entropy.

As can be observed, each of these assumptions relies on a single dominant factor. Indeed, hypothesis *(i)* and *(ii)* are rather intuitive and mechanistic, in the sense that they place the emphasis on environmental and ecological drivers of the phenology. Instead, the scenarios *(iii)* and *(iv)* function as non-mechanistic models based on statistical properties of the distribution of starting times, regarding either their dispersion or their entropy. Of course, since biotic and

abiotic forces do not act separately, one could construct a more complex model where various of these factors operate simultaneously. In this sense, these synthetic models constitute a first-order approach, which nonetheless, as we will see, yield some interesting results. In what follows, we define each of these models one by one and describe how we numerically implemented them.

Synchronized phenology

This model is based on the assumption that the level of synchronization in the community is high, hence most species' activity temporally coincide at the peak of the season. As we reviewed in section 5.1, empirical evidence suggests that seasonal systems usually exhibit non-negligible synchronization, in the sense that the flowering and pollination of species tend to occur simultaneously. Several hypothesis have been proposed to account for this pattern, from the presence of abiotic pressures such as the temperature, the precipitation or the photoperiod –disregarding genetic differences or biotic constraints– (Forrest and Miller-Rushing, 2010), to the existence of facilitative interaction among concurrent species, which obtain an ecological benefit of overlapping their periods of activity. All in all, it is still not clear how the mentioned factors interplay among themselves and with other possible forces to give rise to the observed heterogeneity in starting dates (Forrest and Miller-Rushing, 2010).

In order to attempt to reproduce this pattern, we construct a model were species' periods are approximately centered. To do so, we set the medium dates around the peak of the season and then slightly perturb them, following the numerical procedure detailed in Appendixes I.1 and I.3. This leads to phenological configurations where species are considerably –but not perfectly– synchronized. Indeed, introducing this imperfection is crucial for two reasons: first, to account for the aforementioned heterogeneity in starting and middle dates of activity; second, because a perfectly synchronized system is trivial, in the sense that all species fully overlap, recovering hence the aggregated case.

Minimization of the intra-guild competition

This second model is built upon the hypothesis that the periods of the species are located along the season so as to avoid, as far as possible, overlapping with other species that exploit a common mutualistic resource –i.e. pollinating services in the case of plants or flower availability for pollinators. As discussed above, the evidence for this type of mechanism is controversial, and, when it does occur, its effect is most probably subordinated to other genetic and environmental factors. Nevertheless, we will still explore the consequences of this assumption, given that it is the natural counterexample of the synchronized scenario.

In order to construct a phenological configuration that minimizes the competition among species, we implement a global search algorithm that optimizes an objective function under the constrains in Eqs. 5.7-5.8 (see Appendix I.2 for the numerical details). In this particular model, the objective function corresponds to the total competitive phenological overlap among species, as detailed in Appendix I.4.

Maximization of the variance

We now turn our attention to models that focus directly on the statistical properties of the system's phenology. As a first approach, we propose a model based on maximizing the dispersal of the periods along the season. In particular, we maximize the variance of the middle dates of activity. Indeed, if we define the middle time t_M of a species i as:

$$t_{M,i} = t_{0,i} + \frac{p_i - 1}{2}, \tag{5.9}$$

then its variance $\mathrm{Var}(t_M)$ is an approximate measure of the dispersion of the activity of both plants and pollinators along the season. Once again, the maximization of this quantity is done under the condition that mutualistic interactions present in the aggregated network still occur. The numerical procedure to do so is explained in Appendixes I.2 and I.5.

Maximization of the entropy

Following a similar line of thought, we propose a second model to produce phenological configurations that is based on their statistical properties. In particular, we refine the former approach by characterizing the distribution with a more sophisticated and robust indicator, namely, the entropy. As a matter of fact, this is a plausible alternative to maximizing the variance which may especially outperform the latter when the distribution is multimodal.

Let us define the entropy within the constructed framework for describing phenology. We start by defining a random variable x_i as the number of species whose middle date of activity t_m take place at a given date t_i. Then, its corresponding probability $p(x_i)$ will be:

$$p(x_i) = \frac{\text{number of species with } t_m = t_i}{\text{total number of species}}. \tag{5.10}$$

Given this random variable, it is possible to define its Shannon-Gibbs entropy as follows:

$$S = -\sum_i p(x_i) \ln p(x_i), \tag{5.11}$$

which follows the already familiar and standard form exploited in the first part of thesis. It is straightforward to see that in a scenario of perfect synchronization, the medium dates of activity are the same for all species. Hence if we name such date by the index k, then $p(x_k) = 1$, and the information entropy is zero.

Maximizing the entropy defined in Eq. 5.11 under the constraints imposed by the network of interactions results in a maximum entropy model, that randomizes the distribution of periods of the species yet using only the minimal amount of necessary information. The particular details of how this model was implemented can be found in the Appendixes I.2 and I.6.

Comparison among synthetic models

Given that our ultimate goal is to be able to generate realistic distributions of synthetic phenology, we now proceed to test the performance of the different models proposed above. To do so, we will adopt as input the observed network of interactions –which is to be preserved–, and the empirical distribution of periods. The latter will allow us to focus on the quality of the methodology to produce the starting dates alone, without introducing additional sources of noise.

In order to examine the adequacy of each model to reproduce the empirical phenological patterns, we start by extracting the synthetic starting dates corresponding to the different datasets by applying the numerical methods explained in Appendix I to our three empirical networks. After doing so, we characterize the synthetic phenologies within an analogous framework to the one described in section 5.2. That is, we calculate, on the one hand, the distribution of phenological coefficients defined in Eqs. 5.5-5.6, and, on the other hand, we couple the phenology to the network structure and compute the change of some basic structural features along time. Along the rest of this section we will explain and discuss the results of comparing these synthetic measures with the empirical observations.

Distribution of overlaps

We start by looking at the distribution of the phenological coefficients defined in Eqs. 5.5-5.6, as we had done before for the empirical case (see Fig. 5.5). In order to compare the empirical and the synthetic distributions, we perform two different statistical measures: *(i)* a two-sample Kolmogorov-Smirnov test (see Appendix H.2) and *(ii)* the calculation of the Kullback-Leibler divergence (see Appendix H.3).

Concerning *(i)*, we analyzed separately the competitive and mutualistic overlaps on the one hand, and the distributions for plants and for pollinators on the other hand, as summarized in Table 5.2. In particular, for the Burkle dataset, the null hypothesis that

Model /Dataset	Mutualistic overlap		Competitive overlap	
Synchronized	Plants	Pollinators	Plants	Pollinators
Burkle	0.052	0.051	0.008	**0.021**
Kantsa 1st year	0.015	0.010	0.002	0.002
Kantsa 2nd year	0.009	0.009	0.001	0.0017
Minimum competition	Plants	Pollinators	Plants	Pollinators
Burkle	**0.100**	**0.103**	**0.036**	**0.031**
Kantsa 1st year	0.012	0.013	0.002	0.0015
Kantsa 2nd year	0.007	0.008	0.001	0.001
Maximum variance	Plants	Pollinators	Plants	Pollinators
Burkle	**0.066**	**0.069**	**0.027**	**0.028**
Kantsa 1st year	0.015	0.014	0.004	0.003
Kantsa 2nd year	0.011	0.011	0.003	0.002
Maximum entropy	Plants	Pollinators	Plants	Pollinators
Burkle	0.040	0.042	0.010	**0.015**
Kantsa 1st year	0.009	0.007	0.001	0.001
Kantsa 2nd year	0.006	0.007	0.001	0.0016

Table 5.2: Results of the K-S two sample test among the synthetic distribution and the empirical distribution. We show the KS distance between the two samples, and highlight in bold the cases in which the null hypothesis is rejected, that is, those where the two samples do significantly differ (p-value < 0.05). The smaller the KS distance, the smaller the discrepancy between the two samples. The numerical implementation to calculate these distances is described on Appendix H.2.

both samples come from the same distribution is rejected for the models which minimize the competition and maximize the variance, which are hence incompatible with the empirical data. The model with centered times and maximum entropy are generally compatible with the observed phenology, except for the distribution of coefficients associated to the competition among pollinators. Instead, for the Kantsa dataset, the four models are compatible with the data.

In order to differentiate which model better reproduces the empirical phenology in the cases in which, according to the KS test, various models are statistically compatible, we carry out *(ii)*, that is, the calculation of the KL-divergence. Indeed, the KL distance measures the amount of information lost when we approximate the empirical distribution by the synthetic one, and therefore it can be used as a statistical criterion for model selection. In Table 5.3 we can observe that the model based on maximum entropy generally provides the best approximation, except for the second year of the Kantsa dataset, in which it is slightly outperformed by the model based on minimizing the competition. It is also interesting to observe that the second-best model is not the same among datasets: while the second-best model for the Burkle dataset is the one with synchronized phenology, in the Kantsa dataset it is the model which minimizes the competition.

Structural features

Secondly, in order to complement the information provided by depicting the phenological coefficients, we calculated as well the sequence of temporal networks resulting from considering the phenology. This produces a sequence of networks, each corresponding to a given date, as represented in Fig. 5.6. Repeating the procedure detailed in section 5.11 now for each synthetic model, we calculated a few basic structural quantities as a function of time: the number of active nodes -size-, the number of active links and the maximum degree. The results for each model as well as the empirical case are plotted together in Fig. 5.8.

Dataset / Model	D_{KL} Mutualistic overlap		D_{KL} Competitive overlap		
Burkle	Plants	Pollinators	Plants	Pollinators	Average
Synchronized	0.035	0.038	0.002	0.014	0.022
Minimum competition	0.095	0.101	0.026	0.033	0.064
Maximum variance	0.042	0.056	0.010	0.019	0.032
Maximum entropy	0.022	0.032	0.003	0.008	0.016
Kantsa 1st year	Plants	Pollinators	Plants	Pollinators	Average
Synchronized	0.0116	0.0053	0.0014	0.0010	0.0048
Minimum competition	0.0050	0.0073	0.0009	0.0004	0.0034
Maximum variance	0.0111	0.0047	0.0032	0.0008	0.0049
Maximum entropy	0.0055	0.0051	0.0005	0.0005	0.0029
Kantsa 2nd year	Plants	Pollinators	Plants	Pollinators	Average
Synchronized	0.0048	0.0036	0.0008	0.0008	0.0025
Minimum competition	0.0018	0.0035	0.0005	0.0005	0.0015
Maximum variance	0.0080	0.0036	0.0019	0.0005	0.0035
Maximum entropy	0.0019	0.0035	0.0005	0.0007	0.0016

Table 5.3: Results of the K-L divergence among the synthetic distribution and the empirical distribution. The smaller the KL-divergence, the smaller the difference between the two samples. Further details on the definition and numerical implementation of this measure can be found in Appendix H.3.

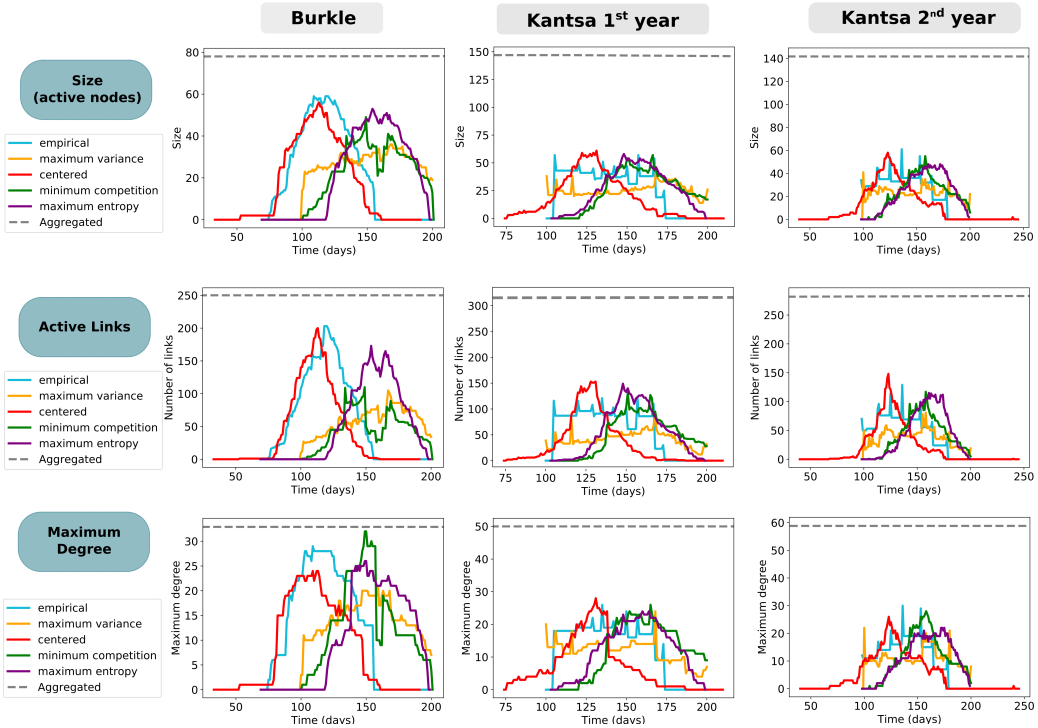

Figure 5.8: Temporal evolution of three fundamental structural features, measured on a daily basis: number of active nodes, active links and maximum degree. Each column corresponds to a different dataset as indicated on the top of the figure. In each plot, we represent the results for the empirical case (light blue), and the four synthetic models based on: synchronized middle times (red), minimum competition (green), maximum variance (yellow) and maximum entroy (violet). In grey and dashed stye, the reference value for the aggregated case.

With this information at hand, we can perform a comparison between the product of

each synthetic model and the empirical observations, specifically addressing the change in fundamental structural properties along time. To quantify these correlations, we calculated the corresponding Pearson coefficient for different values of time lag between the distributions. By doing so, we are taking into account the possibility that the null model reproduces well the empirical scenario but in a delayed or advanced time. That is, we are relaxing the assumption of a perfect matching between the empirical and the synthetic starting dates, focusing instead on the relative position among the starting dates of different species. In table 5.4 we show the maximum value of the Pearson correlation calculated following this procedure, as it is further detailed in Appendix H.4.

Table 5.4 and Fig. 5.8 show that the analysis of the structure lead to similar results to the aforementioned analysis of the phenological overlap. Indeed, the better fitting models for the Burkle dataset are the ones based on synchronized phenology and maximum entropy, while for the Kantsa dataset the maximal correlation is found for the model which minimizes intra-guild competition and, again, the one maximizing the entropy.

Dataset / Property	Maximum Pearson coefficient for each null model			
Burkle	Synchronized	Max Variance	Min competition	Max entropy
Maximum degree	0.98	0.88	0.93	0.98
Number of links	0.98	0.87	0.78	0.98
Size	0.99	0.79	0.92	0.98
Average	0.99	0.85	0.88	0.98
Kantsa 1st year	Synchronized	Max Variance	Min competition	Max entropy
Maximum degree	0.78	0.76	0.91	0.91
Number of links	0.74	0.71	0.89	0.83
Size	0.81	0.58	0.89	0.85
Average	0.78	0.69	0.90	0.86
Kantsa 2nd year	Synchronized	Max Variance	Min competition	Max entropy
Maximum degree	0.90	0.67	0.87	0.93
Number of links	0.85	0.78	0.89	0.85
Size	0.89	0.63	0.90	0.88
Average	0.88	0.69	0.88	0.88

Table 5.4: Maximum Pearson correlation among the empirical and the null expectation of the structural properties along time.

Overall, these multiple statistical tests reveal at least two general conclusions. On the one hand, we find that each dataset is better described by a distinct mechanistic assumption, i.e. the synchronization of the species' phenologies in the Burkle dataset and the minimization of the competition in the Kantsa dataset. This disparity seems to reflect the substantial divergences between the two datasets, that we described in detail in section 5.2. On the other hand, both networks' phenologies are accurately reproduced by the statistical model that maximizes the entropy associated to the distribution of the middle dates of activity, despite the considerable differences among the two datasets. What this latter finding suggests is that the observed network of interactions together with the periods of each species provide sufficient information to reproduce, fairly closely, the observed temporal patterns of activity. This is particularly interesting given the mentioned differences among datasets, which provides, to a certain extent, a warranty of generality despite the limited data at our disposal. This finding does not imply that, forcedly, the starting dates of activity are set at random, but that the information enclosed in the corresponding network of interactions and the species' periods may be sufficient to reproduce well the main characteristics of the community's phenology.

5.4 Conclusions and perspectives

Along this chapter we have addressed the possibility of moving beyond the aggregated paradigm by incorporating –in the form of periods of activity– some of the temporal variability that plant-pollinator communities exhibit along the year. In particular, we have concentrated on seasonal ecosystems, assessing the daily change in both inter-guild, mutualistic relationships and intra-guild, competitive interactions.

The analyses carried out along this chapter have revealed, in the first place, that non-trivial information is lost when portraying the real network of interactions by a static representation, that is, neglecting its temporal dimension. Indeed, we have observed that the consequences of introducing the empirical phenology into the network formalism are system-dependent, and hence no general pattern can be expected a priori. Moreover, the process of aggregation not only disregards the richness of temporal variability, but it also tends to overestimate the value of the main fundamental structural features, as had been remarked as well by Sajjad et al. (2017). This is especially relevant given that structural features like the degree or the connectivity are consistently used to characterize, respectively, the relative vulnerability of species (Dakos and Bascompte, 2014) or the community stability (Thébault and Fontaine, 2010).

In the light of the limitations of the aggregated paradigm, and driven by the scarcity of available datasets, we proposed a group of models to produce, given a fixed mutualistic network, a compatible hypothetical phenology. The comparison of these results with the empirical datasets revealed that the soundness of certain mechanisms is, at least in the first-order approach we have adopted here, specific to the particular system under consideration. Instead, we have found that the purely statistical assumption of maximizing the entropy associated to the distribution of middle dates performs generally well, as we have tested in two dissimilar empirical examples. Importantly, the remarkable performance of the maximum entropy hypothesis is partly explained by the fact that, actually, the network of interactions is closely dependent upon the starting dates, in the sense that the mutualistic contacts observed corresponded, forcedly, to concurrent species –a condition that, indeed, we impose to our models. Therefore, preserving the network of interactions is a strong constraint, which could justify the general adequacy of this model.

In perspective, these synthetic models offer a methodological set that might prove useful in different aspects. On the one hand, they can be exploited merely as a group of realistic models to construct synthetic ensembles in the absence of highly-resolved empirical data, in those cases where the main driving forces of the phenology are known. On the other hand, they can also be applied as null models that permit testing a variety of null hypothesis, from the mechanistic forces shaping the phenology to the existence of temporal, structural or dynamical patterns. At this point, it is worthy to remind as well that ours is just a first approach to modeling the temporal variability of networks. In particular, we considered the description level at which species are active or inactive during a certain fraction of the season. However, it could be possible to refine the scale of description to include the weekly or even daily turnover of interactions, a sort of hyper-realistic depiction of the temporal variability of the network that is gaining attention during the recent years (CaraDonna et al., 2017). This is due, partly, to the technological advances that permit monitoring phenology in great detail, and therefore it is probable that in the coming years we will find a rising number of this type of studies.

In the bigger picture, the interest in moving towards a more realistic portrayal of interacting systems is not exclusive to ecology, and indeed the study of temporal complex networks has received great attention in recent years (Holme and Saramäki, 2012). How this change of paradigm will eventually challenge our understanding of natural systems is something we are just now beginning to explore.

CHAPTER 6

Dynamics *one more time*

This sixth chapter, that closes both the second part and the main body of the thesis, constitutes the natural continuation of the inquiries about the temporal dimension of mutualism we had initiated above. Here, though, we will leave aside the emphasis on the network's structure and tackle instead the impact of considering phenology on the community dynamics. Before starting, it is worthy to forewarn that some of the results presented along this chapter are still inconclusive and call for further investigations, but we will still present them here in order to introduce some of the prospective work that emanates from this thesis.

This chapter is structured as follows. First, we will introduce the tight relation between phenology, ecosystem's dynamics and climate change, a topic that has not ceased to gain attention in recent years. Next, we will propose a methodological approach to incorporate phenology in a dynamical model that considers both the mutualistic and the competitive interactions. Finally, we will test this model on the two empirical datasets we studied in Chapter 5 and discuss the results.

6.1 Stability in a changing climate, or why time matters

Previously, we have investigated how our representation of a mutualistic community changes when we take into account the phenology, concluding that several structural features are distorted by the lens of the aggregated paradigm. Given that the link between structure and dynamics is, certainly, one of the keystones of the field of ecological networks in particular and that of complex networks in general, a pertinent question that naturally follows is how ecosystems' dynamics are modified by the phenology. In this sense, there are, at least, two main queries. First, how does our current understanding of the stability of communities translate into a framework that accounts for temporal variability? And secondly, and maybe even more importantly, what effect does phenology have on our predictions about the future robustness of ecosystems?

Regarding the first question, admittedly the vast majority of studies on stability are based upon aggregated networks, disregarding the phenology of species (Bastolla et al., 2009; Thébault and Fontaine, 2010; Suweis et al., 2013). Arguably, this choice may be justified, to a certain extent, as long as the population effects derived from the ecological interactions build up along the season. Nonetheless, it is clear that the lack of phenological information not only implies a loss of detail, but may also lead to over or underestimating certain ecological relationships. This is especially relevant, as we will discuss below, for indirect interactions such as competition, which can be strikingly modified when considering the temporal dimension of the system. In this line of thought, some works have explored the consequences of accounting for phenology in the characterization of the dynamics. For instance, Encinas-Viso et al. (2012), proposed a microscopic dynamical model that involved both mutualism and competition in order to analyze, by exploring a wide range of theoretical forms for the configuration of phenology, the properties of the resulting hypothetical networks of interactions. More recently, Ramos-Jiliberto et al. (2018) proposed a highly-realistic population model and applied it to study a set of empirical networks with its corresponding phenology, upon which they applied different types of perturbations. In both of these examples, the authors concluded that the phenology plays a fundamental role in driving the

community's stability and dynamics, by producing phenomena that could not be explained from the aggregated perspective alone.

On the other hand, the study of the impact of phenology on the dynamics is inevitably intertwined with a global perturbative process that menaces a great variety of natural systems, namely the climate change. This comes as no surprise if we consider the multiplicity of environmental factors that play a role in determining the starting dates of activity, as reviewed in Chapter 5. In particular, both the onset of flowering and the date of first emergence of insects have been claimed to advance as the environmental temperature raises, which can lead to what is commonly known as *phenological shifts* (Hegland et al., 2009). The most immediate consequence of this phenological perturbation is the possibility that mutualistic partners desynchronize, leading to a lack of temporal overlap –also called *mismatch*– that hampers pollination services and may eventually lead to biodiversity loss. As a result, during the last decade there has been a major explosion in the number of works devoted to quantify the possible extent of such mismatches (Memmott et al., 2007; Hegland et al., 2009; Burkle et al., 2013; Duchenne et al., 2020) as well as their impact on the persistence of species and the community stability (Revilla et al., 2015; Rafferty et al., 2015).

Truth be told, in this chapter we will focus mainly on the first question, although it would be worthy to keep in mind the possible applications of this kind of dynamical models to the study of phenological shifts and mismatches. In what follows, hence, we start by introducing one of these possible models.

6.2 A model to incorporate phenology

The aim of this section is to present a model that permits assessing the effects of phenology on the organization of ecological mutualistic systems, particularly on biodiversity persistence. To this end, we work upon a previous population model proposed by Gracia-Lázaro et al. (2018), that investigates the influence of the network structure on the persistence of species. In particular, this model exploits a bilayer framework like the one depicted in Fig. 6.1, which accounts, simultaneously, for mutualistic links between species of different kind and competitive interactions among members of the same guild. Such competition is driven, as detailed in section 5.2, by the sharing of common mutualistic resources (Jones et al., 2012), therefore being derivable from the empirical network of mutualistic interactions. As we had done in the previous chapter, we will concentrate on the particular case of plant-pollinator communities, although some of the results are in fact generalizable to other ecological or social systems that are equally based on consumer-resource relationships.

Let us focus here on plant-pollinator systems and consider a community consisting of N^P species of plants and N^A species of animals, being $N = N^P + N^A$ the total number of species. The plants' parameters and variables are represented by the superscript P, while A stands for animals. As always, the mutualistic relationships are given by the bipartite $N^P \times N^A$ matrix, B, with $B_{ik} = 1$ if animal species k pollinates the plant species i, and $B_{ik} = 0$ otherwise. Within this framework, in the original model by Gracia-Lázaro et al. (2018) the evolution of the abundance of each species is described by a differential equation, which takes into account both the abundance of other species and the interaction with them, resulting in a system of N coupled differential equations. In detail, let s_i^P be the abundance of the plant species i, being α_i^P its intrinsic growth rate. Then, the relative abundance of a given plant i evolves according to:

$$\frac{1}{s_i^P}\frac{ds_i^P}{dt} = \alpha_i^P - \beta_i^P s_i^P - \beta_0^P \frac{\sum_{jP,i\neq j} s_j^P \sum_{k\in A} B_{ik}B_{jk}s_k^A}{\sum_{k\in A} B_{ik}s_k^A} + \gamma_0^P \frac{\sum_{k\in A} B_{ik}s_k^A}{1 + h^P\gamma_0^P \sum_{k\in A} B_{ik}s_k^A} \quad , \quad (6.1)$$

which takes into account the mean-field *intra*-species competition for resources regulated by parameter β_i^P, the structured *inter*-species competition for mutualistic resources pondered by parameter β_0^P and finally the mutualistic benefit. This last term models the effect of mutualism following a Holling Type II functional response, as proposed by Bastolla et al. (2009), that involves an interaction strength parameter γ_0^P and the so-called handling time term, h^P, which regulates the saturation of the mutualistic term. Moreover, the existence of

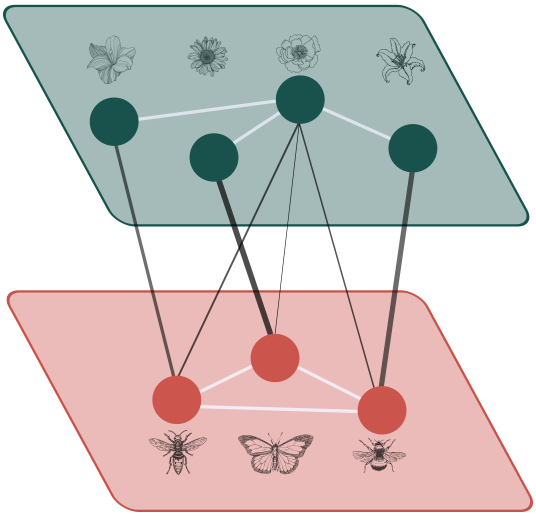

Figure 6.1: Bilayer representation of a plant-pollinator network. Mutualistic interactions are depicted in grey as the inter-layer links, while competitive interactions for shared resources are represented in white as intra-layer connections.

competitive interactions is mediated by the term $B_{ik}B_{jk}$, as previously introduced in Eq. 5.2. Although we focused here on the temporal evolution of the plants' population, an analogous expression can be drawn for the pollinators. Overall, as aforementioned the system can be seen as a multilayer network like the one depicted in Fig. 6.1, where inter-layer connections represent the mutualistic interactions, while intra-layer links account for the competition.

In order to include the temporal dimension into this formalism, we adopt a first-order approach that quantifies the dynamical consequences of phenological overlap in an *effective* manner. This approximation presumes that species interact homogeneously along time, and hence the resulting amount of mutualistic benefit or competition stress is proportional to the fraction of shared overlap in their periods of activity, as defined in section 5.2 and depicted in Fig. 5.4. Subsequently, the mutualistic and competition growth terms can be modulated by a linear function of the temporal coexistence between species. That is, the larger the amount of time during which two species coexist, the larger the corresponding mutualistic or competitive term will be. As a way to model this mechanism, we can exploit the phenological coefficients Ω^P_{ijk} and Φ^P_{ik}, defined in Eqs. 5.5-5.6. Indeed, following the effective assumption describe here, we can introduce them directly into equation 6.1, which leads to:

$$\frac{1}{s_i^P}\frac{ds_i^P}{dt} = \alpha_i^P - \beta_i^P s_i^P - \beta_0^P \frac{\sum_{jP,i\neq j} s_j^P \sum_{k\in A} B_{ik}B_{jk}s_k^A\Omega^P_{ijk}}{\sum_{k\in A} B_{ik}s_k^A\Phi^P_{ik}} + \gamma_0^P \frac{\sum_{k\in A} B_{ik}s_k^A\Phi^P_{ik}}{1+h^P\gamma_0^P\sum_{k\in A} B_{ik}s_k^A\Phi^P_{ik}} \quad , \tag{6.2}$$

where the mutualistic and competitive terms are now rescaled by the phenological coefficients 5.5-5.6.

As a matter of fact, expression 6.2 can be written more compactly. Let M_i^P be the biomass of the pollinators of a given plant species i, then $M_i^P = \sum_{k\in A} B_{ik}s_k^A\Phi^P_{ik}$, and let W_{ij}^P be the biomass of the pollinators shared by two plant species i, j, such that $W_{ij}^P = \sum_{k\in A} B_{ik}B_{jk}s_k^A\Omega^P_{ijk}$. With this notation, Eq. 6.2 turns into:

$$\frac{1}{s_i^P}\frac{ds_i^P}{dt} = \alpha_i^P - \beta_i^P s_i^P - \beta_0^P \frac{\sum_{j\in P,i\neq j} s_j^P W_{ij}^P}{M_i^P} + \gamma_0^P \frac{M_i^P}{1+h^P\gamma_0^P M_i^P} \quad . \tag{6.3}$$

In the same way, the relative abundance variation of an animal species k is given by:

$$\frac{1}{s_k^A}\frac{ds_k^A}{dt} = \alpha_k^A - \beta_k^A s_k^A - \beta_0^A \frac{\sum_{l\in A,k\neq l} s_l^A W_{kl}^A}{M_k^A} + \gamma_0^A \frac{M_k^A}{1+h^A\gamma_0^A M_k^A}. \tag{6.4}$$

It is worthy to remark that the latter equations 6.3-6.4 are formally identical to the original model introduced in the work by Gracia-Lázaro et al. (2018). This illustrates the fact that, following the procedure presented here, we have translated the binary aggregated network into a weighted, but still aggregated, formalism. Certainly, this is still a first-order approach to the modeling of temporal variability, since the structure of the network does not change over time. However, while for the mutualistic network the binary structure is not modified with respect to the aggregated representation –i.e. features like the degree, connectivity, etc, are preserved–, in what concerns the competitive network some links may removed, particularly in those cases in which the interacting species do not coincide along the season. In this sense, the aggregated case presents a sort of worst-case scenario in terms of the competition, that is tempered by the introduction of the phenology.

6.3 Results in two empirical datasets

With this methodology at hand, we are ready now to test the predictions of the aforementioned model on an empirical dataset. In particular, we study the three real networks extracted from the Burkle and the Kantsa datasets. The details on each dataset are given in Appendix A, while the main features of each system have been characterized in section 5.2. Along the present section we will analyze how their community dynamics is affected by phenology: first, by applying the population model introduced above and, secondly, by comparing these results with the predictions of a null model where the starting dates of activity of both guilds are shifted.

To start with, following an analogous procedure to the one proposed by Gracia-Lázaro et al. (2018), we numerically integrate the system of Eqs. 6.4-6.3 for a wide range of different values of mutualistic and competitive strength (see Appendix J for more details on the computational implementation). In Fig. 6.2, we plot the number of surviving species in the steady state, for both the aggregated empirical case as modeled by Eq. 6.1 and the network with empirical phenology as given by Eq. 6.2.

Moreover, in order to complement the information provided by these two scenarios, we construct a null model based on the shifting of the starting dates under the condition of constraining the binary mutualistic network and the periods' distribution. In particular, we apply the numerical procedure described in Appendix I.1. This provides, hence, a randomization of the links' weights associated to the phenological overlap, and will permit assessing the robustness of the results with respect to possible variations in the interaction strength due to shifts in the starting dates. In Fig. 6.2 we plot, together with the results of the aggregated and the weighted networks, the average biodiversity obtained by applying the model of Eq. 6.2 over a set of null configurations generated by synthetically shifting the empirical starting dates.

The results summarized in Fig. 6.2 point out several aspects that are worth discussing. First, in general terms we recover a comparable pattern to the one found by Gracia-Lázaro et al. (2018), in the sense that increasing the mutualism positively affects biodiversity in the low-competition regime, but turns out to be detrimental to species' persistence when competition for mutualistic resources is severe. Moreover, similarly to what we observed when talking about the network's structure, the effect of phenology on the network is highly system-dependent. Indeed, the two datasets exhibit almost opposite behaviors: while for the Burkle dataset the region of maximum persistence increases dramatically in the model with phenology in comparison to the aggregated case, in both years of the Kantsa dataset this region decreases. This can be understood if we consider the substantial differences between the two datasets, thoroughly detailed in section 5.2.

In order to attempt to better understand these results, we investigate the relation between the persistence of a species and its individual characteristics. In particular, we consider two fundamental properties of, respectively, the structural and the temporal dimension of the system, namely the species degree and its period of activity. As shown in Fig. 6.3, in the three empirical examples under study the degree is a strong determinant of the persistence of a species. In detail, having a small degree is a necessary condition –although not sufficient– for a reduced region of persistence, which means that specialists species are more vulnerable to

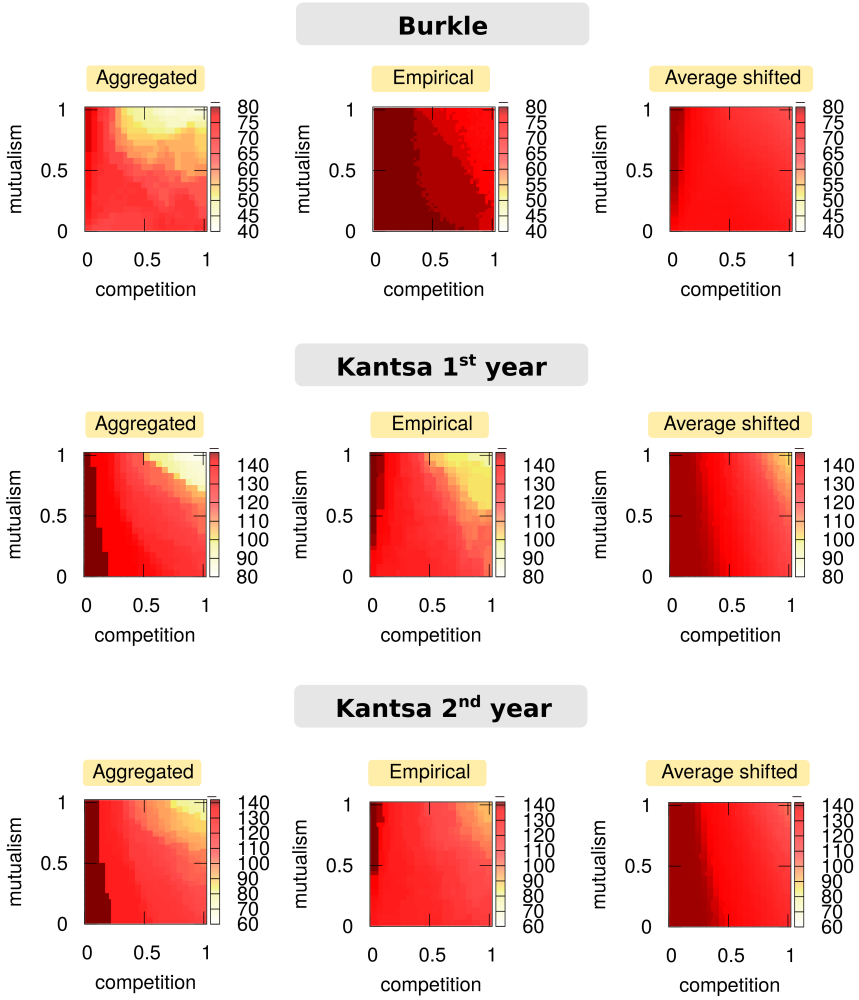

Figure 6.2: Biodiversity persistence as a function of the mutualism and inter-species competition parameters. Panels show the levels of biodiversity in the stationary state of the population model given by Eqs. 6.4-6.3, as a function of the strength of mutualistic and competitive interactions –that is, parameters γ_0 and β_0. The color scale represents the number of species in the steady state. The left panels show the results obtained when phenology is neglected; the middle panels depict the results obtained when considering the observed phenological coefficients; and the right pannels show the results obtained when considering the phenological coefficients corresponding to 100 independent null configurations, generated by shifting the initial times of activity and flowering as explained in Appendix I.1.

extinction. This result is observed for both the aggregated network and the network weighted with the empirical phenology, as well as for the null model where the starting dates are shifted. From an ecological viewpoint, this should come as no surprise since specialists species have been traditionally regarded as more fragile (McKinney, 1997), given the higher specificity of their mutualistic resources, specially pollinators (Memmott et al., 2007; Ramos-Jiliberto et al., 2018).

On the other hand, considering the relation with the species' phenological period yields divergent results depending on the dataset, as can be seen in Fig. 6.3. Interestingly, the analysis of the Burkle dataset reveals that species with short period are benefited from the introduction of the temporal dimension, in comparison to both the aggregated case and the null model. This could explain the sharp increase in the region of maximum persistence, for the empirical case, depicted in Fig. 6.2. Nonetheless, this finding is not general. In the Kantsa dataset we find instead that introducing the phenology is detrimental to the

persistence of species with short periods. In particular, in this dataset there is a bulk of pollinator species with just one or two days of observed activity (see Fig. 5.3) which represent the majority of extinctions in Fig. 6.3.

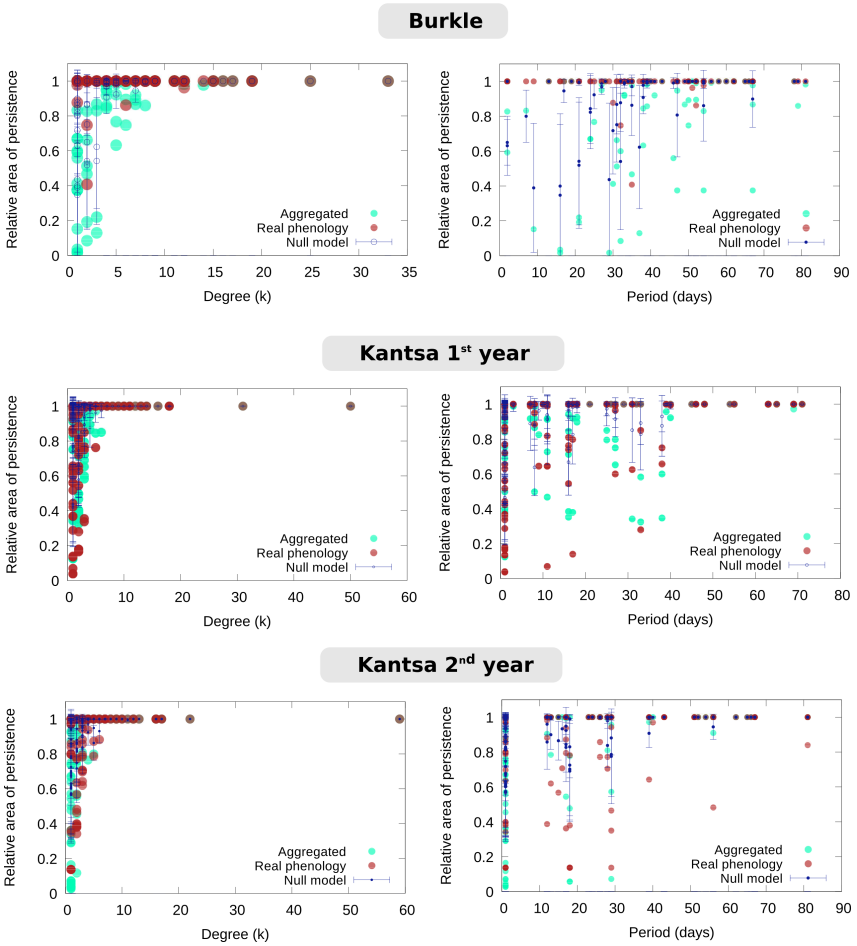

Figure 6.3: Relative size of the region of persistence per species as a function of their degree (left) and period (right). We plot the results for the aggregated case (in red), the empirical case (in light blue) and the null model (in dark blue), in which case we depict the average and the standard deviation of the relative region of persistence of each species over the null ensemble.

The dynamical uncertainty associated to species with short period might be better understood by comparing the empirical results with the estimations provided by the null model. In particular, let us introduce a probability of survival $p_{s,i}$ for each species i. In the null model, $p_{s,i}$ is defined as the ratio between the number of times that species i persists alive on the whole range of exploration of β and γ, among the total number of null configurations. In the study of the empirical network this quantity is binary, such that, if we call it $x_{s,i}$, we have $x_{s,i} = 1$ if species i never gets extinct and $x_{s,i} = 0$ otherwise. Using these quantities, we can define the z-score associated to the empirical observation when compared with the null ensemble as:

$$\text{z-score}_i = \frac{x_{s,i} - p_{i,s}}{\sigma_i}, \tag{6.5}$$

where the standard deviation σ_i is computed as the one corresponding to a Bernoulli process, since the survival/extinction event is binary. Thus, the z-score will be positive if the species survived in the empirical case but got extinct a certain number of times in the null ensemble, and negative otherwise. We plotted this quantity as a function of the degree

of the species and as a function of its period in Fig. 6.4. Here again we observe divergent results among datasets, in the sense that the particular correlations are different for each network. However, we also find that in general the species with short period tend to have a larger z-score –in absolute terms– which means that their persistence is more affected by the introduction of phenology –either in a positive or in a negative way– and hence their long-term robustness is more difficult to predict.

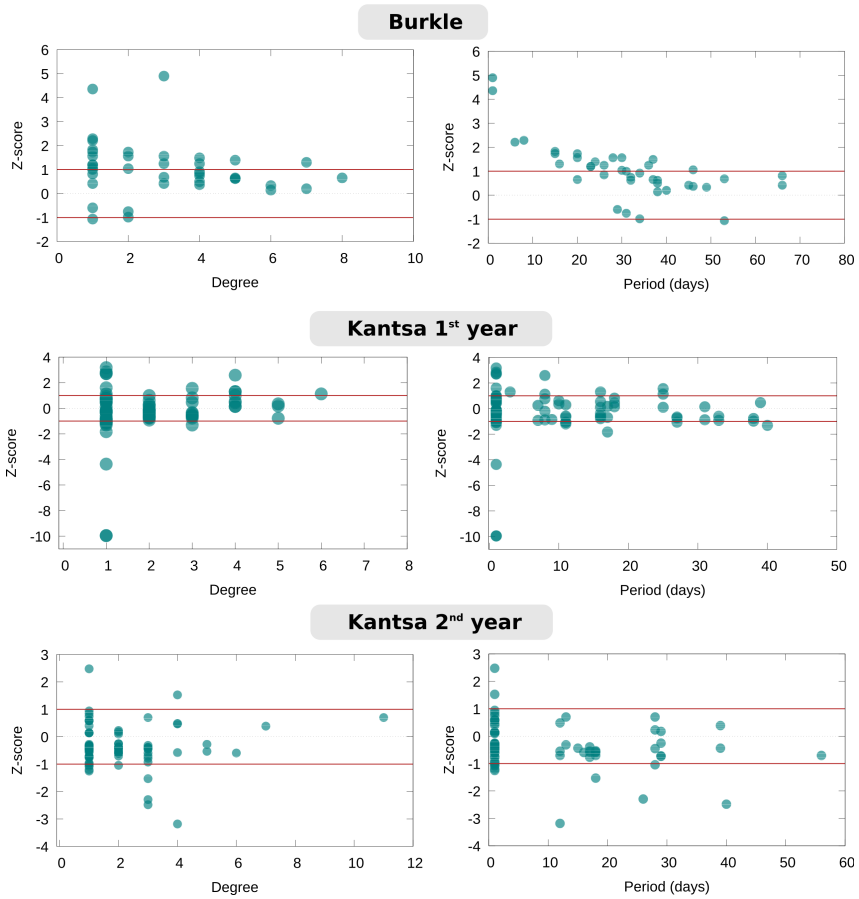

Figure 6.4: Relation between the z-score as defined in Eq. 6.5 and the degree (on the left) or the period (on the right), for the three datasets.

On the whole, we have observed that, together with being a specialist, having a short period is typically a sign of higher vulnerability to extinctions. On the other hand, these results pose probably more questions than answers, as we find once again no universal pattern in how phenology specifically affects ecosystem's dynamics, particularly species persistence. Truth to be told, this should come as no surprise if we take into account the substantial inherent dissimilarities between the two datasets. How to cope with this problems and what could be done as prospective work to try to answer some of the remaining questions is what we discuss in the next section, the last of this chapter.

6.4 Conclusions and perspectives

Along this chapter, we have briefly addressed the question of the interplay between phenology, mutualism and species persistence, by taking as a paradigmatic example the case of plant-pollinator systems. In detail, we have developed a previous dynamical model that accounts for both competitive and mutualistic interactions, in order to include the effect of phenology. We have applied a first-order approximation, consisting in weighting the strength of ecological interactions by the temporal overlap among the partners. After examining this model, our

results point out that specialist species tend to have a larger probability of becoming extinct, in particular due to perturbations on the balance between competitive and mutualistic outcomes, a result which has equally been observed in other experimental (McKinney, 1997) and theoretical studies (Memmott et al., 2007; Gracia-Lázaro et al., 2018; Ramos-Jiliberto et al., 2018). Moreover, the persistence of species with short periods is the most difficult to predict, since they are the most sensitive to changes in the starting dates. A possible future increase in the number of available, highly-resolved datasets could permit assessing the generality of these results, and particularly the existence of local correlations related to the species composition of the site and its geographic or climatic conditions.

All in all, the model presented here represents just a first step towards the modeling of phenology, in the sense that it is greatly limited by the fact that the dynamics still occur on a static network. Other works, like the one by Encinas-Viso et al. (2012), have proposed microscopic models that involve a changing network of interactions, at the expense –all things being said– of introducing some stochasticity. In our case, the effective modeling of phenology using a deterministic setting is hampered by the difficulty in identifying and handling the diverse temporal scales, specially the rate of change in the network. In this sense, it would be interesting to explore how ecological dynamical models would perform in the framework of temporal networks, a field that has received great attention during the recent years (Holme and Saramäki, 2012).

Understanding the often-neglected temporal dimension of mutualistic communities is not only a question of theoretical curiosity, but an urgent challenge in the context of a changing climate. Although we have not addressed this question explicitly here, the null model based on shifting the starting dates is partly based on this philosophy. In this sense, the development of an adequate methodological framework is crucial to assess the consequences of climate change on mutualistic systems around the globe, from the the extent and impact of possible mismatches (Visser and Gienapp, 2019) to the flexibility of the network to rewire and replace missing interactions (Vizentin-Bugoni et al., 2020) or to accommodate invasive species (Hellmann et al., 2008).

CHAPTER 7

Conclusions

Since Darwin introduced his famous metaphor of the entangled bank to describe the intertwined complexity of natural communities, scientists have looked at ecological interactions as potential drivers of the structure and dynamics of ecosystems. However, until a few decades ago these studies primary emphasized the importance of antagonistic interactions, leaving aside mutually beneficial relationships, that remained overlooked as curious but marginally relevant (Bronstein, 1994). Nowadays we know that mutualism does in fact play a major role in the organization of ecological communities, pervading ecosystems around the globe, involving diverse spatial scales and engaging very different kinds of organisms (Bascompte and Jordano, 2013), to the extent that we can find analogous relations in non-ecological contexts such as social and economic systems.

In this thesis we have looked at mutualistic systems from a complex network perspective, considering these communities as a perfect example of a complex system. The network representation of ecosystems entails an inherent tension between the need of providing a stylized description that permits detecting and understanding general patterns, and on the other hand the risk of oversimplifying, missing relevant details about the structure or the dynamics. In other words, when constructing a network we face the challenge of knowing what is the minimum amount of information necessary to obtain a faithful portrayal of the system, in relation, of course, to the questions we would like to answer.

This tension between simplification and attention to detail is somewhat reflected in the two parts in which this thesis is organized. Indeed, along the first part we have looked at the structure of binary mutualistic networks in order to investigate the emergence of a widespread architectural pattern, namely nestedness. Using a null model based on maximum entropy ensembles, we have demonstrated that this pattern can be naturally explained by a reduced set of fundamental network features, particularly the degree sequences. This finding not only carries fundamental implications for our understanding on what structural indexes should be tackled to characterize the dynamics of mutualistic systems, but also on how ecosystems have been assembled and have evolved through time. With these results at hand and by applying once more the constructed null model, we have then explored the functioning and performance of different nestedness metrics, establishing the difficulty of finding an unbiased and universal tool to quantify and rank nested patterns.

In the second part of this thesis, we have followed a different path and, if before we had questioned what is the minimum information needed to reproduce the structure of aggregated networks, here we turned into investigating whether such static network representation is actually realistic enough, or, on the contrary, its lack of detail distorts our perception of mutualistic communities. First, we have explored the consequences from a structural viewpoint of partly accounting for the community's temporal variability, by characterizing two highly-resolved empirical datasets. Furthermore, we have proposed a set of models aimed at producing, under diverse assumptions, synthetic configurations of phenology. From their comparison with the empirical systems, our results suggest that models based on maximum entropy may once again work generally well to reproduce –subject to some constraints– the observed phenology. Instead, the adequacy of mechanistic models seems to be highly system dependent. Secondly, as a natural continuation of these queries, we begun to address the problem of how to translate the existence of temporal variability into a dynamical framework which could permit assessing the influence of phenology upon species coexistence.

Some of the questions addressed along this thesis are still open and call for further investigation, while answering others has lead to the arousal of new queries and avenues of research[1]. To conclude this thesis, we briefly discuss these topics on the bigger picture, relating our findings to broader challenges in the field of ecological networks in particular and that of complex systems in general.

7.1 'Informing' ecology

In his influential book *The Structure of Evolutionary Theory*, Gould (2002) wrote:

> *A. N. Whitehead famously remarked [...] that all later philosophy might well be described as a footnote to Plato. How often, indeed, must any decent scholar invent a formulation with pride in systematic analysis, and with hope for originality –only to discover that one of history's truly great thinkers had established the same principle, recognized its importance, and even specified its full range of application.*

In a similar spirit, we must acknowledge that the application of concepts from information theory and statistical physics to ecology is not entirely new. Indeed, models based on the maximum entropy principle have been applied, especially during the last two decades, to the study of macroecology (Pueyo et al., 2007; Harte et al., 2008), in particular to infer the scaling relation of relevant biodiversity metrics such as the species area relationship (typically shortened as SAR) or the species abundance distribution (the so-called SAD). As discussed by Harte and Newman (2014), this type of approach has not been exempt from criticism, primary because of its lack of a mechanistic background, which somewhat complicates is ecological interpretation. Harte and Newman (2014) provide several reasons to justify the good performance of maximum entropy models, that may as well apply to our study of ecological networks: from the concurrence of various factors and forces whose overall effect can be seen as random –as we argued in Chapter 5–, to the presence of sufficient implicit information in the constrained variables to reproduce macroscopic patterns –similarly to what has been discussed in Chapter 3.

Despite the existence of these precursory applications of information theory to macroecology, admittedly its exploitation in the context of ecological networks is comparatively scarce. All in all, in recent years this tendency seems to have been reverted, and we can find an increasing number of works that use an information theoretic approach to characterize the structure of ecological networks in different ways. On the one hand, statistical models based on maximum entropy assumptions have been used to disentangle the general forces shaping the organization of ecological interactions, similarly to what we have done along this thesis for mutualistic communities. For instance, Williams (2011) proposed a maximum entropy model that solely constrains the number of nodes and links of the network in order to generate synthetic degree distributions, and claimed that the hypothetic distributions are statistically compatible, in around 70% of the studied cases, with the empirical observations of both antagonistic and mutualistic systems [2]. In a more general fashion, Solé and Valverde (2004) analyzed the architectural constraints of diverse types of real complex networks using metrics borrowed from information theory. Doing so, they found that the structure of several technological and biological systems –including an ecological network– falls within a narrow range of the whole space of possible configurations. On the other hand, some works have moved beyond the maximum entropy approach, using methods of statistical inference to refine the depiction of the real structure of ecosystems. For example, Young et al. (2019) have recently proposed the use of tools from Bayesian inference to construct a model that

[1] A translation of this summary into French and Spanish can be found in Appendix K.

[2] Despite the methodological interest of these results, the findings by Williams (2011) are greatly hindered by the small size of the real networks studied (generally having less than 100 species). As a matter of fact, Williams also observed that larger real networks tended to show a larger discrepancy with respect to the synthetic expectation, in particular due the broadening of the degree distribution. This is in agreement with the fact that as the network's size increases, so does the tail of the degree distribution, departing from the distribution generated by the Exponential random graph model.

informs on how a particular, incomplete observation of a network can be used to estimate the real, complete structure of the system. This offers a methodological framework to assess the problem of incompletely sampling ecological networks, which is one of the open questions in the discipline (Ings et al., 2009; Bascompte and Jordano, 2013).

From a broader perspective, and to finish this section, it is worthy to mention that the process of 'informing' ecology is not an isolated phenomenon, since in general the field of complex networks has equally witnessed an increase in information theoretic approaches (Park and Newman, 2004), especially in their applications to real-world problems (Cimini et al., 2019). In this sense, it is also true that many of the methods and results presented along this thesis have implications beyond the field of ecology, given that some of the patterns and features we have analyzed here –such as nestedness or the role of temporal variability– are transversal to many network applications.

7.2 From Madagascar to Delphi

> *This adventure, begun casually enough, served to enrich but also to simplify my life: the future was matter for slight concern. I ceased to question the oracles; the stars were no longer anything more than admirable patterns upon the vault of heaven.*
>
> *Memoirs of Hadrian* - M. Yourcenar

To finally conclude this thesis, let us say that identifying the fundamentally informative properties of mutualistic communities not only is a matter of theoretic accuracy, but also carries far-reaching implications for the predictability of ecosystem's future. As a matter of fact, the role of prediction in ecology is a controversial issue (Carpenter, 2002). In the words of Ings et al. (2009), scientists have been lately advocating for *'moving away from phenomenological studies and moving towards those that are more mechanistic and, ultimately, predictive'*, or in a more poetic fashion, for following the opposite path to the one described above by Yourcenar, that is, extracting interpretations and predictions from the observation of natural patterns.

The difficulty of ecological forecasting is aggravated by the same inherent reasons that lead Darwin to depict ecosystems as an entangled bank: they are composed by many components, subject to various forces and sources of heterogeneity and, as a result of the interplay among all these factors, their dynamics are often non-linear. Indeed, these characteristics are common to complex systems in general, where the question of predictability is a prevailing problem. All in all, ecologists continue struggling to provide accurate predictions, especially in conjunction with policy makers (Clark et al., 2001).

In the context of community ecology, an early but beautiful example of ecological prediction is related to the story of the Darwin's orchid and its pollinating hawk moth (Arditti et al., 2012), briefly described in Chapter 1. As aforementioned, after studying the orchid named *Angraecum sesquipedale*, endemic of Madagascar and characterized by its long nectar spur, Darwin proposed the existence of a particular species, endowed with an equally long tongue, that would pollinate it. Wallace further elaborated upon this hypothesis, envisioning and drawing the plausible form of the pollinator. As a matter of fact, no less than three predictions can be disentangled from this event. First, on the existence of the animal species, about which Wallace (1867) famously wrote:

> *[...] that such a moth exists in Madagascar may be safely predicted: and naturalists who visit that island should search for it with as much confidence as astronomers searched for the planet Neptune [...].*

Next, on the existence of the actual mutualistic relationship between the orchid and the hawk moth. And last but not least, on the robustness of species' persistence, summarized by Darwin (1877)'s sentence: '*If such great moths were to become extinct in Madagascar, assuredly the Angraecum would become extinct*', which predicted a dynamical process of coexinction. Curiously enough, the three predictions have undergone different fates: while the Hawk moth was discovered only two decades after Darwin's death, the mutualistic interaction itself was not explicitly observed until the 1990's (Arditti et al., 2012). The coexinction prediction, on the other hand, has remained a conjecture until today.

This simple example illustrates some of the current problematics for making accurate forecasting in the field of ecological networks. On the one hand, in order to be able to perform suitable predictions one needs an adequate theoretical and methodological framework, that permits modeling the complexity of the system. Along this thesis, we have explored and discussed some of the advantages and limitations of the network formalism. However, at the same time, forecasting is intimately dependent on the quality of the observations, since noisy or incomplete data will certainly undermine the prediction power of any model (Clark et al., 2001). This relates indeed to the second part of this thesis and the discussion about phenology and how it affects mutualistic systems. In this sense, to assess the possible impact of climate change on ecological communities, we need high-resolution data that incorporates, as well, precise information on spatial and temporal heterogeneity (Ings et al., 2009). As aforementioned at the beginning of the thesis, this is a cooperative endeavor that calls for further and interdisciplinary research. In the end, only by doing accurate predictions that can guide concrete actions on natural ecosystems we may fill the gap between science and society.

While this happens, we may continue doing as Emily Dickinson said: *Not knowing when the dawn will come, I open every door.*

Appendices

APPENDIX A

Datasets

A.1 Ecological networks

The Web of Life repository (Bascompte Lab)[1] contains a large dataset of ecological networks, including very diverse species, interaction types, and ecosystems' location and climate. We detail below the main characteristics of the data exploited in Chapters 3 and 4 of this thesis. The number without brackets represents the total number of networks extracted from the repository, while the number between brackets represents the quantity of networks that have a minimum size of 20 nodes, which corresponds to the minimal cutoff used in the study presented in Chapter 4.

- 133 (118) Plant-pollinator networks. Here, the links among guilds represent mutualistic relationships, characterized by benefiting both interacting agents. In this case, animals, including mainly insects, pollinate flowering plants. This activity provides the pollinators with nutrients while pollinated plants enhance their reproductive success. The two set of nodes of the bipartite network represent the species of the plant and pollinator guilds.
- 30 (23) Seed-disperser networks. Here, the links also represent mutualistic interactions, consisting now of birds feeding on the fruits of certain plants and then contributing to their reproduction and dispersal by disseminating their seeds. Hence, one guild is formed by the plant species and the other by the bird species.
- 51 (43) Host-parasite networks. Here, the links depict a parasitic relationship, where one of the species obtains benefits in detriment of the other. Explicitly, these networks are formed by different flea species which feed on diverse mammal species. Although this is not a mutualistic interaction, the system may still be represented by a bipartite network where the two guilds correspond to flea and mammals species.
- 4 (4) Plant-herbivore networks. Here, the links represent a consumer-resource interaction between insect species (one guild) and plant species (the other guild). In detail, the networks depict different communities where macrolepidopteran species feed on several Prunus species.
- 4 (3) Plant-ant networks. These networks include two examples of diverse types of communities: a network depicting ants which feed on plant nectar, this being a consumer-resource interaction, and two networks representing communities where ant species live in a mutualistic association with certain plant species known as Myrmecophytes.

A.2 Economic networks

In Chapter 4 we studied as well a set of economic networks, which are publicly available in Hernandez et al. (2018). In particular, these data consist of:

[1] Publicly available at: www.web-of-life.es

- 8 economic networks representing buyers-sellers interactions in the Boulogne-sur-Mer Fish Market in France (Hernández et al., 2018). These are mutualistic networks taken from a very different context. Each network describes the transactions observed in different days in the bilateral or in the auction Fish Market. These daily networks are typically much denser than ecological ones.

A.3 Phenology and plant-pollinator networks

We used two public datasets which contain observations of mutualistic interactions in plant-pollinator systems together with their phenology. We detail the peculiarities of each dataset below.

The Illinois dataset

The dataset gathered by Burkle et al. (2013) corresponds to a set of woodland sites in Carlinville, Illinois (USA), observed during the springs of 2009 and 2010 from March to May [2]. The observed network of mutualistic interactions contained originally 26 spring-blooming herbaceous plants and 54 bee species. However, 2 plant species did not exhibit any interaction in the empirical network, so we removed them of the analysis and obtained eventually a 24×54 network.

The dataset also included the observed phenology, specifically the starting and ending dates of the active stages of both plants and pollinators. Using those, we extracted as well their periods of activity and the middle dates.

The Lesvos Island dataset

The dataset recorded by Kantsa et al. (2018) is based on a two years study conducted in Aglios Stefanos, Lesvos Island (Greece) during the springs of 2011 and 2012 from April to July. The published dataset[3] includes the aggregated network of interactions over the two years, composed by 41 plant species and 168 pollinators. Moreover, it provides as well mixed information of phenology, including one-year observations and two-years averages. Nonetheless, Kantsa et al. shared with us the observed phenology for each year separately, that is, the starting and ending date of activity for each species in both seasons. Using these, we obtained as well their periods and middle dates.

Remarkably, a large portion of the pollinator species are present in only one of the seasons. In particular, out of the total 168 pollinator species observed along the two years, only 67 species (39.9%) were persistently found in both seasons, while 53 species (31.5%) were observed just during the first year and 48 species (28.6%) just during the second year of observation. This implies that not only there is an important turnover of interactions among the two consecutive years, but also there is a considerable species turnover, as suggested as well by previous studies (Olesen et al., 2008; Chacoff et al., 2018).

In order to obtain the network of interactions specific to each year, we removed those interactions present in the aggregated network that, after including the corresponding information on phenology, occur among species whose periods of activity do not overlap. In such cases, it is clear that the interaction was not possible due to the lack of phenological overlap and hence we can remove it from the yearly network. After doing so for each season, we removed as well those species that do no longer hold mutualistic interactions –i.e. they have zero degree. As a result, both year-specific networks sizes' are reduced to 34 plants species and 113 pollinators in the first year, and 38 plant species and 104 pollinators in the second year of observations.

This method partly approximates the network of interactions corresponding to each year, in the sense that we might be slightly overestimating the number of interactions and underestimating the turnover by keeping all the plausible interactions present in the

[2]The original dataset is publicly available at: https://doi.org/10.5061/dryad.rp321

[3]The original dataset is publicly available partly as Supplementary Material of the article, partly as a repository at: https://figshare.com/articles/dataset/Data_from_Disentangling_the_role_of_floral_sensory_stimuli_to_pollination_networks_/5663455

aggregated network. However, in the absence of a more detailed dataset, it is arguably a valid estimation since it entirely respects the ecological niches.

APPENDIX B

Computational implementation of the null model

Here we give the numerical details on how we obtained the Lagrange multipliers $\vec{x}^*$ and $\vec{y}^*$ that define the corresponding statistical ensembles of the empirical networks. The determination of these multipliers might be achieved following either of two procedures: by directly maximizing the log-likelihood in Eq. 3.11 or by solving the non-linear, coupled set of equations in 3.12-3.13. While in this section we present our particular implementation for bipartite graphs, there is a Matlab package developed by Squartini et al. (2015) which numerically solves this optimization problem for a variety of types of unipartite graphs and constraints [1]. The main difference between their implementation and our approach lies in the numerical functions used to find the optimal Lagrange multipliers. Whereas their package uses a local optimizing function [2], we made a special effort to ensure that the maxima found are global, in particular, by combining the use of a global search algorithm with a local optimization function repeated over a large set of pseudo-random initial conditions.

B.1 Constrained maximization of the entropy

We numerically optimized the log-likelihood by *simulated annealing* (Corana et al., 1987; Goffe et al., 1994, 1996). Given the pseudo-aleatory character of this approach, which allows to overcome the barriers separating local minima, it is extendedly used in situations in which the co-existence of several local optima is expected.

More precisely, in our case we need to take into account that in Eq. 3.11 the degrees may be degenerate. This means that nodes of the same guild having identical degrees satisfy equivalent equations, hence necessarily bearing the same solution. To account for this, we introduced a multiplicity factor m_p for plants and m_a for animals. If we call red_P and red_A the redundancy for plants and for animals (namely, the corresponding numbers of repeated degrees), then the system can be redimensionalized to $N'_P = N_P - red_P$ and $N'_A = N_A - red_A$. This procedure is an extension to the bipartite case of the redimensionalization proposed in Garlaschelli and Loffredo (2008) for a unipartite network. Consequently, the log-likelihood might be rewritten into:

$$L(\vec{x}) = \sum_{p=1}^{N'_P} m_p v_p \, ln(x_p) + \sum_{a=1}^{N'_A} m_a h_a \, ln(y_a) - \sum_{a=1}^{N'_A} \sum_{p=1}^{N'_P} m_p m_a \, ln(1 + x_p y_a) \tag{B.1}$$

[1] The package implements the entire 'Max&Sam' methodology for a general unipartite setting. It provides the functions to find the numerical solution for the maximum entropy ensemble under a number of different constraints for both undirected or directed networks, binary or weighted. Moreover it permits to sample the resulting ensemble. The package is freely available online at https://it.mathworks.com/matlabcentral/fileexchange/46912-max-sam-package-zip. The bipartite case can be reproduced, using this package, by redefining the directed unipartite case in such a way that one guild solely has out-going links, while the other only has incoming links. The formal analogue of preserving the average degree sequences of both guilds would be now to constrain, in average, the in-degree and out-degree sequences.

[2] One can find the documentation of the Matlab function they used to solve the optimization problem in https://es.mathworks.com/help/optim/ug/fmincon.html.

Although, in analytical terms, the original expression in Eq. 3.11 and this latter one are obviously equivalent, from a computational point of view reducing the number of variables enhances the algorithm's efficiency. Besides, imposing from the beginning such identity between variables improves the accuracy of the program.

We have programmed a standard version of the simulated annealing algorithm. The random number generator used is the one by Toral and Chakrabarti (1993), with a starting temperature of $T = 10^3$, a reduction factor of the temperature of $RT = 0.85$, and a total number of updates per fixed temperature of $2 \cdot 10^4$. The algorithm stops when five consecutive iterations differ in less than a parameter $tol = 10^{-6}$. Furthermore, we ran the algorithm 10 times per network with different random seeds, in order to produce independent sequences of explorations. It is considered that the global optimum has been reached when all the runs converge to the same solution.

B.2 Local solution of the system of equations

We have solved the set of equations by means of a local, deterministic algorithm known as the *modified Powell hybrid method*. In particular, we used the MINPACK library (Moré et al., 1980) for FORTRAN, available online (Burton S. Garbow). This method finds the zero of a non-linear system by exploiting its Jacobian, which we analytically calculated and implemented into the program.

As before, we may re-dimensionalize the problem to N'_P equations for plants and N'_A equations for animals, which now read:

$$v_p = \sum_{a=1}^{N'_A} \frac{m_a x_p y_a}{1 + x_p y_a} \quad \text{for } p = 1, ..., N'_P, \tag{B.2}$$

$$h_a = \sum_{p=1}^{N'_P} \frac{m_p x_p y_a}{1 + x_p y_a} \quad \text{for } a = 1, ..., N'_A. \tag{B.3}$$

We implemented these equations and their Jacobian and ran the algorithm with a tolerance $tol = 10^{-11}$ (as defined in the source code). The possibility of exploiting the gradient provides, in general, a greater local accuracy than the simulated annealing technique. However, its shortcoming lies on the risk of getting trapped in local optima, from which, due to its deterministic nature, it is unable to escape. To compensate this drawback we performed a significant sampling of the space of initial conditions, by running 10^4 iterations of the algorithm, each with a different random selection of starting points, covering as well distinct ranges. However, due to the encounter of rough, rather accidental configuration surfaces, the modified Powell hybrid method was not always able to converge to a solution. The rate of success was approximately 50%.

To finally ensure that the maximum found is global, we compared the outcomes of the various independent runs. Moreover, for the cases when the Powell algorithm converged, we could also compare the solutions obtained for both methods which amounts to a total of 10 runs for the simulated annealing and 10^4 for the Powell hybrid method. In all these cases the same maximum was found.

We have also checked that the constraints are correctly met with a relative precision between 0.01% and 10%, by computing the expected degrees from Eq. 3.12-3.13 and comparing to the corresponding values of the observed networks. The worst case of 10% was typically caused by discrepancies in low degrees, generally the most sensitive to imprecisions in the elements of the randomized matrix given that the matrix elements of low degree nodes are usually very small (see Fig. 3.4 in main text as an example).

APPENDIX C

Statistical measures for stable-NODF

C.1 Analytical expressions for the first two moments of stable-NODF

The analytical expression for the average of s-NODF over the ensemble is:

$$\langle \text{s-NODF}(\mathbf{B}) \rangle^* = \frac{1}{K} \sum_{i<j}^{N_P} \left\{ \cdot \frac{\sum_{a=1}^{N_A} \langle b_{ia} \rangle \langle b_{ja} \rangle}{\sum_{a=1}^{N_A} \langle b_{ja} \rangle} \right\} + \frac{1}{K} \sum_{k<l}^{N_A} \left\{ \cdot \frac{\sum_{p=1}^{N_P} \langle b_{pk} \rangle \langle b_{pl} \rangle}{\sum_{p=1}^{N_P} \langle b_{pl} \rangle} \right\}. \tag{C.1}$$

The standard deviation of s-NODF is given by the analogous of Eqs. 3.26-3.27, where the partial derivatives in Eq. 3.27 correspond to:

$$K \, \frac{\partial \, \text{s-NODF}(\mathbf{B})_{\text{plants}}}{\partial b_{rc}} = \sum_{j=r+1}^{N_P} \frac{b_{jc}}{v_j} + \sum_{i=1}^{r-1} \frac{b_{ic}}{v_r} - \sum_{i=1}^{r-1} \sum_{a=1}^{N_A} \frac{b_{ia} \, b_{ra}}{{v_r}^2} \tag{C.2}$$

$$K \, \frac{\partial \, \text{s-NODF}(\mathbf{B})_{\text{animals}}}{\partial b_{rc}} = \sum_{l=c+1}^{N_A} \frac{b_{rl}}{h_l} + \sum_{k=1}^{c-1} \frac{b_{rk}}{h_c} - \sum_{k=1}^{c-1} \sum_{p=1}^{N_P} \frac{b_{pk} \, b_{pc}}{{h_c}^2}, \tag{C.3}$$

C.2 Statistical measures of stable-NODF

We have computed the real nestedness and its statistical significance using stable-NODF, for the 167 networks in our dataset. In particular, for each real network we have calculated the estimated average and the standard deviation using the analytical expressions in Eq. C.1 and Eqs. C.2-C.3. Fig. C.1 and Table C.1 show that real nestedness is not statistical significant when measured by stable-NODF either.

Fraction of ntws with |z-score| ≤ 1		Fraction of ntws with |z-score| ≤ 2	
118 out of 167	70.7%	162 out of 167	97.0%

Table C.1: Fraction of networks whose discrepancy between the real and randomized nestedness is less or equal than one or two sigma, for nestedness measures performed with stable-NODF.

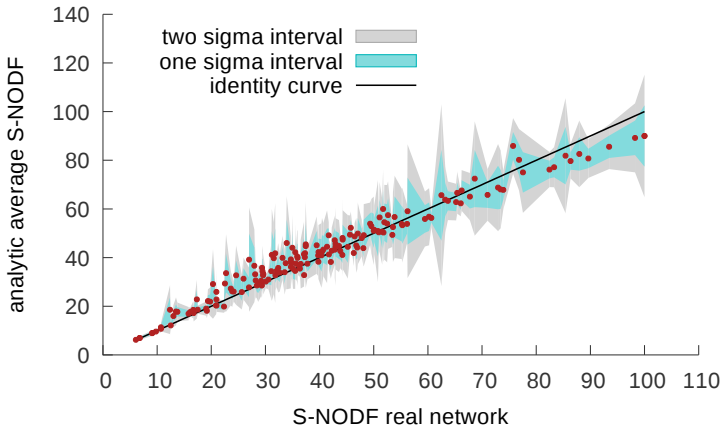

Figure C.1: Comparison between the real measure of stable-NODF and its average in the ensemble estimated using an analytical expression, for the 167 networks of our study.

APPENDIX D

Additional methods to assess the significance of nested patterns

D.1 Significance tests

We quantified the significance of the nestedness measures using the *z-score* index, which for a general property x reads: $\frac{x^*-\langle x\rangle}{\sigma_x}$. For us, $\langle x\rangle$ is the average nestedness computed in the ensemble, either analytically or by explicit sampling, and we compare it with the empirical observations x^*. The standard deviation is σ_x. Given that the NODF values are Gaussian distributed in the random ensemble, the z-scores can be directly related to p-values.

Moreover, we performed a *multiple test correction* which allows accounting for the fact that as the number of statistical tests increases, so does the probability of finding rare events (Benjamini and Hochberg, 1995). Thus, considering the multiple comparisons prevents overstating the number of significant discoveries. It is pertinent to apply this technique here since the 167 cases studied are evaluated under the same *null hypothesis* and all of them follow a normal distribution. We employed the *false discovery rate* method, in particular the Benjamini-Hochberg procedure which applies to independent tests (Benjamini and Hochberg, 1995). The correction was numerically carried out using the $StatsModel$ package in Python (Seabold and Perktold, 2010).

D.2 Self organizing network model

In order to reorganize the original network into an even more nested structure, we numerically implemented the self-organizing network model proposed by Burgos et al. (2007). This methodology keeps constant many aspects susceptible to affect the measure of nestedness, like the size and fill, but modifies the degree sequences through the redistribution of connections. We rewired the links among species following two simple rules: *i)* when changing an interaction, the new partner must have higher degree than the old neighbor *ii)* if the proposed redistribution leaves one of the two nodes with no interactions at all, we reject the change. This operation was repeated until the system achieved a frozen state in which no more reconnections were accepted (we considered this happened when 10^3N consecutive rejections occurred, being N the number of nodes of the network). The final frozen state is normally not perfectly nested, since condition *(ii)* typically leads to configurations which are not utterly optimal. To compensate this, we carried out 10^3 independent rewiring operations for each network. We then averaged the target properties, namely, nestedness (measured using NODF) and the variance of the joint degree sequence of the two guilds.

D.3 Statistical measures of degree assortativity

Assortativity is a network feature that quantifies to what extent nodes tend to match other nodes that are similar (or dissimilar) to them. Here, we used the notion of degree assortativity. We followed the definition proposed by Newman (2002), which consists of a normalized correlation coefficient between degrees. This eventually corresponds to the *Pearson*

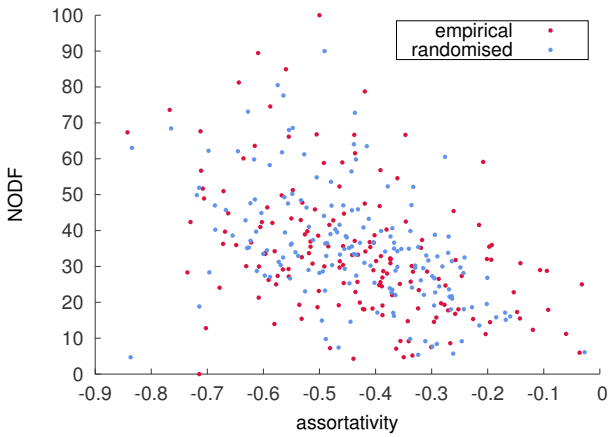

Figure D.1: Relation between the degree assortativity and the nestedness for the real network (in pink) and the average measure for the randomised case (in blue).

correlation coefficient denoted by r, such that $r = -1$ indicates perfect disassortativity, $r = 0$ no correlation at all and $r = 1$ maximum assortativity.

In order to compute the statistical properties of this quantity, we produced for each ensemble a sampling made up by 10^4 networks. We then measured computationally the assortativity of each sampled network using the *assortativity_degree* function from the *igraph* package in *R* (Csardi). Fig. D.1 displays the anti-correlation between the Pearson's coefficient and nestedness, showing that, in general, the more disassortative a network is the more nested. Finally this allowed us to calculate the first and second moments of the assortativity for each ensemble in our set.

APPENDIX E

Measures of nestedness on a sampling

E.1 Statistical measures of NODF on a sampling

Effect of the NODF's normalization

Null networks obtained by sampling the canonical ensemble may include nodes with no interactions and, hence, degree zero. Typically, this corresponds to nodes with low degree in the real network, which are very common in ecological networks having fat-tailed degree distributions. Such zero-degree nodes pose a dilemma when measuring certain network properties which involve normalizing by the size of the network (or a related quantity). This happens, in fact, for NODF, which is normalized by the total number of pairs of rows and of columns.

In particular, we may consider two different criteria for normalizing NODF:

- **Homogeneous normalization.** The dimension is calculated including the zero-degree nodes, so that the size is held constant and equal to the original one. This has the advantage that, since the degree sequences are preserved on average and so is the size, the density of links is preserved on average (and equal to the empirical one). Moreover, from a conceptual perspective it makes sense to consider nodes that are present in the system but not interacting -e.g. a plant which is flowering but is not visited by pollinators-.

- **Heterogeneous normalization.** We may consider as well not to count the zero-degree nodes, which entails that the size of the network changes from one sampled network to another. In this case, the sampled networks are typically smaller that the original one (see Fig. E.1) and, since the degree sequences are still preserved on average, the average density of links on the ensemble differs from the empirical value (actually, it is larger).

The homogeneous choice is more appropriate, since it keeps constant the density of links (an equal to the real value) and it is conceptually sound. Importantly, choosing one or another normalization has a strong impact on the resulting value of NODF, as can be seen in Fig. E.2. Indeed, the heterogeneous normalization leads to a significant discrepancy between the analytical and sampled average, being the sampled average systematically larger than the analytical prediction. On the other hand, by using the homogeneous normalization this discrepancy falls within two standard deviations, meaning that the two measures are statistically compatible.

Altogether, this effect is driven, mainly, by the strong dependency of NODF on the density of links, that has been explictly quantified in Chapter 4. Indeed, given that in the heterogeneous choice smaller networks tend to have a larger density of links, the resulting NODF is biased towards larger values. Consequently, we chose to estimate the distribution of NODF using the homogeneous normalization.

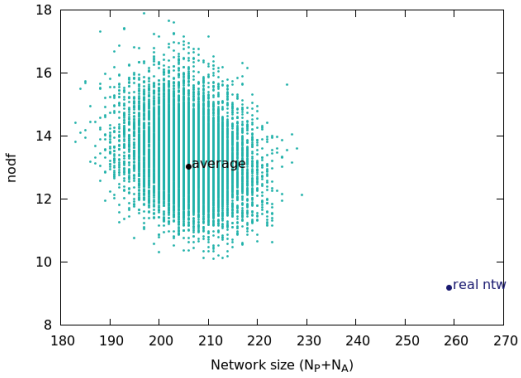

Figure E.1: Comparison between the real (in blue) and sampled values (in green) of the NODF and size of several sampled networks, obtained by neglecting zero-degree nodes. Calculations are made over an empirical pollination network composed by 259 species, and the sampling includes 10^4 null networks.

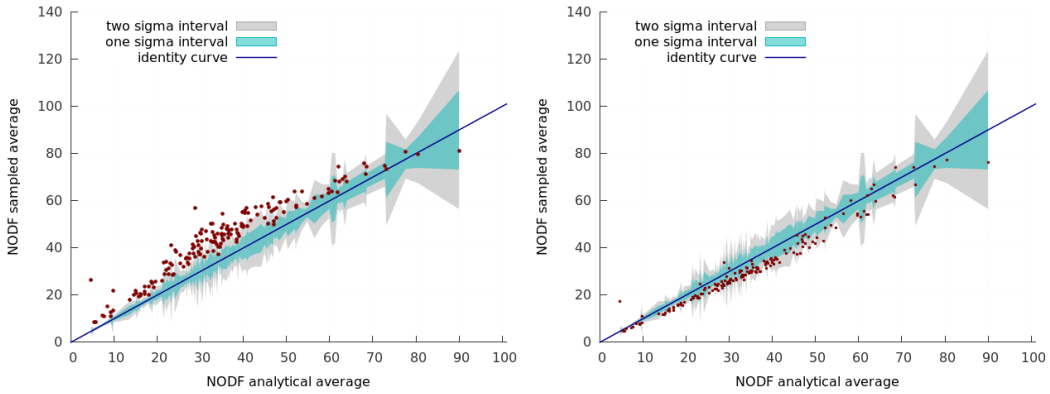

a) Heterogeneous normalization **b)** Homogeneous normalization

Figure E.2: Comparison between the sampled average and the analytical average, measured by NODF, for a set of real mutualistic networks. The expression for the analytical average is the same for both **a)** and **b)**. However, in **a)** the sampled average is calculated by excluding from the normalization the nodes with zero degree. Instead, **b)** keeps the normalization factor constant.

Results using the homogeneous normalization

Using the homogeneous normalization, we performed the statistical measures of NODF on a sampling of the ensemble. The sampling is formed by 10^4 networks generated using the link probabilities in Eq. 3.17 for each one of the 167 empirical networks of the study. As we can see in Fig. E.3 and Table E.1, the real value of nestedness and the average over the sampling are statistically compatible.

E.2 Statistical measures of spectral radius on a sampling

We carried out as well the calculations for the expected average and standard deviation of the spectral radius on a sampling. To this end, we sampled the statistical ensemble by producing 10^4 networks. For each sampled network we computed the spectral radius, ρ,

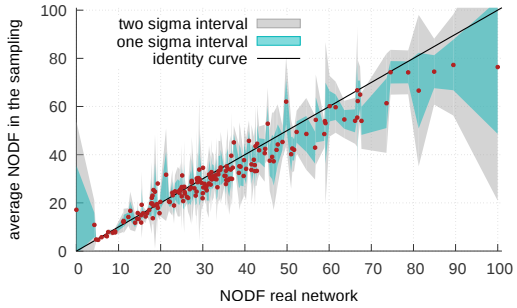

Figure E.3: Comparison between the real measure of NODF and the average computed over the sampling formed by 10^4 networks, for the 167 networks of our study.

Fraction of ntws with |z-score| ≤ 1		Fraction of ntws with |z-score| ≤ 2	
108 out of 167	64.7%	150 out of 167	89.8%

Table E.1: Fraction of networks whose discrepancy between the real and randomized nestedness is less or equal than one or two sigma, for NODF distributions estimated on a sampling of the ensemble.

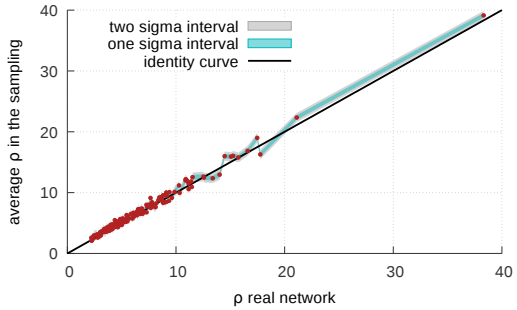

Figure E.4: Comparison between the real observation of the spectral radius $\rho(\lambda)$ and the average estimated over a sampling of the statistical ensemble formed by 10^4 networks, for the 167 networks of our study.

using the *R* package *rARPACK* (Qiu and Mei, 2016). Finally, we calculated the average and the standard deviation of the resulting distribution. Fig. E.4 and table E.2 show the comparison between the real value of spectral radius and the average computed over the ensemble, which turn out to be statistically compatible.

It is important to remark that the sampling and the theoretical approach provide slightly different measures of nestedness when using the spectral radius. This is due to the non-normalized character of the spectral radius, which sets a dependence both on the size of the network and its number of links. Indeed, a superior bound for the spectral radius which depends on these quantities is given by Hong Yuan (1988), who proposed that, for a connected graph A having N nodes and L links, it is fulfilled that: $\rho(A) \leq \sqrt{2L - N + 1}$. In fact, when sampling the ensemble, the number of links is conserved in average, but the average number of nodes with non-zero degree decreases. This entails that the average density grows and, consequently, so does the spectral radius. This explains the difference between the theoretical prediction and the measures over the sampling, and calls for special caution when using the spectral radius to quantify nested patterns.

Fraction of ntws with $\|$z-score$\| \leq 1$		Fraction of ntws with $\|$z-score$\| \leq 2$	
84 out of 167	50.3%	149 out of 167	89.2%

Table E.2: Fraction of networks whose discrepancy between the real and randomized nestedness is less or equal than one or two sigma. Nestedness is measured with the spectral radius $\rho(\lambda)$.

APPENDIX F

Methods for assessing nestedness' metrics performance

F.1 Computation of the nestedness index for each of the studied metrics

Temperature

We calculated the temperature metrics using the *R* software (R Core Team, 2013) and, specifically, the *bipartite* package (Dormann et al., 2009) version 1.13.0. In particular, we used the *nested* function and we set as method the *binmatnest2* option. This calculates the temperature metrics by using an implementation by Oksanen et al. (2017) of the *binmatnest* program by Rodríguez-Gironés and Santamaría (2006). We have redefined the resulting temperature in order to uniform the interpretation of the values yielded by all the metrics such that the higher the value of the corresponding index, the higher the nestedness.

NMD

We calculated the nestedness metrics based in the Manhattan distance (NMD) using the *R* software (R Core Team, 2013). We used the *nestedness.corso* function (currently deprecated) from the *bipartite* package (Dormann et al., 2009) version 0.90. For each measure (both for the real networks and the sampled networks), we set to 500 the number of null networks that eventually permits evaluating the significance. Again, we redefined the index to simplify the interpretation of results.

NODF

We wrote a program in FORTRAN90 that computes the NODF and stable-NODF metrics for the real networks, as well as for the corresponding set of null networks.

Importantly, when performing the calculations over the sample of null networks, we kept the same normalization for all sampled networks. That is, we divided the number of overlapping connections, calculated for each null network, by the original number of rows and columns, independently of whether some of the nodes came to have zero degree in the null network.

Discrepancy

We computed the discrepancy metrics using the *R* software (R Core Team, 2013) and the *bipartite* package (Dormann et al., 2009) version 1.13.0. In particular, we performed the calculation using the method *discrepancy* from the *nested* function.

The final nestedness value measured is directly proportional to the density of links and size of the network. With the aim of removing such dependencies, we divided the resulting value of the metrics by the total numbers of links. This results in a relative discrepancy. Once again, we finally rescaled the index in order to obtain the same monotonic variation for all the indices.

NIR

We implemented a program in FORTRAN90 that calculates the NIR value of the real network and of the corresponding set of null networks. In each case, the resulting value of nestedness is multiplied by 100 in order to preserve the same scale for all the metrics.

In order to account for the possible effects of the degeneracy in the ordering, that is, the fact that multiple configurations are possible when we order rows and columns by their degree, we computed the resulting NIR as the average over a large number of equivalently ordered configurations. These configurations were produced by randomly swapping the matrix position of nodes with the same degree. In more detail, to generate a new ordering we run over all the nodes with degenerate degree and, for each node, we accept a position swap with probability $\frac{1}{2}$.

For each real network, we calculated the degeneracy, *ideg* –that is, the number of repeated degrees. Then, we produced a total of $10 \cdot ideg$ configurations with the same degree order but diverse row and column positions. This procedure was carried out both for the real network and for each null network in the sampling with the exception of the Robertson's network (Robertson, 1929) for which, due to its very large size (1500 species), only 10 degenerate configurations have been computed.

Spectral radius

We computed the largest eigenvalue using the *R* software (R Core Team, 2013), in particular the *eigs_sym* function from the *rARPACK* package.

F.2 Correlations among metrics and network features

The statistical correlations were numerically calculated using Python. The Spearman rank correlation coefficient r_s and its p-value were calculated using the Scipy package (Virtanen et al., 2020), in particular the *scipy.stats.spearmanr* function.

We performed the linear fits using the *Statsmodels* package (Seabold and Perktold, 2010), which carries out a multi-linear least-square regression and provides multiple information, including the adjusted R^2, the partial regression coefficients, their standard deviation and their associated p-value. The t-ratio$_{i,j}$ corresponding to each partial regression coefficient, $\beta_{i,j}$, is calculated as follows:

$$t - \text{ratio}_{i,j} = \frac{\beta_{i,j}}{\sigma_{i,j}} \tag{F.1}$$

where $\sigma_{i,j}$ is the standard deviation associated to that coefficient. This index provides, hence, information on how significantly different from zero is a certain regression coefficient.

APPENDIX G

The *nullnest* repository

In order to complement the theoretical work presented in Chapters 3 and 4, we released an open github repository named *nullnest*[1] that aims at being a practical tool, for both ecologists and network scientist, to assess the nestedness of real and null networks. The repository is thoroughly documented, with examples and ready-to-use programs, and allows performing the analysis discussed in Payrató-Borràs et al. (2019) and Payrató-Borràs et al. (2020).

The *nullnest* repository is divided into two main blocks. The first part is related to the construction of the null model. In particular, it provides a program to compute the maximum-entropy and maximum-likelihood ensemble discussed in section 3.2 for any bipartite network introduced by the user. It also contains the ready-to-use probabilities of interaction in the null ensemble, for the whole dataset of empirical networks described in the Appendix A. On the other hand, the second part of the package is concerned with the measurement of nestedness. In detail, we provide the codes to quantify the real degree of nestedness of a given matrix, together with the first two moments of its null distribution, using any of the six metrics discussed in the first part of the thesis. This can be done either by using the analytical expressions derived in Payrató-Borràs et al. (2019) (only for NODF and the spectral radius) or by numerically sampling the null ensemble, for any of the six metrics studied in Payrató-Borràs et al. (2020).

[1]The codes and the accompanying documentation can be downloaded at: https://github.com/cclaualc/nullnest.

APPENDIX H

Statistical tests on phenology

H.1 Quality of a fit using the Kolmogorov-Smirnov test

In order to assess the quality of the fit and obtain its corresponding p-value, we start by performing a Kolmogorov-Smirnov one-sample test between the fitted function and the empirical distribution, using the *stats.kstest* software from the *SciPy* package (Virtanen et al., 2020) in Python. Next, in order to determine its p-value we explicitly compare the obtained KS-value with the expected statistics, sampled using Monte Carlo simulations.

In more detail, we proceed as follows:

- We calculate the K-S test statistics –using the SciPy software–, that we may call D_{obs}, between the empirical distribution and the fitted function, whose parameters are estimated using the maximum likelihood fitting software from the *stats* function in SciPy.
- Using Monte Carlo methods, we generate a sample of size N_{sampl} composed by synthetic distributions, each sampled from the fitted function and having the same size as the observed, empirical distribution.
- For each synthetic sample indexed by i, we fit a function using the same functional form as in the empirical case and using the maximum likelihood estimator from the *stats* function in SciPy.
- We then calculate the K-S test statistics between this novel fit and the corresponding synthetic sample, which produces a new distance that we will call $D_{syn,i}$.
- Once this procedure has been repeated for all the synthetic distributions generated, we can compare the observed K-S statistics D_{obs} with the distribution of $D_{syn,i}$ in the sample.

After carrying out this computation, the p-value is then calculated as:

$$\text{p-value} = \frac{\text{number of samples with } D_{syn,i} > D_{obs} + 1}{N_{sampl}}, \tag{H.1}$$

which, as normally, quantifies whether the observed KS distance D_{obs} differs significantly from what would be expected if the observed distribution of periods was really generated by the fitted function. Hence, when the p-value is sufficiently large the fit is compatible with this assumption.

H.2 Kolmogorov-Smirnov two sample test

We programmed a Kolmogorov-Smirnov test on two samples by using the *ks_2samp* function from the *SciPy* package. In detail, the K-S test for two samples permits challenging the null hypothesis that two particular samples come from the same statistical distribution. The smaller the KS distance, the smaller the discrepancy between the two samples. In the case where the p-value is relatively small (e.g. p-value < 0.05) the difference among distributions

is significant and hence the null hypothesis is rejected, which in our case implies that the distribution produced by the given synthetic model is incompatible with the empirical observations.

H.3 Kullback-Leibler divergence

The Kullback-Leibler divergence quantifies how one probability distributions $Q(x)$ is different from a second, reference distribution called $P(x)$. In particular, the KL divergence from Q to P is defined as:

$$D_{KL} = \sum_x P(x)\, log \frac{P(x)}{Q(x)}, \tag{H.2}$$

and it measures the amount of information lost when approximating $P(x)$ by $Q(x)$. In our case, we calculate this quantity taking as the reference function $P(x)$ the empirical distribution of phenological overlap, while $Q(x)$ corresponds to distribution of phenological overlaps produced by the null model under consideration. We implement this calculation in a program in Python that uses the *stats.entropy* software from the *SciPy* package.

H.4 Pearson correlation with time lag

In order to calculate the Pearson correlation for different values of time lag, we take the evolution of a given structural property in the synthetic model, and shift it alternatively backwards or ahead in time. For each different value of time lag, we calculate the corresponding Pearson coefficient between the synthetic, shifted array, and the unchanged empirical vector. In particular, we use the *stats.pearsonr* software from the *SciPy* package to compute the Pearson correlation. We repeat this procedure for a wide range of different temporal lags, and eventually extract the maximum value. This also provides the time lag at which the correlation among the empirical and the synthetic sequences is maximized.

APPENDIX I

Numerical implementation of synthetic models

In this appendix we explain the different numerical methods used to encounter the starting dates of species' activity, on the basis of different hypothesis and under the constrain that mutualistic partners share a minimum phenological overlap.

First, we describe two numerical approaches to solve the problem of maintaining the mutualistic overlap: *(i)* by shifting some given starting dates, *(ii)* by optimizing a certain quantity within the constraints imposed by the non-zero overlap. Secondly, we explain how we implemented these methods for each particular synthetic model.

I.1 Shift of starting dates

Here we introduce a method to shift a given set of initial times of activity, with the condition that a minimal mutualistic overlap is preserved. The periods of activity, that we will denote as p_i^P for a plant i and p_k^A for an animal k, are kept unchanged. We solely modify the timing of the beginning of the activity of each species, where we note the initial time by $t_{0,i}^P$ for each plant i and $t_{0,k}^A$ for each animal k.

The program takes as input the aforementioned information together with the starting dates of activity, that, importantly, need to already fulfill the set of inequalities written in Eqs. 5.7-5.8. This can be achieved by taking, depending on the case, a trivial solution –e.g. the same starting dates for all species– or the empirical dataset –if available. Then, the proposal of the novel starting dates is done under the condition that a non-zero amount of temporal overlap between interacting mutualistic partners must be preserved. In detail, we impose, at least, 1 day of overlap, which is the minimal unit of phenology in the studied datasets. To warrant that this occurs, we fix the following boundaries to the new initial times. Let us call $t'^P_{0,i}$ the novel time proposed for plant species i:

- The **upper** bound is given by the neighbor species whose activity ceases earlier. That is, by the minimum of the set of times $\{t_{0,k}^A + p_k^A\}$, where k runs over the indexes of the animal species interacting with plant i (so, if $\mathbf{B}$ is the bipartite matrix, those fulfilling that $\mathbf{B}_{i,k} = 1$). Let us illustrate this with the example on Fig. I.1. The upper boundary for the initial flowering time of plant number 1 is given by the pollinator that finishes pollinating earlier, which is animal number 1. Therefore, as can be seen in the figure, the upper limit for $\{t_{0,1}^P\}$ coincides with $\{t_{f,1}^A\}$.

- The **lower** bound is found by subtracting the period of plant i to the time at which starts the last species. Thus, by the maximum of the set of times $\{t_{0,k}^A\}$, minus p_i^P. In the example of Fig. I.1, the pollinator that begins its activity the latest is animal number 3, at $\{t_{0,3}^A\}$. To $\{t_{0,3}^A\}$, we need to subtract the period of plant number 1 (in yellow) in order to recover the lower limit.

According to these criteria, the new starting dates of activity are extracted from the following uniform distribution:

$$t'^{P}_{0,i} \subset U\Big(\mathbf{max}\big(\{t^{A}_{0,k}\}\big) - p^{P}_{i} + 1\,,\, \mathbf{min}\big(\{t^{A}_{0,k} + p^{A}_{k}\}\big) - 1\Big), \tag{I.1}$$

where the 1 is respectively subtracted and added to the boundaries in order to ensure at least one day of overlap between mutualistic partners.

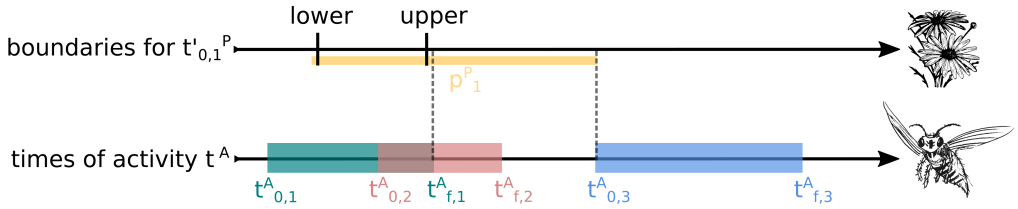

Figure I.1: Example of a plant wich interacts mutualistically with three pollinator species. We calculate the upper and lower boundaries for the new initial time of the plant $t'^{P}_{0,1}$ using, respectively, the minimum final time of activity of its pollinators (here $t^{A}_{f,1} = t^{A}_{0,1} + p^{A}_{1}$) and the maximal initial time (here $t^{A}_{0,3}$) minus the period of the plant (p^{P}_{1}). As can be seen in the figure, to this boundaries we correspondingly added and substracted one day in order to mantain at least one day of mutualistic overlap.

Note again that this procedure requires an initial configuration of starting dates, either empirical or hypothetical, that is then randomized. Subsequently, the resulting set of starting dates shows some dependency on the initial configuration. As explained below, we exploit this feature to generate synthetic phenologies that are approximately centered.

I.2 Constrained optimizations

Here we describe a second procedure to generate a set of starting dates that fulfills the inequalities described in Eqs. 5.7-5.8. In contrast with the algorithm described in section I.1, this method does not require any other input than the network of mutualistic interactions and the periods, and hence there is no initial condition for the starting dates. Instead, we seek a solution that, on the one hand, verifies the system of coupled inequalities, and on the other hand, optimizes a given quantity, described by an objective function.

In particular, given the constraints in Eqs. 5.7-5.8, we may use linear programming techniques to find a feasible solution. Since $L >> N$, the problem is overdetermined, yet we know already that it is consistent because there are some trivial solutions which satisfy all the constraints -e.g., all species starting or finishing the same date-. However, we are particularly interested in non-trivial solutions which can lead to realistic or statistically interesting configurations of phenology. This leads to the introduction of the objective function, which we will seek to optimize over the possible set of solutions. In sections I.4-I.6 we specify the numerical implementation of different forms of this objective function, but the general structure of the algorithm is maintained.

In detail, we solve the constrained optimization problem defined by Eqs. 5.7-5.8 through a two-step process. First, we perform multiple local optimizations with different initial seeds, using the function *minimize* from the *SciPy* package in Python (Virtanen et al., 2020) –specifically the method '*trust-constr*'. Second, we set these local solutions as the starting population for a differential evolution algorithm, which performs a global stochastic search. In particular we use the *differential_evolution* function from *SciPy*. This combination of an iterative local search plus a global optimization aims at ensuring a robust finding of the global optimum.

I.3 Synchronized phenology

In order to produce a configuration where species' periods are relatively synchronized, we proceed in several steps. First, we set the middle dates by sampling a normal probability distribution. Once the medium dates are determined, the location of the period of each species along the seasons is randomized using an algorithmic procedure which conserves the mutualistic interactions provided by the empirical network.

In more detail, we programmed a software in Python that operates as follows:

- We select one of the guilds (for instance, the pollinators) and determine their corresponding starting dates by extracting their middle dates from a normal distribution with standard deviation $\sigma = 0.5$ days and mean $\mu = 120$ days.
- We then set the starting dates for the other guild, by using the randomization process explained in section I.1 of this appendix. In detail, we determine the range -maximum and minimum dates- within which we can extract a random starting date while ensuring that the mutualistic overlap will not be lost. This novel starting date is extracted from a uniform distribution.
- To finish, we re-randomize again the first guild, using the same procedure as in the previous step, in order to relax the assumption of the normality of middle times of activity.

Indeed, we repeat steps *(ii)* and *(iii)* iteratively several times in order to improve the randomization. This eventually yields a non-perfectly synchronized configuration of phenology.

I.4 Minimization of the competition

In order to find the configuration that, under the mentioned constraints, minimizes the competition, we apply the numerical algorithm described in section I.2 where the objective function is the total competitive overlap. In detail, at each iteration of the optimization algorithm, we calculate the total sum of unnormalized phenological overlaps among all competitors, including both competition among plants and among pollinators.

I.5 Maximization of the variance

We perform a constrained search that maximizes the variance of the middle dates by using the algorithm described in section I.2. In this case, the objective function corresponds to the variance, and it is calculated at each iteration of the optimization process.

I.6 Maximization of the entropy

In this model, we find the phenological configuration that maximizes the entropy by using the algorithm explained in section I.2. The objective function corresponds here to the Shannon-Gibbs entropy of the middle dates, as defined in Eq. 5.11, which we explicitly computed using the Python software.

APPENDIX J

Numerical integration of the population model

We simulated the community dynamics as provided by Eq. 6.1 and its counterpart for animals for the aggregated network, and by Eqs. 6.3-6.4 for the network weighted with the phenological overlaps. Each simulation starts from random initial conditions of the relative abundances that are taken at random from a uniform distribution in the interval [0.05, 0.95].

Following references Bastolla et al. (2009); Rohr et al. (2014) and Gracia-Lázaro et al. (2018) we take the values of $\alpha_i^{P,A}$ from a uniform distribution in [0.9, 1.1], the intra-species competition parameter is fixed to $\beta_j^{P,A} = 5$ and the Holling term to $h^{P,A} = 0.1$. For simplicity, we assume that competition and mutualism parameters take the same values for plants and animals. After a transient, equilibrium is assumed when all the species' frequencies remain constant: at that point, we keep the information on final abundances and number of surviving species. A species is considered extinct when its relative abundance is lower than 10^{-9}. This process is repeated for different values of the interaction strength, that is, we modulate β for competition and γ for mutualism homogeneously for all plant and all animal species. Eventually, this provides a heatmap of biodiversity for each pair of β and γ values, as plotted in Fig. 6.2.

APPENDIX K

Translation of summarized conclusions

K.1 Conclusions in French

Depuis que Darwin a introduit sa fameuse métaphore du 'rivage luxuriante' pour décrire la complexité des communautés écologiques, les interactions entre les espèces sont considérées comme des déterminants cruciaux de la structure et de la dynamique des écosystèmes naturels. Cependant, jusqu'à il y a quelques décennies, la plupart de ces travaux soulignaient principalement l'importance des relations antagonistes, laissant de côté les interactions mutualistes – qui étaient considérées comme curieuses du point de vue de l'histoire naturelle mais peu pertinentes (Bronstein, 1994). Aujourd'hui, nous savons que le mutualisme joue en réalité un rôle central dans l'organisation des communautés écologiques, et qu'il est en fait possible de trouver des relations mutuelles dans une multitude d'écosystèmes à travers le monde, à travers différentes échelles spatiales et entre différents types d'organismes (Bascompte and Jordano, 2013).

Dans cette thèse, nous avons étudié les systèmes mutualistes du point de vue du formalisme de réseaux complexes, considérant ces communautés comme un exemple paradigmatique de systèmes complexes. Toutefois, la représentation en réseau implique une tension inhérente entre la nécessité de fournir une description stylisée de l'écosystème permettant de détecter et de comprendre leur propriétés généraux et, d'autre part, le risque d'une simplification excessive, en omettant des détails pertinents de la structure ou de la dynamique. En d'autres termes, en construisant un réseau, nous sommes confrontés au défi de savoir quelle quantité minimale d'informations est nécessaire pour obtenir une représentation fidèle du système, par rapport, bien sûr, aux questions auxquelles nous voudrions répondre.

Cette tension entre nécessité de simplification et attention au détail se reflète dans les deux parties où cette thèse est organisée. En effet, tout au long de la première partie, nous avons examiné la structure des réseaux mutualistes binaires afin d'enquêter sur l'apparition d'un proprieté structurel répandue appelé imbrication. En utilisant un modèle nul basé sur le principe d'entropie maximale, nous avons montré que cet structure peut s'expliquer naturellement par un ensemble réduit de propriétés fondamentales du réseau, à savoir les séquences de degrés. Cette constatation n'a pas seulement d'importantes conséquences sur la question de savoir quels indices structurels doivent être abordés pour caractériser la dynamique des systèmes mutualistes, mais aussi sur notre conception de comment les écosystèmes se forment et évoluent au fil du temps. Ensuite, en appliquant de nouveau le modèle nul construit, nous avons exploré le fonctionnement et la performance de différentes métriques, établissant la difficulté de trouver un outil impartial pour quantifier et classifier universellement les systèmes imbriqués.

Dans la deuxième partie de cette thèse, nous avons suivi une voie différente et, si nous avions auparavant recherché quelles étaient les informations minimales nécessaires pour reproduire la structure des réseaux agrégés, ici nous nous demandons si la représentation statique d'un réseau est réellement suffisamment réaliste ou, au contraire, si son manque de détails fausse notre perception des communautés mutualistes. Premièrement, nous avons exploré les conséquences structurelles de l'introduction de la variabilité temporelle de la communauté, caractérisant deux ensembles de données empiriques à haute résolution. En outre, nous avons proposé un ensemble de modèles destinés à générer, sous diverses hypothèses, des configurations synthétiques de phénologie. À partir de leur comparaison

avec les systèmes empiriques, nos résultats suggèrent que les modèles basés sur le principe de l'entropie maximale reproduisent généralement bien, sous certaines restrictions, la phénologie observée. En revanche, l'adéquation des modèles mécanistes semble dépendre fortement du système étudié. Deuxièmement, en suivant naturellement ce fil de recherche, nous avons abordé la question de savoir comment traduire l'existence de la variabilité temporelle dans un cadre dynamique permettant d'évaluer l'influence de la phénologie sur la coexistence des espèces, un sujet que nous examinons à titre préliminaire et qui nécessite des recherches plus approfondies, notamment dans le contexte du changement climatique.

K.2 Conclusions in Spanish

Desde que Darwin introdujo su famosa metáfora del 'ribazo enmarañado' para describir la complejidad de las comunidades ecológicas, las interacciones entre especies se han considerado determinantes cruciales de la estructura y la dinámica de los ecosistemas naturales. No obstante, hasta hace solo unas décadas se enfatizaba principalmente la importancia de las relaciones antagónicas, dejando de lado las interacciones mutuamente beneficiosas –que se consideraban curiosas desde el punto de vista de la historia natural pero al fin y al cabo poco relevantes (Bronstein, 1994). Hoy en día sabemos que el mutualismo juega, en realidad, un papel central en la organización de las comunidades ecológicas, y que de hecho es posible encontrar relaciones mutualistas en multitud de ecosistemas alrededor del mundo, en diversas escalas espaciales, y entre tipos de organismos muy diferentes (Bascompte and Jordano, 2013).

En esta tesis hemos estudiado los sistemas mutualistas desde el punto de vista del formalismo de redes complejas, considerando estas comunidades como un ejemplo paradigmático de los llamados sistemas complejos. Sin embargo, la representación en forma de red implica una tensión inherente entre la necesidad de proporcionar una descripción estilizada del ecosistema que permita detectar y comprender patrones generales y, por otra parte, el riesgo de simplificar excesivamente, omitiendo detalles relevantes de la estructura o la dinámica. Dicho de otro modo, al construir una red nos enfrentamos al reto de saber cuál es la cantidad mínima de información necesaria para obtener una representación fiel del sistema, en relación, por supuesto, a las preguntas que nos gustaría responder.

Esta tensión entre necesidad de simplificación y atención al detalle se refleja de alguna manera en las dos partes en las que se organiza esta tesis. De hecho, a lo largo de la primera parte hemos examinado la estructura de las redes mutualistas binarias con el fin de investigar la aparición de un extendido patrón estructural, el llamado anidamiento. Usando un modelo nulo basado en el principio de máxima entropía, hemos demostrado que este patrón puede explicarse naturalmente por un conjunto reducido de propiedades fundamentales de la red, concretamente las secuencias de grados. Este hallazgo no solo tiene importantes consecuencias respecto la cuestión de qué índices estructurales deben ser abordados para caracterizar la dinámica de los sistemas mutualistas, sino también sobre nuestra concepción de cómo los ecosistemas se forman y evolucionan a través del tiempo. Seguidamente, aplicando una vez más el modelo nulo construido, hemos explorado el funcionamiento y el rendimiento de diferentes métricas, estableciendo la dificultad de encontrar una herramienta imparcial para cuantificar y clasificar universalmente los patrones anidados.

En la segunda parte de esta tesis, hemos seguido un camino distinto y, si antes habíamos investigado cuál es la mínima información necesaria para reproducir la estructura de las redes agregadas, aquí nos preguntamos si la representación estática de una red es realmente lo suficientemente realista, o, por el contrario, su falta de detalle distorsiona nuestra percepción de las comunidades mutualistas. En primer lugar, hemos explorado las consecuencias desde un punto de vista estructural de introducir la variabilidad temporal de la comunidad, caracterizando dos conjuntos de datos empíricos de alta resolución. Además, hemos propuesto un conjunto de modelos destinados a generar, bajo diversas hipótesis, configuraciones sintéticas de fenología. A partir de su comparación con los sistemas empíricos, nuestros resultados sugieren que los modelos basados en el principio de máxima entropía reproducen generalmente bien –dadas ciertas restricciones– la fenología observada. En cambio, la adecuación de los modelos mecanicistas parece ser sumamente dependiente del sistema

estudiado. En segundo lugar, siguiendo de forma natural este hilo de investigación, hemos abordado el problema de cómo introducir la existencia de la variabilidad temporal en un marco dinámico que permita evaluar la influencia de la fenología en la coexistencia de las especies, un tema que tratamos preliminarmente y que requiere una investigación más detallada, especialmente en el contexto del cambio climático.

Bibliography

Albert, R., H. Jeong, and A.-L. Barabási (2000). Error and attack tolerance of complex networks. *Nature 406*(6794), 378–382.

Aleta, A., S. Meloni, and Y. Moreno (2017). A multilayer perspective for the analysis of urban transportation systems. *Scientific reports 7*, 44359.

Allesina, S. (2012, 07). The more the merrier. *Nature 487*, 175 EP –.

Allesina, S. and S. Tang (2012). Stability criteria for complex ecosystems. *Nature 483*(7388), 205.

Almeida-Neto, M., P. Guimarães, P. R. Guimarães, R. D. Loyola, and W. Ulrich (2008). A consistent metric for nestedness analysis in ecological systems: reconciling concept and measurement. *Oikos 117*(8), 1227–1239.

Amaral, L. A. N., A. Scala, M. Barthelemy, and H. E. Stanley (2000). Classes of small-world networks. *Proceedings of the National Academy of Sciences 97*(21), 11149–11152.

Anderson, P. W. (1972). More is different. *Science 177*(4047), 393–396.

Aono, Y. and K. Kazui (2008). Phenological data series of cherry tree flowering in kyoto, japan, and its application to reconstruction of springtime temperatures since the 9th century. *International Journal of Climatology: A Journal of the Royal Meteorological Society 28*(7), 905–914.

Arditti, J., J. Elliott, I. J. Kitching, and L. T. Wasserthal (2012). 'good heavens what insect can suck it'–charles darwin, angraecum sesquipedale and xanthopan morganii praedicta. *Botanical Journal of the Linnean Society 169*(3), 403–432.

Arthur, W. B. et al. (1993). On the evolution of complexity. Technical report.

Atmar, W. and B. D. Patterson (1993). The measure of order and disorder in the distribution of species in fragmented habitat. *Oecologia 96*(3), 373–382.

Atmar, W. and B. D. Patterson (1995). The nestedness temperature calculator: a visual basic program, including 294 presence-absence matrices. *AICS Research Incorporate and The Field Museum*.

Ayala, F. J. (2007). Darwin's greatest discovery: design without designer. *Proceedings of the National Academy of Sciences 104*(suppl 1), 8567–8573.

Bar-Yam, Y. (2000). Complexity rising: From human beings to human civilization, a complexity profile.

Barabási, A.-L. et al. (2016). *Network science*. Cambridge university press.

Barabási, A.-L. and R. Albert (1999). Emergence of scaling in random networks. *Science 286*(5439), 509–512.

Barber, M. J. (2007). Modularity and community detection in bipartite networks. *Physical Review E 76*(6), 066102.

Bascompte, J. and P. Jordano (2013). *Mutualistic networks*, Volume 70. Princeton University Press.

Bascompte, J., P. Jordano, C. J. Melián, and J. M. Olesen (2003). The nested assembly of plant–animal mutualistic networks. *Proceedings of the National Academy of Sciences 100*(16), 9383–9387.

Bascompte, J., P. Jordano, and J. M. Olesen (2006). Asymmetric coevolutionary networks facilitate biodiversity maintenance. *Science 312*(5772), 431–433.

Bascompte Lab. *Web of Life, ecological networks database*. Bascompte Lab. Available at http://www.web-of-life.es/.

Bastolla, U., M. A. Fortuna, A. Pascual-García, A. Ferrera, B. Luque, and J. Bascompte (2009). The architecture of mutualistic networks minimizes competition and increases biodiversity. *Nature 458*(7241), 1018–1020.

Bawa, K. S., H. Kang, and M. H. Grayum (2003). Relationships among time, frequency, and duration of flowering in tropical rain forest trees. *American Journal of Botany 90*(6), 877–887.

Bell, F. K., D. Cvetković, P. Rowlinson, and S. K. Simić (2008). Graphs for which the least eigenvalue is minimal, ii. *Linear Algebra and its Applications 429*(8-9), 2168–2179.

Ben-Israel, A. and T. N. Greville (2003). *Generalized inverses: theory and applications*, Volume 15. Springer Science & Business Media.

Benjamini, Y. and Y. Hochberg (1995). Controlling the false discovery rate: a practical and powerful approach to multiple testing. *Journal of the royal statistical society. Series B (Methodological)*, 289–300.

Bersier, L.-F. (2007). A history of the study of ecological networks. *Biological networks 3*, 365–421.

Biggs, N., E. K. Lloyd, and R. J. Wilson (1986). *Graph Theory, 1736-1936*. Oxford University Press.

Blüthgen, N., J. Fründ, D. P. Vázquez, and F. Menzel (2008). What do interaction network metrics tell us about specialization and biological traits. *Ecology 89*(12), 3387–3399.

Borge-Holthoefer, J., R. A. Baños, C. Gracia-Lázaro, and Y. Moreno (2017). Emergence of consensus as a modular-to-nested transition in communication dynamics. *Scientific reports 7*, 41673.

Broido, A. D. and A. Clauset (2019). Scale-free networks are rare. *Nature communications 10*(1), 1–10.

Bronstein, J. L. (1994). Our current understanding of mutualism. *The Quarterly Review of Biology 69*(1), 31–51.

Bronstein, J. L. (2001). The costs of mutualism. *American Zoologist 41*(4), 825–839.

Bronstein, J. L., R. Alarcón, and M. Geber (2006). The evolution of plant–insect mutualisms. *New Phytologist 172*(3), 412–428.

Brualdi, R. A. and J. G. Sanderson (1999). Nested species subsets, gaps, and discrepancy. *Oecologia 119*(2), 256–264.

Burgos, E., H. Ceva, L. Hernández, and R. Perazzo (2009). Understanding and characterizing nestedness in mutualistic bipartite networks. *Computer Physics Communications 180*(4), 532–535.

Burgos, E., H. Ceva, L. Hernández, R. Perazzo, M. Devoto, and D. Medan (2008). Two classes of bipartite networks: nested biological and social systems. *Physical Review E 78*(4), 046113.

Burgos, E., H. Ceva, R. P. Perazzo, M. Devoto, D. Medan, M. Zimmermann, and A. M. Delbue (2007). Why nestedness in mutualistic networks? *Journal of theoretical biology 249*(2), 307–313.

Burkle, L. A., J. C. Marlin, and T. M. Knight (2013). Plant-pollinator interactions over 120 years: loss of species, co-occurrence, and function. *Science 339*(6127), 1611–1615.

Burton S. Garbow, Kenneth E. Hillstrom, J. J. M. (1980). Minpack libary source code, subroutine hybrd. Available at: https://www.math.utah.edu/software/minpack/minpack/hybrd.html.

Caldarelli, G., A. Capocci, P. De Los Rios, and M. A. Munoz (2002). Scale-free networks from varying vertex intrinsic fitness. *Physical review letters 89*(25), 258702.

CaraDonna, P. J., W. K. Petry, R. M. Brennan, J. L. Cunningham, J. L. Bronstein, N. M. Waser, and N. J. Sanders (2017). Interaction rewiring and the rapid turnover of plant–pollinator networks. *Ecology letters 20*(3), 385–394.

Carmel, Y., R. Kent, A. Bar-Massada, L. Blank, J. Liberzon, O. Nezer, G. Sapir, and R. Federman (2013). Trends in ecological research during the last three decades–a systematic review. *PloS one 8*(4).

Carpenter, S. R. (2002). Ecological futures: building an ecology of the long now. *Ecology 83*(8), 2069–2083.

Carroll, L. (1872). *Through the looking glass, And what Alice found there*. MACMILLAN AND CO.

Chacoff, N. P., J. Resasco, and D. P. Vázquez (2018). Interaction frequency, network position, and the temporal persistence of interactions in a plant–pollinator network. *Ecology 99*(1), 21–28.

Chuine, I., P. Yiou, N. Viovy, B. Seguin, V. Daux, and E. L. R. Ladurie (2004). Grape ripening as a past climate indicator. *Nature 432*(7015), 289–290.

Chung, F. and L. Lu (2002). Connected components in random graphs with given expected degree sequences. *Annals of combinatorics 6*(2), 125–145.

Cimini, G., A. Gabrielli, and F. S. Labini (2014). The scientific competitiveness of nations. *PloS one 9*(12).

Cimini, G., T. Squartini, F. Saracco, D. Garlaschelli, A. Gabrielli, and G. Caldarelli (2019). The statistical physics of real-world networks. *Nature Reviews Physics 1*(1), 58–71.

Cirtwill, A. R., T. Roslin, C. Rasmussen, J. M. Olesen, and D. B. Stouffer (2018). Between-year changes in community composition shape species' roles in an arctic plant–pollinator network. *Oikos 127*(8), 1163–1176.

Clark, J. S., S. R. Carpenter, M. Barber, S. Collins, A. Dobson, J. A. Foley, D. M. Lodge, M. Pascual, R. Pielke, W. Pizer, et al. (2001). Ecological forecasts: an emerging imperative. *science 293*(5530), 657–660.

Clements, F. E. and F. L. Long (1923). *Experimental pollination: an outline of the ecology of flowers and insects*. Number 336. Carnegie institution of Washington.

Connor, E. F. and D. Simberloff (1979). The assembly of species communities: chance or competition? *Ecology 60*(6), 1132–1140.

Corana, A., M. Marchesi, C. Martini, and S. Ridella (1987). Minimizing multimodal functions of continuous variables with the "simulated annealing" algorithm corrigenda for this article is available here. *ACM Transactions on Mathematical Software (TOMS) 13*(3), 262–280.

Corso, G., A. I. Araujo, and A. M. Almeida (2008). A new nestedness estimator in community networks. *arXiv preprint arXiv:0803.0007*.

Csardi, G. *Assortativity in R igraph package*. Available at: http://igraph.org/r/doc/assortativity.html.

Dakos, V. and J. Bascompte (2014). Critical slowing down as early warning for the onset of collapse in mutualistic communities. *Proceedings of the National Academy of Sciences 111*(49), 17546–17551.

Darwin, C. (1877). *The various contrivances by which orchids are fertilised by insects*. John Murray.

De Benedictis, L. and L. Tajoli (2011). The world trade network. *The World Economy 34*(8), 1417–1454.

Deutsch, E. and M. Neumann (1984). Derivatives of the perron root at an essentially nonnegative matrix and the group inverse of an m-matrix. *Journal of Mathematical Analysis and Applications 102*(1), 1–29.

Domínguez-García, V. and M. A. Muñoz (2015). Ranking species in mutualistic networks. *Scientific reports 5*, 8182.

Dormann, C. F., J. Fründ, N. Blüthgen, and B. Gruber (2009). Indices, graphs and null models: analyzing bipartite ecological networks. *The Open Ecology Journal 2*(1).

Duchenne, F., E. Thébault, D. Michez, M. Elias, M. Drake, M. Persson, J. Piot, M. Pollet, P. Vanormelingen, and C. Fontaine (2020). Phenological shifts alter the seasonal structure of pollinator assemblages in europe. *Nature Ecology & Evolution 4*(1), 115–121.

Dupont, Y. L. and J. M. Olesen (2009). Ecological modules and roles of species in heathland plant–insect flower visitor networks. *Journal of Animal Ecology 78*(2), 346–353.

Egerton, F. N. (2007). Understanding food chains and food webs, 1700–1970. *The Bulletin of the Ecological Society of America 88*(1), 50–69.

Eklöf, A., U. Jacob, J. Kopp, J. Bosch, R. Castro-Urgal, N. P. Chacoff, B. Dalsgaard, C. de Sassi, M. Galetti, P. R. Guimarães, et al. (2013). The dimensionality of ecological networks. *Ecology letters 16*(5), 577–583.

Elton, C. S. (1927). *Animal ecology*. The Macmillan Company.

Encinas-Viso, F., T. A. Revilla, and R. S. Etienne (2012). Phenology drives mutualistic network structure and diversity. *Ecology Letters 15*(3), 198–208.

Euler, L. (1741). Solutio problematis ad geometriam situs pertinentis. *Commentarii academiae scientiarum Petropolitanae*, 128–140.

Feng, W. and K. Takemoto (2014). Heterogeneity in ecological mutualistic networks dominantly determines community stability. *Scientific reports 4*, 5912.

Fisher, R. A. (1935). *The design of experiments.* Oliver and Boyd. London and Edinburgh.

Forrest, J. and A. J. Miller-Rushing (2010). Toward a synthetic understanding of the role of phenology in ecology and evolution.

Fort, H., D. P. Vázquez, and B. L. Lan (2016). Abundance and generalisation in mutualistic networks: solving the chicken-and-egg dilemma. *Ecology letters 19*(1), 4–11.

Fortuna, M. A., D. B. Stouffer, J. M. Olesen, P. Jordano, D. Mouillot, B. R. Krasnov, R. Poulin, and J. Bascompte (2010). Nestedness versus modularity in ecological networks: two sides of the same coin? *Journal of Animal Ecology 79*(4), 811–817.

Galeano, J., J. M. Pastor, and J. M. Iriondo (2009). Weighted-interaction nestedness estimator (wine): a new estimator to calculate over frequency matrices. *Environmental Modelling & Software 24*(11), 1342–1346.

Gallotti, R. and M. Barthelemy (2015). The multilayer temporal network of public transport in great britain. *Scientific data 2*(1), 1–8.

Garlaschelli, D. and M. I. Loffredo (2004). Fitness-dependent topological properties of the world trade web. *Physical review letters 93*(18), 188701.

Garlaschelli, D. and M. I. Loffredo (2008). Maximum likelihood: extracting unbiased information from complex networks. *Physical Review E 78*(1), 015101.

Goffe, W. L. et al. (1996). Simann: A global optimization algorithm using simulated annealing. *Studies in Nonlinear Dynamics and Econometrics 1*(3), 169–176.

Goffe, W. L., G. D. Ferrier, and J. Rogers (1994). Global optimization of statistical functions with simulated annealing. *Journal of econometrics 60*(1-2), 65–99.

Gotelli, N. J. (2000). Null model analysis of species co-occurrence patterns. *Ecology 81*(9), 2606–2621.

Gotelli, N. J. and G. L. Entsminger (2001). Swap and fill algorithms in null model analysis: rethinking the knight's tour. *Oecologia 129*(2), 281–291.

Gotelli, N. J. and G. R. Graves (1996). *Null models in ecology*. Smithsonian Institution Press.

Gould, S. J. (2002). *The structure of evolutionary theory*. Harvard University Press.

Gould, S. J. and R. C. Lewontin (1979). The spandrels of san marco and the panglossian paradigm: a critique of the adaptationist programme. *Proceedings of the royal society of London. Series B. Biological Sciences 205*(1161), 581–598.

Gracia-Lázaro, C., L. Hernández, J. Borge-Holthoefer, and Y. Moreno (2018). The joint influence of competition and mutualism on the biodiversity of mutualistic ecosystems. *Scientific reports 8*(1), 9253.

Graham, E. A., E. C. Riordan, E. M. Yuen, D. Estrin, and P. W. Rundel (2010). Public internet-connected cameras used as a cross-continental ground-based plant phenology monitoring system. *Global Change Biology 16*(11), 3014–3023.

Greve, M. and S. L. Chown (2006). Endemicity biases nestedness metrics: a demonstration, explanation and solution. *Ecography 29*(3), 347–356.

Grilli, J., M. Adorisio, S. Suweis, G. Barabás, J. R. Banavar, S. Allesina, and A. Maritan (2017). Feasibility and coexistence of large ecological communities. *Nature communications 8*, 14389.

Guimarães, P. R. and P. Guimaraes (2006). Improving the analyses of nestedness for large sets of matrices. *Environmental Modelling & Software 21*(10), 1512–1513.

Guimaraes Jr, P. R., V. Rico-Gray, S. Furtado dos Reis, and J. N. Thompson (2006). Asymmetries in specialization in ant–plant mutualistic networks. *Proceedings of the Royal Society B: Biological Sciences 273*(1597), 2041–2047.

Harary, F. (1969). *Graph theory*. Addison-Wesley, Reading, MA.

Harte, J. and E. A. Newman (2014). Maximum information entropy: a foundation for ecological theory. *Trends in ecology & evolution 29*(7), 384–389.

Harte, J., T. Zillio, E. Conlisk, and A. B. Smith (2008). Maximum entropy and the state-variable approach to macroecology. *Ecology 89*(10), 2700–2711.

Havens, K. and S. Henderson (2013). Citizen science takes root. *American Scientist 101*(5), 378–385.

Hegland, S. J., A. Nielsen, A. Lázaro, A.-L. Bjerknes, and Ø. Totland (2009). How does climate warming affect plant-pollinator interactions? *Ecology letters 12*(2), 184–195.

Heleno, R., C. Garcia, P. Jordano, A. Traveset, J. M. Gómez, N. Blüthgen, J. Memmott, M. Moora, J. Cerdeira, S. Rodríguez-Echeverría, et al. (2014). Ecological networks: delving into the architecture of biodiversity. *Biology Letters*.

Hellmann, J. J., J. E. Byers, B. G. Bierwagen, and J. S. Dukes (2008). Five potential consequences of climate change for invasive species. *Conservation biology 22*(3), 534–543.

Hernandez, L., A. Vignes, and S. Saba (2018). *Figshare dataset*. Available at: https://figshare.com/articles/data_used_for_article_zip/6080396/1.

Hernández, L., A. Vignes, and S. Saba (2018). Trust or robustness? an ecological approach to the study of auction and bilateral markets. *PloS one 13*(5), e0196206.

Holme, P. and J. Saramäki (2012). Temporal networks. *Physics reports 519*(3), 97–125.

Ings, T. C., J. M. Montoya, J. Bascompte, N. Blüthgen, L. Brown, C. F. Dormann, F. Edwards, D. Figueroa, U. Jacob, J. I. Jones, et al. (2009). Ecological networks–beyond food webs. *Journal of Animal Ecology 78*(1), 253–269.

Inoue, T., M. Kato, T. Kakutani, T. Suka, and T. Itino (1990). Insect-flower relationship in the temperate deciduous forest of kibune, kyoto: an overview of the flowering phenology and the seasonal pattern of insect visits.

James, A., J. W. Pitchford, and M. J. Plank (2012). Disentangling nestedness from models of ecological complexity. *Nature 487*(7406), 227–230.

James, A., J. W. Pitchford, and M. J. Plank (2013). James et al. reply. *Nature 500*(7463), E2–E3.

Jaynes, E. T. (1957). Information theory and statistical mechanics. *Physical review 106*(4), 620.

Johnson, S., J. J. Torres, J. Marro, and M. A. Muñoz (2010). Entropic origin of disassortativity in complex networks. *Physical review letters 104*(10), 108702.

Johnson, S. D. and K. E. Steiner (2000). Generalization versus specialization in plant pollination systems. *Trends in Ecology & Evolution 15*(4), 140–143.

Jones, E. I., J. L. Bronstein, and R. Ferrière (2012). The fundamental role of competition in the ecology and evolution of mutualisms. *Annals of the New York Academy of Sciences 1256*(1), 66–88.

Jonhson, S., V. Domínguez-García, and M. A. Muñoz (2013). Factors determining nestedness in complex networks. *PloS one 8*(9), e74025.

Joppa, L. N., J. M. Montoya, R. Solé, J. Sanderson, and S. L. Pimm (2010). On nestedness in ecological networks. *Evolutionary Ecology Research 12*(1), 35–46.

Jordano, P. (1987). Patterns of mutualistic interactions in pollination and seed dispersal: connectance, dependence asymmetries, and coevolution. *The American Naturalist 129*(5), 657–677.

Jordano, P., J. Bascompte, and J. M. Olesen (2003). Invariant properties in coevolutionary networks of plant–animal interactions. *Ecology Letters 6*(1), 69–81.

Kaiser-Bunbury, C. N., J. Memmott, and C. B. Müller (2009). Community structure of pollination webs of mauritian heathland habitats. *Perspectives in Plant Ecology, Evolution and Systematics 11*(4), 241–254.

Kaiser-Bunbury, C. N., S. Muff, J. Memmott, C. B. Müller, and A. Caflisch (2010). The robustness of pollination networks to the loss of species and interactions: a quantitative approach incorporating pollinator behaviour. *Ecology Letters 13*(4), 442–452.

Kallimanis, A., T. Petanidou, J. Tzanopoulos, J. Pantis, and S. Sgardelis (2009). Do plant–pollinator interaction networks result from stochastic processes? *Ecological modelling 220*(5), 684–693.

Kamilar, J. M. and Q. D. Atkinson (2014). Cultural assemblages show nested structure in humans and chimpanzees but not orangutans. *Proceedings of the National Academy of Sciences 111*(1), 111–115.

Kantsa, A., R. A. Raguso, A. G. Dyer, J. M. Olesen, T. Tscheulin, and T. Petanidou (2018). Disentangling the role of floral sensory stimuli in pollination networks. *Nature communications 9*(1), 1–13.

Kéfi, S., V. Miele, E. A. Wieters, S. A. Navarrete, and E. L. Berlow (2016). How structured is the entangled bank? the surprisingly simple organization of multiplex ecological networks leads to increased persistence and resilience. *PLoS biology 14*(8), e1002527.

Kirkland, S. J. and M. Neumann (2012). *Group inverses of M-matrices and their applications*. Chapman and Hall/CRC.

Kochmer, J. P. and S. N. Handel (1986). Constraints and competition in the evolution of flowering phenology. *Ecological monographs 56*(4), 303–325.

Kondoh, M., S. Kato, and Y. Sakato (2010). Food webs are built up with nested subwebs. *Ecology 91*(11), 3123–3130.

König, M. D., C. J. Tessone, and Y. Zenou (2014). Nestedness in networks: A theoretical model and some applications. *Theoretical Economics 9*(3), 695–752.

Krishna, A., P. R. Guimaraes Jr, P. Jordano, and J. Bascompte (2008). A neutral-niche theory of nestedness in mutualistic networks. *Oikos 117*(11), 1609–1618.

Kropotkin, P. et al. (1902). Mutual aid: A factor of evolution. *History of Economic Thought Books*.

Kwapień, J. and S. Drożdż (2012). Physical approach to complex systems. *Physics Reports 515*(3-4), 115–226.

Levin, S. A. (1992). The problem of pattern and scale in ecology: the robert h. macarthur award lecture. *Ecology 73*(6), 1943–1967.

Levin, S. A. (1998). Ecosystems and the biosphere as complex adaptive systems. *Ecosystems 1*(5), 431–436.

Lewinsohn, T. M., P. Inácio Prado, P. Jordano, J. Bascompte, and J. M. Olesen (2006). Structure in plant–animal interaction assemblages. *Oikos 113*(1), 174–184.

Lin, J.-H., C. J. Tessone, and M. S. Mariani (2018). Nestedness maximization in complex networks through the fitness-complexity algorithm. *Entropy 20*(10), 768.

Lloyd, S. (2001). Measures of complexity: a nonexhaustive list. *IEEE Control Systems Magazine 21*(4), 7–8.

Mariani, M. S., Z.-M. Ren, J. Bascompte, and C. J. Tessone (To appear in 2019). Nestedness in complex networks: observation, emergence, and implications. *Physics Reports*.

May, R., A. R. McLean, et al. (2007). *Theoretical ecology: principles and applications*. Oxford University Press on Demand.

May, R. M. (1972). Will a large complex system be stable? *Nature 238*, 413–414.

Maynard, D. S., C. A. Serván, and S. Allesina (2018). Network spandrels reflect ecological assembly. *Ecology letters 21*(3), 324–334.

McCann, K. S. (2000). The diversity–stability debate. *Nature 405*(6783), 228–233.

McIntosh, R. P. (1986). *The background of ecology: concept and theory*. Cambridge University Press.

McKinney, M. L. (1997). Extinction vulnerability and selectivity: combining ecological and paleontological views. *Annual review of ecology and systematics 28*(1), 495–516.

Medan, D., R. P. Perazzo, M. Devoto, E. Burgos, M. G. Zimmermann, H. Ceva, and A. M. Delbue (2007). Analysis and assembling of network structure in mutualistic systems. *Journal of theoretical biology 246*(3), 510–521.

Memmott, J., P. G. Craze, N. M. Waser, and M. V. Price (2007). Global warming and the disruption of plant–pollinator interactions. *Ecology letters 10*(8), 710–717.

Memmott, J., N. M. Waser, and M. V. Price (2004). Tolerance of pollination networks to species extinctions. *Proceedings of the Royal Society of London B: Biological Sciences 271*(1557), 2605–2611.

Milo, R., S. Shen-Orr, S. Itzkovitz, N. Kashtan, D. Chklovskii, and U. Alon (2002). Network motifs: simple building blocks of complex networks. *Science 298*(5594), 824–827.

Mitchell, M. (2009). *Complexity: A guided tour*. Oxford University Press.

Montoya, J. M., S. L. Pimm, and R. V. Solé (2006). Ecological networks and their fragility. *Nature 442*(7100), 259–264.

Moré, J. J., B. S. Garbow, and K. E. Hillstrom (1980). User guide for minpack-1. Technical report, CM-P00068642.

Newman, M. (2010). *Networks: An Introduction*. Oxford University Press.

Newman, M. E. (2002). Assortative mixing in networks. *Physical review letters 89*(20), 208701.

Nowak, M. A. (2006). Five rules for the evolution of cooperation. *Science 314*(5805), 1560–1563.

Nuismer, S. L., P. Jordano, and J. Bascompte (2013). Coevolution and the architecture of mutualistic networks. *Evolution: International Journal of Organic Evolution 67*(2), 338–354.

Odum, E. P. (1977). The emergence of ecology as a new integrative discipline. *Science 195*(4284), 1289–1293.

Oksanen, J., F. G. Blanchet, M. Friendly, R. Kindt, P. Legendre, D. McGlinn, P. R. Minchin, R. B. O'Hara, G. L. Simpson, P. Solymos, M. H. H. Stevens, E. Szoecs, and H. Wagner (2017). *vegan: Community Ecology Package*. R package version 2.4-4.

Olesen, J. M., J. Bascompte, Y. L. Dupont, H. Elberling, C. Rasmussen, and P. Jordano (2010). Missing and forbidden links in mutualistic networks. *Proceedings of the Royal Society of London B: Biological Sciences*, 13–71.

Olesen, J. M., J. Bascompte, Y. L. Dupont, and P. Jordano (2006). The smallest of all worlds: pollination networks. *Journal of theoretical Biology 240*(2), 270–276.

Olesen, J. M., J. Bascompte, Y. L. Dupont, and P. Jordano (2007). The modularity of pollination networks. *Proceedings of the National Academy of Sciences 104*(50), 19891–19896.

Olesen, J. M., J. Bascompte, H. Elberling, and P. Jordano (2008). Temporal dynamics in a pollination network. *Ecology 89*(6), 1573–1582.

Olito, C. and J. W. Fox (2015). Species traits and abundances predict metrics of plant–pollinator network structure, but not pairwise interactions. *Oikos 124*(4), 428–436.

Park, J. and M. E. Newman (2003). Origin of degree correlations in the internet and other networks. *Physical Review E 68*(2), 026112.

Park, J. and M. E. Newman (2004). Statistical mechanics of networks. *Physical Review E 70*(6), 066117.

Patterson, B. D. and W. Atmar (1986). Nested subsets and the structure of insular mammalian faunas and archipelagos. *Biological journal of the Linnean society 28*(1-2), 65–82.

Payrató-Borràs, C., L. Hernández, and Y. Moreno (2019). Breaking the spell of nestedness: The entropic origin of nestedness in mutualistic systems. *Physical Review X 9*(3), 031024.

Payrató-Borràs, C., L. Hernández, and Y. Moreno (2020). Measuring nestedness: A comparative study of the performance of different metrics. *Ecology and evolution 10*(21), 11906–11921.

Perazzo, R. P., L. Hernández, H. Ceva, E. Burgos, and J. I. Alvarez-Hamelin (2014). Study of the influence of the phylogenetic distance on the interaction network of mutualistic ecosystems. *Physica A: Statistical Mechanics and its Applications 394*, 124–135.

Petanidou, T. (1991). Pollination ecology in a phryganic ecosystem.

Petanidou, T., W. N. Ellis, N. S. Margaris, and D. Vokou (1995). Constraints on flowering phenology in a phryganic (east mediterranean shrub) community. *American Journal of Botany 82*(5), 607–620.

Pierce, W. D., R. A. Cushman, C. E. Hood, et al. (1912). Insect enemies of the cotton boll weevil.

Pilosof, S., M. A. Porter, M. Pascual, and S. Kéfi (2017). The multilayer nature of ecological networks. *Nature Ecology & Evolution 1*(4), 1–9.

Post, E., B. A. Steinman, and M. E. Mann (2018). Acceleration of phenological advance and warming with latitude over the past century. *Scientific reports 8*(1), 1–8.

Poulin, R. (2010). Network analysis shining light on parasite ecology and diversity. *Trends in parasitology 26*(10), 492–498.

Prado, P. I. and T. M. Lewinsohn (2004). Compartments in insect–plant associations and their consequences for community structure. *Journal of Animal Ecology 73*(6), 1168–1178.

Pueyo, S., F. He, and T. Zillio (2007). The maximum entropy formalism and the idiosyncratic theory of biodiversity. *Ecology letters 10*(11), 1017–1028.

Qiu, Y. and J. Mei (2016). rarpack: Solvers for large scale eigenvalue and svd problems. Available at: https://CRAN.R-project.org/package=rARPACK.

R Core Team (2013). *R: A Language and Environment for Statistical Computing*. Vienna, Austria: R Foundation for Statistical Computing.

Rafferty, N. E., P. J. CaraDonna, and J. L. Bronstein (2015). Phenological shifts and the fate of mutualisms. *Oikos 124*(1), 14–21.

Ramos-Jiliberto, R., P. M. de Espanés, M. Franco-Cisterna, T. Petanidou, and D. P. Vázquez (2018). Phenology determines the robustness of plant–pollinator networks. *Scientific reports 8*(1), 1–10.

Rathcke, B. and E. P. Lacey (1985). Phenological patterns of terrestrial plants. *Annual review of ecology and systematics 16*(1), 179–214.

Revilla, T. A., F. Encinas-Viso, and M. Loreau (2015). Robustness of mutualistic networks under phenological change and habitat destruction. *Oikos 124*(1), 22–32.

Rezende, E. L., J. E. Lavabre, P. R. Guimarães, P. Jordano, and J. Bascompte (2007). Non-random coextinctions in phylogenetically structured mutualistic networks. *Nature 448*(7156), 925–928.

Robertson, C. (1929). Flowers and insects lists of visitors of four hundred and fifty three flowers.

Robins, G., P. Pattison, Y. Kalish, and D. Lusher (2007). An introduction to exponential random graph (p*) models for social networks. *Social networks 29*(2), 173–191.

Robins, G., T. Snijders, P. Wang, M. Handcock, and P. Pattison (2007). Recent developments in exponential random graph (p*) models for social networks. *Social networks 29*(2), 192–215.

Rodríguez-Gironés, M. A. and L. Santamaría (2006). A new algorithm to calculate the nestedness temperature of presence–absence matrices. *Journal of Biogeography 33*(5), 924–935.

Rohr, R. P., S. Saavedra, and J. Bascompte (2014). On the structural stability of mutualistic systems. *Science 345*(6195), 1253497.

Saavedra, S., F. Reed-Tsochas, and B. Uzzi (2009). A simple model of bipartite cooperation for ecological and organizational networks. *Nature 457*(7228), 463.

Saavedra, S. and D. B. Stouffer (2013). Disentangling nestedness disentangled. *Nature 500*(7463), E1–E2.

Saavedra, S., D. B. Stouffer, B. Uzzi, and J. Bascompte (2011). Strong contributors to network persistence are the most vulnerable to extinction. *Nature 478*(7368), 233–235.

Sajjad, A., S. Saeed, M. Ali, F. Z. A. Khan, Y. J. Kwon, and M. Devoto (2017). Effect of temporal data aggregation on the perceived structure of a quantitative plant–floral visitor network. *Entomological Research 47*(6), 380–387.

Santamaría, L. and M. A. Rodríguez-Gironés (2007). Linkage rules for plant–pollinator networks: trait complementarity or exploitation barriers? *PLoS biology 5*(2), e31.

Saracco, F., R. Di Clemente, A. Gabrielli, and T. Squartini (2015). Randomizing bipartite networks: the case of the world trade web. *Scientific Reports 5*(10595).

Scoones, I. (1999). New ecology and the social sciences: what prospects for a fruitful engagement? *Annual review of anthropology 28*(1), 479–507.

Seabold, S. and J. Perktold (2010). Statsmodels: Econometric and statistical modeling with python. In *9th Python in Science Conference*.

Shelford, V. E. (1913). *Animal communities in temperate America: as illustrated in the Chicago region: a study in animal ecology*. Number 5. University of Chicago Press.

Siegenfeld, A. F. and Y. Bar-Yam (2019). An introduction to complex systems science and its applications. *arXiv preprint arXiv:1912.05088*.

Silva, W. (2002). Patterns of fruit-frugivore interactions in two atlantic forest bird communities of south-eastern brazil: implications for conservation. *Seed dispersal and frugivory: Ecology, evolution and conservation*, 423–435.

Simon, H. A. (1991). The architecture of complexity. pp. 457–476.

Skeat Walter, W. (1980). *A Concise Etymological Dictionary of the English Language*. The Putnam Publishing Group: Perigee Books.

Small, E. (1976). Insect pollinators of the mer bleue peat bog of ottawa. *Canadian field-naturalist*.

Solé, R. and S. Valverde (2020). Evolving complexity: how tinkering shapes cells, software and ecological networks. *Philosophical Transactions of the Royal Society B 375*(1796), 20190325.

Solé, R. V. and S. Valverde (2004). Information theory of complex networks: on evolution and architectural constraints. In *Complex networks*, pp. 189–207. Springer.

Solé, R. V. and S. Valverde (2006). Are network motifs the spandrels of cellular complexity? *Trends in ecology & evolution 21*(8), 419–422.

Solé-Ribalta, A., C. J. Tessone, M. S. Mariani, and J. Borge-Holthoefer (2018). Revealing in-block nestedness: Detection and benchmarking. *Physical Review E 97*(6), 062302.

Squartini, T. and D. Garlaschelli (2011). Analytical maximum-likelihood method to detect patterns in real networks. *New Journal of Physics 13*(8), 083001.

Squartini, T., R. Mastrandrea, and D. Garlaschelli (2015). Unbiased sampling of network ensembles. *New Journal of Physics 17*(2), 023052.

Stang, M., P. G. Klinkhamer, and E. Van der Meijden (2007). Asymmetric specialization and extinction risk in plant–flower visitor webs: a matter of morphology or abundance? *Oecologia 151*(3), 442–453.

Staniczenko, P. P., J. C. Kopp, and S. Allesina (2013). The ghost of nestedness in ecological networks. *Nature communications 4*, 1391.

Straka, M. J., G. Caldarelli, T. Squartini, and F. Saracco (2018). From ecology to finance (and back?): A review on entropy-based null models for the analysis of bipartite networks. *Journal of Statistical Physics 173*(3-4), 1252–1285.

Strona, G., W. Ulrich, and N. J. Gotelli (2018). Bi-dimensional null model analysis of presence-absence binary matrices. *Ecology 99*(1), 103–115.

Suweis, S., F. Simini, J. R. Banavar, and A. Maritan (2013). Emergence of structural and dynamical properties of ecological mutualistic networks. *Nature 500*(7463), 449–452.

Tébar, F., L. Gil, and L. Llorens (2004). Flowering and fruiting phenology of a xerochamaephytic shrub community from the mountain of mallorca (balearic islands, spain). *Plant Ecology 174*(2), 295–305.

Thébault, E. and C. Fontaine (2010). Stability of ecological communities and the architecture of mutualistic and trophic networks. *Science 329*(5993), 853–856.

Toral, R. and A. Chakrabarti (1993). Generation of gaussian distributed random numbers by using a numerical inversion method. *Computer physics communications 74*(3), 327–334.

Trøjelsgaard, K., P. Jordano, D. W. Carstensen, and J. M. Olesen (2015). Geographical variation in mutualistic networks: similarity, turnover and partner fidelity. *Proc. R. Soc. B 282*(1802), 20142925.

Ulrich, W., M. Almeida-Neto, and N. J. Gotelli (2009). A consumer's guide to nestedness analysis. *Oikos 118*(1), 3–17.

Ulrich, W. and N. J. Gotelli (2007). Null model analysis of species nestedness patterns. *Ecology 88*(7), 1824–1831.

Ulrich, W. and N. J. Gotelli (2012). A null model algorithm for presence–absence matrices based on proportional resampling. *Ecological Modelling 244*, 20–27.

Valverde, S., J. Piñero, B. Corominas-Murtra, J. Montoya, L. Joppa, and R. Solé (2018). The architecture of mutualistic networks as an evolutionary spandrel. *Nature ecology & evolution 2*(1), 94.

Vázquez, D. P., N. Blüthgen, L. Cagnolo, and N. P. Chacoff (2009). Uniting pattern and process in plant–animal mutualistic networks: a review. *Annals of botany 103*(9), 1445–1457.

Vázquez, D. P., N. P. Chacoff, and L. Cagnolo (2009). Evaluating multiple determinants of the structure of plant–animal mutualistic networks. *Ecology 90*(8), 2039–2046.

Vázquez, D. P., C. J. Melián, N. M. Williams, N. Blüthgen, B. R. Krasnov, and R. Poulin (2007). Species abundance and asymmetric interaction strength in ecological networks. *Oikos 116*(7), 1120–1127.

Vázquez, D. P., R. Poulin, B. R. Krasnov, and G. I. Shenbrot (2005). Species abundance and the distribution of specialization in host–parasite interaction networks. *Journal of Animal Ecology 74*(5), 946–955.

Venables, W. N. and B. D. Ripley (2002). *Modern Applied Statistics with S* (Fourth ed.). New York: Springer. ISBN 0-387-95457-0.

Virtanen, P., R. Gommers, T. E. Oliphant, M. Haberland, T. Reddy, D. Cournapeau, E. Burovski, P. Peterson, W. Weckesser, J. Bright, S. J. van der Walt, M. Brett, J. Wilson, K. Jarrod Millman, N. Mayorov, A. R. J. Nelson, E. Jones, R. Kern, E. Larson, C. Carey, İ. Polat, Y. Feng, E. W. Moore, J. Vand erPlas, D. Laxalde, J. Perktold, R. Cimrman, I. Henriksen, E. A. Quintero, C. R. Harris, A. M. Archibald, A. H. Ribeiro, F. Pedregosa, P. van Mulbregt, and S. . . Contributors (2020). SciPy 1.0: Fundamental Algorithms for Scientific Computing in Python. *Nature Methods*.

Visser, M. E. and P. Gienapp (2019). Evolutionary and demographic consequences of phenological mismatches. *Nature ecology & evolution 3*(6), 879–885.

Vizentin-Bugoni, J., V. J. Debastiani, V. A. Bastazini, P. K. Maruyama, and J. H. Sperry (2020). Including rewiring in the estimation of the robustness of mutualistic networks. *Methods in Ecology and Evolution 11*(1), 106–116.

Wallace, A. R. (1867). Creation by law. *The Quarterly Journal of Science 4*(16), 470–488.

Waser, N. M., L. Chittka, M. V. Price, N. M. Williams, and J. Ollerton (1996). Generalization in pollination systems, and why it matters. *Ecology 77*(4), 1043–1060.

Watts, D. J. and S. H. Strogatz (1998). Collective dynamics of 'small-world'networks. *Nature 393*(6684), 440.

Williams, R. J. (2011). Biology, methodology or chance? the degree distributions of bipartite ecological networks. *PLoS One 6*(3), e17645.

Young, J.-G., F. S. Valdovinos, and M. E. Newman (2019). Reconstruction of plant–pollinator networks from observational data. *bioRxiv*, 754077.

Yuan, H. (1988). A bound on the spectral radius of graphs. *Linear Algebra and its Applications 108*, 135–139.

Zhang, X., M. A. Friedl, C. B. Schaaf, A. H. Strahler, J. C. Hodges, F. Gao, B. C. Reed, and A. Huete (2003). Monitoring vegetation phenology using modis. *Remote sensing of environment 84*(3), 471–475.